Isotopes of sulphur, oxygen, strontium and carbon in groundwater as tracers of mixing and geochemical processes, Murray Basin, Australia

Submitted by

Shawan Shwket Dogramaci (MSc.)

as requirement in full for the degree of

Doctor of Philosophy

in the

Department of Geology & Geophysics

The University of Adelaide

January 1998

Table of Contents

List of Tables

List of Figures

Abstract

Salinisation of groundwater and surface water of the semi-arid Murray Basin is an issue of vital importance to the viability of agriculture in south-east Australia. Furthermore, the understanding of the transport and transfer of water and salts in large sedimentary aquifers is necessary for better management of water resources in the future.

The salinity of groundwater of the regional Murray Group Aquifer increases from 500 mg/l at the south-eastern basin margin, to ~ 23,000 mg/l about 300 km downgradient near the discharge area (River Murray). Addition of saline local recharge and upward leakage from the underlying saline Renmark Group Aquifer are thought to be the most likely causes for the increase in salinity in the Murray Group Aquifer.

The chemical composition and $\delta^{18}O$ and $\delta^{2}H$ of water molecules of the two regional aquifers are not sufficiently different to be used as tracers to identify the locations and extent of mixing. The main aim of this thesis is to assess the usefulness of $\delta^{34}S$ and $\delta^{18}OSO_4^{2-}$ of dissolved SO_4^{2-} and $^{87}Sr/^{86}Sr$ ratios as tracers of inter-aquifer mixing and rock-water interaction between and within the Murray and Renmark Group aquifers in the south-west Murray Basin.

The $\delta^{2}H$ and $\delta^{18}O$ composition of groundwater from both aquifers is depleted in ^{2}H and ^{18}O relative to sea water, and indicates that groundwaters are derived from rain fall and is not remnant sea water or connate seawater. Major ion distribution in both aquifers indicates that the combination of evapotranspiration of rainfall prior to recharge, carbonate dissolution and cation exchange on clays are major processes determining the current chemical composition of groundwater.

The $\delta^{34}S$, $\delta^{18}OSO_4^{2-}$ and SO_4^{2-}/Cl^- ratios suggest that vertical input of sulphate into the Murray Group Aquifer through local recharge is the dominant process relative to the

sulphate derived from groundwater flowing laterally from the basin margin. Further modification of the sulphate concentration in the discharge area near the River Murray occurs due to upward leakage from the Renmark Group Aquifer that has enriched $\delta^{34}S$ and $\delta^{18}OSO_4^{2-}$ values due to bacterial sulphate reduction.

The $^{87}Sr/^{86}Sr$ ratio of groundwater from the south and central part of the Murray Group Aquifer is controlled by dissolution of carbonate as recharge water percolates through the soil zone, and mixes with laterally flowing groundwater. Incongruent dissolution of carbonate minerals in the aquifer is also shown to occur by a model of $^{87}Sr/^{86}Sr$ and Sr^{2+}/Ca^{2+} ratio variations. This conclusion is further supported by $\delta^{13}C$ data, which shows that $\delta^{13}C$ becomes progressively more enriched as the $^{87}Sr/^{86}Sr$ ratio evolves towards that of the calcite $^{87}Sr/^{86}Sr$ ratio of the aquifer matrix. Sr^{2+} concentrations and $^{87}Sr/^{86}Sr$ ratios of the groundwater in the northern part of the Murray Group Aquifer suggest that the most likely processes influencing groundwater chemistry is mixing with more radiogenic groundwater from the Renmark Group Aquifer through upward leakage. The $^{87}Sr/^{86}Sr$ ratios also suggest that in addition to upward leakage, significant amounts of water from the Murray Group Aquifer in the northern part of the study area is derived from local recharge. This is supported by a measurable amount of ^{14}C content in groundwater throughout the study area. The measured ^{14}C content of groundwater in the south and central part of the Murray Group Aquifer was adjusted for the effect of carbonate mineral dissolution and, the adjusted ^{14}C data was used to estimate recharge rates in different parts of the Murray Group Aquifer.

Declaration of originality

I certify that this thesis does not contain or incorporate without acknowledgment any material previously submitted for the degree or diploma in any university; and that to the best of my knowledge and belief it does not contain any material previously published or written by another person except where due reference is made in the text.

I give consent to this copy of my thesis, when deposited in the University Library, being available for loan and photocopying.

Shawan Shwket Dogramaci.

Publications Associated with this Thesis

Journal Papers

1. Dogramaci, S. S., Herczeg, A. L., Schiff, S., and Bone, Y. (1998) Interpretation of Sulphur and Oxygen isotopes of Dissolved Sulphate In Semi-arid Regional Aquifers of the Murray Basin, Southeastern Australia. In prep. (Journal of Applied Geochemistry)
2. Dogramaci, S. S., Herczeg, A. L., Bone, Y. (1998) The Strontium Isotope Geochemistry of Regional Groundwater Systems: Applications To Water-Rock Interaction and Inter-Aquifer Mixing in the South-Western Murray Basin, Australia. In prep. (Journal of Hydrology).
3. Herczeg, A. L., Dogramaci, S. S. (1998) Hydrogeochemistry and Stable Isotope study of Groundwater in Tertiary Aquifers of the Mallee Region, South-Western Murray Basin, Australia. In prep. (Journal of Hydrology).

National and International Conference Publications

1. Dogramaci, S. S., Herczeg, A. L., Bone, Y. 1998. Strontium Isotope as a Tracer of Carbonate-Groundwater Reactions in the Semi-Arid Regional Aquifer of Southwestern Australia. 9th International Symposium on Water-Rock Interaction, 30 March- 3 April. Taupo, New Zealand.
2. Dogramaci, S. S., Herczeg, A. L., Bone, Y. 1997. Strontium Isotope Evolution in Groundwaters from a Carbonate Aquifer in the South-Western Murray Basin, Australia. 6th New Zealand/Australian Conference on Environmental Isotope Science. 2-4 April, Wellington, New Zealand.

3. Dogramaci, S. S., Herczeg, A. L., Bone, Y. 1997. Interpretation of Sulphur and Oxygen Isotopes of Dissolved Sulphate in Regional Aquifers of the Murray Basin, South-Eastern Australia. 6th New Zealand/Australian Conference on Environmental Isotope Science. 2-4 April, Wellington, New Zealand.
4. Dogramaci, S. S., Herczeg, A. L., Schiff, S., 1996. Sulfur and Oxygen-18 Isotopic Composition of Dissolved Sulfate as a Tool for Identifying Inter-Aquifer Mixing in the Mallee Region of South Australia: American Geophysical Union, Western Pacific Geophysics Meeting, Vol. 77, No. 22, July 23-27.
5. Dogramaci, S. S., Herczeg, A. L., Bone, Y. 1996. Strontium and Sulphur Isotopes as Tracers of Inter-Aquifer Mixing and Water-Rock Interaction, South-Western Murray Basin. Geological Society of Australia. Abstract No. 41. 13th AGC Canberra. pp. 159.
6. Dogramaci, S. S., Herczeg, A. L., Bone, Y. 1995. Strontium and Sulphur Isotopes as Tracers of Flow Systems in Regional Aquifers, southwestern the Murray Basin. Murray Darling 1995 Workshop, Wagga Wagga, Record No. 1995/61.

Acknowledgments

The work described in this thesis was carried out with the CSIRO Land and Water and the University of Adelaide. I gratefully acknowledge the assistance, patience, insight and infectious enthusiasm of my principal supervisor Dr. Andrew Herczeg throughout my work and for introducing me to the misty world of isotope hydrology. I also thank my second supervisor Dr. Yvonne Bone for her advice and encouragement and useful comments on the drafts of this thesis.

I extend my gratitude to all of the staff of the CSIRO Land and Water for their support and assistance. In particular Fred Leaney, John Dighton and Megan Easterbrook for teaching me isotope analysis. I also thank Dr. Peter Cook for useful discussions on numerous isotope and hydrological matters.

I would like to especially thank Dr. Corrine Le Gal La Salle from The Flinders University of South Australia for numerous discussion sessions in which many important concepts were developed and challenged.

Many thanks to all staff of the University of Adelaide, Department of Geology and Geophysics for their help and support, in particular Dr. Keith Turnbull, David Bruce and John Stanley for their help and advice in strontium and sulphur isotope analysis.

I am also grateful to the following people for their help and assistance throughout this work: Steve Barnett, Andrew Love from Department of Mines and Energy and Robbie Lennard from The Flinders University.

I gratefully acknowledge the financial support awarded by the University of Adelaide and CSIRO, Division of Land and Water and Centre for Groundwater Studies.

Operating funds were provided by LWRRDC research grant CWS3 (Potential for Groundwater Salinisation, Mallee area, Murray Basin) and the University of Adelaide.

Finally, much appreciation goes to my family for their support and encouragement, and to my wife Andrea whose dedication and sacrifice has fueled me throughout my post graduate studies.

CHAPTER 1

Introduction

1.1 Background and scope of the problem

Groundwater has been an integral part of human day to day activity from the beginning of civilization. The Old Testament contains many references to groundwater, springs and wells, e.g., Abraham and Isaac were famous for their success as well diggers. The importance of groundwater supplies is illustrated in the twenty-six chapters of Genesis which refers to Isaac's effort to find water for his tribe and the text reads as follows:

"And Isaac departed thence, and pitched his tent in the valley of Gerar, and dwelt there.

And Isaac digged again the wells of water which they had digged in the days of Abraham his father; for the Philistines had stopped them after the death of Abraham: and he called their names after the names by which his father had called them.

And Isaac's servants digged in the valley, and found there a well of springing water. And the herdmen of Gerar did strive with Isaac's herdmen, saying, The water is ours; and he called the name of the well Esek; because they strove with him....."

Tolman (1937) describes the large underground water tunnels of Kanats, in Persia and Egypt dating back from 800 BC. Thirty six of these Kanats (Tunnels) still supply Tehran and the highly cultivated agricultural area around Tehran.

Many theories have been proposed by Greek and Roman philosophers to explain the origin of groundwater. Some of the theories were accurate accounts, and others were just reverie and fantasies (Meinzer, 1934; Baker and Horton, 1936). For example, in ancient times springs where considered as miraculous gifts of gods; they wrought miracles and were places where temples were built (Meinzer, 1934). The Greek philosophers Plato and Homer, on the other hand, thought that spring water was derived from the ocean by direct flow through subterranean channels, then purified and raised to the surface. In describing rain water formation, Aristotle thought that the air surrounding the earth is turned into water by the cold of the heavens and falls as rain and that the air which penetrates and passes into the crust of the earth also becomes transformed into water, owing to the cold which it encounters there (Baker and Horton, 1936). It was only in the late seventeenth century that a clear understanding of the hydrological cycle had been achieved (Todd, 1959).

Furthermore, groundwater tracing also dates from ancient times. Mazor (1976 a) describes tracing experiments carried out by Philip, the ruler of the Holy Land nearly 2000 years ago, to confirm his belief that the source of the Banias Spring is Ram Lake which is located 600 m above the spring on the slope of Mount Hermon. The experiment was carried out by throwing chaff into Ram lake and observing it in Banias

Spring. The result of Philip's tracing experiments have been ruled out by the recent observations of stable isotopic content of both sources. However, his basic idea is as sound as it was 2000 years ago.

The use of groundwater due to scarcity of fresh surface water in many parts of the world has greatly preceded the understanding of its origin, occurrence and movement. Groundwater accounts for about two-thirds of the freshwater of global water resources. Neglecting the amount of fresh water held in polar ice caps and glaciers, groundwater accounts for 98% of fresh water resources on a global scale (Todd, 1970; Freeze and Cherry, 1979). Moreover, groundwater is especially important in arid and semi-arid regions where potential evaporation exceeds precipitation, resulting in a small or negligible and unreliable runoff (Peak, 1979). In such areas only a small fraction of precipitation contributes to groundwater recharge, a major portion of precipitation being lost by evaporation from the surface layers. In this case the total dissolved solids (TDS) in rainwater are concentrated in the soil zone and can produce highly concentrated recharge water.

Infiltration of high TDS water via local recharge to the water table can directly affect the quality and chemical composition of groundwater. The small flux of recharge water in arid and semi-arid regions may result in long residence times for water in the unsaturated zone which in turn results in extensive water-rock interactions. A consequence of this is that the concentration of TDS in groundwater may increase and reach extremely high levels. In addition, arid and semi-arid regions of the globe are

generally characterised by flat topography and low relief. This is especially true for the Australian continent and some parts of Africa, Asia and North America. Low relief and flat topography have resulted in low hydraulic gradients, causing a long residence time of groundwater, especially in regional aquifers. The accumulated effects of these factors make accurate identification of recharge and discharge characteristics, as well as physical and chemical processes occurring in the aquifers over a long period of time almost impossible by conventional hydrologic methods alone. Understanding the large scale processes that can take place over a long period of time can therefore only be accomplished through a combination of conventional methods and chemical and isotopic measurements.

1.2 Isotopes in hydrological studies

The isotopes of light elements (H, C, O, S) can fractionate through physical and chemical processes due to mass differences between the isotopes of a given element. It is, therefore, often possible to identify these processes by studying the various isotopic compositions of aquifer minerals and that of solutes and water molecules in groundwater. The isotopes of heavier elements with an atomic mass > 40, on the other hand, are not affected by mass fractionation because relative mass differences of these isotopes are too small to become measurably separated during physical and chemical processes.

A large number of hydrologic investigations of arid and semi-arid regions have been carried out over the last 30 years using a combination of hydrologic data and stable isotope ratio of water molecules ($^{2}H/^{1}H$, $^{18}O/^{16}O$) as well as carbon isotopes ($^{13}C/^{12}C$, and ^{14}C) of dissolved inorganic carbon. For example, Salati et al. (1974) found some indication for climate change from stable isotope composition of groundwater in the Brazilian Northeastern region. Edmunds and Walton (1980) described methods to estimate recharge in semi-arid regions by stable isotope and Cl^- content in soil profiles. Sonntag et al. (1980) also used stable isotopes in combination with the tritium content of water in the unsaturated zone and groundwater to determine the age and estimate the amount of recharge in the Dahna sand dune (Saudi Arabia). Lloyd (1980) examined the groundwater gradients in old groundwaters in southwestern Egypt using radiocarbon data and concluded that the hydraulic gradient in old groundwaters could persist for a long period of time in arid regions.

The ^{2}H and ^{18}O isotopes of water molecules are conservative at ambient temperature and will remain constant in groundwater unless affected by physical processes, such as mixing with groundwater with a different isotopic signature, or variation in evaporation during recharge. Therefore, the effect of these processes on groundwater can be identified by comparing the $\delta^{2}H$ and $\delta^{18}O$ of groundwater and of the rainfall which recharges the aquifer (Mazor et al., 1985; Herczeg et al., 1992; Love et al., 1993; Chambers et al., 1995).

The ^{14}C concentration of total inorganic carbon species ($CO_{2(aq)} + HCO_3^- + CO_3^{2-}$), in combination with the $^{13}C/^{12}C$ ratio and carbonate chemistry can be used to determine the residence time of groundwater (Mook, 1980). In addition to this, $\delta^{13}C$ can provide information on sources and sinks of inorganic carbon, which is an important step in understanding the geochemistry of groundwater because bicarbonate is a major anion in groundwater. For example, Pearson and Swarzenki (1974) used ^{14}C concentration and carbonate chemistry to delineate the sources and age of the groundwater in the Northern Province of Kenya and concluded that groundwater can be divided into two distinct groups, each representing different recharge events in the past.

Sulphur isotopes (^{34}S, ^{32}S) of dissolved sulphate can reveal information on the sources and sinks of sulphate and geochemical processes that modify sulphate concentration and groundwater (Hendry et al., 1989; Nielsen et al., 1991; Edmunds et al.,1995). Different sulphur compounds can display distinct isotopic signatures (Nielsen et al., 1991), potentially allowing the identification of the relative contributions of SO_4^{2-} to groundwater from different sources. Oxygen isotopes (^{18}O, ^{16}O) of dissolved sulphate ($\delta^{18}OSO_4^{2}$), on the other hand, may reveal information about the sulphur cycle in conditions where sulphur isotopes information is ambiguous. Often the $\delta^{18}OSO_4^{-2}$ isotope have provided information on sulphate reduction-oxidation (redox) reactions, whereas the sulphur isotope provided no evidence of these reactions (van Everdingen et al., 1982; Tylor et al., 1984 a, b).

Strontium isotopes ($^{87}Sr/^{86}Sr$) unlike light isotopes, are not affected by mass fractionation. Therefore, if the groundwater has reached chemical and isotopic equilibrium with the aquifer minerals, the $^{87}Sr/^{86}Sr$ of the groundwater reflects that of the aquifer minerals. In contrast, if equilibrium has not been achieved or only partially achieved, then the $^{87}Sr/^{86}Sr$ for the two phases will be different and will depend on the extent of the reaction between the groundwater and the respective minerals. The $^{87}Sr/^{86}Sr$ isotopes are particularly good tracers as indicators of the interaction of water and carbonate minerals and its effect on the chemical composition of groundwater.

Utilisation of the above mentioned isotope techniques have led to the advancement of several hypotheses to explain the occurrence of brackish, saline and hyper-saline groundwater in the Stripa aquifer in Sweden (Nordstrom et al., 1989; Moser et al., 1989; Fritz et al., 1989; Clauer et al., 1989) and in the Canadian Shield (Frape and Fritz, 1982; Fritz and Frape, 1982; Frape et al., 1984 a, b; Fritz and Frape, 1987). Some of these studies have been motivated by the need to find a safe repository for high-level radioactive waste and are focused on groundwater in fractured rocks. However, similar studies in sedimentary basins have been carried out to understand and interpret some of the complex features and characteristics of groundwater on a regional scale, for example the Milk River Aquifer in Alberta, Canada (Hendry and Schwartz, 1988; Hendry et al., 1991; Drimmie et al., 1991; Frohlich et al., 1991), Snake River Plain Regional Aquifer System, Idaho, and Eastern Oregon in United States (Wood and Low, 1988), and the Great Artesian Basin in Australia (Bentley et al., 1986; Collerson et al., 1988; Herczeg et al., 1991; Mazor, 1992; Phillips, 1993).

Similarly, the Regional Aquifer-System Analysis (RASA) Program in the United States has developed quantitative appraisals of the major groundwater systems. For examples: the Madison Aquifer in parts of Montana, South Dakota, and Wyoming (Busby et al., 1991); Cambrian-Ordovician Aquifer in Northern Midwest (Siegel, 1989); Florida Aquifer, in Florida and parts of Georgia, South Carolina, and Alabama (Sprinkle, 1989); Sandstone Aquifers of the Northern Great Plains (Henderson, 1984); Alluvial Aquifers of Arizona (Robertson, 1987); and groundwater in the Sacramento Valley, California (Hull, 1984). These studies have used a combination of mass balance calculations and various isotopic compositions as a constraint on geochemical models to quantitatively predict the amount of salts introduced to the aquifers via various physical and geochemical processes.

Despite the large body of research into regional groundwater studies, and application of various conventional and novel methods in hydrologic and geochemical investigations, the majority of these studies have been carried out in temperate regions of Europe North America, and United States, and there are very few comprehensive geochemical and isotopic studies on a regional scale in semi-arid regions.

This study concentrates on the use of $^{87}Sr/^{86}Sr$, $\delta^{34}S$ and $\delta\ ^{18}OSO_4^{2-}$ in regional aquifers within the Murray Basin of south-eastern Australia in combination with major ions and δ^2H, $\delta^{18}O$, $\delta^{13}C$, ^{14}C. The main emphasis is to test the usefulness of $^{87}Sr/^{86}Sr$, $\delta^{34}S$ and $\delta^{18}OSO_4^{2-}$ in a semi-arid environment as tracers to provide information on specific locations of inter-aquifer mixing and water-rock interaction in the two regional aquifers.

Application of these isotopes may reveal information on long term processes which cannot be obtained by conventional methods. Furthermore, protection of the water quantity and quality can only be achieved through a thorough understanding of large scale processes that can best be measured through chemical and isotopic measurements.

1.3 Aims of the thesis

Groundwater in the Murray Group Aquifer is the only water resource for irrigation, stock, domestic and municipal use in the western Murray Basin. The TDS increases along the hydraulic gradient from ~500 mg/l at the south-eastern basin margin to ~ 23,000 mg/l, 350 km downgradient at the discharge area near the River Murray. The spatial distribution of salinity in deep groundwater of the underlying confined Renmark Group Aquifer is similar to that of the Murray Group Aquifer. The hydraulic head distribution between the two major aquifers indicates the potential for inter-aquifer mixing through upward leakage from the Renmark Group Aquifer in the north and north-western part of the study area. Hydrochemistry and δ^2H, $\delta^{18}O$ in both aquifers are also similar, so that the assessment of the effect of mixing on water quality in the Murray Group Aquifer is not possible by these techniques. Therefore, alternative environmental isotopes are sought to assess the extent of inter-aquifer mixing and groundwater geochemical processes.

The main objectives of this thesis are:

1. to evaluate the usefulness of strontium, sulphur, and oxygen isotopes of dissolved sulphate in a semi-arid regional aquifer to identify specific locations for inter-aquifer mixing and to provide information on rock-water interactions in the Murray Group Aquifer;

2. to determine the extent of mixing between the two aquifers, via upward leakage from the Renmark Group Aquifer;

3. to estimate the extent and rate of upward leakage from the Renmark Group Aquifer;

3. to estimate the relative importance of water derived from diffuse local recharge relative to recharge at the basin margin followed by lateral flowing groundwater in the Murray Group Aquifer;

4. to investigate the major geochemical and physical processes causing the increase of salinity in the Murray Group Aquifer along the hydraulic gradient.

In order to address these objectives, the thesis is divided into seven chapters. Chapter 1 describes the study area (the south-western Murray Basin), the physiography, and the geological and hydrological setting of the two principal aquifers. Chapter 2 describes groundwater sampling techniques and chemical and isotopic analysis of groundwater

and the aquifer matrix. Chapter 3 provides background chemical and water stable isotope data and addresses the main physical and geochemical processes affecting the chemical composition of groundwater from the Murray and Renmark Group aquifers. Chapter 4 discusses the geochemistry of sulphur and oxygen-18 isotopes of dissolved sulphate in groundwater and their use as tracers, to determine the source of sulphate and to identify inter-aquifer mixing. In Chapter 5 the use of strontium isotope and concentration data to provide information on water-rock interaction is discussed. The main part of chapter 5 develops geochemical models using strontium and carbon-13 data to elucidate the effect of rock-water interaction on total dissolved solids in groundwater from the Murray Group Aquifer. Strontium isotope data are also used to quantify inter-aquifer mixing though upward leakage. Chapter 6 discusses the effect of geochemical processes occurring in the Murray Group Aquifer on radiocarbon concentration of groundwater. Recharge rates have been estimated from radiocarbon data to the Murray Group Aquifer in various parts of the basin. The main conclusions are presented in chapter 7.

1.4 Previous investigations in the study area

A comprehensive geological investigation was carried out by Brown and Stephenson (1991) describing the structural and stratigraphic framework of groundwater in the Tertiary sediments of the Murray Basin. Lawrence (1975) and Barnett (1989) carried out regional-scale hydrogeological investigations of the major aquifers in the south-

western part of the Murray Basin. A detailed study on the spatial distribution of salinity in the Murray and Renmark Group aquifers throughout the Murray Basin was conducted by Evans and Kellett (1989), showing that the spatial distribution of salinity is similar in both aquifers and salinity generally increases from the basin margin towards the central part of the basin. Lindsay and Barnett (1989) have studied the effect of structure and stratigraphy of the Murray and Renmark Group aquifers on upward leakage from the Renmark Group Aquifer to the Murray Group Aquifer near the River Murray in South Australia. Hydrochemical investigations in this area using stable isotopes and hydrochemistry showed that the Renmark Group Aquifer may be contributing significant amounts of water to the Murray Group Aquifer (Herczeg et al., 1989). Arad and Evans (1987), using hydrochemistry and stable isotope composition in the Campaspe River aquifer system in Victoria, suggested that irrigation has a significant effect on the salinity distribution in the groundwater. Jones et al. (1994) have investigated the sources of dissolved salts in the groundwater of the Murray Basin by using hydrochemistry and stable isotope composition of pore water in an aquitard (Geera Clay) ~ 300 km to the east of the study area and concluded that the pore water is derived from meteoric water.

A detailed hydrologic and hydrochemical study was conducted on the interaction between groundwater and surface water systems in northern Victoria by Macumber (1991). This subject has been the focus of several investigations to understand the dynamics of groundwater discharge and geochemical processes occurring in these zones (Herczeg et al., 1992; Long et al., 1992; Hines et al., 1992; Lyons et al., 1995).

More detailed research on the source of salinity in the River Murray, which is the main discharge area for the groundwater in the Murray and Renmark Group aquifers, was carried out by Simpson and Herczeg (1991a, b; 1994) and Herczeg et al. (1993). Despite the extensive research conducted in the past on the origin and the cause of salinity in the Murray Basin, few studies exist concerning the use of chemical and isotopic composition of groundwater at a regional scale to assist in understanding the increase in salinity of the groundwater (Arad and Evans, 1987; Evans and Kellet, 1989; Davie et al., 1989; Kellet et al., 1990; Telfer, 1989, 1990).

1.5 Site description and physiography

The study area lies between latitude 34° to 36° 30′ South and longitude 140° to 142° East and encompasses 60,000 km^2 of the south-western Murray Basin (Fig.1.1 & 1.2). It stretches 400 km from the River Murray in the north, and is bounded by Padthaway Ridge in the southwest and Dundas Plateau in the southeast. The study area is generally characterised by low relief with the exception of the Dundas Plateau (max. elevation 300m) on the southeastern margin of the basin. Mean annual precipitation ranges from less than 250 mm/year in the north, to over 600 mm/year in the south and southwest. Rainfall is winter dominated, falling mainly between May and October, and annual evaporation ranges from approximately 1,700 to 2,200 mm /year (Cook 1992). Runoff in the study area is negligible due to low relief and highly permeable sandy soils cover much of the region.

Prior to 1850, the study area was mostly covered by native Eucalyptus woodland, known locally as Mallee. Mallee refers to low shrubby trees or tall shrubs with two or usually more stems. The most common trees are Red Mallee (*Eucalyptus socialis*), Gray Mallee (*Eucalyptus dumosa*), Ridge-Fruit Mallee (*Eucalyptus incrassata*), Oil Mallee (*Eucalyptus oleosa*), and White Mallee (*Eucalyptus gracilis*). There is also a wide variety of grass and shrub species between the trees, including Porcupine Grass (*Triodia irritans* and *Chenopods*). The Mallee trees are characterized by roots up to 20m deep and are capable of intercepting and transpiring most of the rainfall (Walker et al., 1990). Over the last 150 years ~ 80% of the study area was cleared for dryland cropping. The present predominant land use comprises of rotational cereal cropping and sheep and cattle grazing.

1.7 Geological setting

The Murray Basin is a low-lying, saucer-shaped, intra-cratonic groundwater basin containing Cenozoic sediments deposited in shallow-marine, fluvio-lacustrine and eolian environments (Brown, 1989; Brown and Stephenson, 1991). It underlies an area of about $3x10^5$ km^2. This closed groundwater basin contains 200-600 m of unconsolidated sediments, and sedimentary rocks with a number of regional aquifer systems. A simplified NW-SE geological cross-section is shown in Fig. 1.3.

The earliest deposition of Cenozoic fill in the study area was during the Paleocene to Oligocene about 20-60 million years ago, when continental deposition of the Warina

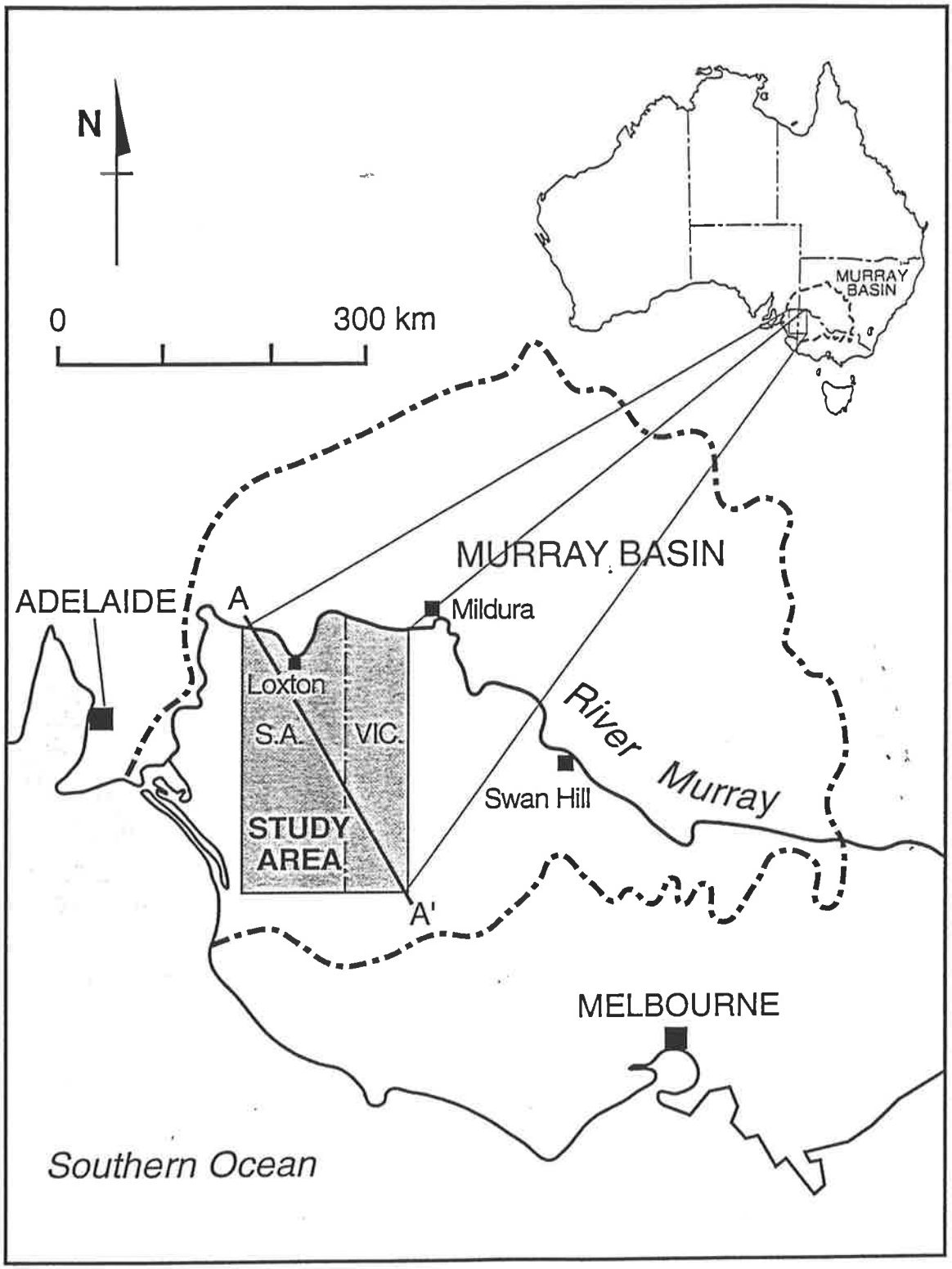

Fig. 1.1 Location map, showing the Murray Basin and the study area. Location of geological cross-section A-A` (Fig. 1.3) is also shown.

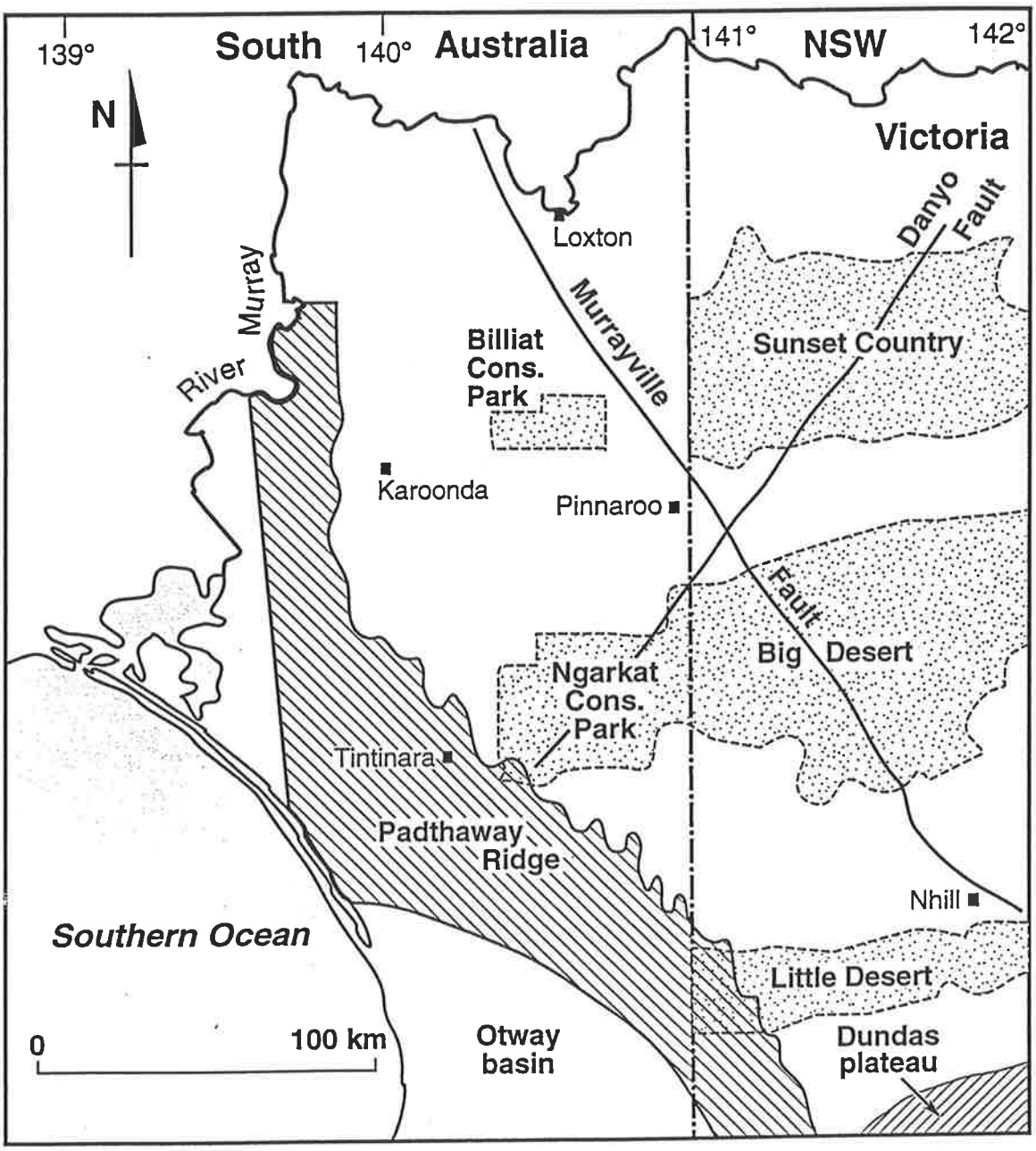

Fig 1.2 Location of study area, the south-western Murray Basin, showing the relationship to adjacent geological provinces. The Dundas Plateau acts as a hydraulic basement high in the southeastern margin of the basin.

Sands and Olney Formation, which make up the Renmark Group Aquifer, occurred. The Warina Sand is a fluvial unit of pale gray to pale brown, medium to coarse quartz sand and sandstone, soft silt, clay and minor pebble conglomerate (Harris, 1966; Lawrence, 1975; Brown and Stephenson, 1991). The sand is poorly-sorted at the base of the formation (Ludbrook, 1961), and moderate- to well-sorted elsewhere (Lawrence,1975). It is overlain by laterally discontinuous beds of poorly-consolidated, dark brown, gray carbonaceous silt, sand and clay known as the Olney Formation, originating from a fluvio-lacustrine environment (Brown, 1989). The Olney Formation is characterised by an abundance of carbonised plant remains, including fossil logs, woody peat, and leaf litter debris (Brown and Stephenson, 1991).

The marine transgression into the Murray Basin occurred in the Early Oligocene about 32 million years ago, and was caused by a rise in sea level resulting in deposition of marine and marginal-marine sediments (Murray Group) over the western Murray Basin. These marine and marginal-marine sediments attain a thickness of up to130 m in north-west Victoria, and consist of gray to white bryozoal calcarenite. In some places, the calcarenite contains a high content of quartz and skeletal debris. Lack of cements and voids in the skeletal remains of this temperate environment fauna give the Murray Group Limestone its high permeability (Lawrence, 1975). The Renmark Group Aquifer is separated from the Murray Group Aquifer by a 20 to 30 m thick aquitard known as the Ettrick Formation, which disconformably overlies the Renmark Group and consists of fine grained silt, and sandy glauconitic marl (Fig 1.3).

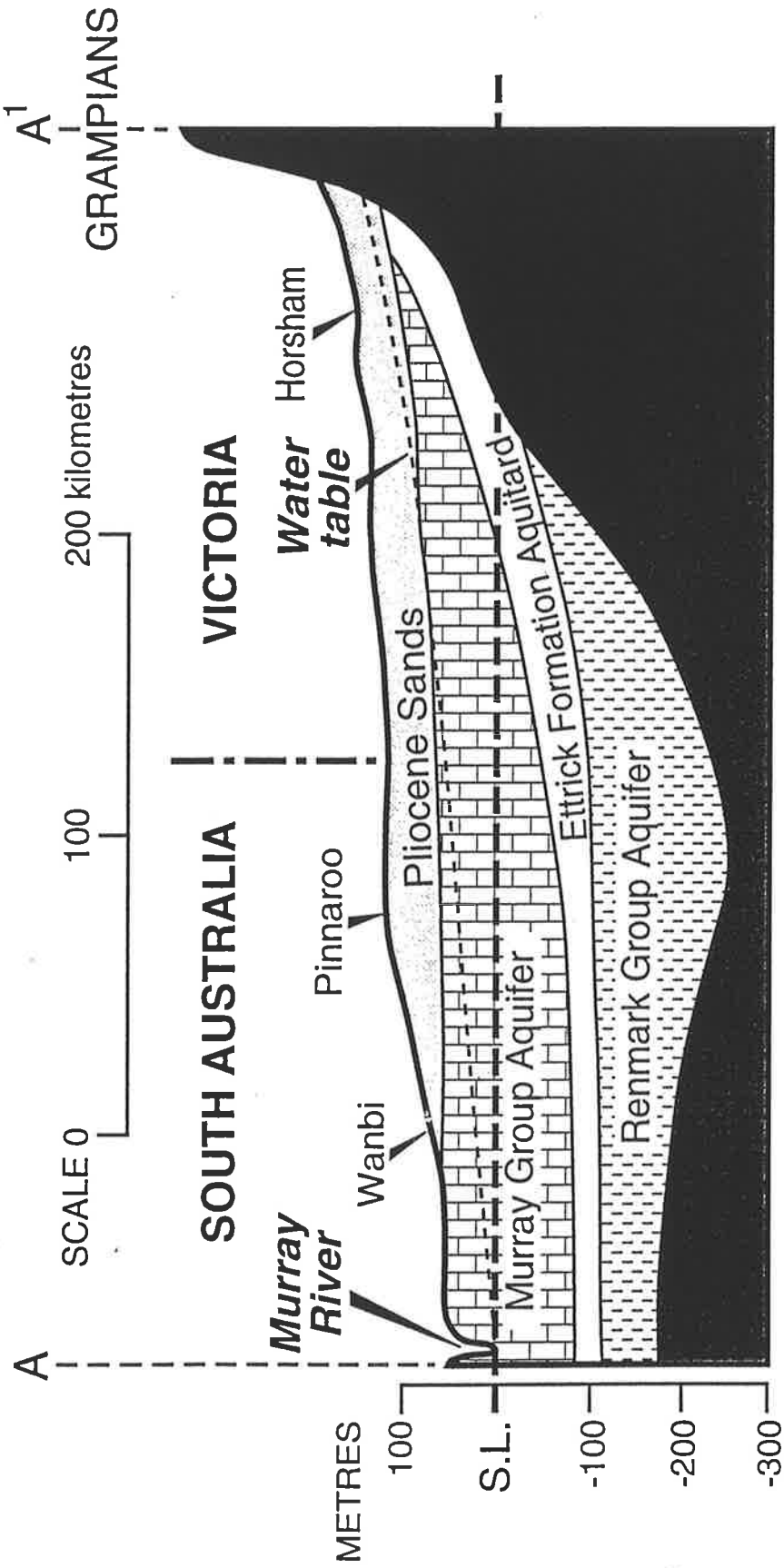

Fig. 1.3 Simplified SE-NW geological cross-section located as Fig. 1.1 from Allison *et al.* (1990).

A marine transgression-regression about 6 million years ago resulted in shallow marine deposition of the Bookpurnong beds. The sediments are glauconitic and highly fossiliferous. This formation is absent over the western part of the study area due to uplift along the Murrayville Fault (Fig 1.2) (Brown and Stephenson, 1991). During the final retreat of the sea from the Basin in the early Pliocene between 4 to 2 million years ago, the marginal marine quartz sand of the Loxton sands and Parilla sands were deposited (Ludbrook, 1961; Firman, 1973; Brown and Stephenson, 1991). The Loxton and Parilla sands consist mainly of weakly cemented and unconsolidated yellow-brown, fine to coarse, well-sorted quartz sand and sandstone with minor clay, silt and pebble conglomerate.

1.7 Hydrogeology

1.7.1 Murray Group Aquifer

The compiled potentiometric contours (Barnett, 1989; Murray Basin Hydrogeological Map Series, AGSO-Fig. 1.4) show that groundwater movement in the Murray Group Aquifer is from the Dundas Plateau in western Victoria to the north north-west and west under a very low gradient of 1:4,000 where it discharges into the River Murray. The longest inferred flow line travels north in a northwesterly direction up to 350 km and the shortest is 150 km to the west. The hydraulic conductivity of the Murray Group Aquifer ranges from 3 m/day in the south and 1-2 m/day in the north and northwest (Lawrence, 1975; Barnett, 1983). Under the present day hydraulic gradient,

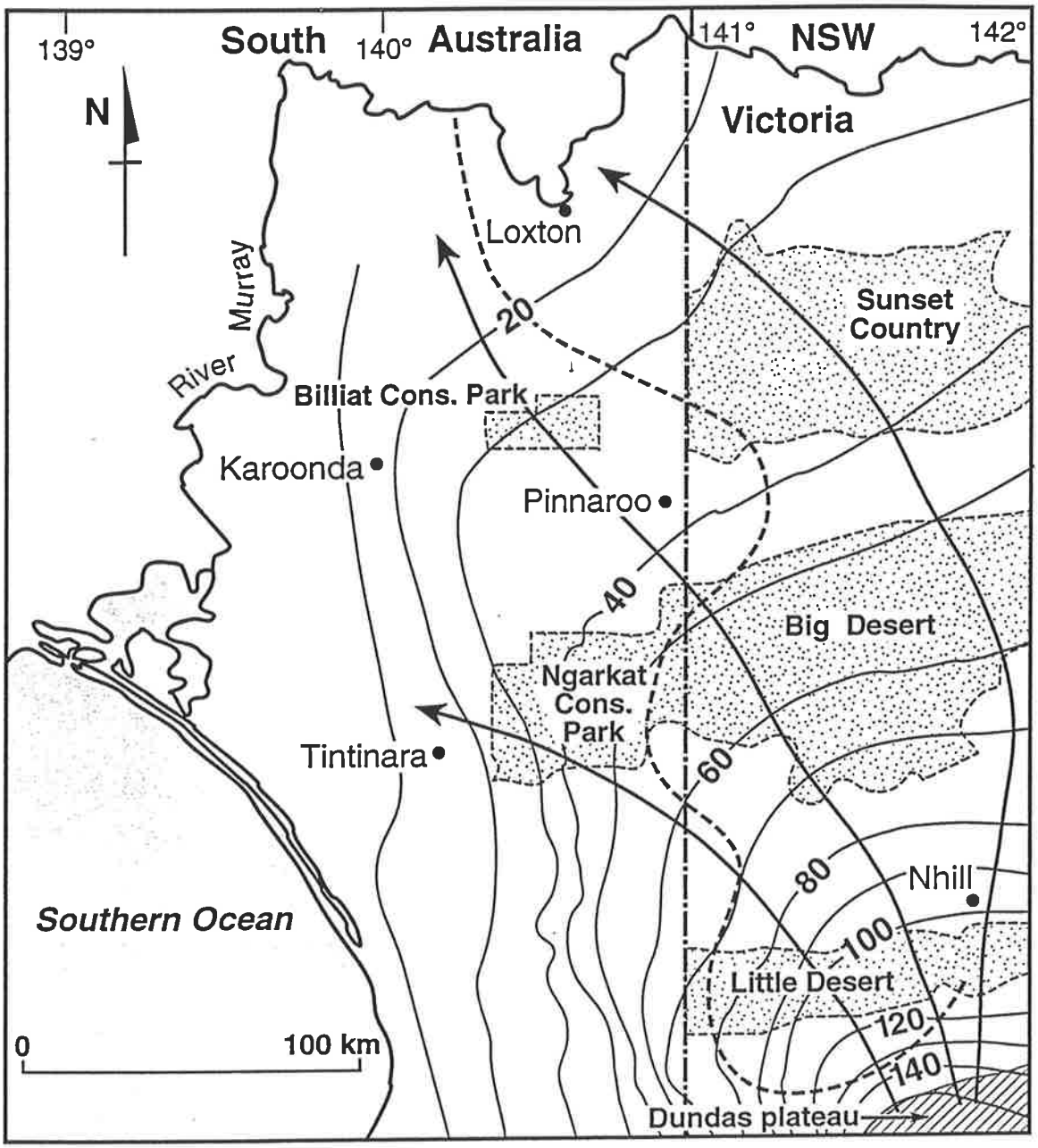

Fig. 1.4 Potentiometric surface and groundwater flow directions for the Murray Group Aquifer. The dashed line represents the confined and unconfined boundary, i.e. east of the boundary the water table is in the Pliocene sand aquifer

a travel time along the longest flow path from the basin margin in the southeast to the discharge area in the north-west was estimated using Darcy's lawto be ~ 200,000 years Barnett (1989).

The Murray Group Aquifer in Victoria is partly confined by the Bookpurnong Beds, and unconfined further west in South Australia. This formation is overlain by the Loxton-Parilla Sand aquifer throughout the study area. The boundary between the confined and unconfined part of the Murray Group Aquifer is shown in Fig. 1.4.1 The water table in the confined part lies in the overlying sand aquifer, whereas in the unconfined part it lies in the Murray Group Aquifer.

1.7.2 Renmark Group Aquifer

Groundwater flow in the Renmark Group Aquifer is to the north and northwest from the Dundas Plateau (western Victoria), towards the River Murray where it discharges by upward leakage into the unconfined Murray Group Aquifer (Barnett, 1983). Horizontal hydraulic conductivity in the Renmark Group Aquifer averages 10-30 m/day at the eastern part of the Murray Basin and decreases to the west towards the study area to 1-5 m/day (Lawrence, 1975; Woolley and Williams, 1978; Tickell and Humphreys, 1987). There is no measured data on vertical hydraulic conductivity for the Murray and Renmark Group aquifers.

The hydraulic head difference contour (Barnett, 1989) shows the potential for downward leakage through the Murray Group Aquifer to the south, but further down gradient the situation is reversed with a head difference of up to 20 m indicating a potential for upward leakage from the Renmark Group Aquifer in the north and north west of the area (Fig 1.5).

1.8 Groundwater recharge rates

Recharge rates under Mallee vegetation have been estimated in the northern part of the study area and ranged from 0.04 mm a^{-1} to 0.09 mm a^{-1} (Allison 1985; Cook et al., 1989; Cook and Walker, 1989). Localized recharge through depressions in the landscape may also contribute significantly to groundwater recharge. Cook et al. (1991) estimated recharge through natural clearings in the study area as 7.5 mm a^{-1}, and concluded rates of up to 100 mm a^{-1} may be possible through sinkholes in karstic areas near Murbko (Fig 1.6). Kennett-Smith et al. (1994) studied the relationship between recharge rates and soil texture and found that the recharge rate is strongly related to the average clay content in the top 2 m of the soil profiles. That is, heavy-textured soils tended to represent low recharge areas especially where native vegetation has been cleared.

The clearing of native vegetation and replacement by pasture and shallow-rooting crops such as wheat have increased the recharge rate and altered the hydrologic balance in the

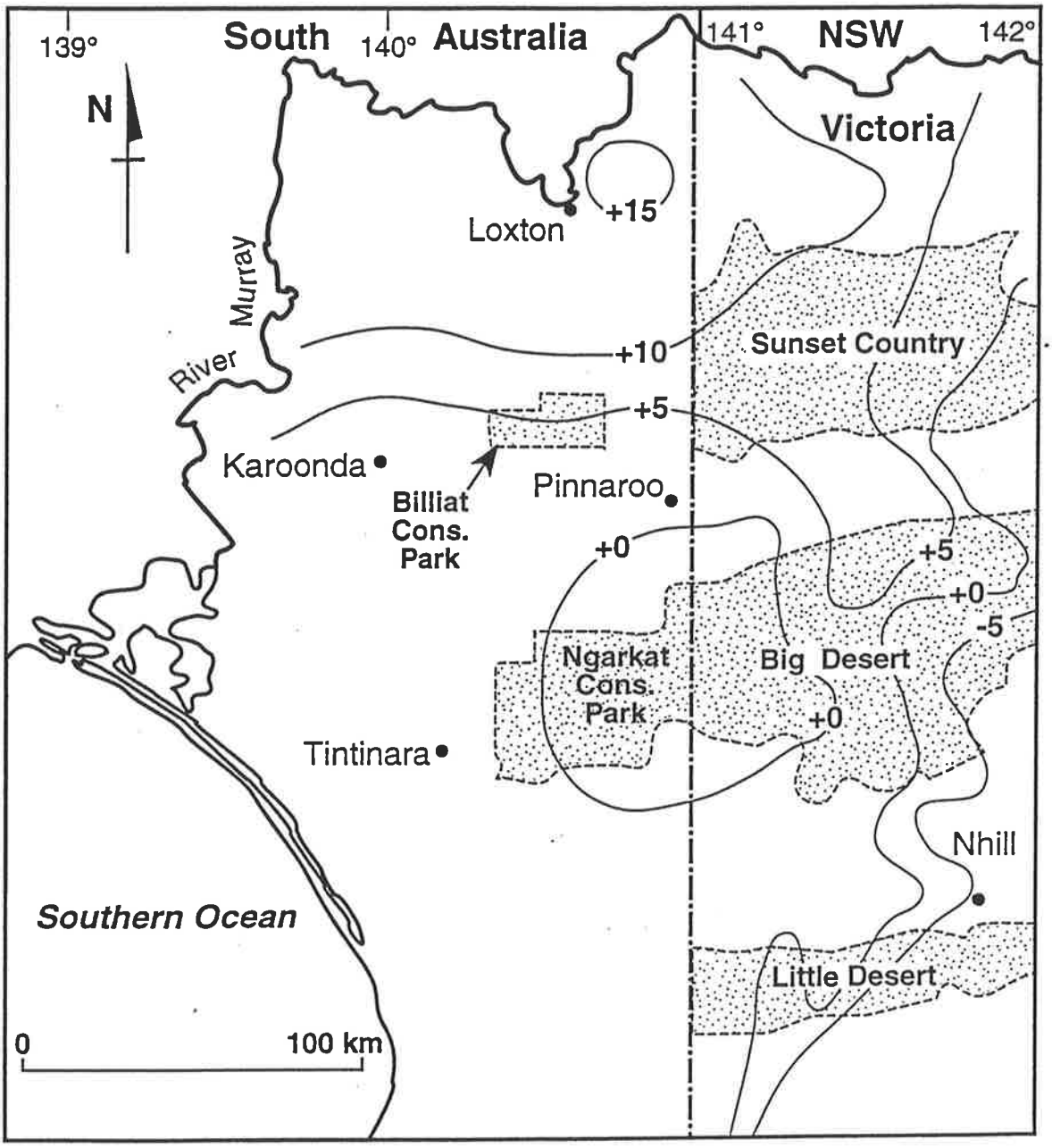

Fig. 1.5 Hydraulic head difference between the Renmark and Murray Group aquifers. Positive signs indicate potential for upward leakage from the Renmark Group Aquifer.

Murray Basin (Macumber, 1990). The drainage flux under this new agricultural land use has been estimated by Allison et al. (1990) to be between 1 mm a^{-1} and 50 mm a^{-1} and they give a mean for all sites studied of approximately 17 mm a^{-1}. This constitutes an increase in recharge of more than two orders of magnitude from that under native vegetation. However, the time delay in transmitting this increase in recharge to the water table is estimated to be between 50 and 500 years (Allison et al., 1990) and depends on the depth to the water table.

Groundwater recharge estimates in various parts of this study area were first carried out nearly twenty years ago using the chloride mass balance method (Allison and Hughes, 1978). The range of Cl^- concentration in the unsaturated zone profile in the study area varies depending on the location, vegetation cover and soil texture (Allison et al., 1990, Kennett-Smith et al., 1994; Leaney et al., 1995). In the northern and central part of the area at Wanbi, Kulkami, Borrika and Maggea (Fig 1.6) the Cl^- concentrations in soil water range from 7,500 mg/l to 16,000 mg/l (Hughes et al., 1988 a, b, c; Cook et al., 1992). In these unsaturated profiles the Cl^- concentrations increased with depth and reached peak values of between 12,000 and 16,000 mg/l at 2 to 6 m depth. Below the chloride maximum there is a gradual decrease in Cl^- concentration with depth due to diffusion of chloride to the groundwater (Cook et al., 1992). The only information on the Cl^- concentration of the unsaturated profile in the southern part of the study area is given by Leaney et al. (1994, 1995). Their study suggests that, whereas the form of the Cl^- distribution in the profile was similar to that obtained from the northern part of the study area, the Cl^- concentration was much lower and ranged from 500 to 2,000 mg/l.

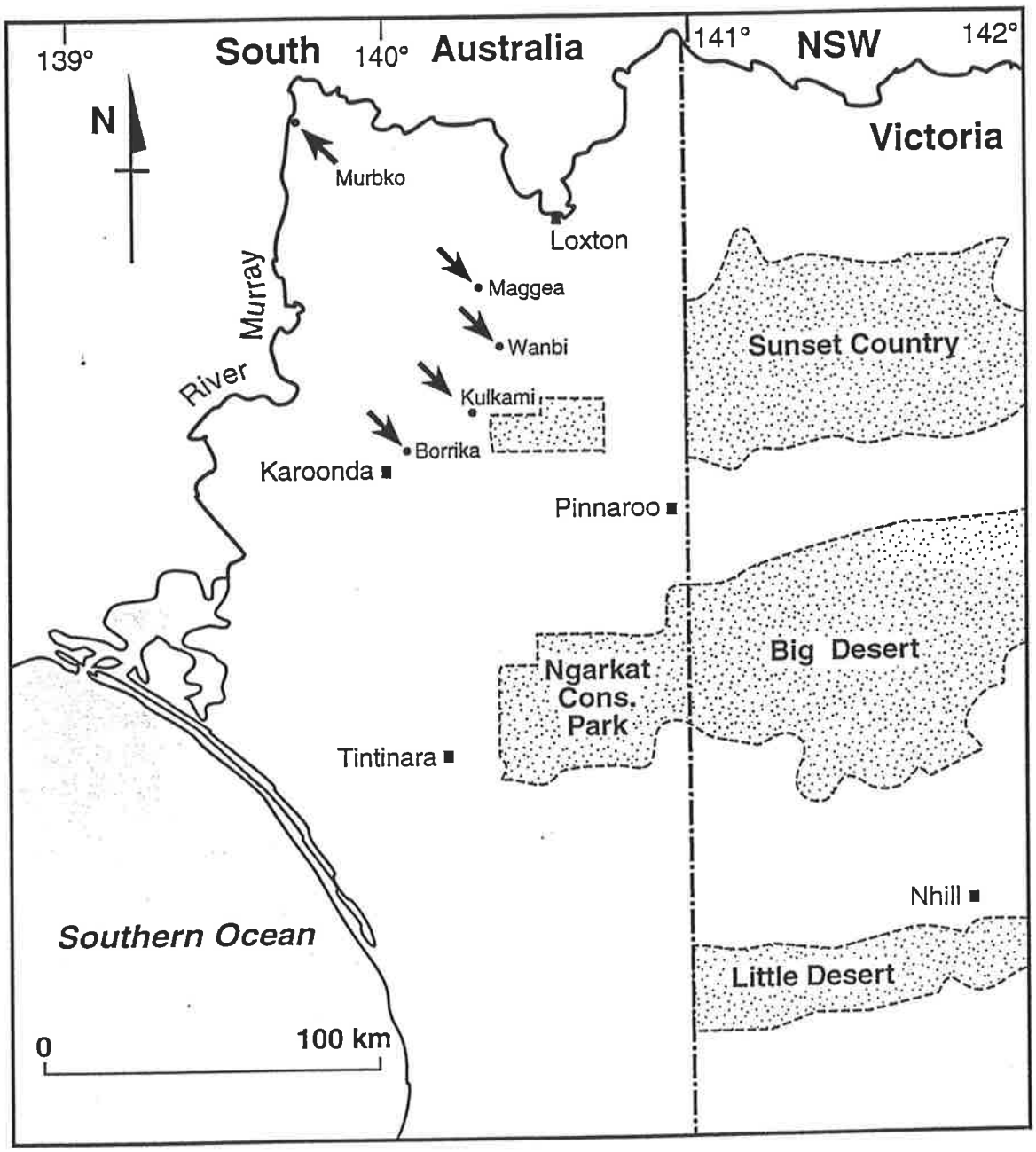

Fig. 1.6 Locations of the core holes for recharge estimates in the previous investigations.

CHAPTER 2

Sampling and analytical methods

2.1 Groundwater sampling

The sampling methodology of regional scale aquifers is a vital part of any hydrochemical and isotopic investigation and is probably the major source of error in the processes of obtaining representative samples of groundwater. The extent to which small sample in a certain depth of an aquifer may be considered to be reliably representative of a large volume of groundwater at that point depends on several factors. These include homogeneity of the groundwater, number of groundwater samples, the method of sample collection, and the size of the individual samples. The groundwater sampled from a certain depth interval may not represent exactly the composition of all the water in that specific vertical section due to the variation of horizontal and vertical hydraulic conductivity of the aquifer. However, it is usually assumed that the groundwater represents the average composition of available water at that interval.

Furthermore, a general relationship has been recognised between the concentration and chemical composition of groundwater and the types of groundwater flow systems

(local, intermediate, regional). For example, regional groundwater flow systems are generally characterized by relatively higher dissolved salt concentrations (Back, 1961). This occurs due to a relatively longer residence time of groundwater along the flow paths in regional aquifers. This causes a higher rate of mineral dissolution, thus increase in concentration of dissolved salt in groundwater (Back, 1960).

Accordingly the depth of groundwater sampled below the water table from the unconfined Murray Group Aquifer is critical in understanding whether the variation of the chemical composition along the hydraulic gradient is due to the chemical evolution of groundwater, or just an artifact of sampling methodology. Therefore, in addition to the selected bores and wells along the hydraulic gradient (AA` transect) of the Murray Group Aquifer, three boreholes were drilled and sampled from discrete intervals below the water table to test the effect of flow systems and sampling depth on chemical and isotopic composition of groundwater (Fig. 2.1). The depths of these bores were 40, 50 and 60m below the water table respectively.

The groundwater samples were collected over a 2 year period between 1995-1996 on 4 field trips. A total of 91 groundwater samples from the Murray Group Aquifer were collected from a number of observation boreholes, private wells and town water supply wells. The bores, and wells penetrating the Murray Group Aquifer were selected on the longest flow path of the Murray Group Aquifer (AA`, Fig. 1.1) and were divided into three groups; (1) observation boreholes that are open 2 m to 100 m, to the aquifer thickness (2) private irrigation and town water supply wells that are open to more than

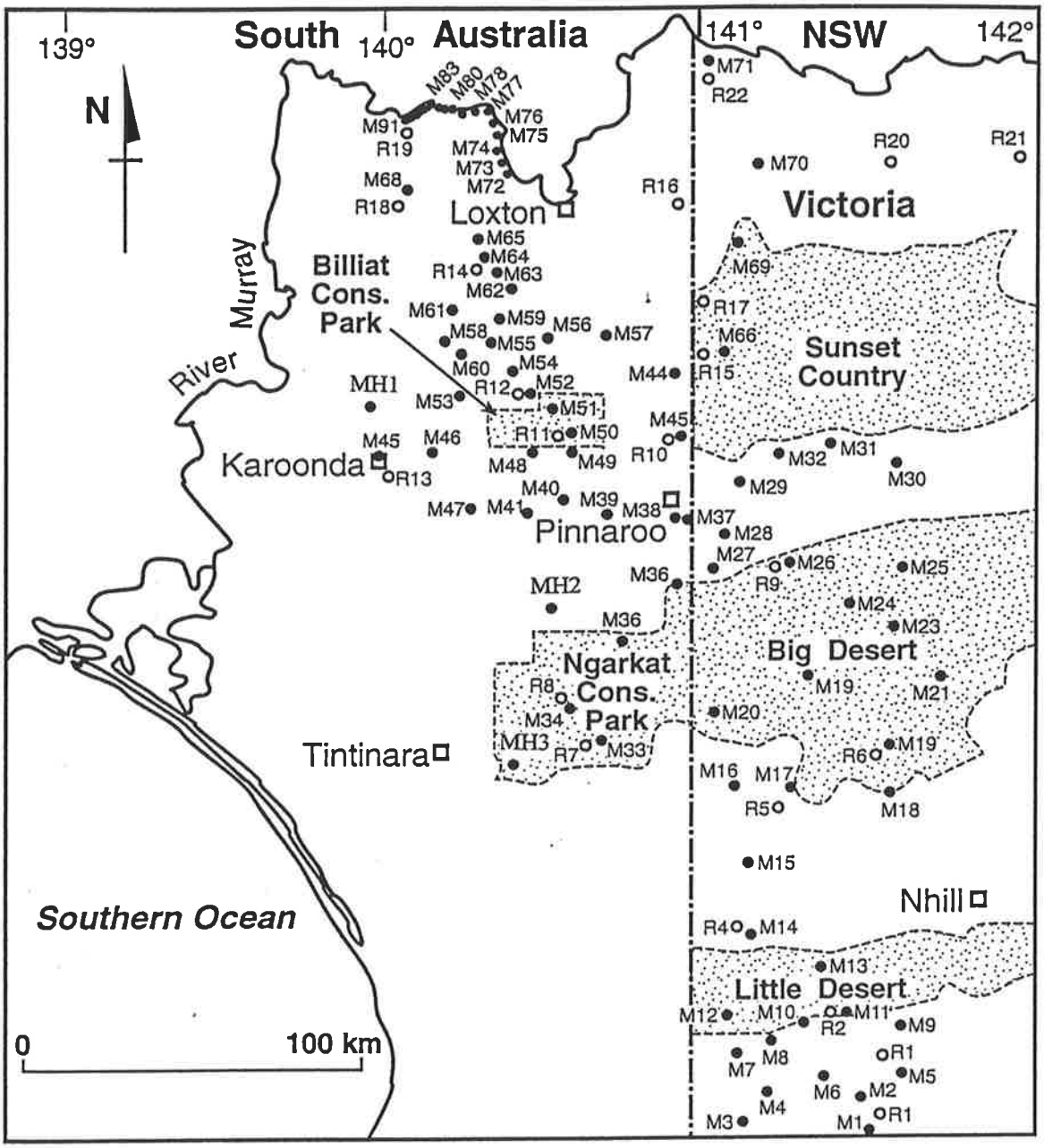

Fig 2.1 Groundwater sample location map. `M` denotes the wells sampled from the Murray Group Aquifer while `R` denotes the wells sampled from the Renmark Group Aquifer. Locations of the 3 drilled bores (MH1, MH2, MH3) are also shown.

a half of the total aquifer thickness and (3) domestic wells that penetrate the top 5 m to 20 m of the Murray Group Aquifer.

Groundwater from the Renmark Group Aquifer was sampled from observation boreholes, which had relatively short screens ranging from 2 to 20 m. The locations of groundwater sampling sites are shown in Fig 2.1.

Groundwater samples from the observation boreholes were collected using a (MP1, GRUNDFOS) submersible pump. The privately-owned wells were sampled from existing installed pumps. Groundwaters from discrete intervals of the three open boreholes were sampled using a (MP1, GRUNDFOS) submersible pump equipped with an inflatable rubber packer. Three groundwater samples from the Renmark Group Aquifer were artesian. At least three times the casing volume of each well was pumped prior to sample collection. The groundwater samples were collected after the pH, Eh and temperature had stabilized. Electrical conductivity, temperature, Eh, and pH were measured immediately in the field by an enclosed, flowing, in-line sampling cell (Yellow Spring Inc. 3560, Water Quality Monitoring System). The Eh was measured using a Pt electrode (YSI 3540 ORP) with Ag/AgCl reference calibrated with Zobell solution. The pH was measured using a glass/AgCl combination pH electrode (YSI 3530) calibrated with standard pH 4 and 7 buffer solution to an accuracy of ± 0.05 pH units.

Water samples for major ions were filtered through a 0.45 μm cellulose acetate membrane filter (Millipore), and collected in acid-washed polyethylene bottles.

Samples for stable isotopes ($\delta^{18}O$ and $\delta^{2}H$) of water molecules were collected in unfiltered 25 ml glass bottles and filled directly from the sampling outlet.

Groundwater samples for $\delta^{34}S$, and $\delta^{18}OSO_4^{2-}$ of dissolved sulphate and $^{87}Sr/^{86}Sr$ ratio were filtered through a 0.45 μm cellulose acetate membrane filter in the field in order to remove suspended particles. The filtered samples for the $\delta^{34}S$ and $\delta^{18}OSO_4^{2-}$ were then acidified to pH ~ 4 with dilute HCl and stored in two litre plastic bottles. One hundred millilitres of filtered groundwater-samples were acidified with high-purity HNO_3, and stored in sealed polyethylene bottles for Sr^{2+} isotope analysis.

Groundwater for ^{14}C analysis was collected in a 25 litre plastic container. Barium carbonate ($BaCO_3$) and barium sulphate ($BaSO_4$) were precipitated by the addition of 100 ml of 10M sodium hydroxide (NaOH), 750 ml of saturated barium chloride ($BaCl_2$), and 40 mg Magnafloc 156 (IAEA. 1975). The pH was maintained between 9 and 10 during precipitation by the addition of aliquots of (NaOH).

2.2 Analytical Methods

2.2.1 Major ions

Chemical analyses of all the major ions were performed by CSIRO (Commonwealth Scientific and Industrial Research Organisation) Land and Water chemistry laboratory

in Perth, Western Australia. The samples were sealed in polyethylene bottles and shipped over-night.

Total alkalinity was determined by the potentiometric titration method to a fixed end point using 0.1N H_2SO_4. Carbonate species concentrations ($CO_{2(aq)}$, HCO_3^-,CO_3^{2-}) were calculated using the computer code PHREEQM (Nienhuis et al., 1993, based on PHREEQE, Parkhurst et al., 1980) from alkalinity, pH and major ion concentrations.

Sulphate concentration was determined on an auto-analyser by reduction of sulphate to hydrogen sulphide, distillation of the latter and its subsequent colourimetric determination (Keay et al., 1972).

Chloride concentration was determined by the automated ferricyanide method. This method relies on the liberation of the thiocyanate $(SCN)_2$ ion from mercuric thiocyanate $Hg_2(SCN)_2$ by the formation of soluble chloride. In the presence of ferric ions the liberated thiocyanate forms a highly coloured ferric thiocyanate $Fe(SCN)_2.3H_2O$ proportional to the original chloride concentration (O'Brien, 1962).

Bromide concentration was determined by the High-Performance Liquid Chromatography (HPLC) technique. The HPLC procedure for bromide determination uses UV detection at a wavelength of 200 nm and a buffered (NaCl) eluent. Bromide has significant UV absorption, so by monitoring at a low UV wavelength and using a

UV absorbing eluent such as chloride, a sensitive and selective detection can be achieved (Millipore Corporation 1989).

The concentration of Ca^{2+}, Mg^{2+}, Na^{+}, K^{+} and Sr^{2+} were determined by Atomic Absorption spectroscopy (AAS). This method is based on directing a light beam through the vaporised sample into a monochromator, and on to a detector that measures the amount of light absorbed by the atomised element in the flame. The amount of light absorbed is proportional to the concentration of each respective measured element in the water sample.

2.2.2 $\delta\ ^{2}H$ and $\delta\ ^{18}O$ of water molecules

The removal of isotopically representative water from brackish and saline groundwater samples was carried out using the azeotropic distillation method (Horita and Gat, 1988). An azeotrope is a mixture of two or more liquids where the boiling point may be higher or lower than the original individual components. For the case of the kerosene-water azeotrope, the boiling point of the mixture is 96°C (Walker et al., 1994) which is lower than the boiling point of water (100 °C) and kerosene (185 °C) separately (Walker et al., 1994).

During distillation, the azeotrope boiling point is maintained at 96°C until the water is depleted. The temperature is then raised to the boiling point of kerosene 185°C. The heated mixture is cooled in a straight condenser and both condensed phases, water and

kerosene are collected in a funnel situated under the condenser (Revesz and Woods, 1990). The apparatus allows the kerosene overflow to drip back into the flask without clogging the funnel and to participate again in the distillation. At the beginning of distillation, water and kerosene evolve together, causing a cloudy appearance and the distillation continues until the cloudy part of the distillation apparatus turns from cloudy to clear. A complete distillation lasts from 150 to 180 minutes. The water is collected in an air tight glass bottle and any trace of kerosene is removed by adding wax and warming the wax to melting point (60°C to 70°C), thereby dissolving the kerosene in the wax.

Deuterium concentration was determined on hydrogen gas introduced by the reduction of the distilled water over uranium (Bigeleisen et al ., 1959; Dighton et al., 1997). The preparation line consists of a quartz tube filled with approximately 15 gm of crushed, depleted uranium turnings. The tube is inserted into a temperature controlled furnace and connected to the sample inlet tap by two Cajon "ultra-torr" brass unions. The sample inlet tap consists of a 2 mm bore Springham high vacuum glass valve, with a 2 mm diameter hole through one side to inject the water sample into the preparation line. The line is connected to the diaphragm-type vacuum to provide circulation of the gas until complete reduction has occurred.

For $\delta^{18}O$ measurements, 5 ml of distilled water samples was equilibrated with CO_2 for 24 hours at 25 °C (Epstein and Mayeda, 1953). The $\delta^{2}H$ and $\delta^{18}O$ were analysed using standard techniques on a VG 602 D or Europa Scientific Tracermass stable

isotopes gas ratio mass spectrometer. The mass spectrometer separates charged atoms and molecules on the basis of their masses in magnetic fields. After passing through the magnetic field, the separated ions are collected in the ion detector and converted into an electrical pulse, which is then fed into an amplifier. The ion beams of the respective isotopes (e.g. $^{13}C^{16}O_2$, $^{12}C^{18}O^{16}O$, $^{12}C^{16}O_2$) are collected and measured simultaneously (Nier et al., 1947; Mckinny et al., 1950).

Deuterium and $\delta^{18}O$ are expressed in per mil notation (parts per thousand) relative to standard V-SMOW(Vienna Standard Mean Ocean Water) according to the following equation:

$$\delta(\text{SMOW}, ‰) = \left(\frac{R_{sample} - R_{SMOW}}{R_{SMOW}}\right) X1000 \qquad (2.1)$$

where R is the $^{18}O/^{16}O$ or $^{2}H/^{1}H$ ratio of the sample and R_{SMOW} is the $^{18}O/^{16}O$ or $^{2}H/^{1}H$ ratio of the standard. Precision for the analysis are ± 0.15‰ for $^{18}O/^{16}O$ and ± 1‰ for $^{2}H/^{1}H$.

2.2.3 $\delta\ ^{34}S$ of dissolved SO_4^{2-}

The 2 litre acidified water samples were heated to boiling point to ensure removal of CO_2 and thus minimize co-precipitation of $BaCO_3$. Fifty millilitres of 10% $BaCl_2$ solution was added to the boiled samples to precipitate $BaSO_4$. The $BaSO_4$ was washed with warm, deionised, distilled water. The washed $BaSO_4$ was dried overnight

in an oven at 70°C. After 24 hours, the $BaSO_4$ was scraped from the dried beaker and stored for analysis.

The $BaSO_4$ samples for sulphur analysis were converted to SO_2 gas by the method described by Coleman and Moore (1978). About 40 mg of $BaSO_4$ was mixed thoroughly in an agate mortar with 250 mg of Cu_2O and 700 mg of SiO_2. The mixture was placed in a vertical 9 mm O.D. silica glass tube and silica glass wool was placed on the top and bottom of the tube. The tube was connected to the preparation line and evacuated. The tube was heated to 1200°C until no appreciable outgassing was observed by a Pirani vacuum gauge. At this temperature, $BaSO_4$ thermally decomposes to SO_3 and SO_2, with the former converted to SO_2 and collected. The sulphur isotope composition of SO_2 was determined with a VG 602 D mass spectrometer. The results were expressed on the international CDT scale, with a reproducibility of ±0.2‰.

2.2.4 $\delta\ ^{18}O$ of dissolved SO_4^{2-}

For $\delta^{18}O$ analysis of dissolved sulphate, sub-samples from $BaSO_4$ were separated and sent to the Environmental Isotope Laboratory, University of Waterloo, Canada. Oxygen-18 was determined using the method described by Shakur (1982). About 10 mg of $BaSO_4$ was mixed thoroughly with ~10 mg pure (99.99%) graphite in an agate mortar until the mixture was homogeneous. The mixture was placed in platinum foil, folded and clamped between two electrodes in a reaction chamber. The chamber was

evacuated and the sample was preheated to 400°C to release water and other impurities. The temperature was then raised to ~ 1000°C. At this temperature, $BaSO_4$ thermally decomposes and oxygen reacts with graphite to form CO and CO_2. The CO_2 produced was trapped in liquid N_2 and the CO was excited by a high voltage electric discharge between two platinum electrodes converting it to CO_2, and then collected in a cold finger by liquid N_2. When the reaction was completed, the produced CO_2 was purified and separated from any remnant H_2O by cold traps using a combination of liquid N_2 and a mixture of dry ice-alcohol. The purified CO_2 was collected in glass ampoules. The $\delta^{18}O$ isotopic composition of CO_2 was measured by the mass spectrometer using standard techniques, and the results were expressed in per mil notation (parts per thousand) relative to standard V-SMOW, with a reproducibility of ±0.5‰.

2.2.5 $^{86}Sr/^{87}Sr$ ratio

Rock samples were taken for $^{87}Sr/^{86}Sr$ isotope analysis from cuttings from five drill holes that penetrate the Murray and Renmark Group aquifers. In addition to the whole rock $^{87}Sr/^{86}Sr$ analysis, the rock samples were crushed and leached with 0.05 M acetic acid (CH_3COOH) in order to determine the $^{87}Sr/^{86}Sr$ ratio of the carbonate component of the rock samples. The rock samples were totally digested in sealed Teflon vessels using distilled HF and HNO_3 and quartz distilled HCl. The water

samples were evaporated in the Teflon vessels and dissolved in distilled HCl and centrifuged in order to separate any undissolved precipitate.

Strontium ions in the water and rock samples were separated from other ions using a standard cation exchange column procedure. The purified Sr^{2+} was converted to nitrate form, and taken up in 30 µl of 0.15 M H_3PO_4, and loaded on to a single tantalum (Ta) filament for mass spectrometer measurements.

The isotopic composition of Sr^{2+} was measured on a Finnigan MAT 261 multi-collector mass spectrometer, using a double collection static mode. Data blocks of ten scans were run until acceptable within-run statistics were achieved (8-15 blocks). All reported values of $^{88}Sr/^{86}Sr$ have been corrected for natural and analytical stable isotope fractionation to $^{88}Sr/^{86}Sr = 8.3752$. The $^{87}Sr/^{86}Sr$ ratio measurement errors are 2σ mean and apply to the last decimal place. The average and reproducibility of measured values during data acquisition of the international standard material NBS987, were 0.710245±0.000022 (2 s.d.), N=20.

2.2.6 Radiocarbon and $\delta\ ^{13}C$

The mixed precipitate of $BaCO_3$ and $BaSO_4$ from 20 litre water samples was placed in a glass flask, and the $BaCO_3$ was converted to CO_2 by the addition of 5% HCl. The evolved CO_2 was purified and separated from other impurities (e.g. H_2O, N_2, O_2) by a combination of cold traps (liquid N_2 and a mixture of dry ice-alcohol). The evolved

CO_2 was collected and frozen on the cold finger with liquid N_2 (Qureshi et al., 1989). The flask containing CO_2 was then attached to a circulation line which was pre-evacuated and the CO_2 expanded into a bladder. The circulation line was isolated, and the volume of CO_2 produced was estimated by measuring the volume of displaced water from the outer vessel enclosing the bladder (Leaney et al., 1994). The circulation pump was started and the CO_2 was bubbled through a mixture of Carbosorb® (Packard Instr. Co.) and Permaflour® (Packard Instr. Co.) for 20 minutes. The C/P solution was removed and weighed into a vial. The radiocarbon activity of the samples was determined on a LKB Wallac 1220 Quantulus Liquid Scintillation Counter.

Subsamples of evolved CO_2 during radiocarbon analysis were taken for $\delta^{13}C$ analysis. The collected CO_2 was further purified by the cold finger using liquid N_2 on a specially designed line to ensure complete removal of H_2O. The $^{13}C/^{12}C$ composition was determined on a VG 602 D mass spectrometer.

Carbon-13 values for limestone were determined on the CO_2 released from carbonates acidified in a sealed tube with 100% H_3PO_4. The sample was equilibrated at 25 °C for 24 hours. Analysis of the $^{13}C/^{12}C$ ratio was determined on a Europa Scientific Tracermass stable isotope gas ratio mass spectrometer. The precision of the analysis is quoted as ± 0.2 ‰. The $^{13}C/^{12}C$ ratio is expressed in per mil notation relative to standard PDB (*Bellemnitella americana* from the Cretaceous Pee Dee Formation, South Carolina).

2.3 Mineralogy and chemical composition of rocks

Detailed petrographic study of the aquifer matrix were carried out on the thin sections prepared from the rock samples taken from the aquifer matrix. Mineralogical composition of the rock specimens was also determined by XRD analysis.

The whole rock samples were carefully ground by hand in a small mortar, and smear mounted with organic solvent (acetone) on to a glass slide. The sample was then inserted into the X-ray diffractometer for XRD analysis. Analysis was performed using a Philips PW-1050 diffractometer, utilising Co Kα radiation of wavelength 1.7902 nm (normal focus) with an operating voltage at 50 kV and current 30mA. Samples were usually analysed in the 2-theta angle range of 3 to 75° in steps of 0.02°.

The X-rays produced in the diffractometer are first collimated to produce a sub-parallel beam with the angle of divergence depending on the size of the divergent slit. The divergent beam is then directed at the sample and rotated at a regular speed. The X-rays will be defracted according to Bragg's Law as follows:

$$n\lambda = 2d \sin\theta \qquad (2.2)$$

where n is an interger, λ is the wavelength of the X-rays, d is the lattice spacing in angstroms and θ is the angle of diffraction. The beam passes from the receiving crystal in the rock samples to the detector. The signal produced by the X-ray photons on the

detector is amplified and passed on to the electronic recording equipment. Minerals were identified from the diffractrometer digital out put using computer code XPLOT (Raven, 1992) as well as the JCPDS (Joint Committee on Powder Diffraction Standard) data books.

The major element analysis of the rock samples from the Murray and Renmark Group aquifers were determined by X-ray fluorescence (XRF). The rock samples were crushed by Roller crushers employing rotating eccentric ribbed hard steel rollers in a cone grinder. The powdered rock was then made into pressed pellets by mixing with a binder and pressed to 20,000 psi (1400 kg/cm^2- Norrish and Chappell, 1977) and analysed by a Philips PW 1480 X-ray Fluorescence Spectrometer, using an analysis program calibrated against several international and local Standard Reference Materials (SRMís). A dual-anode (Sc-Mo) X-ray tube was used, operating at 40 kV, 75 mA. The principal behind this technique is that when a sample is bombarded with high energy X-rays, secondary radiation is emitted, with the wavelengths and intensities dependent on the elements present. Measurements of the intensity of the characteristic radiation for a particular element give a value reflecting its concentration in the sample.

CHAPTER 3

Hydrochemistry and stable isotopes

3.1 Introduction

The concentrations and types of dissolved ions in groundwater play a major role in the suitability of the water for intended use. Understanding the processes that might produce the present day major ion distribution in the groundwater from the Murray and Renmark Group aquifers is essential for present and future management of this important water resource. A knowledge of whether the chemical composition of the groundwater is caused by natural processes or induced by human activities is a prerequisite in many groundwater management issues such as potential exploitation, sustainable yield and groundwater contamination.

The main objectives of this chapter are to provide an insight into possible mechanisms that control the chemical composition of groundwater in the Murray and Renmark Group aquifers, and to describe physical and geochemical processes that cause the increase of the total dissolved solid (TDS) observed along the hydraulic gradient in the Murray Group Aquifer. The information provided in this chapter also serves to

underpin the discussion of more exotic groundwater tracers in the following three chapters.

The integrated use of natural tracers such as dissolved ions, various isotopes, and physical parameters (e.g. temperature and depth to the water table) has proved to be an effective approach to hydrological and geochemical investigations. Each of the natural tracers provide specific information and when combined, can be used to elucidate processes such as the origin of groundwater, the mixing between different groundwater bodies, quality of water, location of recharge, groundwater residence time, and the sources of dissolved ions in groundwater (Mazor, 1976 b; Wallick and Toth, 1976; Elliot, 1990; Le Gal La Salle, 1995). For example, Mazor et al. (1985), have identified the sources of groundwater in the spa of Schinznach in Switzerland by using a combination of dissolved ions, stable isotopes and temperature of groundwater. Love et al. (1993) have used dissolved ions, stable isotopes, and radiocarbon data in combination with groundwater hydraulic data to determine the origin of groundwater and the flow regime in the Otway Basin in Australia.

Investigations into the processes that can affect the chemical composition of groundwater on a regional a scale have been well documented (see below). An early model describing the mechanisms that control the evolution of chemical composition of groundwater was presented by Chebotarev (1955). According to his model, the general sequence of major ion evolution in groundwater was from freshwater, dominated by

bicarbonate ions, towards a sea water-like composition with the following major anion sequence as a function of the increasing residence time of groundwater.

$HCO_3^- \rightarrow HCO_3^- + SO_4^{2-} \rightarrow SO_4^{2-} + HCO_3^- \rightarrow SO_4^{2-} + Cl^- \rightarrow Cl^-$

Back (1960, 1966), and Back and Hanshaw (1965), expanded this model and suggested that the concentration and type of chemical composition that develop in groundwater are controlled largely by flow pattern, and by mineralogy of the aquifer matrix. In general, groundwater flow systems and the associated chemical composition is divided into three types; (i) local systems that are characterised by shallow depth and high intensity of circulation. The effect of these conditions on chemistry is reflected by thorough flushing, resulting in low TDS, and Ca^{2+}-HCO_3^- type water, (ii) intermediate systems which are characterised by relatively intermediate flow and residence time, and with higher TDS compared to water in local systems. Water in this zone is of sulphate type with relatively low concentrations of Na^+ and Cl^- ions, (iii) regional systems which are characterised by relatively greater depth, longer flow paths and longer residence time resulting in high TDS, and Na^+-Cl^- dominance (Back, 1961; Domenico, 1972; Wallick and Toth, 1976).

The studies carried out by Chebotarev (1955), and Back (1960, 1961, 1966) have demonstrated that the chemical composition of groundwater is also dependent on the type of minerals forming the aquifer matrix. However, this relationship is not simple, due to the various factors that can affect the chemical composition of groundwater, for example, (i) solubility of the elements forming aquifer minerals, (ii) temperature of

groundwater, (iii) the contact area between water and rock, (iv) the amount and distribution of soluble ions in minerals and (v) length of contact time.

In sedimentary aquifers the concentration of TDS of groundwater can vary from $< 10^2$ mg/l to $>10^5$ mg/l depending on the type of the sedimentary host rock. Four main geochemically related groups of sedimentary rocks can be identified (Domenico, 1972); (1) resistates that are mainly of sandstone and coarse clastic materials, (2) hydrolysates that are formed from insoluble material as a result of chemical weathering of parent rocks such as shale, (3) precipitates that are formed mainly by chemical or biological precipitation such as limestone and, (4) evaporites that are formed by deposition from highly concentrated brines (e.g. gypsum and halite).

Although earlier researchers recognised variations in groundwater composition, which formed the basis for interpretation of evolutionary reaction processes on regional scales, they were unable to quantitatively assess and predict the amount of major ion contribution derived from the aquifer matrix. Garrels and Mackenzie (1967), Helgeson (1968), and Helgeson et al., (1969) presented quantitative models for mineral dissolution and precipitation to account for the change in chemical composition of the associated water. Parkhurst et al. (1980) and Plummer et al. (1980, 1983, 1991) expanded these models, and developed more comprehensive models based on mass balance calculations to quantitatively predict the geochemical evolution of groundwater.

However, the evolution of groundwater chemistry, particularly in arid and semi-arid regions, can be affected by processes other than water-rock interaction. The general conclusions from regional groundwater studies on the Australian continent suggest that rock-water interaction alone cannot explain the chemical composition of groundwater (Evans, 1982; Martin and Harris, 1982; Black, 1989; Herczeg et al., 1991, Mazor and George 1992). Evans (1982) showed that the chemical composition of groundwater in the regional fractured-rock aquifer of the Australian Capital Territory cannot be explained by the type of rocks in the aquifer matrix. Investigation into the evolution of groundwater chemistry in the Great Artesian Basin (Herczeg et al., 1991) and Otway Basin (Love et al., 1993) showed that evapotranspiration prior to recharge has a significant effect on groundwater chemistry.

This study uses dissolved ion concentrations and variations in the stable isotope composition of groundwater to identify the physical processes and water-rock interactions that may be responsible for the observed increase in major ion concentrations in the Murray and Renmark Group aquifers. The stable isotope composition (δ^2H and $\delta^{18}O$) is a conservative property of the water mass during subsurface flow. Therefore, it is possible to relate the isotopic composition of the groundwater to that of the weighted mean isotopic composition of rainfall recharging the aquifer. Because the average δ^2H and $\delta^{18}O$ composition of rainfall is a function of elevation, latitude, distance from the coast and temperature, it is often possible to determine the geographic origin of recharge to groundwater (Gat, 1971; Darling and Bath, 1988). On the other hand, physical processes such as evaporation prior to

recharge or mixing with waters with different δ^2H and $\delta^{18}O$ signatures can change the original δ^2H and $\delta^{18}O$ composition of groundwater. The effect of these processes on the δ^2H and $\delta^{18}O$ composition can be identified by comparing the isotopic composition of the groundwater with initial recharge water (Mazor et al., 1985; Herczeg et al., 1992; Love et al., 1993; Chambers et al., 1995).

Dissolved Cl^- is a conservative ion in groundwater because it does not take part in chemical reactions in fresh and saline waters at ambient temperature (Feth, 1981). Moreover, the Cl^- concentration can also be conserved if groundwater is undersaturated with respect to halite (NaCl), and Cl^- bearing minerals such as halite or sylvite do not exist in the aquifer matrix. Under these circumstances, Cl^- concentration can be used as a physical tracer to delineate mixing between groundwaters with different Cl^- concentrations as well as changes in evapotranspiration amounts prior to recharge.

The relative importance of chemical reactions taking place in the groundwater of the Murray and Renmark Group aquifers can also be demonstrated by observing the variation of major ion concentration along the hydraulic gradient with respect to conservative ions such as Cl^-. On the basis of major ion variations, mass-balance calculation can be made and geochemical or conceptual models can be developed to illustrate geologic, climatic and physiographic effects on groundwater chemistry.

3.2 Results

3.2.1 Aquifer mineralogy and mineral chemistry

Fifty four rock samples were collected from five drill holes (M33, M34, M50, M52, M64) penetrating both aquifer systems through to the bedrock (Fig 3.1). The bores are located in the middle and upper part of the study area representing aquifer mineralogy along 120km of AA` transect. The samples were analysed by X-ray diffraction, and X-ray fluorescence for their mineralogical and chemical composition. The results of XRD analysis for the Murray and Renmark Group aquifer matrix are given in appendix 1, and the results of the major element composition are given in Table (3.1).

Calcium and silica are the major elements of the Murray and Renmark Group aquifers matrix respectively (Table 3.1). The CO_2 and H_2O liberated from carbonate and other minerals during ignition accounts for ~ 33% by weight of the Murray Group Aquifer and 9% by weight of the Renmark Group Aquifer matrix. The percent MgO concentration of the Murray and Renmark Group aquifers matrix is ~ 4 and ~ 0.7 respectively. Whereas Na_2O, K_2O, Al_2O_3 from silicates (clay minerals and feldspars), SO_3 from sulphur compounds and Fe_2O_3 comprise < 5% by weight of the Murray Group Aquifer matrix, they comprise ~ 10% by weight of the Renmark Group Aquifer matrix. The relatively higher Ca concentration is due to the dominance of carbonate minerals in the Murray Group Aquifer matrix, whereas, the relatively high Si concentration is due to the dominance of quartz and chert in the Renmark Group Aquifer matrix.

Table 3.1
Average chemical composition of the aquifer matrix in % weight of the Murray and Renmark Group aquifers from core cuttings collected from four boreholes.

Oxides	Average the Murray Group Aquifer matrix (n = 35)		Average the Renmark Group Aquifer matrix (n = 18)	
	%	SD	%	SD
SiO_2	16.84	15.00	68.85	17.94
Al_2O_3	1.73	2.08	3.39	2.58
Fe_2O_3	1.63	1.43	3.83	3.47
MgO	4.62	1.50	0.71	0.44
CaO	39.74	9.69	9.58	6.57
Na_2O	0.39	0.11	0.40	0.38
K_2O	0.31	0.28	0.57	0.37
SO_3	0.53	0.90	2.23	1.69
Organic C	0.70	1.10	2.95	1.90
Loss on ignition 960 C°	33.54	7.45	9.25	14.28

The Murray Group Aquifer is composed primarily of calcite and quartz, with minor dolomite, organic carbon, and trace amounts of glauconite, clay minerals, and iron oxides. Quartz is the major mineral in the Renmark Group Aquifer with minor calcite, lignite and trace amounts of feldspars and clay minerals.

Whereas the carbonate minerals calcite, Mg-calcite and dolomite are the most abundant minerals ranging from 35% to 93 % by weight in the Murray Group Aquifer, their concentration ranges from 2% to 30% by weight in the Renmark Group Aquifer matrix. Mg-calcite accounts for 5% to 10 % by weight of total calcite in the Murray Group Aquifer. The weight percent of dolomite in the Murray Group Aquifer varies laterally and vertically within the formation, and ranges from < 1% to 3% by weight. Quartz and

chert are the major minerals and contribute 60% to 93% by weight of the Renmark Group Aquifer.

The minor components of the Renmark Group Aquifer, and to a lesser extent the Murray Group Aquifer, are organic substances (organic carbon and lignite) with organic carbon being between 1% and 3%. Small amounts of feldspars and glauconite were present in the Murray Group Aquifer. Kaolinite and smectite were recognised by their corresponding XRD peaks in the Murray and Renmark Group aquifers. Trace amounts of sulphide minerals (primarily pyrite) are present in the Renmark Group Aquifer.

The Renmark Group Aquifer matrix is composed of clastic sediments, mainly quartz sand and poorly consolidated silt (Brown, 1989). These minerals are the product of mechanical and chemical weathering of parent rocks. The deficiency of alkali earth elements (Mg^{2+}, K^{+}, Na^{+}) which accounts only for 2% by weight of the aquifer matrix indicates that these deposits have also been affected by extensive weathering. Hydrolysis of major silicate minerals results in liberation of the cations which ultimately causes deficiency of cations within the residual deposit.

3.2.2 Major ion concentrations of groundwater

Results of chemical and isotopic analysis of groundwaters from the Murray and Renmark Group aquifers are presented in Table 3.2 and 3.3 respectively. The TDS concentration of groundwater from the Murray Group Aquifer is variable, ranging from

550 mg/l at the basin margin in the south and south-east, to 22,700 mg/l in the north and north-east in the wells adjacent to the River Murray. Groundwater in the Renmark Group Aquifer has a similar TDS to that in the Murray Group Aquifer, and generally increases to values of 22,300 mg/l near the River Murray.

Based on major ion concentrations, two hydrochemical zones are delineated in the Murray and Renmark Group aquifers:

Zone A. Fresh to brackish groundwater in the Murray and Renmark Group aquifers, TDS ranges from < 1000 to 5000 mg/l. This zone covers approximately 80% of the study area extending from the basin margin in the south, to 250 km towards the north and north-west (Fig. 3.1).

Zone B. Saline groundwater that has a TDS ranging from 5,000 mg/l to ~ 21,000 mg/l in both aquifers. The groundwater of this zone occurs in the north and northwestern part of the study area, 60 km south of the River Murray (Fig. 3.1).

Chloride concentrations in the Murray and Renmark Group aquifers range from 3.3 mmol/l to 336 mmol/l. There is a general increase in Cl^- concentration in the Murray Group Aquifer towards the north and north-west along the hydraulic gradient, with a much greater rate of increase in Zone B near the River Murray. The increase in Cl^- concentration is not monotonic. Rather it shows an irregular distribution with rapid increase and decrease along the hydraulic gradient. This is also observed for the Cl^- concentration in the Renmark Group Aquifer (Fig. 3.2 a).

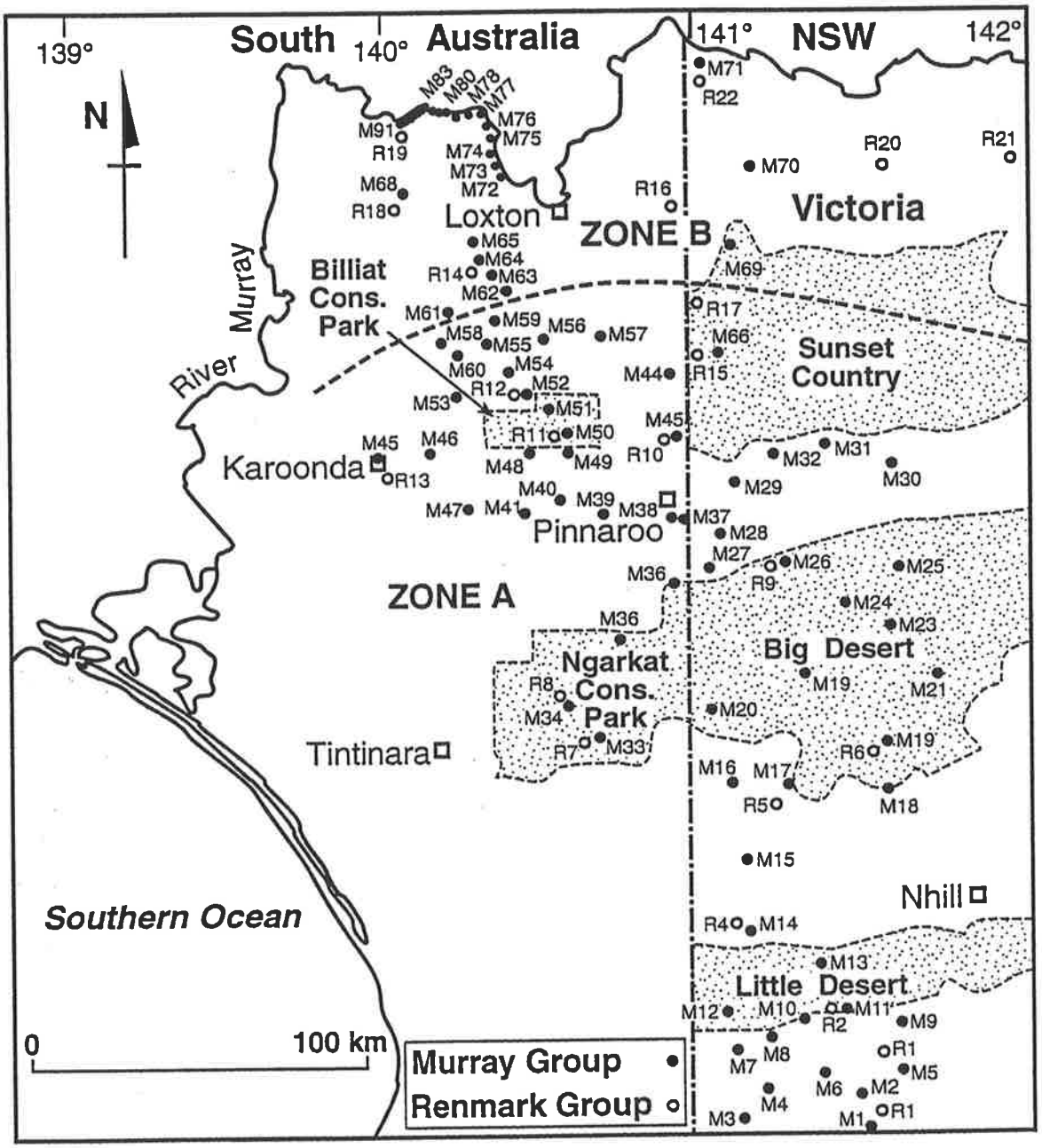

Fig. 3.1 Groundwater sample location map and boundary between Zone A and B.

Table 3.2 Chemical and $\delta^{18}O$ and $\delta^{2}H$ analysis of groundwaters from the Murray Group Aquifer. The ID numbers refer to our internal code. The registered number (*) is the Victorian Sinclair Knight Merz (Groundwater data base GDB number), and Registered Bore number of the South Australian Department of Mines and Energy. TDS is expressed as milligrams per litre and is calculated by summing the ion data. The results of major and minor ions are expressed in millimole and micromole. $\delta^{18}O$ and $\delta^{2}H$ are expressed in per mil notation relative to SMOW. SI refers to saturation state of the groundwater with respect to calcite and dolomite. Dist. refers to approximate distance in kilometres from the basin margin (Dundas Plateau).

Well Reg. No.	Well ID.	pH	Temp. (°C)	TDS	HCO_3^-	Cl^-	SO_4^{2-}	Na^+	K^+	Mg^{2+}	Ca^{2+}	Si^{4+}	Br^-	Sr^{2+}	$\delta^{18}O$	$\delta^{2}H$	SI		pCO_2	Dist.
				(mg/l)	(mmol/l)								(µmol/l)		(‰, SMOW)		Calcite	Dolomite	(atm.)	(km)
61922*	M1			543	4.1	3.27	0.21	3.8	0.10	1.19	0.94	0.22	6	15	-5.2	-34.3	-0.3	-0.5	0.012	15
61930*	M2			1498	7.9	14.27	0.66	13.5	0.14	3.17	1.28	0.27	22	52	-5.5	-31.0	-0.0	0.4	0.021	22
77850*	M3			1547	5.9	16.64	0.76	16.2	0.16	2.10	2.32	0.24	23	19	-4.5	-28.0	0.0	0.2	0.016	34
111321*	M4			1260	5.1	13.71	0.51	11.4	0.14	1.31	2.72	0.22	17	14	-3.5	-24.6	0.1	0.0	0.014	38
67829*	M5			893	4.1	9.11	0.31	8.1	0.24	1.16	1.66	0.27	12	9	-5.8	-36.8	-0.0	-0.2	0.008	32
51846*	M6	6.93	18.4	1445	6.0	14.98	0.83	14.1	0.23	2.10	2.03	0.41	21	14	-4.4	-26.4	-0.4	-0.7	0.029	34
92808*	M7	7.11	18.2	1075	5.0	10.24	0.58	9.8	0.17	1.88	1.78	0.41	14	16	-5.6	-36.1	-0.3	-0.5	0.017	50
50946*	M8	6.82	19	702	4.9	4.68	0.28	4.5	0.11	1.20	1.80	0.33	6	13	-3.7	-25.1	-0.6	-1.2	0.030	51
60610*	M9	7.48	19.9	587	4.1	3.98	0.18	4.1	0.26	0.97	1.19	0.49	7	10	-6.1	-35.3	-0.0	-0.0	0.007	36
79530*	M10	7.42	20.6	904	4.8	8.07	0.41	7.4	0.17	1.51	1.87	0.43	10	13	-6.5	-34.5	0.1	0.2	0.009	50
48559*	M11			2613	12.8	23.98	2.18	24.7	1.15	3.57	1.71	0.17	35	40	-5.0	-30.8	0.5	1.5	0.020	48
60436*	M12	7.29	19.2	1413	5.8	14.41	0.93	13.4	0.26	2.38	2.11	0.40	22	24	-5.5	-32.3	0.0	0.2	0.014	59
84741*	M13	7.44	18.2	885	5.2	7.62	0.26	6.4	0.23	1.60	1.96	0.39	14	21	-5.9	-35.9	0.2	0.3	0.009	60
75651*	M14	7.53	19.8	998	5.1	9.65	0.54	8.3	0.26	1.91	1.74	0.39	15	20	-5.7	-34.3	0.2	0.5	0.007	80
75365*	M15	7.35	18.8	1602	5.4	17.86	1.10	14.8	0.30	3.56	2.31	0.42	34	40	-5.5	-34.4	0.0	0.4	0.011	98
75351*	M16	7.43	19.8	1406	5.6	14.58	0.93	12.5	0.30	3.06	2.05	0.42	26	34	-5.7	-35.8	0.2	0.6	0.010	124
60450*	M17	7.48	21.8	1500	5.0	17.52	0.93	16.1	0.37	2.83	1.82	0.42	34	24	-5.8	-35.5	0.1	0.6	0.008	126
79655*	M18	7.45	22.1	1676	2.9	23.92	0.71	16.6	0.45	2.82	3.74	0.29	47	16	-5.7	-37.7	0.2	0.3	0.005	108
58079*	M19	7.64	21.6	1408	4.3	16.56	1.04	16.7	0.38	1.78	1.63	0.46	29	9	-5.9	-38.0	0.2	0.5	0.005	119
98297*	M20	7.56	18.7	1015	5.6	8.66	0.83	9.0	0.24	2.02	1.47	0.41	15	19	-6.0	-37.2	0.2	0.6	0.008	137

Table 3.2 Contd.

Well Reg. No.	Well ID.	pH	Temp. (C°)	TDS mg/l	HCO_3^-	Cl^-	SO_4^{2-}	Na^+	K^+	Mg^{2+}	Ca^{2+}	Si^{4+}	Br^-	Sr^{2+}	$\delta^{18}O$	δ^2H	SI		pCO_2	Dist.
					mmol/l								µmol/l		(‰, SMOW)		Calcite	Dolomite	(atm.)	(km)
103369*	M21			725	4.2	6.01	0.32	5.8	0.18	0.99	1.55	0.38	12	6	-6.0	-38.4	0.1	0.1	0.007	142
98254*	M22	7.68	20.5	857	5.0	7.14	0.53	7.2	0.20	1.63	1.44	0.33	12	14	-5.8	-39.0	0.3	0.7	0.005	143
49951*	M23			1144	4.1	12.07	0.89	11.3	0.26	2.97	0.96	0.45	19	11	-6.1	-41.0	-0.2	0.2	0.006	159
49952*	M24			708	3.3	6.35	0.53	6.3	0.18	2.17	0.58	0.40	10	9	-6.0	-39.1	-0.4	-0.2	0.005	171
49950*	M25			733	3.4	6.43	0.59	6.8	0.18	2.08	0.58	0.40	13	9	-6.0	-35.5	-0.4	-0.2	0.006	174
66477*	M26	7.18		1275	5.5	12.89	0.74	10.0	1.20	2.09	2.09	0.43	16	13	-5.7	-31.2	-0.0	0.1	0.018	185
54642*	M27			849	3.9	6.74	1.03	7.9	0.17	1.19	1.31	0.39	11	10	-6.5	-38.6	-0.0	-0.0	0.008	182
54636*	M28			1135	5.6	7.56	1.73	11.4	0.17	1.42	1.43	0.46	12	11	-5.6	-38.9	0.0	0.3	0.012	190
82220*	M29	7.31	24.9	1496	8.4	12.10	1.04	14.2	0.33	2.22	1.54	0.39	18	27	-6.1	-40.0	0.2	0.6	0.021	202
61571*	M30	7.87	22.4	1425	4.4	15.23	1.47	14.7	0.41	2.80	1.33	0.51	22	21	-5.9	-43.0	0.4	1.1	0.003	204
65758*	M31			906	3.9	8.52	0.90	8.0	0.26	1.33	1.39	0.48	11	13	-6.3	-42.4	0.0	0.2	0.007	216
77199*	M32			1175	4.4	12.44	0.91	11.0	0.33	1.93	1.51	0.45	16	19	-6.0	-40.0	0.1	0.5	0.007	212
7026-113	M33	7.66	20.8	781	4.4	6.18	0.53	6.1	0.18	1.59	1.12	0.43	11	11	-5.9	-38.3	0.1	0.5	0.005	149
7026-110	M34	7.56	22.1	866	3.6	8.60	0.46	7.1	0.64	1.53	1.42	0.33	16	11	-6.4	-38.1	0.0	0.2	0.005	164
7027-566	M35	7.30	20.9	891	4.3	8.38	0.50	7.8	0.18	0.95	1.61	0.24	14	6	-5.8	-39.8	-0.1	-0.3	0.011	177
7027-650	M36	7.48	22	707	4.2	5.36	0.43	5.2	0.16	1.09	1.37	0.40	8	7	-5.7	38.3	0.0	0.0	0.007	183
7027-606	M37	7.37	23.9	961	5.3	6.23	1.12	8.5	0.19	1.43	1.43	0.45	11	14	-5.8	-38.8	0.0	0.2	0.012	204
7027-592	M38	7.45	22.4	850	4.7	5.78	0.95	7.4	0.20	1.20	1.15	0.48	11	12	-5.9	-40.4	-0.0	0.0	0.009	204
7027-597	M39	7.60	22.0	768	3.7	6.40	0.61	7.8	0.16	0.80	1.02	0.37	11	6	-5.9	-39.7	-0.0	-0.0	0.005	214
7027-669	M40	7.26	23.5	997	4.5	9.11	0.76	10.7	0.23	1.60	0.66	0.32	12	0	-6.0	-40.7	-0.4	-0.3	0.014	218
7027-602	M41	7.58	21.4	1030	4.6	9.00	0.93	11.2	0.20	0.74	1.05	0.41	15	6	-6.2	-39.0	0.0	-0.0	0.008	220
7027-405	M42	7.49	22.5	1370	4.9	14.50	0.93	15.4	0.33	1.54	1.16	0.40	23	5	-5.7	-38.2	0.0	0.2	0.008	224
7027-586	M43	7.60	24.0	1340	3.9	14.70	1.18	14.9	0.30	1.84	1.34	0.35	22	14	-5.8	-40.3	0.0	0.4	0.005	228
7027-579	M44	7.43	24.2	986	3.7	9.79	0.91	8.8	0.21	1.26	1.73	0.42	15	9	-6.0	-43.1	0.0	0.0	0.007	240
6827-1536	M45	7.23	21	2363	7.9	25.11	1.94	27.0	0.49	3.48	1.55	0.46	43	23	-5.1	-37.1	0.0	0.3	0.021	255
7026-120	M46	7.38	28	2473	6.8	27.53	2.32	29.5	0.64	3.11	1.62	0.42	40	16	-5.3	-38.3	0.1	0.7	0.015	249

Table 3.2 Contd.

Well Reg. No.	Well ID.	pH	Temp. (C°)	TDS mg/l	HCO_3^-	Cl^-	SO_4^{2-}	Na^+	K^+	Mg^{2+}	Ca^{2+}	Si^{4+}	Br^-	Sr^{2+}	$\delta^{18}O$	δ^2H	SI		pCO_2	Dist.
					mmol/l								µmol/l		(‰, SMOW)		Calcite	Dolomite	(atm.)	(km)
6927-591	M47	7.12	19.7	1474	7.6	12.10	1.13	13.9	0.31	3.09	1.26	0.48	24	21	-5.2	-38.6	-0.3	-0.0	0.026	234
6927-644	M48	7.39	25.4	2092	4.7	25.53	1.97	23.1	0.41	2.82	1.92	0.40	40	17	-5.6	-39.1	0.0	0.4	0.010	239
6927-590	M49	7.54	24.5	2054	4.4	24.46	1.89	24.4	0.44	2.83	1.87	0.40	34	16	-5.6	-40.1	0.2	0.6	0.006	234
6927-588	M50	7.92	28.6	2055	4.4	24.37	1.88	24.8	0.41	2.44	2.01	0.38	38	13	-5.8	-41.6	0.6	1.5	0.003	240
6927-601	M51	7.53	22.9	1323	4.4	14.50	0.96	14.4	0.25	1.73	1.40	0.34	24	10	-5.7	-38.2	-0.1	-0.0	0.010	245
6928-567	M52	7.60	23.1	1802	6.5	16.93	1.98	21.5	0.42	1.77	1.08	0.51	27	14	-5.6	-39.3	0.1	0.6	0.008	251
6928-411	M53	7.19	25.3	1996	6.1	20.93	2.05	23.0	0.50	2.37	1.62	0.36	36	15	-5.3	-36.0	-0.1	0.0	0.019	258
6928-49	M54	7.16	27.4	2005	7.5	18.87	1.98	23.7	0.46	2.33	1.22	0.50	33	26	-5.2	-41.2	-0.2	0.1	0.026	260
6928-260	M55	7.48	24.6	1234	4.9	11.79	1.08	13.6	0.28	1.39	1.10	0.34	21	11	-4.9	-38.1	-0.0	0.2	0.009	268
7028-503	M56	7.28	25.2	2339	8.3	22.76	2.34	27.0	0.55	3.44	1.34	0.54	35	46	-5.1	-37.8	0.0	0.5	0.021	262
7025-422	M57	7.35	23.4	2446	6.2	28.66	2.11	27.7	0.71	3.49	2.03	0.47	47	34	-5.5	-39.0	0.0	0.5	0.013	258
6928-477	M58	7.35	22.7	3785	9.4	42.96	4.31	45.7	0.61	4.48	1.71	0.48	68	53	-5.1	-37.9	0.1	0.7	0.019	271
6928-27	M59	7.20	23.7	3644	8.4	42.28	3.81	45.2	0.61	4.20	1.80	0.53	67	56	-5.4	-38.5	-0.0	0.4	0.024	273
6828-112	M60	7.10	22.9	3273	10.8	34.95	3.01	37.4	0.56	5.10	1.52	0.46	57	44	-5.1	-35.7	-0.1	0.4	0.038	275
6928-528	M61	7.08	24.8	5063	13.2	60.06	3.91	64.4	0.59	6.58	1.63	0.45	93	70	-4.9	-36.0	-0.0	0.6	0.048	281
6928-424	M62	7.07	26.1	6376	15.1	72.21	6.81	85.4	0.71	6.46	1.66	0.30	120	73	-4.5	-35.9	-0.0	0.7	0.056	285
6929-154	M63	7.40	25.4	6093	12.9	72.75	5.16	87.8	0.76	4.69	1.16	0.45	109	55	-5.0	-36.9	0.0	0.9	0.024	289
6929-169	M64	7.20	23.2	6086	13.2	71.14	6.38	83.6	0.75	4.40	1.45	0.48	116	63	-4.7	-36.9	0.0	0.5	0.037	293
6928-2	M65	7.16	24.8	6751	11.5	87.84	4.44	95.1	1.15	6.66	2.08	0.50	133	102	-5.5	-38.7	0.0	0.7	0.035	300
49677*	M66	7.50		2096	5.5	24.82	1.27	25.8	0.78	2.98	1.06	0.46	36	25	-6.2	-42.8	-0.0	0.8	0.009	243
64363*	M67	7.51		7434	9.0	101.3	4.75	113.8	1.24	3.81	1.28	0.54	143	34	-5.6	-37.4	0.0	0.8	0.013	254
96929-356	M68	6.70	26.4	15750	8.7	250.9	4.94	212.7	2.03	18.22	10.08	0.25	353	0	-5.0	-33.0	-0.0	0.3	0.059	319
85570*	M69	7.45		18310	6.5	271.3	13.53	268.8	2.74	17.19	5.66	0.52	333	287	-4.4	-33.1	0.3	1.3	0.009	281
81833*	M70			18130	3.8	290.7	7.84	241.1	3.12	26.45	10.43	0.53	402	793	-4.0	-33.3	-0.3	-0.7	0.020	295
86775*	M71	6.90	24	21160	5.9	339.3	7.34	291.4	3.17	27.81	11.15	0.61	439	770	-5.1	-34.5	0.0	0.6	0.026	324
6929-705	M72	6.67	25.9	19930	8.0	302.3	11.75	278.8	3.38	20.49	12.15	0.60	424	294	-4.5	-30.1	-0.0	0.2	0.056	330

Table 3.2 Contd.

Well Reg. No.	Well ID.	pH	Temp. (C°)	TDS mg/l	HCO_3^-	Cl^-	SO_4^{2-}	Na^+	K^+	Mg^{2+}	Ca^{2+}	Si^{4+}	Br^-	Sr^{2+}	$\delta^{18}O$	δ^2H	SI		pCO_2	Dist.
					mmol/l								µmol/l		(‰, SMOW)		Calcite	Dolomite	(atm.)	(km)
6929-700	M73	6.56	25.9	17180	8.2	267.4	7.44	241.0	2.31	17.32	9.43	0.50	347	216	-4.7	-33.2	-0.3	-0.2	0.071	330
6929-711	M74	6.54	27.2	18570	8.5	296.8	6.94	250.0	2.58	19.58	11.78	0.55	401	220	-4.9	-35.1	-0.2	0.0	0.077	332
6929-712	M75	6.43	26.6	19751	8.2	315.5	7.31	266.6	2.69	21.51	13.45	0.56	418	237	-4.6	-31.5	-0.3	-0.2	0.087	334
6929-710	M76	6.39	27	22950	7.6	367.1	8.94	313.2	3.04	24.93	15.54	0.49	474	271	-4.6	-32.3	-0.4	-0.3	0.085	336
6929-702	M77	6.46	26.9	20820	7.6	333.8	8.78	274.5	2.71	23.53	15.82	0.30	438	253	-4.6	-32.1	-0.2	-0.1	0.076	337
6929-701	M78	6.50	26.6	21960	7.6	346.1	10.88	292.3	2.58	24.76	17.17	0.26	448	268	-4.6	-32.1	-0.2	0.0	0.071	338
6929-684	M79	6.50	26.4	23080	6.7	362.7	13.13	307.1	2.61	27.93	16.14	0.26	464	277	-4.5	-33.9	-0.3	-0.1	0.062	340
6929-651	M80	6.50	26.4	22840	6.7	361.9	11.19	304.9	2.58	26.16	17.89	0.25	449	277	-4.7	-34.3	-0.2	-0.0	0.062	342
6929-682	M81	6.47	25.8	22610	6.3	350.6	14.94	298.8	2.47	25.05	17.94	0.28	442	277	-4.3	-36.1	-0.3	-0.3	0.061	345
6929-685	M82	6.62	26.4	22720	6.2	353.1	17.63	289.7	2.38	25.17	17.61	0.22	437	284	-4.3	-32.3	-0.1	0.0	0.048	348
6929-686	M83	6.65	25.5	22190	6.3	349.4	13.88	289.3	2.43	24.15	17.27	0.21	463	293	-4.5	-33.3	-0.0	0.1	0.044	348
6929-687	M84	6.62	25.6	21620	7.5	335.6	10.97	297.5	2.56	25.79	14.42	0.22	416	279	-4.9	-31.8	-0.1	0.2	0.057	350
6929-689	M85	6.70	25.9	19450	7.9	304.6	10.44	263.2	2.42	19.00	12.55	0.26	432	226	-5.0	-37.3	-0.0	-0.3	0.053	350
6929-691	M86	6.63	26.6	18700	7.7	296.1	9.06	252.3	2.42	17.32	12.03	0.35	437	221	-5.1	-31.4	-0.1	0.0	0.059	350
6929-692	M87	6.65	27.3	16680	8.3	259.9	8.78	228.8	2.20	14.27	9.33	0.36	379	178	-5.1	-34.0	-0.2	0.0	0.063	350
6929-693	M88	6.70	25.4	13570	8.7	205.0	6.69	192.7	1.97	13.25	6.34	0.37	312	146	-5.2	-35.8	-0.2	0.0	0.060	350
6929-1046	M89	6.69	22	23570	9.0	336.1	23.84	332.8	2.81	24.89	9.58	0.47	456	225	-4.4	-35.0	-0.2	0.1	0.057	351
6929-1041	M90	6.85	25.2	17990	9.2	262.2	15.63	251.8	2.52	17.24	6.59	0.45	353	180	-4.7	-32.7	-0.0	0.4	0.047	354
6929-1082	M91	6.66	22.6	22290	8.6	334.0	18.69	300.2	2.71	26.74	9.83	0.53	461	293	-4.3	-32.1	-0.2	0.0	0.057	355

Table 3.3 Chemical and $d^{18}O$ and $d^{2}H$ analysis of groundwaters from the Renmark Group Aquifer. The ID numbers refer to our internal code. The registered number (*) is the Victorian Sinclair Knight Merz (Groundwater data base GDB numbers), and the Registered Bore number of the South Australian Department of Mines and Energy. TDS is expressed as milligrams per litre and is calculated by summing the ion data. The results of major and minor ions are expressed in millimoles and micromoles. $d^{18}O$ and $d^{2}H$ are expressed in per mil notation relative to SMOW. Dist. refers to approximate distance in kilometres from the basin margin (Dundas Plateau).

Well Reg. No.	Well ID.	pH	Temp. (°C)	TDS (mg/l)	HCO_3^-	Cl^-	SO_4^{2-}	Na^+	K^+	Mg^{2+}	Ca^{2+}	Si^{4+}	Br^-	Sr^{2+}	$\delta^{18}O$	$\delta^{2}H$	Dist. (km)
					(mmol/l)								(µmol/l)		(‰, SMOW)		
67847*	R1	8.00	18.9	795	2.82	9.65	0.32	8.7	0.27	1.00	0.86	0.05	15	9	-5.8	-34.2	5
60623*	R2	8.72	22.1	677	3.72	4.80	0.21	6.7	0.61	0.90	0.43	0.11	8	11	-6.0	-37.4	15
48554*	R3	8.48	17.1	2058	5.62	25.30	1.21	26.7	0.43	1.65	0.72	0.22	42	8	-5.5	-37.2	48
75669*	R4	7.71	22.3	1317	5.63	12.69	1.02	12.0	0.46	2.67	1.61	0.23	20	14	-5.7	-39.1	60
60475*	R5	7.68	20.5	2206	5.93	25.30	1.92	24.1	0.51	3.74	2.33	0.49	41	23	-5.8	-38.2	126
58111*	R6	8.64	21.6	1855	3.37	22.65	1.79	23.3	0.73	2.02	1.41	0.15	38	13	-5.0	-33.7	119
7026-112	R7	7.49	23.9	875	4.06	8.46	0.57	7.5	0.23	1.37	1.41	0.34	13	6	-5.7	-38.7	149
7026-111	R8	7.84	25.3	740	4.11	6.23	0.43	6.2	0.17	1.06	1.28	0.38	11	6	-6.2	-40.7	164
66476*	R9			1525	7.25	14.87	0.33	20.5	0.54	0.65	0.31	0.18	23	5	-5.8	-39.4	185
7027-585	R10	7.98	28.5	1270	6.14	11.71	0.53	16.7	0.41	0.53	0.35	0.23	17	5	-6.4	-43.1	228
6927-588	R11	7.92	28.6	1108	4.76	10.72	0.70	12.2	0.37	1.37	0.98	0.22	19	6	-6.1	-41.0	240
6928-542	R12	8.10	28.8	1870	10.94	15.35	0.34	25.8	0.47	0.21	0.16	0.22	25	0	-6.0	-41.0	251
6827-1530	R13	7.65	27.1	2189	10.15	19.80	1.04	32.1	0.41	0.14	0.18	0.20	33	1	-3.4	-34.0	255
6929-423	R14	7.72	26.3	3284	11.30	36.70	1.22	48.5	0.55	0.75	0.44	0.22	54	7	-5.5	-38.5	289
49676*	R15	7.10	33.1	4562	6.79	61.89	2.59	64.5	1.09	4.01	1.73	0.16	103	37	-5.0	-36.8	243
7028-469	R16	7.90	21.9	4636	5.55	66.46	1.96	70.8	1.13	2.75	0.09	0.01	90	33	-5.8	-37.1	278
109458*	R17			4816	7.27	64.29	3.38	67.9	0.98	4.07	1.53	0.17	94	35	-5.8	-35.9	250
6929-760	R18	6.99	28.7	14566	9.09	232.0	4.50	195.3	1.97	16.33	8.83	0.15	295	159	-5.2	-34.6	319
6829-992	R19	7.25	25.5	15859	6.89	234.0	12.84	222.3	2.45	15.55	7.14	0.20	312	148	-4.5	-39.3	350
81832*	R20	7.04		19176	8.15	304.6	7.97	255.9	2.58	24.64	11.63	0.19	476	310	-3.5	-30.3	295
104800*	R21	7.01	25.1	18609	7.68	291.0	7.72	250.1	2.50	25.55	13.45	0.19	390	283	-4.4	-32.6	304
86774*	R22	7.94	24	21576	7.37	336.9	11.91	286.2	2.46	28.71	15.14	0.18	438	282	-4.6	-30.0	324

Variations in bicarbonate concentration are not as pronounced as the Cl^- concentration. However, there is a moderate increase in dissolved HCO_3^- to as much as 12 mmol/l occurring in the downgradient part of the Murray Group Aquifer in Zone A. In Zone B the concentration of HCO_3^- decreases to ~ 4 mmol/l (Fig. 3.2 b).

Sulphate concentrations in the Murray and Renmark Group aquifers range from 0.4 to 22 mmol/l, and 0.09 to 12. 84 mmol/l respectively and generally follow the same pattern as Cl^- in both aquifers. However, the SO_4^{2-} concentration in Zone B of the Murray Group Aquifer is considerably higher than that in the Renmark Group Aquifer corresponding to the large increase in Cl^- concentration down gradient near the River Murray (Fig. 3.2 c).

Bromide concentrations in the Murray and Renmark Group aquifers also follow a similar pattern as Cl^- concentrations. The Br^- concentration in both aquifers in Zone A ranges from 0.01 to 0.14 mmol/l and is relatively lower compared with Br^- concentration in groundwater of Zone B (0.4 mmol/l-Fig. 3.2 d).

Sodium follows a similar trend with concentrations of ~3.8 mmol/l, increasing to 85 mmol/l along the 250 km of Zone A, then rapidly increasing to 260 mmol/l in Zone B (Fig. 3.3 a).

The plot of Ca^{2+} and Mg^{2+} versus distance (Fig. 3.3 b, c)), shows a similar trend to that observed for Na^+ and Cl^-. However the magnitude of Ca^{2+} and Mg^{2+} increase is

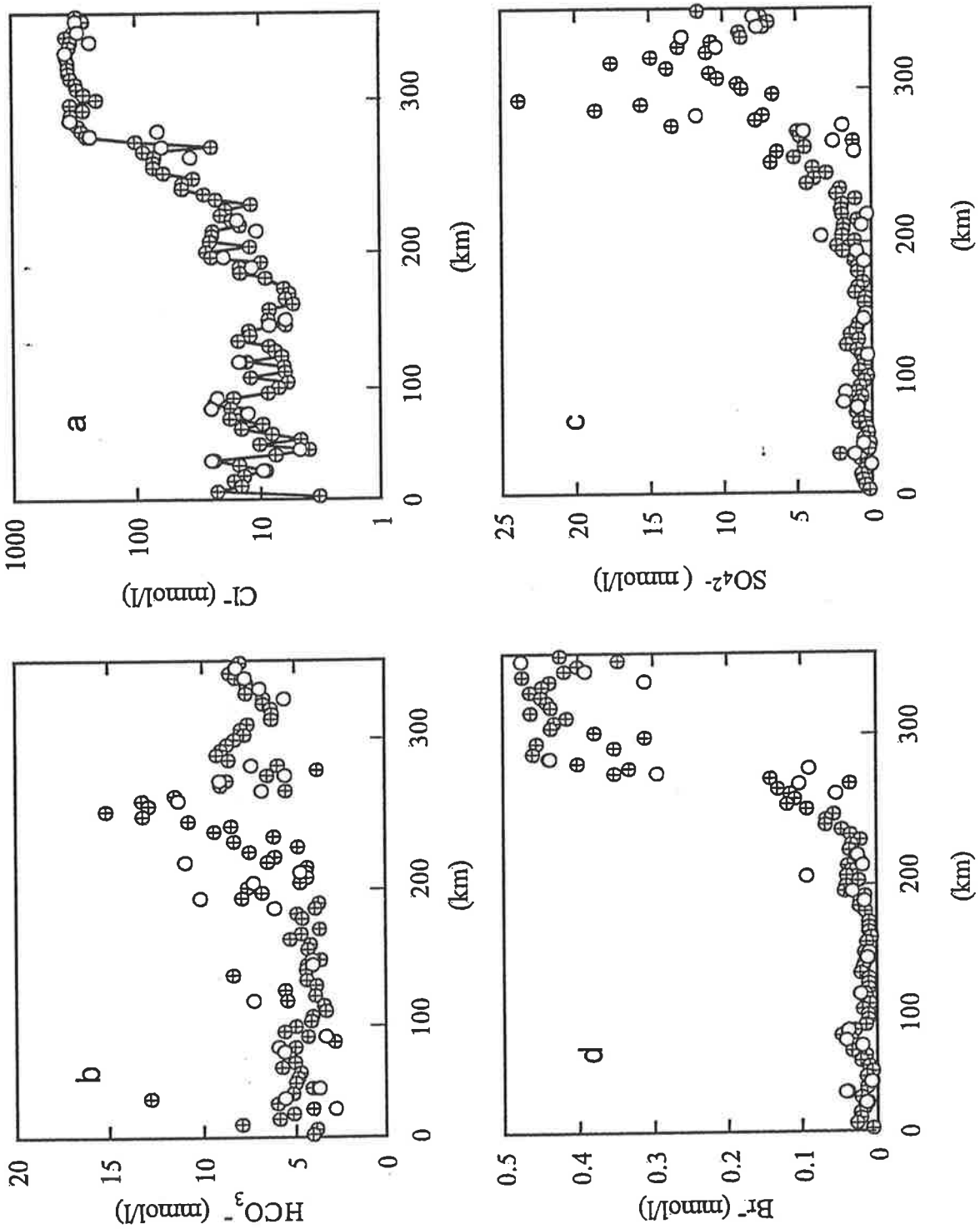

Fig. 3.2 a, b, c, d Major anion concentrations in mmol/l along the AA` transect (see Fig. 1.1). The Km axis refers to distance from the basin margin. The crossed circles denote the Murray Group Aquifer whereas the open circle denotes the Renmark Group Aquifer. The variation of Cl^- concentration is shown on a log scale whereas the variation of the HCO_3, $SO_4^{2-}$and Br^- concentrations are shown on a normal scale. Note the sudden increase and decrease of Cl^- concentration (Fig. 3.2 a) in adjacent wells in both aquifers.

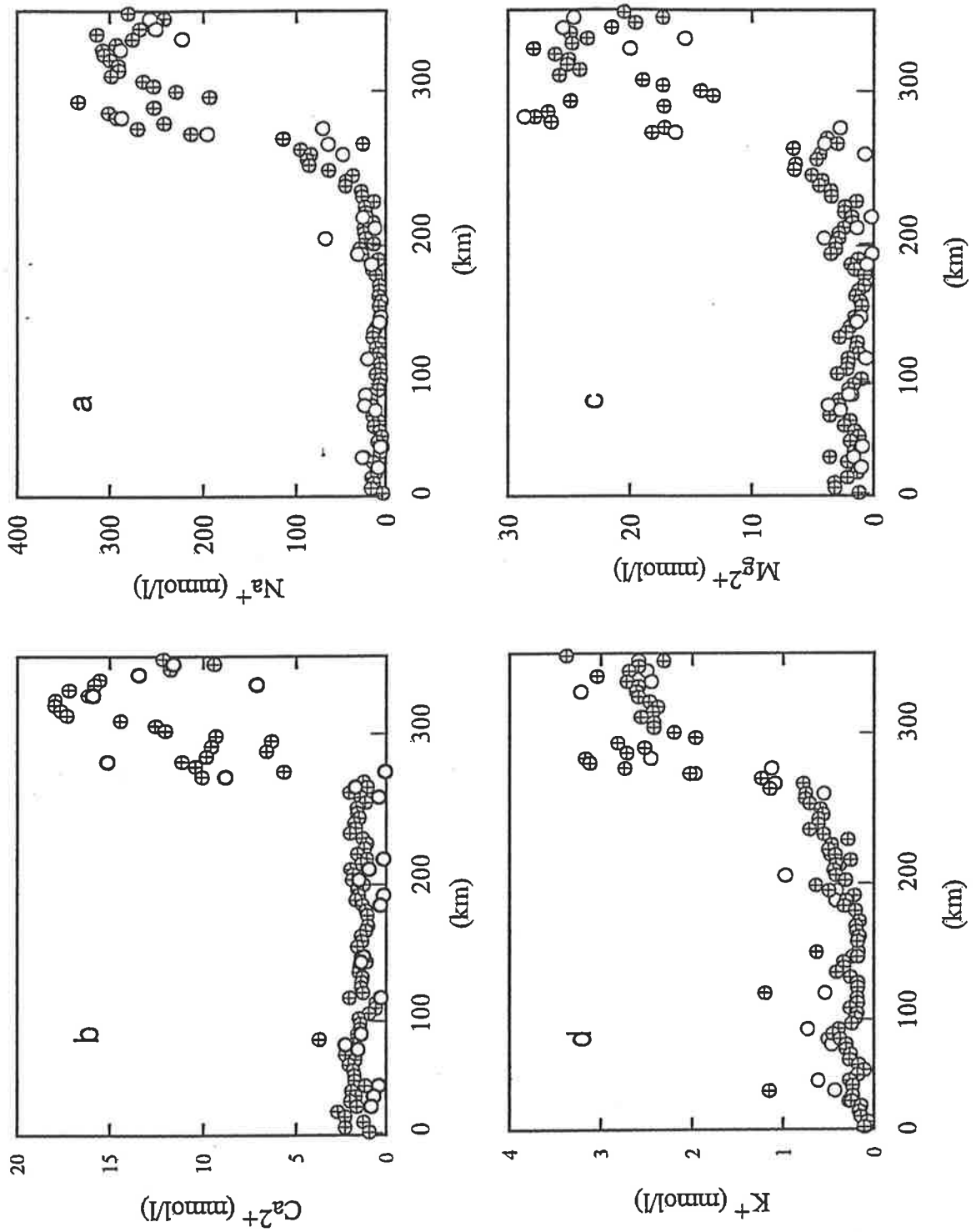

Fig. 3.2 a, b, c, d Major cation concentrations in mmol/l along the AA` transect (see Fig. 1.1). The Km axis refers to distance from the basin margin. The crossed circles denote the Murray Group Aquifer whereas the open circles denote the Renmark Group Aquifer. The variation of Cl^- concentration is shown on a log scale whereas the variation of the HCO_3, $SO_4^{2-}$and Br^- are shown on a normal scale. Note the sudden increase in major cation concentration in both aquifers in the northern part of the study area.

much less. There are slight increases in Ca^{2+} and Mg^{2+} concentrations in Zone A from 0.58 to 2.72 mmol/l and 0.95 to 6.4 mmol/l respectively, then a rapid increase to values of 17.8 mmol/l for Ca^{2+}, and 27.9 mmol/l for Mg^{2+} in Zone B.

Potassium concentrations range from 0.14 to 0.71 mmol/l in Zone A , then increases downgradient in Zone B to values of 3.38 mmol/l in the Murray and Renmark Group aquifers (Fig. 3.3 d).

Silica concentrations in the Murray and Renmark Group aquifers range from 0.17 to 0.8 mmol/l, and 0.01 to 0.4 mmol/l respectively. The variation in silica concentrations in both aquifer systems is very small compared with other major ions (Table 3.2).

A Piper diagram for the major ions in groundwater from the Murray Group Aquifer is shown in (Fig. 3.4). Groundwater chemistry throughout the Murray Group Aquifer is dominated by Na^+ and Cl^- ions. The general concentration pattern for dissolved major ions in the sampled waters is:

$Cl^- > HCO_3^- > SO_4^{2+}$ and $Na^+ > Mg^{2+} > Ca^{2+} > K^+$.

The percent equivalent of Na^+ and Cl^- increases along the hydraulic gradient from the basin margin from ~ 50% in the south and south-east to > 90% down gradient near the River Murray.

Groundwater from the Renmark Group Aquifer has a similar chemical composition to that in the Murray Group Aquifer (Fig. 3.5). Sodium and chloride are the dominant

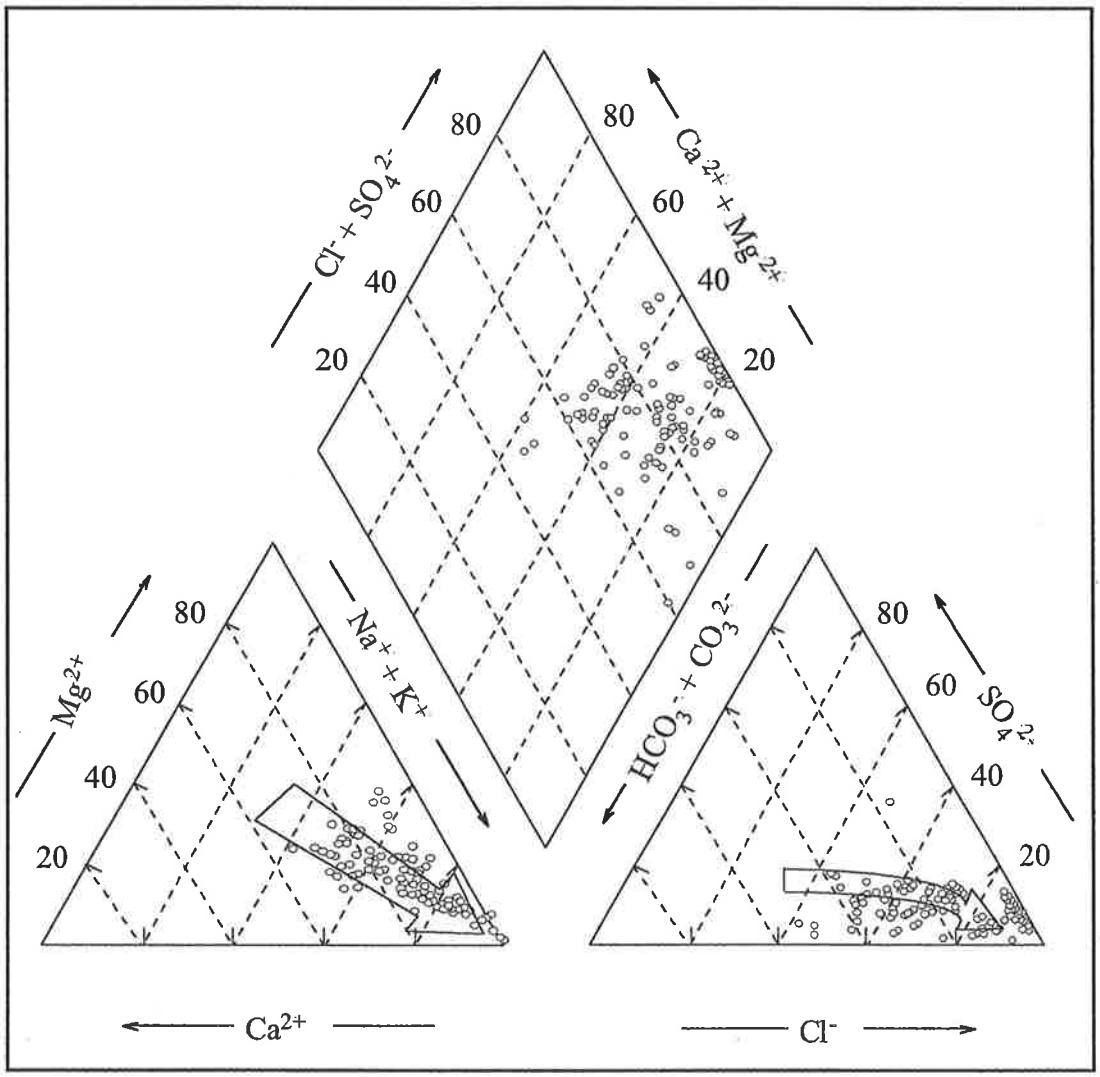

Fig. 3.4 Piper diagram showing chemical composition of groundwater from the Murray Group Aquifer, in mole percent of cations and anions. Note that all groundwater samples are Na^+-Cl^- type water. Arrows show evolution of groundwater from the basin margin in the south and southeast towards the discharge area in the north and north-west near the River Murray. Na^+ and Cl^- mole percent increase from 50% near the basin margin to > 90% in Zone B near the River Murray.

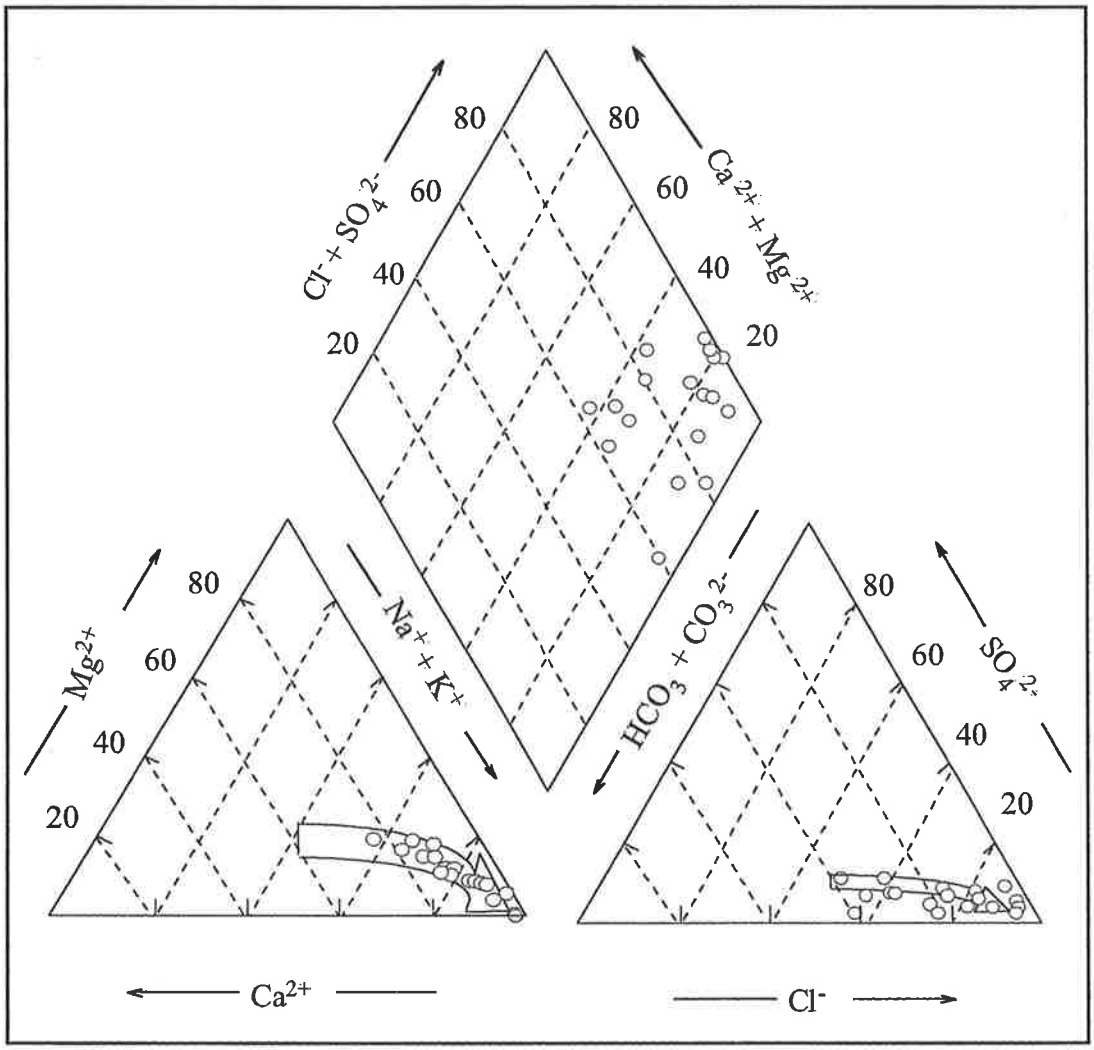

Fig. 3.5 Piper diagram showing chemical composition of groundwater from the Renmark Group Aquifer, in mole percent of cations and anions. All groundwater samples are Na^+-Cl^- type water similar to that in the Murray Group Aquifer. Arrows show evolution of groundwater from the basin margin in the south and southeast towards the discharge area in the north and north-west near the River Murray. Na^+ and Cl^- mole percent also increase from ~ 50% near the basin margin to > 90% in Zone B near the River Murray.

cations and anions regardless of the location or relative major ion concentrations.

3.2.3 δ^2H and $\delta^{18}O$ composition of groundwater in the Murray and Renmark Group aquifers

The δ^2H and $\delta^{18}O$ values in the Murray Group Aquifer range from -42‰ to -32‰ and -6.5‰ to -4.2‰ respectively. Groundwater in the Renmark Group Aquifer has similar δ^2H and $\delta^{18}O$ values and ranges from -43‰ to -30‰ and -6.4‰ to -3.1‰. Most of the water samples fall on or slightly to the right of the World Meteoric-Water Line defined as $\delta^2H = 8\ \delta^{18}O + 10$ (Fig. 3.6).

The plot of δ^2H and $\delta^{18}O$ values along the AA` transect shows that both δ^2H and $\delta^{18}O$ values decrease from the basin margin towards the interior of the basin in Zone A. The most depleted groundwater samples in ^2H and ^{18}O are located 120 km from the basin margin (Fig. 3.7 a, b). Further inland the δ^2H and $\delta^{18}O$ values of groundwater in both aquifers show continued enrichment in ^2H and ^{18}O along the AA` transect and reach a maximum δ^2H and $\delta^{18}O$ value of -34‰ and -4.6‰ respectively at Zone A. Generally the δ^2H and $\delta^{18}O$ values of groundwater in Zone B are more enriched relative to groundwater in the southern and central part of Zone A.

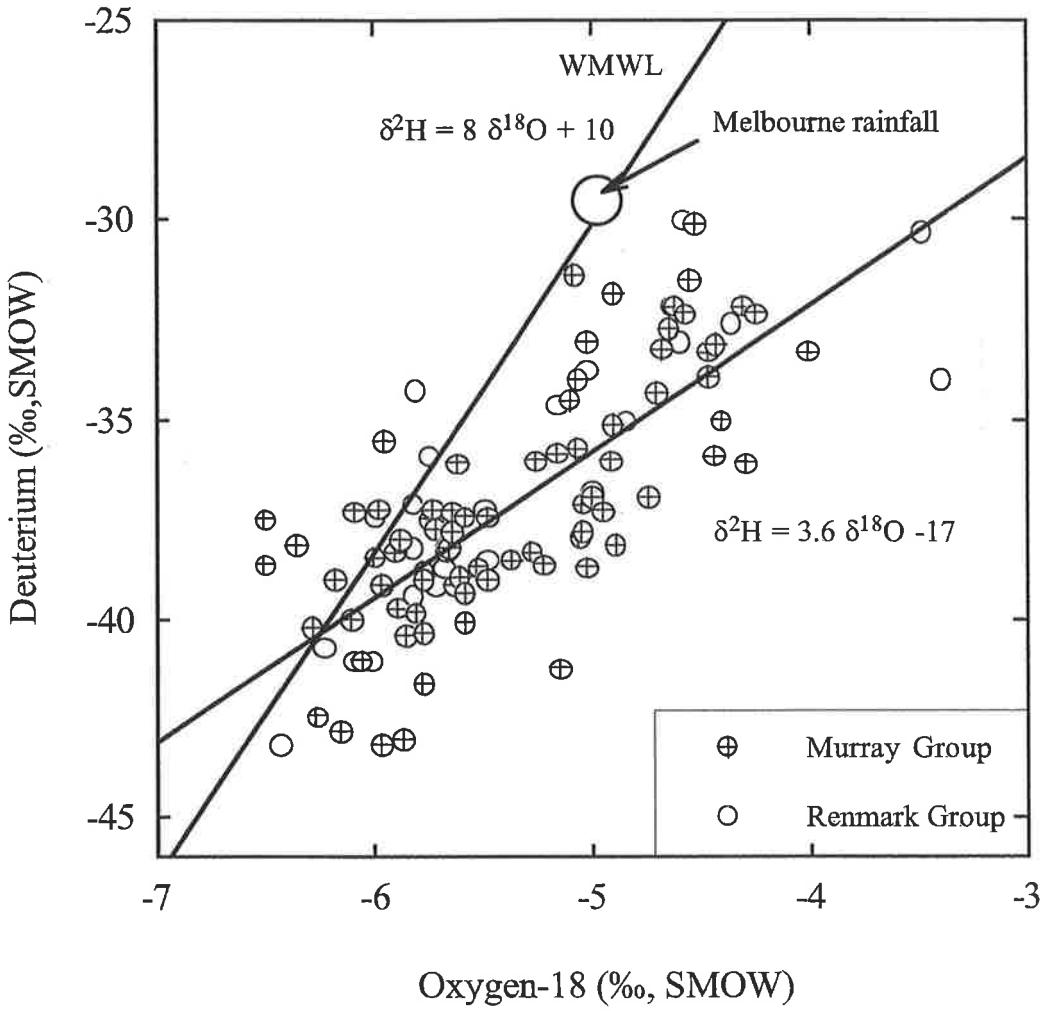

Fig. 3.6 δ^2H vs. $\delta^{18}O$ diagram for groundwaters of the Murray and Renmark Group aquifers. WMWL = World Meteoric Water Line defined as $\delta^2H = 8\ \delta^{18}O + 10$. No clear distinction can be recognised between groundwaters of the Murray and Renmark Group aquifers.

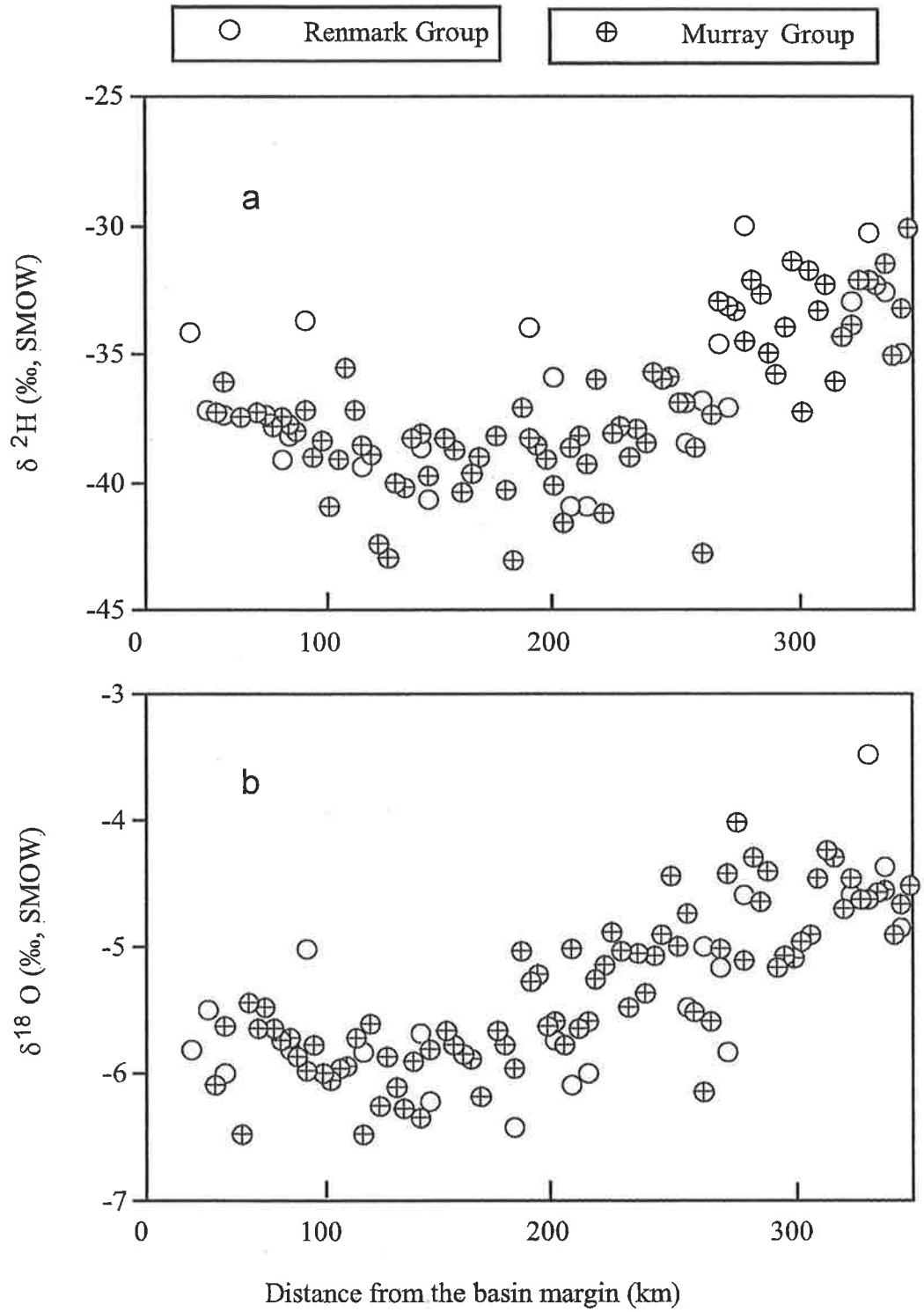

Fig. 3.7 a, b δ^2H and $\delta^{18}O$ composition in the Murray and Renmark Group aquifers along the AA` transect. Groundwaters from the northern part of the study area in both aquifers have relatively enriched ^2H and ^{18}O composition.

3.3 Discussion

3.3.1 Dominance of chloride and sodium ions in groundwater

Attempts to interpret the origin of saline surface waters and groundwaters in the Australian continent date back more than 100 years. Some of these studies have variously ascribed the source of high salinity to sea water transgression (Streich, 1893), evaporation (Bonython, 1956), remnant of sea water entrapped in the sedimentary basins at the time of their deposition (Wopfner and Twidale, 1967; Johnson, 1979), airborne oceanic aerosol transported inland into basins by rainfall (Jack, 1921), and evapotranspiration of rain water prior to recharge (Herczeg and Lyons, 1991). The majority of the high saline waters in the Australian continent are dominated by Na^+ and Cl^- ions. Therefore, understanding the sources of high salinity is commensurate with understanding the dominance of Na^+ and Cl^- ions. Based on the previous studies and distribution of Na^+ and Cl^- ions, the plausible scenarios for the dominance of Na^+ and Cl^- in groundwater from the Murray and Renmark Group aquifers are discussed below.

3.3.1.1 Remnant Sea water dilution

The plot of Na^+ versus Cl^- concentrations in the Murray and Renmark Group aquifers shows that the data falls on the sea water dilution line (Fig. 3.8 a). The same trend is observed in the Br^--Cl^- relationship (Fig. 3.8 b). The line of regression between Na^+ and Cl^- has a slope of 0.82, similar to the marine-derived regression line of (0.85), and a

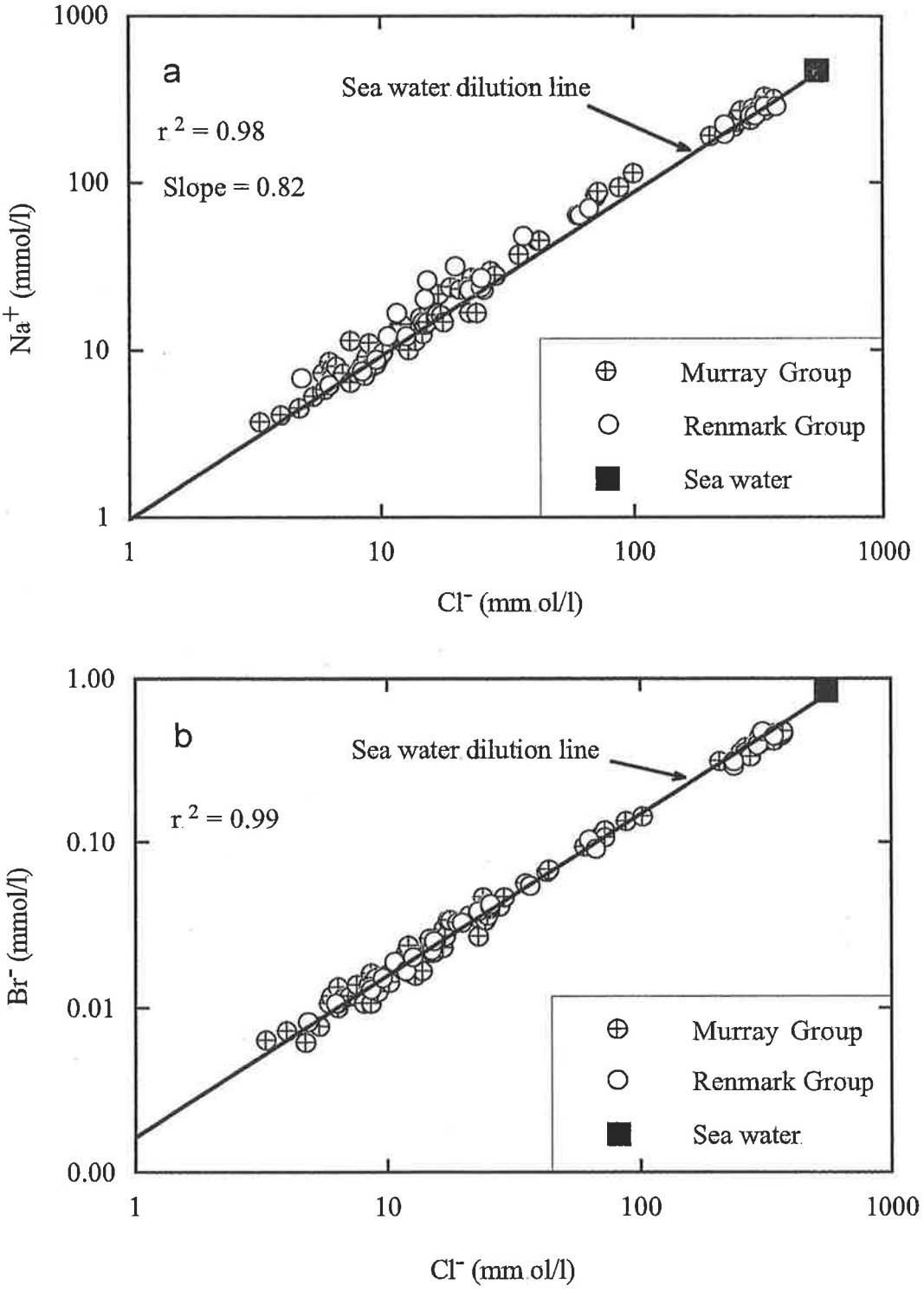

Fig. 3.8 Sodium and Br^- vs. Cl^- concentration of groundwater from the Murray and Renmark Group aquifers. The Na^+ vs. Cl^- (Fig. 3.8 a) and Br^- vs. Cl^- (Fig. 3.8 b) data fall on the sea water dilution line. This suggests that groundwater may be derived from rainfall that has Na^+: Br^-: Cl^- ratios the same as sea water.

correlation coefficient (r^2) of 0.98, implying a marine origin for Cl^- and Na^+ of the groundwater. The marine type Na^+ and Cl^- distribution could be due to dilution of remnant seawater trapped in the basin at the time of deposition.

However, most of the $\delta^{18}O$ and δ^2H data from the groundwater from both aquifers falls on or slightly to the right of the WMWL (Fig. 3.6) indicating the presence of only meteoric water in both aquifers. Stable isotope analysis of pore water from the marine aquitard (Geera Clay), which is the same age as the Murray Group limestone and lies ~ 300 km north-east of the study area, also showed that both δ^2H and $\delta^{18}O$ values are derived from meteoric water (Jones et al., 1994). Furthermore, based on Darcy's law, Barnett (1989) has estimated an average groundwater travel time of the Murray Group Aquifer from the main recharge area at the south-east to discharge area at northwest (at River Murray) to be ~ 200,000 years. The last sea retreat occurred in the study area approximately 2 million years ago (Evans et al., 1990). Therefore, groundwater in both aquifers has been replenished in the study area at least 10 times since the last sea invasion, flushing out any remnants of seawater trapped in the aquifer.

These two lines of evidence suggest that seawater like Na^+ and Cl^- distribution of groundwater from the Murray and Renmark Group aquifers cannot be explained by remnant seawater dilution.

3.3.1.2 Dissolution of Halite

Groundwaters in both aquifers are characterised by a wide range of Na^+ and Cl^- concentration. However, in no case was the activity product of Na^+ and Cl^- close to saturation with respect to halite (~3.5 g/l-Table 3.2). This indicates the absence of Cl^- bearing salts in the saturated aquifer matrix but does not rule out its presence in the unsaturated zone. X-ray diffraction analysis and petrographic study of the aquifer minerals did not reveal any evaporite minerals such as halite or sylvite (Appendix 1).

Dilution of waters saturated with halite during recharge can also cause the dominance of Na^+ and Cl^- of groundwater and cannot be ruled out. This can be checked by observing the Cl^-/Br^- ratio in groundwater. The Cl^-/Br^- mass ratio of halite is one to two orders of magnitude higher than the marine Cl^-/Br^- ratio of ~ 290 due to the exclusion of Br^- from the NaCl crystal lattice during halite precipitation (Braitsch, 1971). The observed Cl^-/Br^- ratio in groundwater samples in both aquifers ranges from 250 to 350 typical of the marine Cl^-/Br^- ratio. This eliminates halite dissolution being the process that modifies the Cl^- and Br^- concentrations.

3.3.1.3 Evaporation of water dominated by Cl^- and Na^+ ions prior to recharge

In order to examine this scenario, we assume that dissolved Na^+ and Cl^- in groundwater in the Murray Group Aquifer is derived entirely from rainfall. Data on the distribution of major ions in rainfall over the Murray Basin showed that Na^+ and Cl^- ions are the

dominant major anion and cation in rainfall, and their mean concentrations are 4.3 and 2.5 mg/l respectively (Blackburn and McLeod, 1983). Chloride concentration in the fresh groundwater at the basin margin (south-east) in the Murray Group Aquifer is about 300 mg/l (Table 3.2). Assuming the average Cl^- concentration in rainfall is 4.3 mg/l, the estimated water loss by evaporation calculated from equation (3.1) is 98%,

$$Q = \frac{Cl_g - Cl_r}{Cl_g} x100 \qquad (3.1)$$

where Q is the percent of water loss and Cl_g and Cl_r are the concentrations of chloride in groundwater and rainwater respectively.

Evaporation of water prior to recharge not only increases the major ion concentration but also leads to enrichment in ^2H and ^{18}O isotopes in the remaining water. Simpson and Herczeg (1991) found a δ^2H enrichment of about 0.75‰ per 1 % evaporation loss in surface waters of the semi-arid regions of the Murray Basin by using a model by Gonfiantini (1986). Using a mean δ^2H value for rainfall in the study area of -24‰ (Leaney et al., 1995), and water loss by evaporation of 98%, the amount of evaporation causes enrichment in δ^2H of ~72 ‰. Accordingly the measured δ^2H of the groundwater would be +48‰. This value is much higher than the measured δ^2H values in both aquifers (Table 3.2), therefore evaporation alone cannot explain the dominance of Na^+ and Cl^- in groundwater.

3.3.1.4 Evapotranspiration of soil water prior to recharge

The study area was mostly covered by native vegetation prior to European settlement ~ 200 years ago. This vegetation is dominated by mallee form 'eucalyptus' that are characterised by multi-trunks and deep roots up to 20 m, capable of intercepting and transpiring most of the infiltrating rainfall (Walker et al., 1990). Water uptake by these plants increases the major ion concentration in recharge water. However the original $\delta^{18}O$ and $\delta^{2}H$ composition (derived from rainfall) is maintained. This occurs because no significant fractionation of the heavy isotopes is observed during plant transpiration (Zimmerman et al., 1967; Allison et al., 1983 b). The $\delta^{18}O$ and $\delta^{2}H$ values reported for pore water from many deep soil profiles in the study area, are similar to the mean $\delta^{18}O$ and $\delta^{2}H$ values in rainfall (Hughes et al., 1988 a, b; Jolly et al., 1990; Cook et al., 1992). Therefore, the most likely scenario for the dominance of Na^{+} and Cl^{-} ions in groundwater of the Murray and Renmark Group aquifers is the removal of water by transpiration of deep rooted native vegetation prior to recharge.

3.3.2 Variation of Cl^{-} concentration in the Murray Group Aquifer

Whereas the concentration of Cl^{-} in the Murray Group Aquifer generally increases along the hydraulic gradient, the spatial distribution of Cl^{-} indicates that the lowest Cl^{-} concentration (~ 250 mg/l) occurs in the middle of Zone A rather than at the basin margin (Fig. 3.9). The rapid increase and decrease of Cl^{-} in adjacent wells can be clearly seen when Cl^{-} concentrations are plotted along the hydraulic gradient (Fig. 3.2 a).

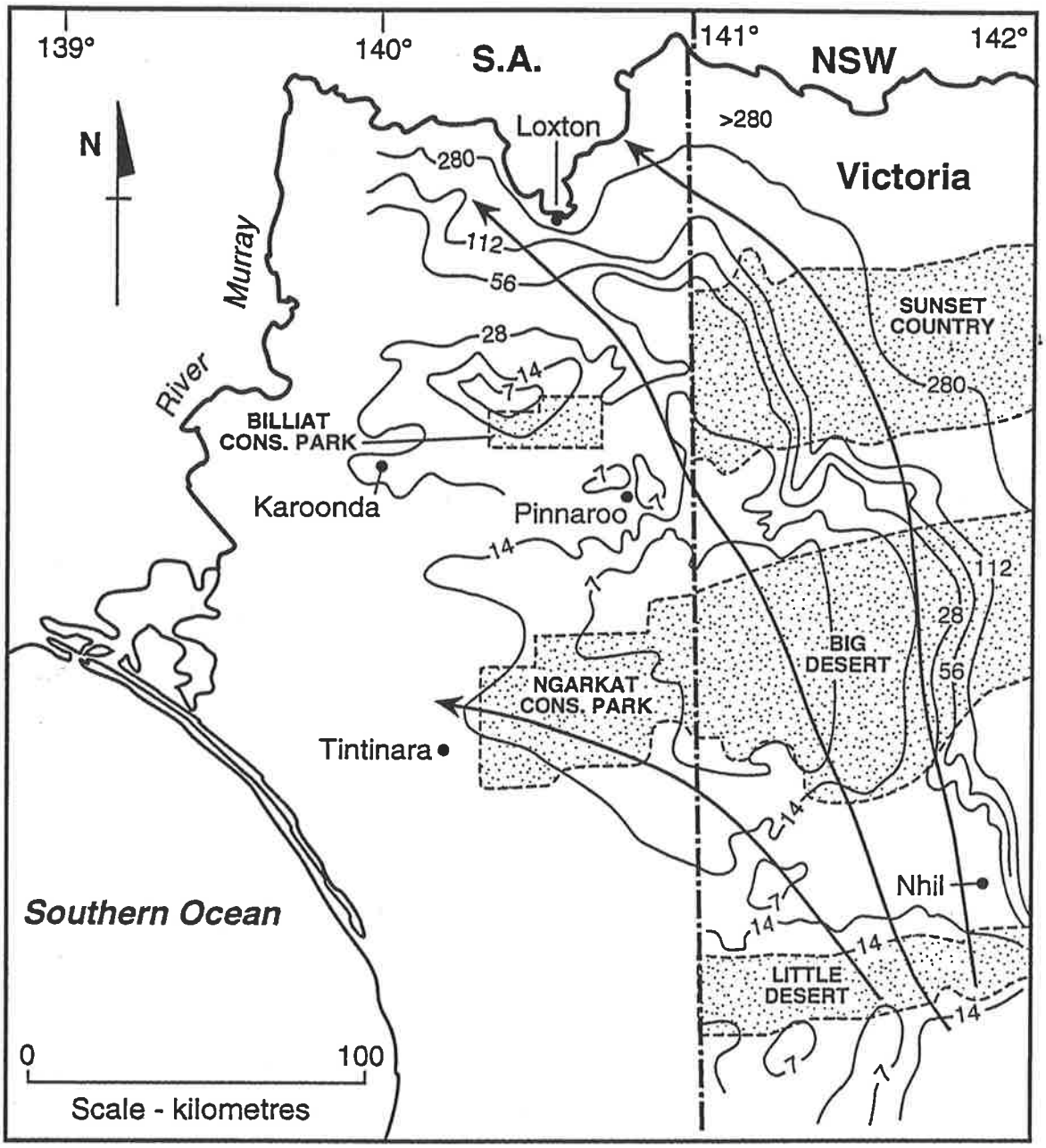

Fig. 3.9 Spatial distribution of chloride concentration in mmol/l in the Murray Group Aquifer. Arrows represent inferred groundwater flow direction.

Chloride is a conservative ion which does not take part in chemical reactions within the range of salinity discussed here (Feth, 1981), and there are no other sources for Cl^- in the Murray Group Aquifer but rainfall. Therefore, the variation of Cl^- observed along the gradient can only occur via mixing with waters with different Cl^- concentrations. Because marine relative abundance of Cl^-, Na^+ and Br^- is maintained over the entire range of Cl^- concentration (Fig. 3.8 a, b), the end member which is mixing with laterally flowing groundwater must be from the local recharge derived from rainfall which also has a marine relative abundance of Cl^-, Na^+, and Br^-.

The concentration of Cl^- in soil water that eventually recharges the aquifer depends on several factors; (1) concentration of Cl^- in rainfall plus contribution of dry fallout, (2) evapotranspiration (3) soil texture, and (4) vegetation type (Allison and Hughes, 1983; Leaney and Allison, 1986; Simpson and Herczeg, 1993; Kennett-Smith et al., 1994). Mixing of this water along the hydraulic gradient with laterally flowing groundwater can cause the variable distribution of Cl^-, whilst maintaining the marine relative abundance of Cl^-, Na^+ and Br^- in groundwater. If the contribution of local recharge on the other hand was not significant, and the Cl^- concentration originated from one single input at the basin margin, followed by lateral flow, the Cl^- distribution would be uniform along the gradient.

3.3.3 Sulphate distribution in the Murray and Renmark Group aquifers

Sulphate concentrations in groundwater shows a positive linear relationship with Cl^-

concentrations with a slight scatter around the sea water dilution line (Fig. 3. 10 a). The SO_4^{2-} concentrations in Zone A tend to fall to the left of the line, whereas the SO_4^{2-} concentration of Zone B and the Renmark Group Aquifer fall to the right of the sea water dilution line. The scatter is probably due to variation of the SO_4^{2-} content of rainfall which eventually recharges the Murray Group Aquifer. Although the SO_4^{2-}/Cl^- ratio of soil water derived from rainfall in the coastal areas is similar to that of sea water, often the SO_4^{2-}/Cl^- ratio increases further inland in rainfall due to a contribution of biogenic derived sulphur to the sulphate pool of the atmosphere (Newman et al., 1991). Therefore, the "excess" SO_4^{2-} in groundwater in Zone A may be due to addition of this biogenic SO_4^{2-} to the sulphate pool of rainfall which recharges the Murray Group Aquifer (A detailed discussion of SO_4^{2-} concentrations in groundwater from the Murray and Renmark Group aquifers is given in chapter 4). The relatively low SO_4^{2-} concentrations in the Zone B of the Murray Group Aquifer and the Renmark Group Aquifer may be due to bacterial sulphate reduction. Bacterial sulphate reduction results in the decrease of sulphate concentration in groundwater. The evidence for the occurrence of bacterial sulphate reduction in Zone B and in the Renmark Group Aquifer is obtained from sulphur and oxygen isotopic values of sulphate (see Chapter 4).

3.3.4 Potassium distribution in the Murray and Renmark Group aquifers

Potassium concentrations in groundwater positively correlate with Cl^- in the Murray and Renmark Group aquifers. The K^+ concentrations of relatively fresh groundwater in Zone A are slightly higher compared with the sea water composition and falls to the

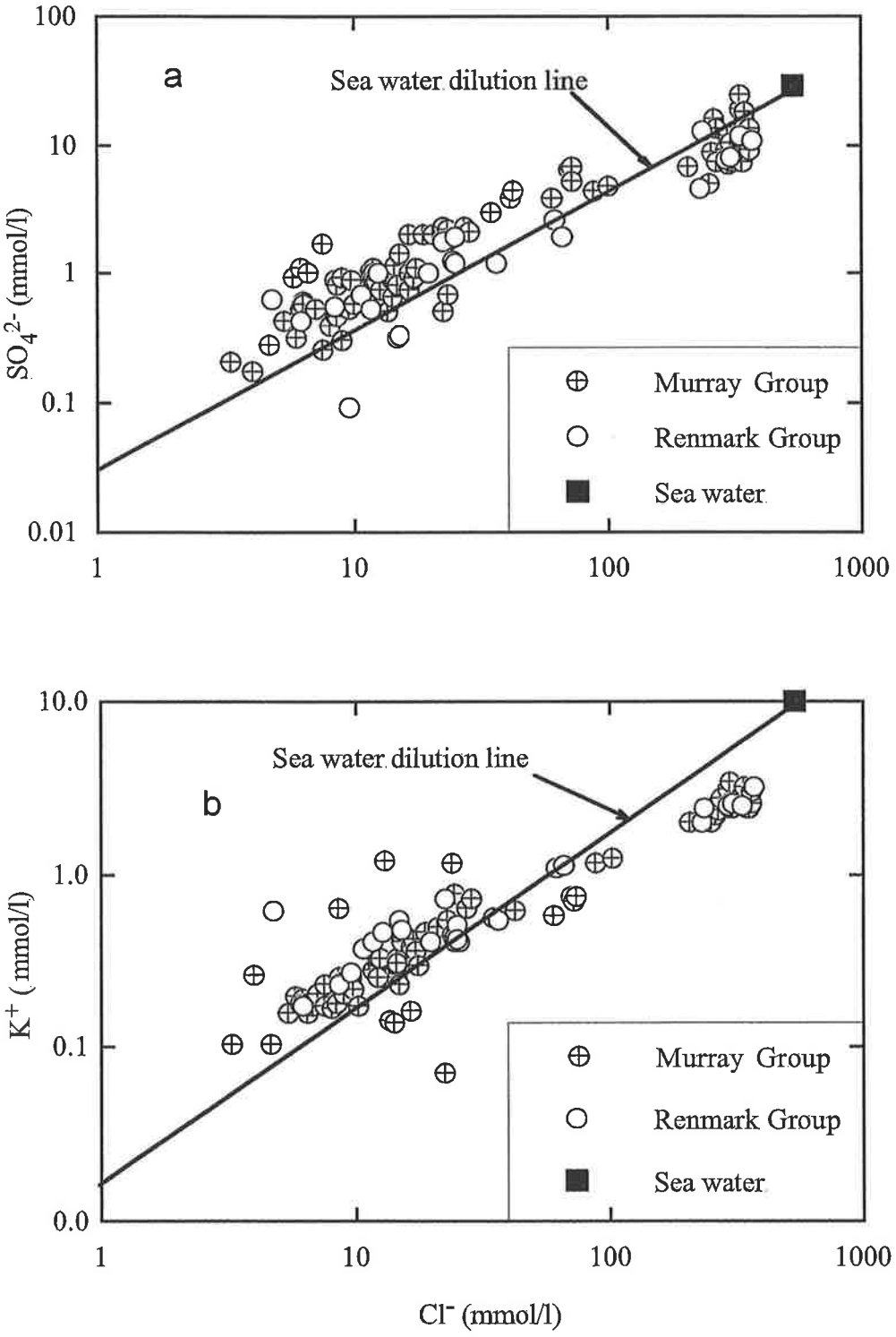

Fig. 3.10 a, b Sulphate and K^+ vs. Cl^- concentration of groundwater from the Murray and Renmark Group aquifers. The higher SO_4^{2-} concentration relative to sea water in the Murray Group Aquifer is probably due to the contribution of biogenically derived SO_4^{2-} to the rainfall that recharges the aquifer. K^+ vs. Cl^- data in both aquifers deviate from the sea water dilution line indicating that groundwater has been modified by cation exchange reaction within the aquifer.

left of sea water dilution line. Whereas, at Zone B the K^+ concentration of more saline groundwater falls to the right of the sea water dilution line (Fig. 3.10 b) indicating removal of K^+ ions from groundwater by chemical reactions. Reactions involving K^+ that take place at ambient temperature and pressure involve cation exchange with clay minerals. The exchange of K^+ for Na^+ on clay minerals could be the process that is responsible for the partial removal of K^+ from the groundwater. Exchange of K^+ for Na^+ is a well known process in dilute groundwaters (Eugster and Jones, 1979). Potassium concentration increases approximately 10 fold from 0.4 mmol/l to 5 mmol/l, whereas Na^+ concentration increases 100 fold. The Na^+/Cl^- ratio for the majority of the groundwater samples is slightly higher than the sea water ratio, the lower than expected K^+ value in the Murray and Renmark Group aquifers in Zone B may be caused by removal of K^+ from groundwater by exchange with Na^+ on clay minerals via a cation exchange reaction.

3.3.5 Ca^{2+}-Mg^{2+}-HCO_3^- relationship in the Murray Group Aquifer

Groundwater in the Murray Group Aquifer is enriched relative to the sea water dilution line in Ca^{2+}, and Mg^{2+} (Fig. 3.11 a, b). Ca^{2+} and Mg^{2+} have a relatively small concentration range of 0.8 to 2.5, and 0.8 to 6.5 mmol/l respectively, compared with the large range of 10 to 370 mmol/l for Cl^- concentration. This suggests that in addition to evapotranspiration, the Ca^{2+} and Mg^{2+} concentrations are affected by chemical reactions in the unsaturated zone or in the aquifer. The processes which are likely to be most important in modifying the Ca^{2+} and Mg^{2+} concentrations within the Murray

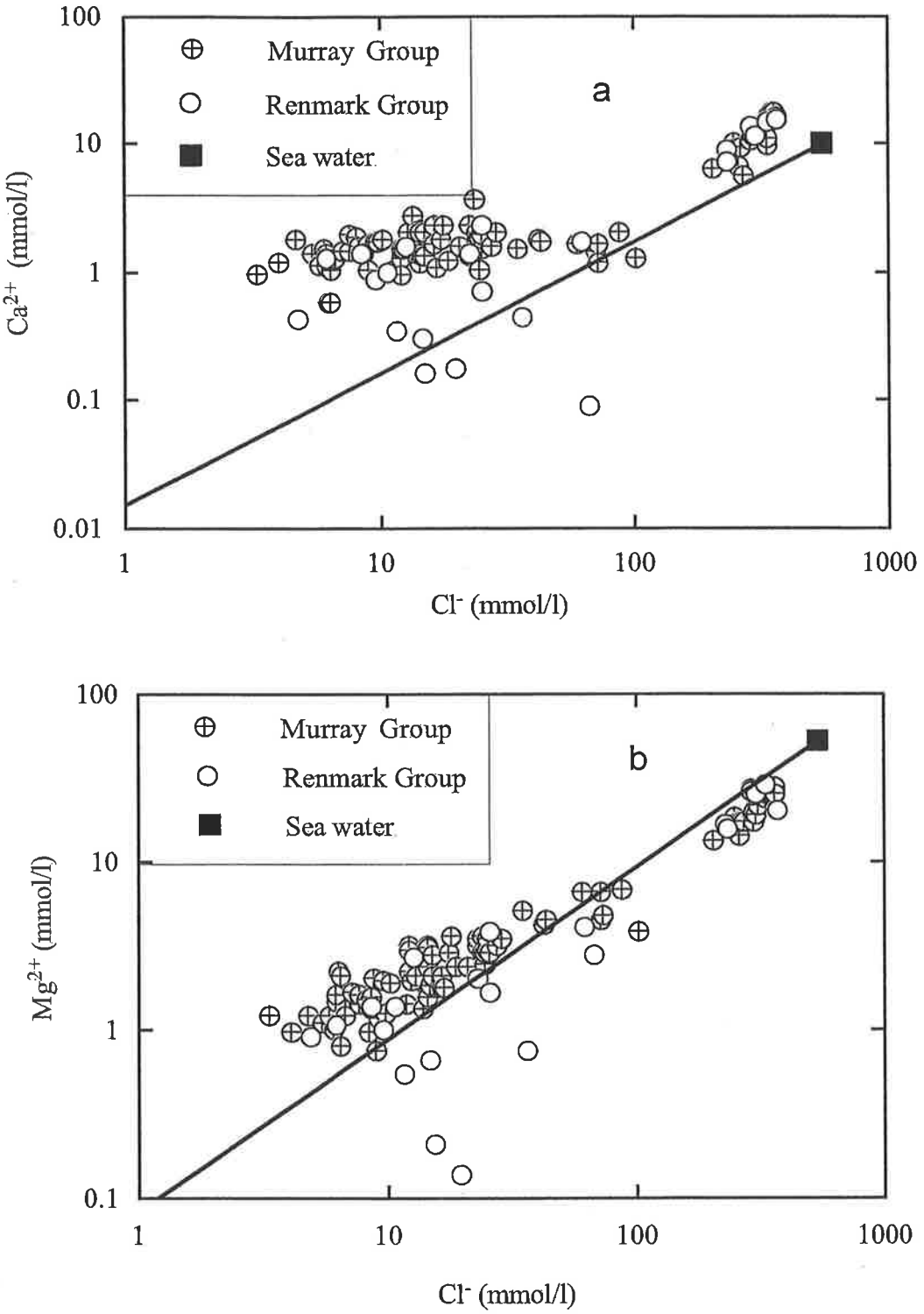

Fig 3.11 a, b Calcium and Mg^{2+} vs. Cl^- concentration of groundwater from the Murray and Renmark Group aquifers. The higher Ca^{2+} and Mg^{2+} concentrations relative to sea water in the Murray Group Aquifer in Zone A suggest that groundwater has been modified by reactions occuring within either the unsaturated zone or the aquifer.

Group Aquifer include congruent and incongruent dissolution of carbonate minerals, and silicate weathering.

Carbonate dissolution reactions in the unsaturated zone occurs in two steps; (1) acquisition of CO_2 in soil water derived from respiration of plants and bacterial oxidation of organic matter in the soil zone followed by, (2) reaction with carbonate minerals, resulting in the addition of Ca^{2+}, Mg^{2+} and HCO_3^- to the solution. The carbonate dissolution reactions may be expressed by the following reactions:

Congruent Dissolution of carbonate minerals

$$(Ca_{1-x}Mg_x)CO_3 + H_2O + CO_2 \leftrightarrow (1-x)\ Ca^{2+} + xMg^{2+} + 2HCO_3^- \qquad (3.2)$$

Incongruent Dissolution of carbonate minerals

$$(Ca_{1-x}Mg_x)CO_3 + Ca^{2+}{}_x \leftrightarrow CaCO_3 + xMg^{2+} \qquad (3.3)$$

Carbonate minerals are ubiquitous in the soil zone in the study area and their concentration varies over three order of magnitude from < 0.1% to ~ 50% by weight (McCord, 1997). The mole fraction of Mg^{2+} of 28 Murray Group limestone samples were estimated from XRD analysis and ranged from 5% to 11%. However, no information exists on the mole fractions of Mg^{2+} in carbonates in the soil zone. However, if dissolved Ca^{2+}, Mg^{2+} and HCO_3^- in the groundwater results mainly from dissolution of carbonate minerals according to equation 3.1, then the molar proportions of (Ca^{2+}+Mg^{2+}) to HCO_3^- should be linear with a slope of 0.5. The Ca^{2+} and Mg^{2+} concentrations are summed together because of the variability of the Mg^{2+} mole

fraction within the carbonate minerals. The line of regression of Ca^{2+}+Mg^{2+} versus HCO_3^- (Fig. 3.12 a) for groundwater samples in the Murray Group Aquifer has a slope of 0.41 with a correlation coefficient (r^2) of 0.5. The scatter and poor correlation coefficient of data suggest additional processes modifying the (Ca^{2+}+Mg^{2+}) and HCO_3^- relationship in the Murray Group Aquifer.

One possible mechanism responsible for the deviation of (Ca^{2+}+Mg^{2+}) vs. HCO_3^- data from the carbonate dissolution line of 0.5 is calcite precipitation during evapotranspiration. Progressive water loss by evapotranspiration causes an increase in the HCO_3^- and Ca^{2+} concentration of soil water until calcite saturation is attained. Beyond the calcite saturation point, the increase in HCO_3^- and Ca^{2+} concentrations of soil water is coupled with their removal by calcite precipitation. Because calcite precipitation removes half as much Ca^{2+} as HCO_3^- according to the stoichiometry of the calcite precipitation reaction (Eq. 3.2), the ratio of Ca^{2+}/HCO_3^- remains unchanged if the initial Ca^{2+}/HCO_3^- ratio in soil water was 0.5. That is, the amounts of Ca^{2+} and HCO_3^- increase beyond calcite saturation by evapotranspiration equals the amount of Ca^{2+} and HCO_3^- removed from the solution by calcite precipitation. However, if the Ca^{2+}/HCO_3^- ratio of soil water was greater than or less than 0.5, then calcite precipitation causes change of the Ca^{2+} /HCO_3^- ratio of the residual water due to the removal of Ca^{2+} and HCO_3^- with a ratio of 0.5. This is known as a chemical divide which was articulated by Eugster and Jones (1979). The higher the amount of water loss from soil water beyond calcite saturation the greater the shift will be from the evaporation line (3.12 b).

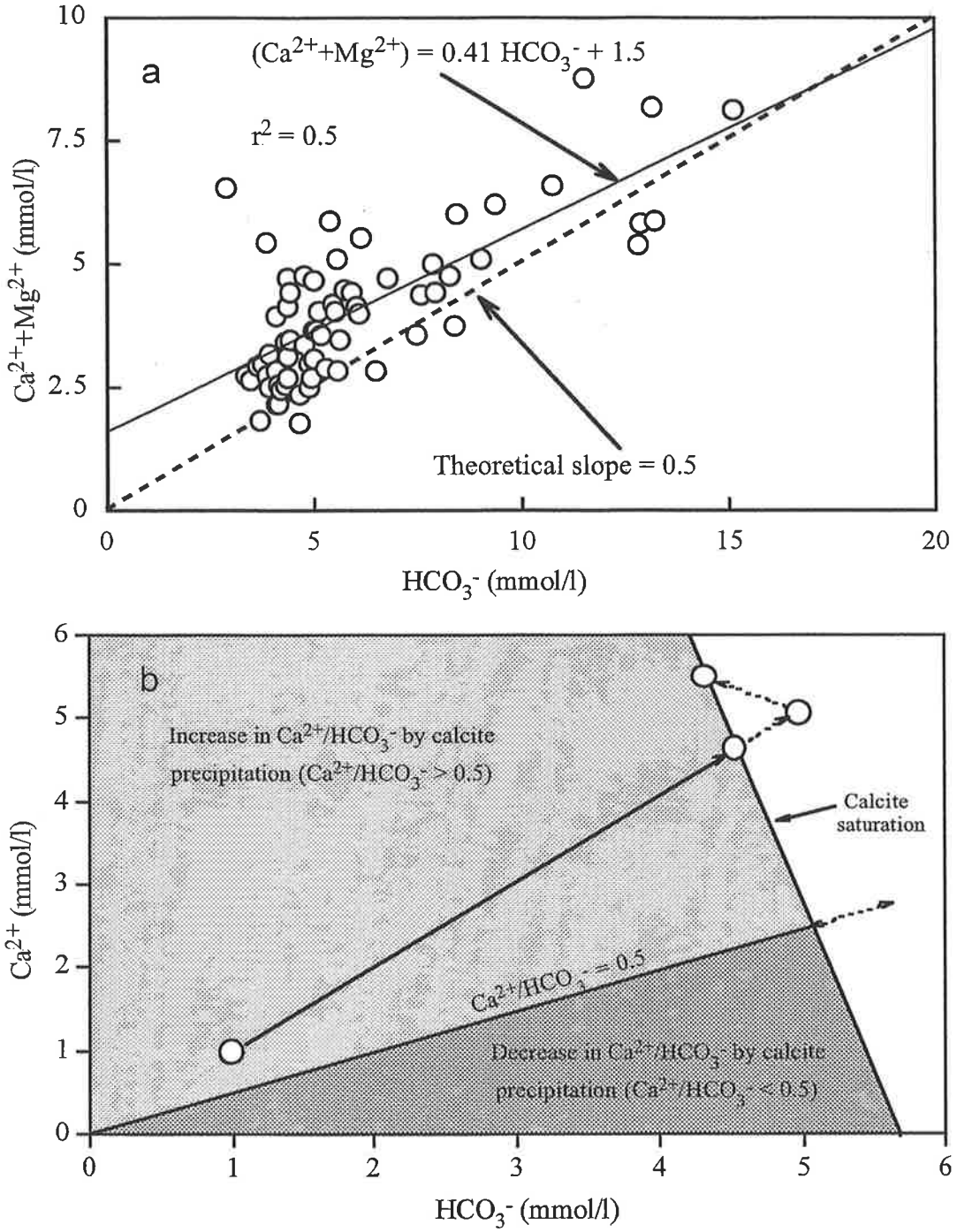

Fig. 3.12. a, b The relationship between (Ca^{2+} + Mg^{2+}) and HCO_3^- of groundwater of the Murray Group Aquifer in Zone A. (b) Schematic diagram for the evolution of soil water during evapotranspiration and calcite precipitation. Diagonal line represent calcite saturation. Evapotranspiration of soil water that falls into the light gray area (Ca^{2+} / HCO_3^- > 0.5) beyond calcite saturation causes an increase in Ca^{2+} / HCO_3^- ratio whereas, evapotranspiration of soil water that falls into the dark gray area (Ca^{2+} / HCO_3^- < 0.5) beyond calcite saturation causes a decrease of the Ca^{2+} / HCO_3^- ratio. Open circles represent various stages of soil water evolution that have an initial Ca^{2+} / HCO_3^- ratio of 1 by evapotranspiration.

The deviation of the data from the carbonate dissolution line in Fig. 3.12 a therefore, may be caused by calcite precipitation during evapotranspiration of soil water. However, incongruent dissolution of carbonate minerals in the aquifer can also result in an increase of the (Ca^{2+}+Mg^{2+}) concentration relative to HCO_3^-, causing the deviation observed from the carbonate dissolution line. The effect of this process on the Ca^{2+} and Mg^{2+} is discussed below.

3.3.6 Incongruent dissolution of Mg-calcite

The degree of calcite saturation that results from the mixing of soil water in equilibrium with respect to calcite with groundwater flowing laterally depends on the final pCO_2, temperature, final chemical composition and the proportion of mixing of the two end members (Wigley and Plummer, 1976). Often, the calculated activities of individual ions in a mixture are not equal to that calculated by conservative mixing of the two end members, and this is particularly true in a carbonate system, due to the differences of ionic strength and the redistribution of carbonate species (H_2CO_3, HCO_3^-,CO_3^{2-}) in the mixture. For example, two end members which are both saturated with respect to calcite can yield a mixture that is either saturated or undersaturated depending on the relative proportions and chemical characteristics of the two end members (Thrailkill, 1968; Wigley and Plummer, 1976).

Most of the groundwater samples from the Murray Group Aquifer in Zone A are close to saturation with respect to calcite (Table 3.2), indicating that no further dissolution of

calcite occurs in the groundwater following addition of soil water to laterally flowing groundwater. However, incongruent dissolution of Mg-calcite (equation 3.3) and subsequent precipitation of calcite can change the relative concentration of Ca^{2+} and Mg^{2+}, by releasing more Mg^{2+} than Ca^{2+} to groundwater which causes the Mg^{2+}/Ca^{2+} ratio to increase. Because the overall change in Ca^{2+} and HCO_3^- during this process is small (Wigley et al., 1978), the change in the Mg^{2+}/Ca^{2+} ratio is a useful indicator of the extent of this process in the Murray Group Aquifer. Groundwater with a Mg^{2+}/Ca^{2+} ratio <1 tends to occur in relatively fresh water in the south and south-eastern part of Zone A (Fig. 3.13-Table 3.2).

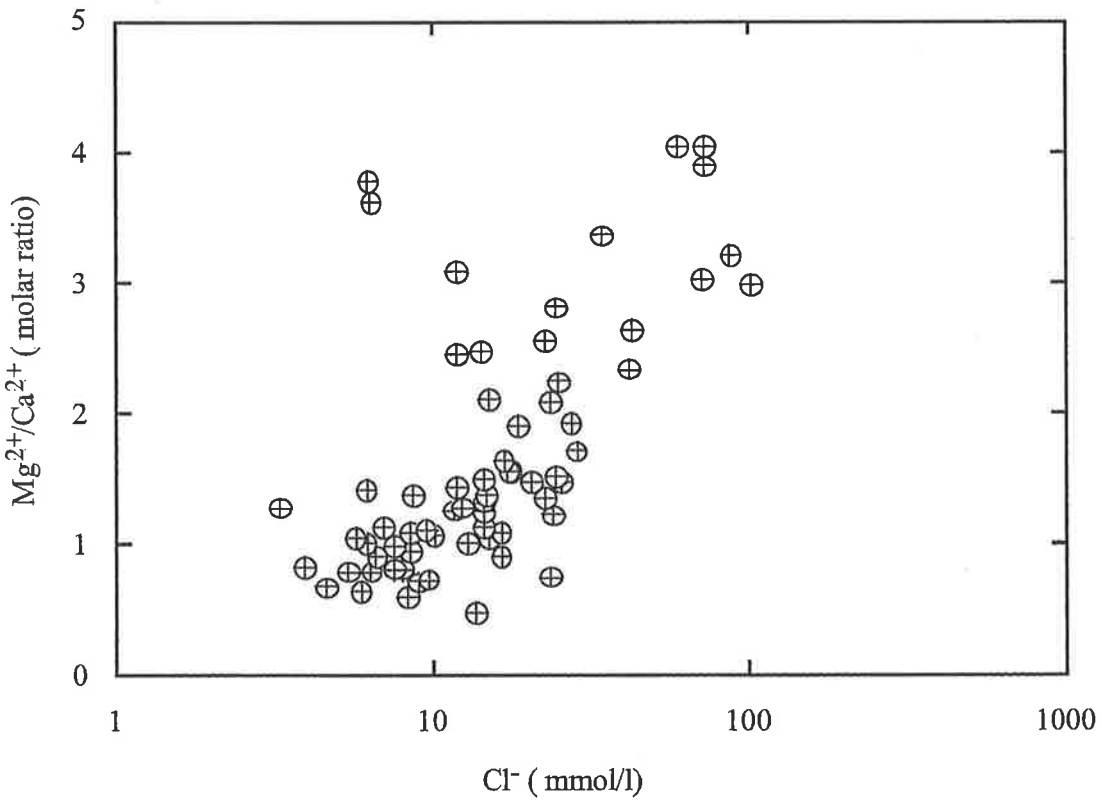

Fig. 3.13 The relationship between Cl^- concentration and Mg^{2+}/Ca^{2+} ratio in the Murray Group Aquifer. Note that the Mg^{2+}/Ca^{2+} ratio increases with an increase in Cl^- concentration

The Mg^{2+}/Ca^{2+} ratio increases with the increase of Cl^- concentration and reaches values of ~ 4 in groundwaters that are located to the northern part of Zone A (Table 3.2). Incongruent dissolution of Mg^{2+} calcite and the addition of Mg^{2+} to the groundwater may be the second process that causes the observed (Ca^{2+}+Mg^{2+}) and HCO_3^- relationship in the Murray Group Aquifer (Fig. 3.12 a). The effect of incongruent dissolution of Mg-calcite on the increase of Mg^{2+} and Sr^{2+} concentrations relative to Ca^{2+}, as well as the Sr^{2+} isotope distribution, will be discussed in more detail in Chapter 5.

3.3.7 Silicate weathering

Addition of Ca^{2+} to the soil water can be accomplished by dissolution of primary silicates (anorthite) or conversion of Ca-smectite to kaolinite according to the following equations:

Anorthite (Gibbsite)

$$CaAl_2Si_2O_8 + 2CO_2 + 8H_2O \leftrightarrow 2Al(OH)_3 + Ca^{2+} + 2H_4SiO_4 + 2HCO_3^- \quad (3.5)$$

Ca-smectite (beidellite) (Kaolinite)

$$6Ca_{0.167}Al_{2.33}Si_{3.67}O_{10}(OH)_2 + 2CO_2 + 25H_2O \leftrightarrow 7Al_2Si_2O_5(OH)_4 + Ca^{2+} + 8H_4SiO_4 + 2HCO_3^- \quad (3.6)$$

Because these reactions release 2 mole of HCO_3^- for each mole of Ca^{2+} produced, their effect on the overall Ca^{2+}/ HCO_3^- ratio of groundwater cannot be distinguished from the calcite dissolution. However, because these reactions also add significant amounts of dissolved silica to the solution, the concentration of dissolved silica should increase if the source of Ca^{2+} and HCO_3^- in groundwater of the Murray Group Aquifer was

primary silicate dissolution or conversion of Ca-smectite. Silica concentration in the Murray Group Aquifer unlike other chemical species does not increase in Zone A (Table 3.2), therefore the above mentioned reactions are not likely to be the cause for the modification of Ca^{2+} and HCO_3^- concentrations.

3.3.8 Development of a reaction model to explain Ca^{2+} Na^+ and HCO_3^- distribution

Geochemical mass balance calculations were performed to test whether evapotranspiration of rain water that ultimately recharges the aquifer, followed by equilibrium with carbonate minerals and cation exchange reactions are responsible for the observed chemical composition of the groundwater in the Murray Group Aquifer. The evapotranspiration of rain water, calcite equilibrium and cation exchange in the soil zone performed under different soil gas CO_2 partial pressures simulating the range of pCO_2 measured in the study area (Dighton and Allison, 1985). The rainfall data in the study area is the average of rainfall chemical composition measured in the south-eastern Murray Basin by Blackburn and McLeod (1983-Table 3.4).

Table 3.4 The Average chemical composition of rain water in the south-eastern Murray Basin in mg/l (Blackburn and McLeod, 1983)

Na^+	K^+	Ca^{2+}	Mg^{2+}	Cl^-	SO_4^{2-}	HCO_3^-
			(mg/l)			
2.48	0.35	1.2	0.57	4.25	3.84	0.91

A geochemical speciation, mass transfer and mixing computer code PHREEQM (Nienhuis et al., 1993, based on PHREEQE, Parkhurst et al., 1980) was used to perform this exercise. PHREEQM is an interactive computer code that can be used to predict the results of a set of hypothetical reactions by defining initial water composition and associated minerals. Mass transfer between the aqueous and solid phases in the hypothetical irreversible mineral-water reactions can be calculated and the chemical composition of the computed solution is compared with the measured chemical data to validate the reaction model hypothesis.

Evapotranspiration was simulated by subtracting H_2O molecules from the rainwater in 10 steps representing progressive water loss from the recharge water until 99.9% of the initial amount of water was lost. The residual solution in each step was equilibrated with calcite and cation exchange between Ca^{2+} with Na^+ under a fixed soil pCO_2. The equilibrium constant (Kd) of 0.5 was used for the cation exchange reaction. Na^+ and Ca^{2+} concentration increases due to evapotranspiration, and Na^+ is released from clay minerals in exchange for Ca^{2+}. The Na^+/Ca^{2+} ratio therefore increases with the evolution of chemical composition of soil water. In addition to this, removal of Ca^{2+} may perturb the calcite equilibrium state, allowing the dissolution of more calcite, which adds bicarbonate into the solution, thus increasing the total bicarbonate concentration. Therefore, the HCO_3^- concentrations, and the Na^+/Ca^{2+} ratio were used as indicators in comparing the modeled and observed groundwater data.

The modeled results are shown in Fig. 3.14 by solid lines on a graph of bicarbonate concentration versus Na^+/Ca^{2+} ratios in equilibrium with calcite, at pCO_2 of 10^{-1}, $10^{-1.5}$ and 10^{-2} atmospheres.

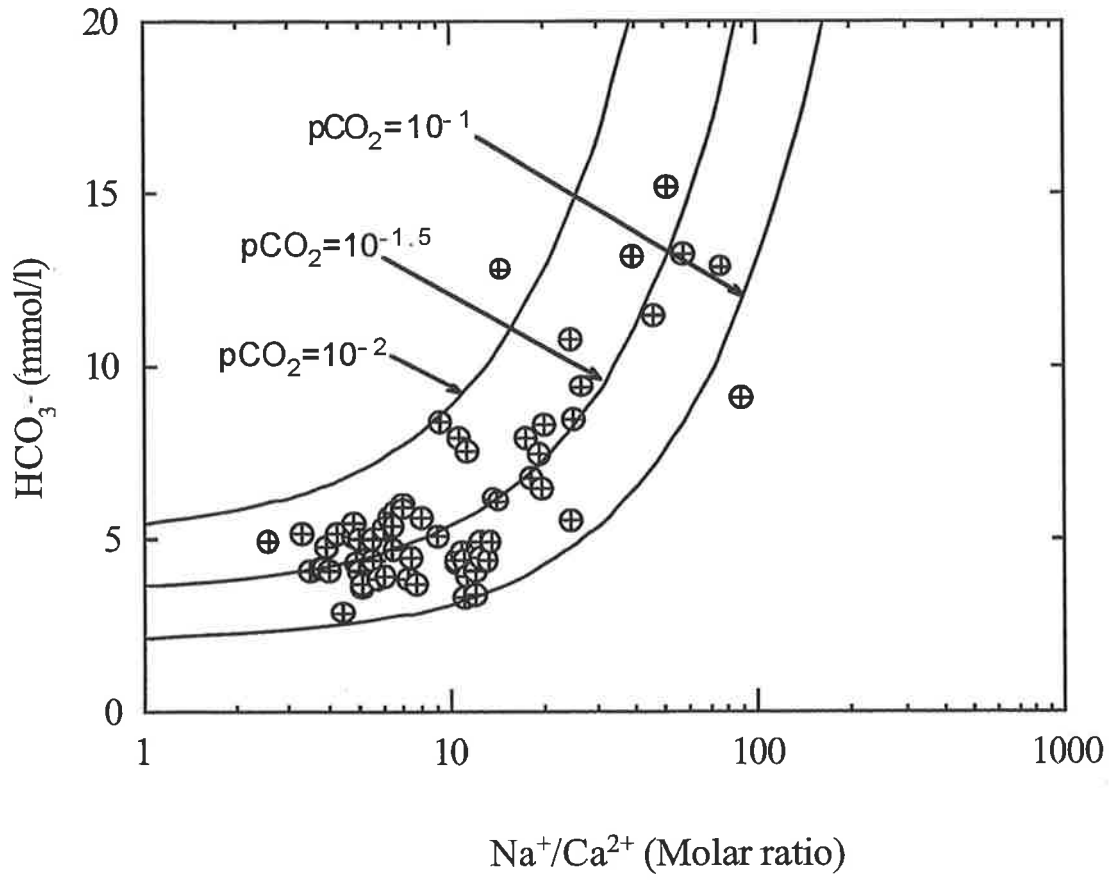

Fig. 3.14 The relationship between Na^+/Ca^{2+} molar ratio and bicarbonate concentration of groundwater from the Murray Group Aquifer. The solid lines on the graph are bicarbonate concentrations and Na^+/Ca^{2+} ratio in equilibrium with calcite, at pCO_2 of 10^{-1}, $10^{-1.5}$ and 10^{-2} atmosphere calculated by computer code PHREEQM (see text).

The observed data from the Murray Group Aquifer suggest that the evolution of recharge water occurs at pCO_2 between 10^{-1} and 10^{-2} atmospheres, which is typical of CO_2 concentrations in the soil zone in the study area (Dighton and Allison, 1985).

This suggests that the model proposed above adequately accounts for the distribution of the dissolved Na^+, Ca^{2+}, and HCO_3^- observed in the Murray Group Aquifer in Zone A.

3.3.9 Variation of TDS in the Renmark Group Aquifer (Zone A)

The dominance of Cl^- and Na^+ ions and their linear relationship, along with the δ^2H and $\delta^{18}O$ data, suggests that the major source for these ions in groundwater from the Murray and Renmark Group aquifers is evapotranspiration of soil water derived from rainfall (see section 3.3.1). Marine relative abundances of Cl^-, Na^+ and Br^- are maintained in both aquifers throughout the study area. However, the Cl^- concentration of the confined Renmark Group Aquifer plotted along the hydraulic gradient (Fig. 3.15) displays an irregular distribution with sharp increases and decreases in adjacent wells. One possible reason is a variable Cl^- concentration due to downward leakage from the overlying Murray Group Aquifer. Figure 3.15 shows that the Cl^- concentrations in the Renmark Group Aquifer along the AA` transect mimic the Cl^- variations in the Murray Group Aquifer. However, the Cl^- concentration of groundwater at Zone A (Fig 3.15) is higher than those measured in the Murray Group Aquifer at the same locations. If the downward leakage was the main mechanism affecting Cl^- concentration in the Renmark Group Aquifer then the maximum Cl^- concentration in the Renmark Group Aquifer would be similar to that of the Murray Group Aquifer at the same location, assuming all the Cl^- was derived through downward leakage and that the measured Cl^- concentrations of the groundwater are identical to the Cl^- concentrations at the bottom of the Murray Group Aquifer.

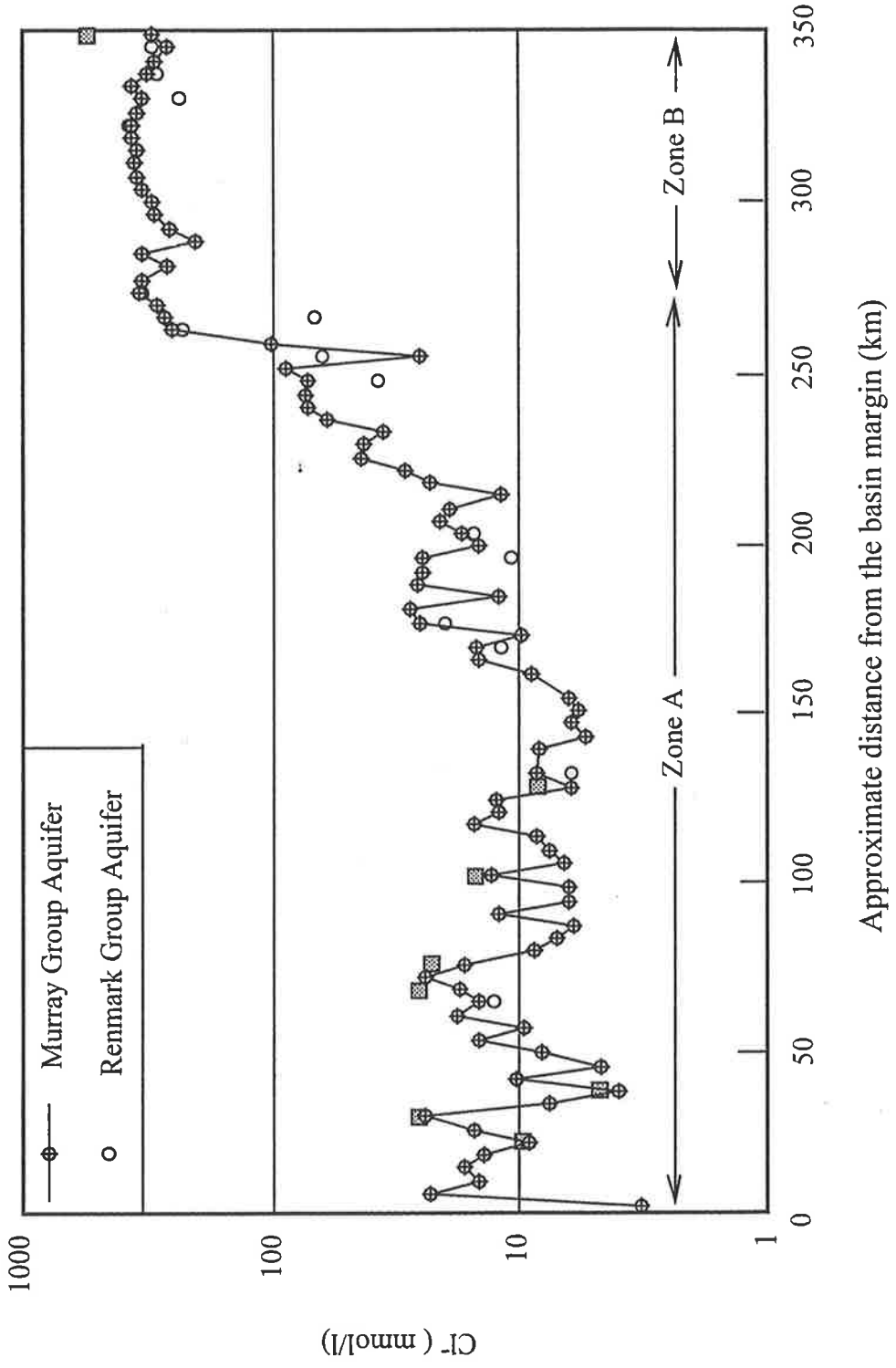

Fig. 3.15 The variation of Cl⁻ concentration in mmol/l of groundwater from the Murray and Renmark Group aquifers along the AA` transect. The rectangular symbols denote the groundwater samples from the Renmark Group Aquifer that have higher Cl- concentration compared to the groundwater samples from the Murray Group Aquifer at the same location.

There is no evidence for an increase of Cl^- concentration with depth from the water table in the Murray Group Aquifer (see chapter 4). Barnett (1983) sampled thirty wells throughout the central and northern part of the study area at different depths below the water table, and found that the Cl^- concentration decreases with depth. He attributed the decrease in Cl^- concentration with depth to the mixing of more saline local recharge water with laterally flowing groundwater. This suggests that the Cl^- concentration at the bottom of the aquifer may be lower than that measured in the water samples because the water samples obtained in this study are mainly from the top 50-70 m of the Murray Group Aquifer. Therefore, mixing through downward leakage is not the process causing the irregular distribution of Cl^- in the Renmark Group Aquifer.

The variation of Cl^- concentration in the Renmark Group Aquifer along the hydraulic gradient is more likely due to variations in the amount of water loss by evapotranspiration prior to recharge over time at the basin margin (Dundas Plateau). Alternating wet and dry periods can potentially cause a variation in the concentration of Cl^- in recharge water due to the change in net evapotranspiration (Schwartz et al., 1981; Love, 1993) which in turn is affected by a change in the type of vegetation cover (Bowler, 1990). A consequence of this is that the concentration of major ions will change in the recharge water, with higher concentrations corresponding to drier climates. The mean travel time of groundwater in the Renmark Group Aquifer, along the longest flow path is ~200,000years (Evans and Kellett, 1989). The change in climate of the

Australian continent and other parts of the world over the last 200,000 years is well documented (Luly et al., 1986; Bowler, 1990; Wasson and Donnelly, 1991; Wood and Imes, 1995; Stute et al., 1995) and shows alternating humid and dry periods. Therefore, variations in Cl^- concentrations in the confined Renmark Group Aquifer may represent a proxy record of the alternating humid and dry climate over the past 200,000 years.

3.3.10 The effect of evapotranspiration on chemical composition of groundwater in the Renmark Group Aquifer

The variable amount of water loss during evapotranspiration causes variation in the concentration of Cl^- and other major ions at the same rate. Thus the cation or anion to Cl^- ratios remain constant with an increase in the absolute concentration of Cl^- if all ions behave conservatively during evapotranspiration. If this were true and the only process for the distribution of major ions was the variation in evapotranspiration, the ions/Cl^- versus Cl^- concentration from the Renmark Group Aquifer should fall on a straight line parallel to the X axis in Fig. 3.16 a, b, c, d. On the other hand, if the major ion concentration was modified by reactions with the aquifer matrix, the ion/Cl^- and Cl^- concentration might fall on a line with a positive or negative slope, depending on the net addition or removal of respective ions from the groundwater. Mixing of groundwater in the Renmark Group Aquifer through downward leakage from the Murray Group Aquifer can also cause the latter relationship. However, groundwater from the Renmark Group Aquifer in Zone A has a higher Cl^- concentration than the Murray

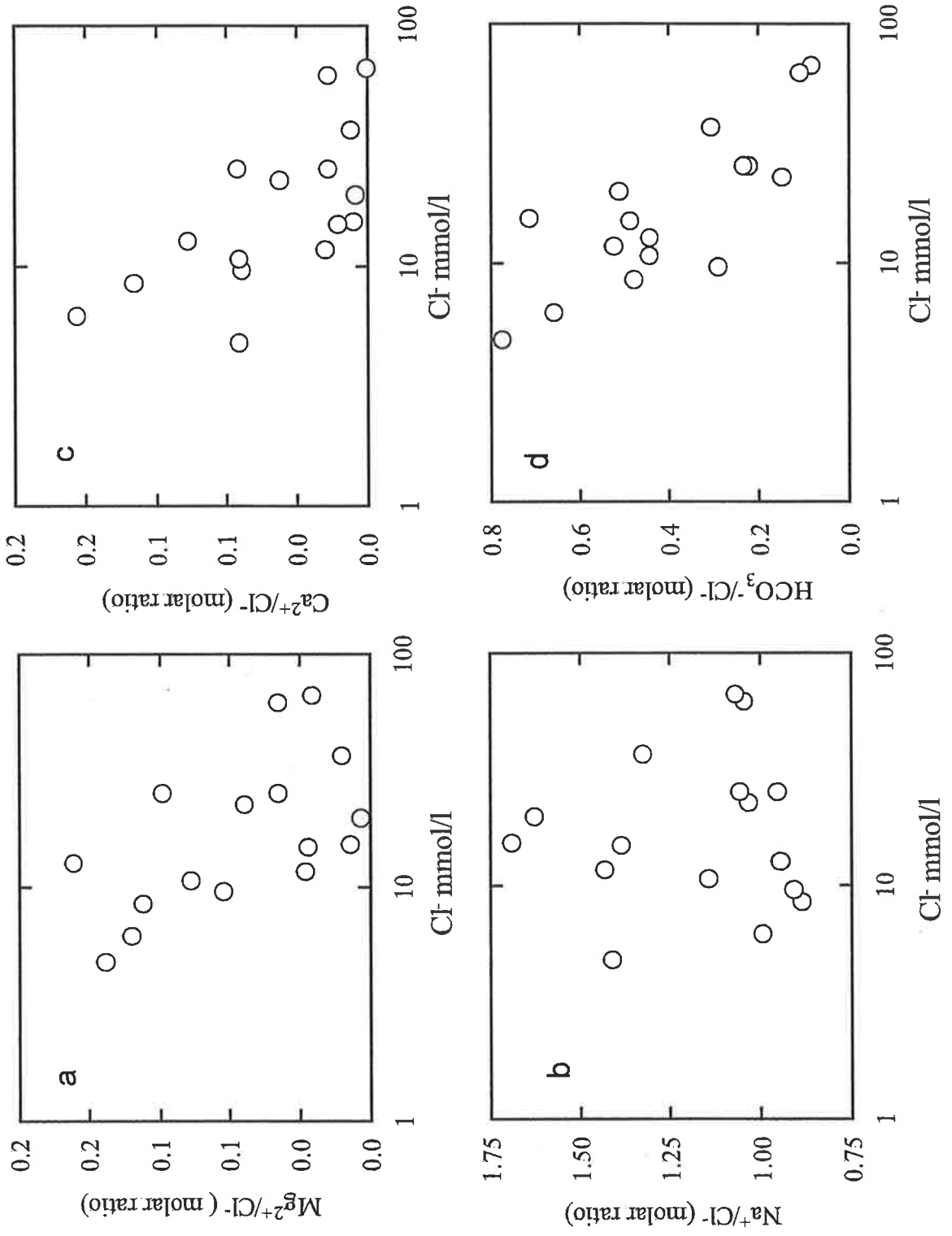

Fig. 3.16 a, b, c, d The relationship between the Mg^{2+}, Na^+, HCO_3^-, Ca^{2+}/Cl^- ratio and Cl^- concentration in the Renmark Group Aquifer in Zone A. The Ca^{2+}/Cl^- and Mg^{2+}/Cl^- ratio decreases with an increase in Cl^- concentration suggesting removal of Ca^{2+} and Mg^{2+} from the groundwater.

Group Aquifer at the same locations (Fig. 3.15) suggesting that downward leakage from the Murray Group Aquifer is not likely to control the variation in the ion/Cl^- ratio.

Figures 3.16 a, c show the decrease of Mg^{2+}/Cl^- and Ca^{2+}/Cl^- ratios with an increase in the Cl^- concentration, indicating the removal of Mg^{2+} and Ca^{2+} ions from the groundwater. In contrast, the Na^+/Cl^- versus Cl^- concentration shows a highly scattered distribution of Na^+/Cl^- with an increase in Cl^- concentrations, but the majority of the water samples have a Na^+/Cl^- ratio higher than the marine ratio of 0.86.

Variations of one major ion/Cl^- ratio in groundwater can be related to other major ion/Cl^- ratios by a number of processes that are schematically depicted in Fig. 3.17, using the Na^+/Cl^- and Ca^{2+}/Cl^- relationship as an example. If the groundwater was dominated by lateral flow and there was no alteration of Ca^{2+} and Na^+ via interaction with the aquifer matrix, the Na^+/Cl^- and Ca^{2+}/Cl^- data would be represented by a single point. If the concentration of Na^+ or Ca^{2+} was altered by the addition or removal of only Na^+ or Ca^{2+}, the data would fall on a straight line, parallel to the X or Y axis, depending on the respective ion variation. However, if the variation of Na^+ concentrations were related to the variation of Ca^{2+} concentrations due to reactions involving both ions, the data would show a relationship between the Na^+/Cl^- and Ca^{2+}/Cl^- ratio.

The data in Fig. 3.18 a, b show a negative relationship between Ca^{2+}/Cl^-, Mg^{2+}/Cl^- and Na^+/Cl^-, indicating removal of Ca^{2+} and Mg^{2+} and an addition of Na^+ to the groundwater

in the Renmark Group Aquifer. This process may be initiated by exchange of Ca^{2+} and/or Mg^{2+} for Na^{+} on clay minerals which may perturb calcite and dolomite equilibria.

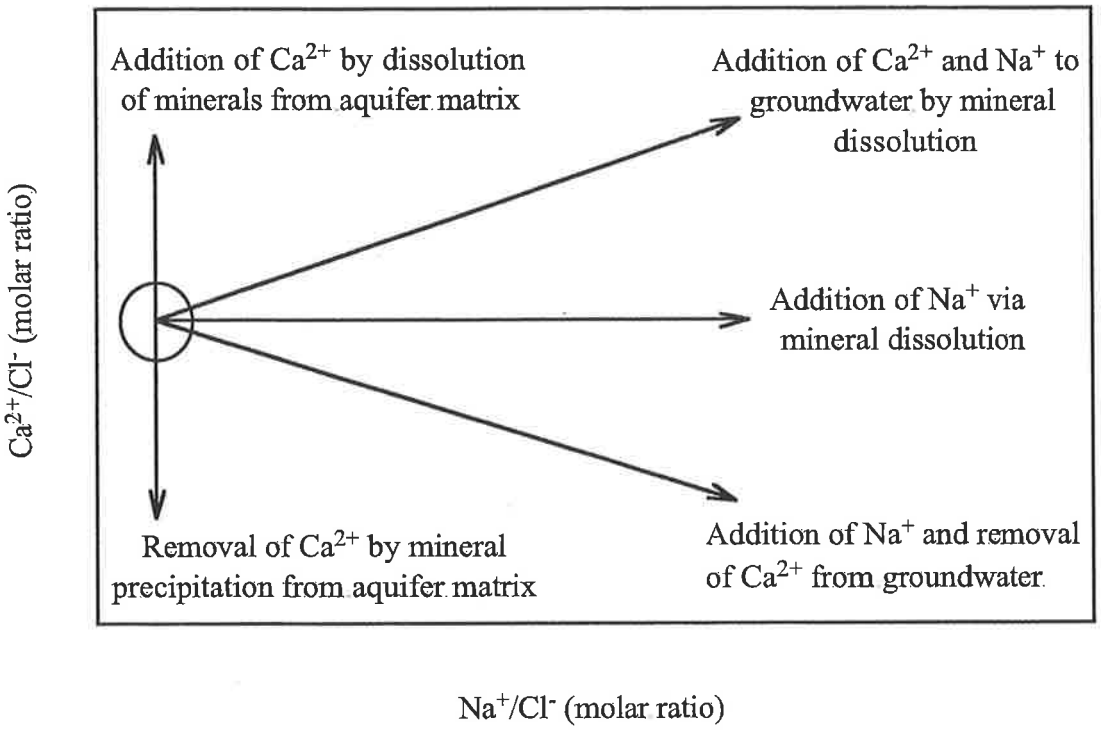

Fig. 3. 17 Conceptual diagram illustrating the change in Na^{+}/Cl^{-} and Ca^{2+}/Cl^{-} ratio by various potential chemical and physical processes in confined aquifers. The open circle represents major ion concentrations in rain water. Variation of evapotranspiration does not change the ion/Cl ratio.

The removal of Ca^{2+} and/or Mg^{2+} may cause calcite and dolomite to dissolve, thus adding Ca^{2+}, Mg^{2+} and HCO_3^{-} to the groundwater. The addition of Na^{+} ions to the groundwater by cation exchange reaction may also cause Na^{+} ion reaction with clay minerals, particularly kaolinite, to produce a secondary clay mineral such as Na-smectite. The presence of kaolinite and Na-smectite was detected from X-ray analysis of the Renmark Group Aquifer matrix and these proposed reactions are discussed below.

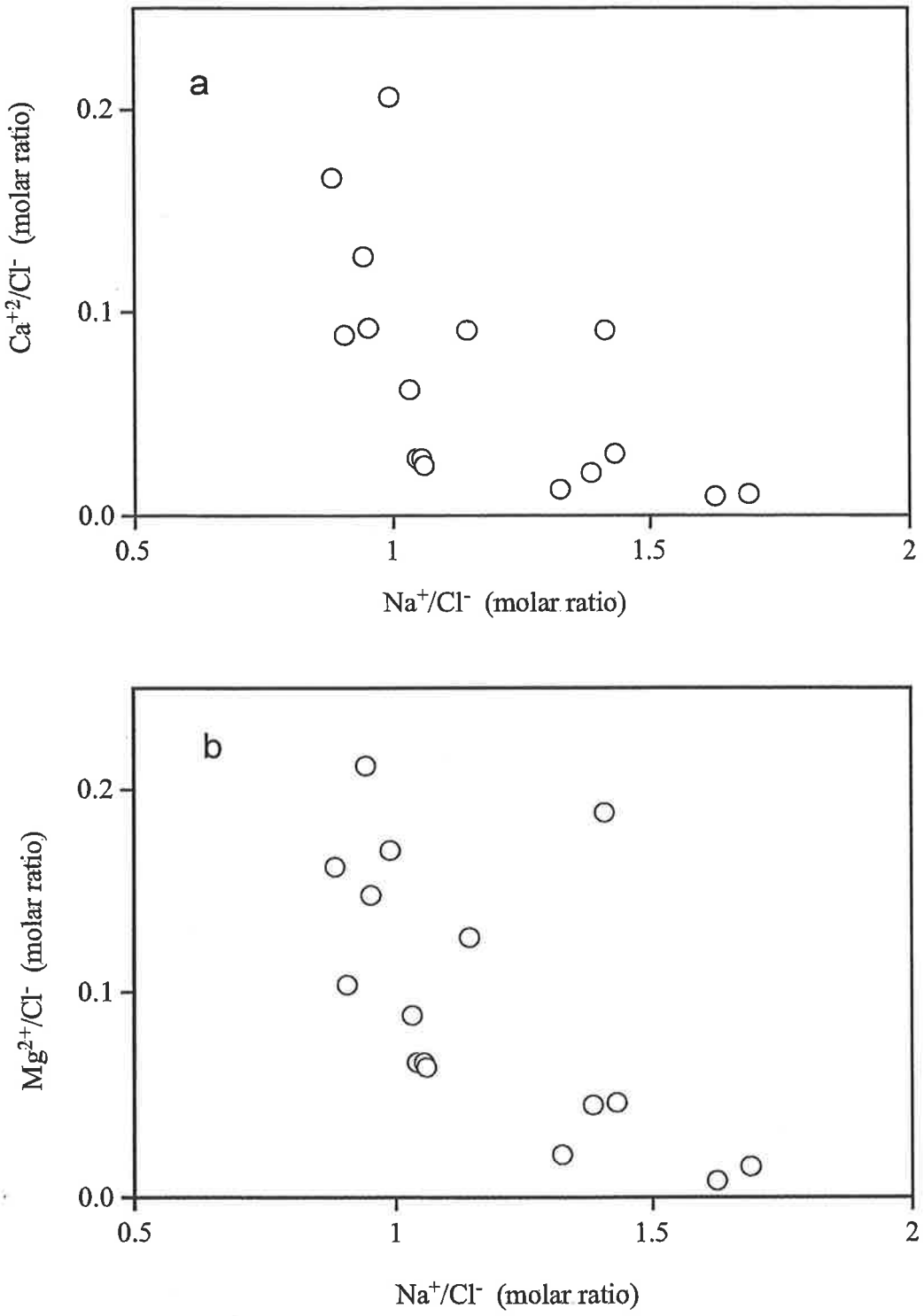

Fig. 3.18 a, b The Ca^{2+}/Cl^-, Mg^{2+}/Cl^- vs Na^+/Cl^- relationship of groundwater from the Renmark Group Aquifer in Zone A. The decrease in the Ca^{2+}/Cl^- and Mg^{2+}/Cl^- ratio and the increase in Na^+/Cl^- ratio suggests the removal of Ca^{2+} and Mg^{2+} and the addition of Na^+ to the groundwater.

3.3.11 Mass balance model to explain the major ion distribution in the Renmark Group Aquifer in Zone A

Mass balance calculations were done using the sequence of reactions proposed by Black (1989) to establish whether a series involving, cation exchange, dissolution of calcite and formation of cation rich clay mineral reactions is responsible for the current major ion distributions in the groundwater. The reactions used in the model along with the mass balance equations are:

Cation exchange;

$$Ca^{2+} + 2Na\text{-}X \rightarrow Ca\text{-}X + 2Na^{+} \quad (3.7)$$

$$-\Delta Na = 2\Delta (Ca^{2+} + Mg^{2+}) \quad (3.8)$$

Dissolution of calcite (i) and/or dolomite (ii)

$$(I)\ CaCO_3 + CO_2 + H_2O \rightarrow 2\ HCO_3^{-} + Ca^{2+} \quad (3.9)$$

$$(ii)\ 2CO_2 + CaMg(CO3)_2 + 2H_2O \rightarrow 4HCO_3^{-} + Ca^{2+} + Mg^{2+} \quad (3.10)$$

$$\Delta\ HCO_3^{-} = 2\Delta (Ca^{2+} + Mg^{2+}) \quad (3.11)$$

Formation of cation rich clay bearing minerals

$$3Al_2Si_2O_5(OH)_4 + Na^{+} + 4H_4SiO_4 \rightarrow 3Na_{0.33}Al_{2.33}Si_{3.67}O_{10}(OH)_2 + H^{+} + 11.5H_2O. \quad (3.12)$$

Kaolinite Na-smectite

$$-\Delta\ Na^{+} = \Delta\ H^{+} \quad (3.13)$$

In order to express all the variable ions in term of HCO_3^{-}, Na^{+}, Ca^{2+} and Mg^{2+}, the change in proton concentrations by kaolinite back reaction expressed as change in HCO_3^{-} concentration as follows:

$$\Delta\ H^{+} = -\Delta\ HCO_3^{-} \quad (3.14)$$

combining Eq. 3.13 and Eq. 3.14 results in

$$- \Delta Na^+ = - \Delta HCO_3^- \quad (3.15)$$

To calculate the change in major ion chemistry along the transect AA`, only those wells located on or near the transect were included in the mass balance calculation. The major ion concentration for each well was normalised to the Cl^- concentrations in the downgradient well to eliminate the effect of evapotranspiration. The method for normalising major ion concentrations is demonstrated for the first two wells R1 and R2 (Table 3.3) and an example is given for normalising Na^+ concentrations:

1. The Cl^- concentration in the upgradient well (R1) is divided by the Cl^- concentration in the downgradient well (R2):

$9.65 \div 4.80 = 2.01$

2. The above factor was multiplied by the Na^+ concentration in the downgradient well (R2):

$2.0 \text{ X } 6.7 = 13.4$ mmol/l

3. The measured Na^+ value in the upgradient well was subtracted from the normalised Na^+ value

$13.4 - 8.7 = 4.7$ mmol/l

4. The above procedure was carried out for Na^+, Ca^{2+}, Mg^{2+} and HCO_3^- for all the wells along the AA` transect shown in Fig. 3.1 and the normalised Na^+ concentration was compared with the calculated Na^+ concentration by a mass balance equation (sum of Eq. 3.8, 3.11 and 3.15)

$$\Delta Na^+ = \Delta HCO_3^- - 2 \Delta (Ca^{2+} + Mg^{2+}) \quad (3.16)$$

The normalised and calculated ΔNa^+ values from mass balance (Eq. 3.16) are presented

in Table 3.5. The calculated Δ Na^+ from the mass balance model generally agrees with the normalised Na^+ value. The positive or negative numbers represent the net addition or removal of Na^+ to the groundwater as a result of exchange with Ca^{2+} and Mg^{2+} minus removal of Na^+ via the back reaction with kaolinite (Eq. 3.12).

Activity-activity diagrams are often used to qualitatively illustrate saturation conditions of groundwater with respect to silicate minerals. The details of the method of construction of activity diagrams are given by Faure (1992). In this study, the activities of different species were calculated using the computer code PHREEQEM.

Table 3.5
Mass balance calculations in mmol/l of Ca^{2+}, Mg^{2+}, HCO_3^- and Δ Na^+ of groundwater along the AA` transect. The calculation of the measured Δ Na^+ was done after normalising all data to Cl^- (see text).

Well Reg. No	Well ID	Cl^-	HCO_3^-	Na^+	Ca^{2+}	Mg^{2+}	ΔHCO_3^-	ΔCa^{2+}	ΔMg^{2+}	ΔNa^+ Measured	ΔNa^+ Calculated
67847	R1	9.65	2.82	8.7	0.86	1.00	4.62	0.01	0.80	4.7	3.0
60623	R2	4.80	3.72	6.7	0.43	0.90	-2.65	-0.30	-0.59	-1.7	-0.9
48554	R3	25.30	5.62	26.7	0.72	1.65	5.61	2.49	3.68	-2.8	-6.7
75669	R4	12.69	5.63	12.0	1.61	2.76	-2.66	-0.44	-0.80	0.1	-0.2
60475	R5	25.30	5.93	24.1	2.33	3.74	-2.17	-0.76	-1.49	1.9	2.3
58111	R6	22.65	3.37	23.3	1.41	2.02	7.48	2.35	1.65	-3.3	-0.5
7026-112	R7	8.46	4.O6	7.5	1.41	1.37	1.58	0.35	0.08	1.0	0.7
7026-111	R8	6.23	4.11	6.2	1.28	1.06	-1.09	-1.15	-0.79	2.4	2.8
66476	R9	14.87	7.3	20.5	0.31	0.65	0.57	0.14	0.03	0.7	0.2
7027-585	R10	11.71	6.14	16.7	0.41	0.53	-0.93	0.72	0.96	-3.4	-4.3
6927-588	R11	10.72	4.76	12.2	0.98	1.37	2.89	-0.87	-1.22	5.9	7.1
6928-542	R12	15.35	10.94	25.8	0.16	0.21	-9.21	0.21	0.76	-9.7	-11.1
109458	R17	64.29	7.27	67.9	1.53	4.07	12.45	-0.76	-2.76	16.7	19.5
7028-469	R14	36.7	11.3	48.5	0.44	0.75					

The activity-activity diagram for the Na^+- H^+ - H_2SiO_4 system (Fig. 3.19) indicates that the groundwater samples plot within the kaolinite and Na-smectite field, and that the hypothesized reaction between kaolinite and Na-smectite may be valid. The presence of both kaolinite and smectite in the Renmark Group Aquifer matrix is probably further evidence that the proposed back reaction of Na^+ with kaolinite is occurring in the groundwater.

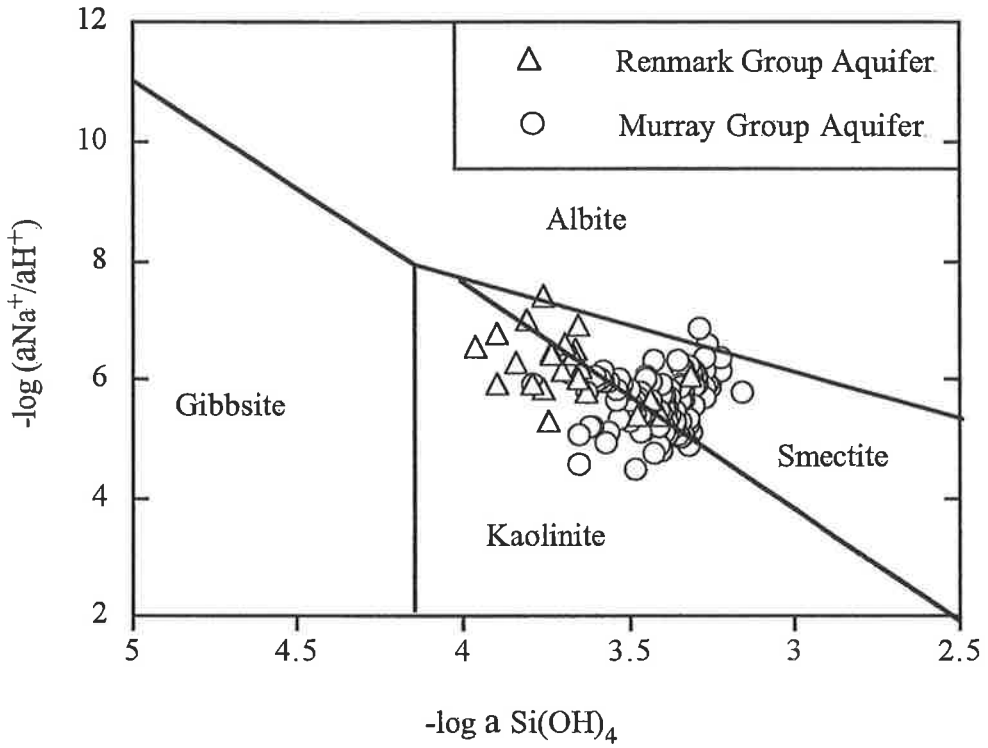

Fig. 3.19 Activity-activity diagram depicting the stability field of Na minerals. Thermodynamic data for calculation of mineral stability are at 25°C (Faure, 1992). The activities of dissolved species are at groundwater temperature 25-30°C. Note that all the groundwater data from the Murray and Renmark Group aquifers are at or close to equilibrium with respect to kaolinite and Na-smectite.

Distribution of major ions of the Renmark Group Aquifer in Zone A appear to be controlled by a combination of evapotranspiration prior to recharge, and water-rock

interaction which modifies the concentration of Na^{+}, Ca^{+2}, Mg^{+2}, and HCO_3^{-} ions relative to Cl^{-}. However, because the magnitude of the Cl^{-} increase or decrease is much higher compared with the other major ions, it is concluded that the overall effect of evapotranspiration in modifying the TDS concentration of groundwater is more significant than the alteration effect of water rock interaction in Zone A.

3.3.12 Chloride concentration of groundwater in the Murray and Renmark Group aquifers in Zone B

Groundwater in both aquifers in Zone B has an average Cl^{-} concentration one order of magnitude higher than the average Cl^{-} concentration in Zone A. The hydraulic head differences of groundwater between the two aquifers in the northern part of Zone A and in Zone B are reversed, and there is the potential for upward leakage from the Renmark Group Aquifer (Fig. 1.4). Therefore, the increase in Cl^{-} concentration in this part of the study area cannot be due to mixing through downward leakage from the Murray Group Aquifer. The increase in Cl^{-} concentration in the confined Renmark Group Aquifer over one order of magnitude cannot be explained by a variation in the evapotranspiration rate, because this process occurs over a relatively long period of time, hence causing a monotonic increase in Cl^{-} concentrations rather than an abrupt increase.

Evans and Kellett 1989. suggested that the higher Cl^{-} concentration of the Renmark Group Aquifer in Zone B is due to mixing with relatively saline (TDS ~ 22,000 mg/l)

groundwater flowing from the Riverine Province east and northeast of the study area. The causes for high salinity of the water flowing from the Riverine Province is attributed to two main reasons; (1) surface discharge of the groundwater and subsequent reflux of solutes back into the groundwater, and (2) mixing with more saline groundwater from the overlying Calivil Sand aquifer which overlies the Renmark Group Aquifer in the Riverine Province. A similar trend is observed for the Cl^- concentration increase in the Murray Group Aquifer in Zone B to that in the Renmark Group Aquifer. This increase could be due to upward leakage from the more saline Renmark Group Aquifer. Hydraulic head gradients indicate the potential for upward leakage (Fig 1.5), suggesting the possibility of mixing between the aquifers. The mechanism leading to a highly saline water and the physical evidence for inter-aquifer mixing in Zone B will be discussed in more detail in the following chapters (4, 5, 6).

3.4 Stable isotopes of water molecules in the Murray and Renmark Group aquifers

Evaporation of water from ocean surface causes the formation of air masses containing water vapour that is depleted in ^2H and ^{18}O compared to sea water. This occurs because light isotopes of water molecules evaporate more efficiently than the heavy isotopes, causing isotopic fractionation. In contrast, during condensation and precipitation, the condensate is enriched in the heavy isotopes relative to the vapor phase. Because both the hydrogen and oxygen components of water molecules experience the same sequence of events during evaporation and condensation, the δ^2H and $\delta^{18}O$ of meteoric water is

related by the empirical equation known as the World Meteoric Water Line WMWL (Craig, 1961):

$$\delta^2H = 8\,\delta^{18}O + 10 \qquad (3.17)$$

The slope of the WMWL in δ^2H versus $\delta^{18}O$ space is related to the equilibrium isotopic fractionation factor of H and O during evaporation, and condensation of water (Craig et al., 1963) by the following equation:

$$\frac{\alpha_{(H)} - 1}{\alpha_{(O)} - 1} = \frac{0.074}{0.0092} = 8 \qquad (3.18)$$

where $\alpha_{(H)}$ and $\alpha_{(O)}$ are the equilibrium fractionation factors for H and O respectively. An added kinetic fractionation during partial evaporation from surface water or from the soil water in the unsaturated zone affects the fractionation between ^{18}O and ^{16}O to a greater extent than that between ^2H and ^1H, causing a shift from the meteoric water line. The relationship between δ^2H and $\delta^{18}O$ for the evaporated waters, therefore, has a lower slope than the meteoric water line. The slope depends on humidity and salinity and can range from ~4 to ~7 (Gonfiantini, 1986) for evaporation from the free surface, and ~2 to ~5 for evaporation from soil water (Allison, 1982; Allison et al., 1983).

Isotopic data from the Murray and Renmark Group aquifers falls mainly on or slightly to the right of the WMWL (3.4). The majority of the groundwater samples from the Murray and Renmark Group aquifers are depleted by 6 to14‰ in δ^2H, and by 0.5 to 1.5‰ in $\delta^{18}O$ compared to the current mean weighted precipitation in Melbourne 300

km south-east and Adelaide ~ 250 km west and north-west of the study area. The current precipitation weighted mean of δ^2H and $\delta^{18}O$ from 10 years of measurement in Melbourne are -28.3‰ and -4.91‰ respectively and in Adelaide are -23.3‰ and - 4.36‰ respectively. Extrapolation of the linear regression of the δ^2H and $\delta^{18}O$ relationship back to the WMWL gives an intersection at values of $\delta^{18}O$ = -6.4‰ and δ^2H of -41‰. These values are similar to the δ^2H and $\delta^{18}O$ values of the groundwater from the south and south-eastern part of the study area at the basin margin (Dundas Plateau).

One explanation for general isotope depletion of the groundwater in the south and south-eastern part of the study area is the "amount effect" (Dansgaard, 1964; Rozanski et al., 1993) where negative δ^2H and $\delta^{18}O$ values are correlated with an increase in rainfall. This implies that the relatively negative δ^2H and $\delta^{18}O$ values of the groundwater correspond to relatively higher rainfall episodes. This explanation is probably justified in the semi-arid climates of the study area in which potential evaporation exceeds the amount of rainfall, and where water from high rainfall events can potentially contribute to recharging the aquifer.

A second explanation for the depleted δ^2H and $\delta^{18}O$ values is the "continental effect" which results in more negative δ^2H and $\delta^{18}O$ values in precipitation with increasing distance from the coast. This occurs due to the gradual removal of moisture from air masses because of preferential removal of the heavy isotopes during condensation

processes. The ^{2}H and ^{18}O depleted rain water eventually recharges the aquifer further inland with relatively more negative values compared to the isotope values of rainfall near the coastal area. The continental effect has been documented in rainfall from Europe and North Africa (Sonntag et al., 1978) and in North America (Sheppard, 1969). The $\delta^{2}H$ gradient in these studies ranges from 1 to 20‰ per 100 km. The location of the groundwater samples (Fig 3.1) in the Murray and Renmark Group aquifers at the south and south-eastern part of the study area range from ~150 to 250 km inland from the coast, therefore the depletion of 16‰ in $\delta^{2}H$ may be due to continental effect if the gradient in the Australian continent is similar to that measured in Europe and North Africa.

Although the $\delta^{18}O$ composition of groundwater from the Murray Group Aquifer is generally depleted in ^{18}O compared to that of rainfall in the coastal cities (i.e. Melbourne and Adelaide), groundwater $\delta^{18}O$ composition further inland is more enriched compared to $\delta^{18}O$ composition from downgradient wells (Fig. 3.7-Table 3.2). Therefore, there must be additional processes affecting $\delta^{18}O$ composition of groundwater from the Murray Group Aquifer further inland. The $\delta^{2}H$ and $\delta^{18}O$ data for groundwater in the Murray Group Aquifer fall to the right of WMWL (Fig. 3.6). The best fit line for the $\delta^{2}H$ and $\delta^{18}O$ relationship is defined by $\delta^{2}H = 3.6\ \delta^{18}O - 17$. The slope of 3.6 for the groundwater is probably due to partial evaporation of the recharge water from the soil zone (Zimmerman et al., 1967; Dincer et al., 1974; Allison, 1982; Barnes and Allison, 1988). The slope of the $\delta^{18}O$ and $\delta^{2}H$ relationship for soil

water from various unsaturated zone profiles in the study area ranged from 2.6 to 4 (Allison, 1982, 1986; Allison and Hughes, 1983; Allison et al., 1983). The theory for the enrichment of ^{18}O and the development of the low slope of the δ^2H and $\delta^{18}O$ in the soil water is discussed in detail by Barnes and Allison (1983). They attributed the higher enrichment in ^{18}O in the unsaturated zone to kinetic fractionation during evaporation from the soil zone. The δ^2H and $\delta^{18}O$ relationship of water evaporated from the saturated soil has a slope of ~5, similar to that observed for evaporation of water from free surface (i.e. water body open to atmosphere). As evaporation proceeds, the initially saturated soil dries out and becomes unsaturated then the soil water vapor will diffuse through the increasing thickness of the dry surface layer. The increase of the thickness of the dry surface through which the soil water must diffuse causes an increase in the kinetic fractionation, leading to a concomitant change of the slope in the δ^2H and $\delta^{18}O$ relationship (Allison, 1982; Barnes and Allison, 1988). Allison et al. (1993b) showed the variation in the slope of the δ^2H and $\delta^{18}O$ relationship ranging from 5 to 2 for different thickness of the same dry porous material over which soil water evaporated under identical conditions. Following this, if the soil water is displaced by subsequent recharge events, and this becomes the main source for groundwater recharge, the groundwater will also have a similar δ^2H and $\delta^{18}O$ relationship. This type of relationship between the δ^2H and $\delta^{18}O$ slope of water from the unsaturated zone and groundwater is also observed in other arid regions in Africa (Dincer et al., 1974).

The δ^2H and $\delta^{18}O$ values in the groundwater from the Renmark Group Aquifer generally have a similar range as those in the Murray Group Aquifer, and are indistinguishable from the Murray Group Aquifer throughout the study area. This implies that the groundwater in the Murray and the Renmark Group aquifers have the same source of recharge which is the cause for the similar δ^2H and $\delta^{18}O$ values in groundwater from both aquifers.

The difference in chemical composition of the groundwater in the Renmark Group Aquifer between Zone A and B is also reflected in the δ^2H and $\delta^{18}O$ composition (Fig. 3.7 a, b). Groundwater in Zone B is more enriched in δ^2H and $\delta^{18}O$ compared with Zone A. This is probably due to the difference in the recharge area for the two water types and a difference in flow regime. The more ^2H and ^{18}O enriched groundwater in Zone B represents groundwater recharge in the Riverine Province 400 km to the east of the study area. This may have evolved through mixing with various waters such as the reflux of evaporated waters in the surface discharge area, and mixing with groundwater from the overlying Calival aquifer (Evans and Kellett, 1989). Groundwater in Zone A on the other hand is mostly derived from the Dundas Plateau south-east of the study area (Fig 1.4).

3.5 Conclusions

Groundwater from the Murray and Renmark Group aquifers shows a progressive increase in salinity along the hydraulic gradient. The interpretation of hydrochemical,

and stable isotope (δ^2H, $\delta^{18}O$) data suggests the following physical and geochemical processes occur in the Murray and Renmark Group aquifers:

1. The relative abundance of Cl^-, Na^+, and Br^- are similar to that of sea water, indicating the dominance of marine airborne salts as a source of these ions to the Murray and Renmark Group aquifers.

2. The Na^+/Cl^- molar ratio, and Ca^{2+}, Mg^{2+} and HCO_3^- distributions indicate that evapotranspiration prior to recharge, carbonate dissolution and cation exchange on clays are major processes causing the current chemical composition of groundwater in the Murray Group Aquifer.

3. The δ^2H and $\delta^{18}O$ composition of water molecules suggests that groundwater of the Murray and Renmark Group aquifers is derived from meteoric water. The relatively enriched $\delta^{18}O$ and the slope of δ^2H and $\delta^{18}O$ relationship of 3.6 may be caused by partial evaporation of rainfall from the soil zone.

4. The progressive increase in Cl^- concentration, whilst maintaining marine relative abundance of Na^+ and Br^- in the groundwater of the Murray Group Aquifer in Zone A, is due to mixing with more saline recharge water with a marine relative abundance of Cl^-, Na^+ and Br^-. Upward leakage from the more saline Renmark Group Aquifer in Zone B is probably the mechanism that causes further increase in Cl^- concentration and in TDS reaching values up to 23,000 mg/l in the Murray Group Aquifer.

5. The variation in the amount of water loss by evapotranspiration during recharge is the main process causing the variation in Cl^- concentration in Zone A in the Renmark Group Aquifer. The mass balance calculations for the carbonate mineral dissolution, cation exchange, and back reaction of Na^+ with kaolinite shows the added influence of theses reactions which further modify the concentration of Na^+, Ca^{2+}, Mg^{2+}, and HCO_3^- in the Renmark Group Aquifer.

6. The information obtained from chemical and stable isotope data on the possible geochemical and physical processes occurring in both aquifers can be used as a basis for further discussions (chapter 4 and 5) on (a) the usefulness of $\delta^{34}S$ and $\delta^{18}O$ of dissolved SO_4^{2-} and $^{87}Sr/^{86}Sr$ ratios as tracers of mixing and (b) the nature of carbonate mineral - groundwater reactions and their effect on radiocarbon data in the groundwater.

CHAPTER 4

Isotopic behaviour of sulphur and oxygen of dissolved SO_4^{2-} in the groundwater of the Murray Basin

4.1 Introduction

Sulphur and oxygen isotopes of dissolved sulphate (SO_4^{2-}) can be used to provide information about the source of sulphate in groundwater, and to elucidate the geochemical and physical processes affecting sulphate concentration (Nriagu et al., 1991). Stable sulphur isotope (^{34}S & ^{32}S) fractionation arises in many processes in the sulphur cycle and this causes the variation in $\delta^{34}S$ values of different sulphur compounds (Nielsen et al., 1991). For example, primary sulphide originating in the upper mantle of the earth has an average $\delta^{34}S$ close to zero (Grinenko and Thode, 1970; Mitchell and Krouse, 1975). However, sedimentary sulphides have a large range of $\delta^{34}S$ values (+30 ‰ to -30 ‰), with a tendency to be depleted in ^{34}S (Lein, 1983). On the other hand, marine evaporite sulphates are enriched in ^{34}S ranging from ~ +10 ‰ to +35%, due to temporal variation in the isotopic composition of marine dissolved sulphate (Holser and Kaplan, 1966; Davies and Krouse, 1975; Claypool et al., 1980). The distinct $\delta^{34}S$ of the various forms of sulphur can be advantageous in many aqueous systems in identifying the sources and sinks of sulphur and in understanding the geochemical and biogeochemical processes that can occur in these systems.

The isotopic composition of sulphate in the rainwater that may eventually recharge groundwater is highly variable, depending on the source of the sulphate in atmospheric aerosols. For example, in coastal areas, rainfall chemistry is generally dominated by sea spray. Therefore the $\delta^{34}S$ and $\delta^{18}OSO_4^{2-}$ of the dissolved sulphate in the rainfall in these areas has a marine signature (Newman et al., 1991).

The $\delta^{34}S$ and $\delta^{18}O$ composition of dissolved sulphate in groundwater, on the other hand, depends on a number of factors, such as: (1) the $\delta^{34}S$ and $\delta^{18}OSO_4^{2-}$ ratio of sulphate of rainfall that recharges groundwater; (2) dissolution of evaporite minerals (gypsum, anhydrite) and/or oxidation of sulphide minerals (e.g. pyrite); (3) bacterial sulphate reduction in the groundwater; and (4) mineralisation of organic sulphur in soil, which modifies the $\delta^{18}OSO_4^{2-}$.

The mineralogy of the aquifer matrix and the redox state of the groundwater also play a major role in modifying the concentration of the dissolved SO_4^{2-} and in changing isotopic composition. Because the redox conditions within the Murray and Renmark Group aquifers are different, the $\delta^{34}S$ and $\delta^{18}OSO_4^{2-}$ of sulphate in each aquifer system are also likely to exhibit different $\delta^{34}S$ and $\delta^{18}OSO_4^{2-}$ signatures. In the highly reducing Renmark Group Aquifer, the $\delta^{34}S$ and $\delta^{18}OSO_4^{2-}$ of the residual dissolved SO_4^{2-} may be relatively enriched through the preferential metabolisation of ^{32}S during bacterial sulphate reduction. In contrast, the $\delta^{34}S$ and $\delta^{18}OSO_4^{2-}$ values in the aerobic unconfined

Murray Group Aquifer may be dominated by SO_4^{2-} having $\delta^{34}S$ and $\delta^{18}O$ values similar to rainfall isotope values, if there are no other sources of SO_4^{2-} in the aquifer.

Several studies have used sulphur or oxygen isotopes as tracers to delineate the sources of sulphate and the mixing of different groundwaters. For example, Edmunds et al. (1995) assigned the origin of dissolved sulphate in the groundwater of the East Midlands Triassic Aquifer to a number of sources using sulphur isotope data. Rye et al. (1980) showed that sulphur isotopic fractionation between dissolved sulphate and the sulphide formed from bacterial sulphate reduction can be related to groundwater residence time and flow path. Rightmire et al. (1974) used $\delta^{34}S$ as a tracer for groundwater mixing with ocean water in the Floridain Aquifer. Bottrell (1991) identified mixing between different groundwaters by using a profile of $\delta^{34}S$ values of aqueous sulphur species in groundwater from Bahamian blue holes. $\delta^{34}S$ and $\delta\,^{18}OSO_4^{2-}$, combined with hydrogeology, have been used to identify the origin and distribution, as well as the sources, of groundwater recharge in Saskatchewan, Canada (Dowuona et al., 1993).

In this chapter, the combination of $\delta^{34}S$ and $\delta^{18}OSO_4^{2-}$ isotopes have been used in the large scale regional aquifers of the south-east Murray Basin:

- to evaluate their usefulness as physical tracers to identify inter-aquifer mixing in Zone B;
- to establish the significance of mixing and its effect on the salinity in the Murray Group Aquifer;

- to identify the source(s) of sulphate in the groundwater of both aquifer systems;
- to elucidate the importance of the vertical solute input through local recharge relative to lateral inputs to the Murray Group Aquifer.

4.2 Background

4.2.1 Sulphur isotope variation of different sulphur forms

Sulphur has four stable isotopes with the following relative abundances, $^{32}S = 95.02\%$, $^{33}S = 0.75\%$, $^{34}S = 4.21\%$ and $^{36}S = 0.02\ \%$ (Macnamara and Thode, 1950). Sulphur occurs as sulphate, sulphide, sulphite, and elemental sulphur in the +6 +4, 0 and -2 valence states respectively.

Gaseous sulphide emitted during volcanic activity in the oceans is in the form of H_2S and SO_2. These gaseous forms of sulphur may react with metals producing sulphides which may form deposits or may oxidise to sulphates and circulate in oceans. Transformation of sulphur compounds during sulphur cycling in the earth biosphere occurs mainly by bacterial organisms, which are also responsible for the variation of $\delta^{34}S$ values between different forms of sulphur. This results mainly from kinetic isotopic fractionation during dissimilatory and assimilatory bacterial reduction and oxidation processes (Harrison and Thode, 1958; Kaplan and Rittenberg, 1964). Dissimilatory reduction of sulphate occurs under anaerobic conditions in which bacteria uses sulphate as a terminal electron acceptor to support respiratory metabolism.

The generalised form of this reaction is as follows:

$$SO_4^{2-} + 2\ CH_2O \rightarrow H_2S + 2HCO_3^- \qquad (4.1)$$

where CH_2O in this reaction is a simplified representation of organic matter.

Laboratory experiments using sulphur reducing bacteria such as *Desulfovibrio* or *Desulfotomaculum* have produced H_2S with $\delta^{34}S$ that are 3 ‰ to 46 ‰ depleted relative to $\delta^{34}S$ values in the initial sulphate (Kaplan and Rittenberg, 1964; Krouse and McCready, 1979; Chambers and Trudinger, 1979).

In contrast to sulphate reducing bacteria, there are many microorganisms that are able to oxidise sulphides under aerobic conditions, using the oxygen from the water molecule, gaseous or dissolved O_2, and nitrate. Some of these organisms, e.g. *Thiobacillus thiooxidans* can exist and oxidise sulphur under extremely acidic conditions (pH as low as 0.5) and high temperatures (>100 °C) (Schoen and Rye, 1970). However, the fractionation of sulphur isotopes between sulphur compounds during oxidation processes is relatively small ranging from > 1% up to 18%, compared with the fractionation during sulphate reduction (Kaplan and Rittenberg, 1964; Fry et al., 1992). Assimilatory reduction of sulphate is the process by which plants and other biota (e.g. bacteria, fungi) take up sulphate from the surrounding environment, reduce it and then fix it into sulphur-containing compounds and other organic compounds. A detailed review of assimilatory reduction of sulphate is given by Anderson (1980). The $\delta^{34}S$ fractionation during assimilatory reduction of sulphate stored in plants or atmospheric

SO_2 is very small, ranging from 0 to 4 ‰ with the organic sulphur generally depleted in heavy isotopes relative to that in sulphate (Mekhtiyeva et al., 1976).

The $\delta^{34}S$ of dissolved sulphate in the ocean has changed over geologic time due to variations in $\delta^{34}S$ of input sulphate from rivers and the output of sulphate from the oceans by bacterial reduction and gypsum precipitation (Thode and Monster, 1965; Holser and Kaplan, 1966; Davies and Krouse, 1975). The $\delta^{34}S$ of marine evaporites (mainly gypsum) has varied over geologic time from +35 ‰ in the early Cambrian, to +10 ‰ by late Permian, and subsequent increase to +21 ‰ in contemporary sea water (Davies and Krouse, 1975; Claypool et al., 1980). Gypsum precipitating from a sulphate bearing solution at ambient temperature is isotopically enriched by only 1.65 ‰ relative to the sulphate in solution (Thode and Monster, 1965).

4.2.2 Oxygen isotope variation of dissolved sulphate

The oxygen isotope composition of dissolved sulphate ($\delta\ ^{18}OSO_4^{2-}$) can vary over a large range of values (-20% to +20%) depending on the environment under which the sulphates are formed. Further modification of the $\delta\ ^{18}OSO_4^{2-}$ can occur after formation of sulphate molecules, via sulphate reduction, precipitation of sulphate minerals or mixing between two end members with different $\delta\ ^{18}OSO_4^{2-}$ values.

The $\delta\ ^{18}OSO_4^{2-}$ during oxidation of sulphur depends on the $\delta^{18}O$ value of the oxygen

source and a fractionation factor between oxygen sources and dissolved SO_4^{2-}. Lloyd (1967) measured the fractionation during oxidation of sulphide to sulphate by bubbling O_2 through Na_2S solution and found that the SO_4^{2-} produced was depleted by 8.7 ‰ in ^{18}O relative to the O_2. The fraction of oxygen contributed from the water molecules was estimated to be two thirds of the overall oxygen pool within the dissolved SO_4^{2-}. Taylor et al. (1984) also studied sulphur oxidation, using pyrite in their experiment, and found that 87.5% of the oxygen in the sulphate came from the O_2 and the rest came from the water molecules. These results were further substantiated by laboratory experiments carried out by Van Everdingen and Krouse (1985) and Gould et al. (1989). The various experimental results suggest that during sulphide oxidation, the $\delta^{18}OSO_4^{2-}$ depends on the available source of oxygen and the reaction conditions.

During sulphate reduction by bacteria, light isotopes of sulphate (^{16}O and ^{32}S) are preferentially metabolised, resulting in relative enrichment of the remaining sulphate in ^{18}O and ^{34}S. Mizutani and Rafter (1969a, 1973) have shown from laboratory experiments that during sulphate reduction there is a linear relationship between $\delta^{34}S$ and $\delta^{18}OSO_4^{2-}$ of the remaining sulphate. However, the slope of best fitted line of the $\delta^{34}S$ vs. $\delta^{18}OSO_4^{2-}$ data of the remaining sulphate varied in each experiment. Therefore, Mizutani and Rafter (1973) concluded that there are additional processes affecting the $\delta^{18}OSO_4^{2-}$ of the remaining sulphate.

The fractionation of $\delta^{18}OSO_4^{2-}$ during precipitation of anhydrite from a sulphate rich solution is 3.2 ‰ at 25 °C whereas precipitation of gypsum results in a fractionation of 2 ‰ (LIoyd, 1968), the $\delta^{18}OSO_4^{2-}$ of the solution being more depleted relative to the precipitated sulphates.

4.2.3 Sulphur isotope variation of sulphate in rainfall

Dissolved sulphate in continental rainfall can be derived from three main sources. These include sea spray sulphate, biogenic aerosols and anthropogenic sulphate. Sea spray sulphate has the same $\delta^{34}S$ signature as marine sulphate (~ +21 ‰ - Rees et al.,1978). The $\delta^{34}S$ values of rainfall more negative than +21 ‰ are attributed to a biogenic sulphur contribution via aerosols, which are mainly ocean derived (Newman et al., 1991). Biogenic sulphur bearing aerosols are mainly formed by oxidation of dimethyl sulphide (DMS) and H_2S, the dominant volatile sulphur compound in ocean waters (Turner et al., 1988; 1989). $\delta^{34}S$ values of ~ +17 ‰ were found for DMS by direct measurement (Calhoun, 1990). There are several other sulphur compounds in the atmosphere, including CS_2 (carbon disulphide) and COS (carbonyl sulphide) but their contribution relative to DMS is less than 5% (Andreae and Jaechke, 1988). Oxidation may occur in gas-phase reactions, in the surface of solid particles, and in the liquid-phase of cloud drops. About half of the SO_2 emitted into the atmosphere is removed by dry deposition (Garland, 1978). The other half is removed by wet deposition consisting of oxidation, hydration, and condensation. The chemistry of oxidation of

organic sulphur compounds to SO_2 has been described by Heicklen (1976), and Davis and Klauberge (1975).

As a result of its association with photoplankton production, dimethylsulphide is the predominant volatile sulphur compound in open ocean waters. Many observations suggest that DMS in aquatic environments is derived, to a significant extent, from the bacterial decomposition of DMSP (dimethylsulphonium propionate) in algal cells, the main precursor of DMS or from zooplankton grazing on these cells. High concentrations of DMS have been observed during the bacterial putrefaction of algae following algal blooms (Bremner and Steele, 1978). The $\delta^{34}S$ value reported for DMSP of ~ +19.8 ‰ (Calhoun and Bates, 1989) is slightly enriched in ^{34}S compared with the $\delta^{34}S$ value of DMS.

The contribution of H_2S to the atmosphere as a result of bacterial sulphate reduction on the continent is much higher than that from the ocean (Andreae and Jaeschke, 1988). The $\delta^{34}S$ values of H_2S depend on the rate of reduction of SO_4^{2-}, the redox conditions of the environment (Nakai and Jensen, 1964; Rees, 1978), and the ability of H_2S to move from the aqueous environment into the atmosphere. Whereas $\delta^{34}S$ of H_2S varies in shallow marine regions from -28 ‰ to -15 ‰, the values in estuaries and coastal tidal zones range from -22 ‰ to +12 ‰ (Grinenko and Grinenko, 1974). Furthermore, the $\delta^{34}S$ values of the H_2S produced by sulphate respiration can be as low as -40 ‰ (Chambers and Trudinger, 1979). The average $\delta^{34}S$ for H_2S formed under different

conditions is probably close to -10 ‰ (Volkov and Rozanov, 1983). The average $\delta^{34}S$ of all biogenic sulphur compounds emitted to the atmosphere from the oceans and continents, calculated by the isotopic mass balance equation, is close to 0 ‰ (Newman et al., 1991).

In industrial areas, anthropogenic sources of sulphate from the combustion of coal and fossil fuels, power plants, and the combustion and refining of oil and gas can be significant. $\delta^{34}S$ values of sulphate from these sources can vary from -30 ‰ to +30 ‰ (Newman et al., 1992). The emission of SO_2 from the Pb-Zn ($\delta^{34}S = 0$) smelter at Port Pirie (~ 300 km west of the study area) has occurred for 94 years. However, a study of heavy metal contamination of soils in the area (Cartwright et al, 1976) suggests that the effect is minimal. Therefore, contribution of this source to the atmospheric sulphate pool is not significant in the Murray Basin.

The excess-sulphate (biogenic) contribution to the sulphate pool in rainfall can be estimated by comparing the ratio of SO_4^{2-}/Cl^- in rainfall samples to that of marine SO_4^{2-}/Cl^- ratios (Mizutani and Rafter, 1969 a, b). The SO_4^{2-}/Cl^- ratio in rainfall near the coast areas is similar to that of the ocean. However, this tends to increase further inland due to the contribution of finer aerosol particles from the oxidation of biogenic sulphur compounds, which travel further inland across the continent and increase sulphate concentration in the atmosphere relative to sea spray (Wakshal and Nielsen, 1982). Aerosols derived from sea spray that are produced by the mechanical action of wind on the ocean surface are larger than particles generated from the oxidation of reduced

biogenic sulphide (Duce, 1981; Georgii, 1978; Husar et al., 1978). Therefore, the larger particles derived from sea spray are likely to be deposited via rainfall nearer the coast, and from lower altitude air masses than the smaller particle size sulphate produced from oxidation of the biogenic sulphur compounds. This effect was suggested by Chivas et al. (1991) to explain the relationship between the increasingly negative $\delta^{34}S$ values found in gypsum in the west and south-west Australian salt lakes with the distance from the coast.

4.2.4 Oxygen isotope variation of sulphate in rainfall

$\delta^{18}OSO_4^{2-}$ values in rainfall are influenced by the same sources as $\delta^{34}S$. These are: (1) sea spray sulphate; (2) oxidation of biogenic sulphur compounds; and (3) anthropogenic SO_2. The final value is primarily controlled by the conditions under which the sulphur is oxidised.

The $\delta^{18}OSO_4^{2-}$ values of rainfall in coastal areas, dominated by sea spray are similar to ocean $\delta^{18}OSO_4^{2-}$ values (+9.6 ‰ - Lloyd, 1967, 1968). However, oxidation of biogenic sulphur can have a significant effect on the overall $\delta^{18}OSO_4^{2-}$ composition of rainfall. The oxygen in SO_2 may come from O_2 molecules in the atmosphere which have $\delta^{18}O \cong +23$ ‰, or from water vapour which has a variable $\delta^{18}O$ values, depending on its sources in the atmosphere.

The $\delta^{18}OSO_4^{2-}$ value resulting from oxidation of biogenic sulphur compounds is variable due to the combination of the oxidation reactions that produce the SO_2. Holt et al.

(1981, 1983) showed that the $\delta^{18}OSO_4^{2-}$ produced by different chemical oxidation reactions in laboratory experiments was always more negative than those observed in the atmospheric aerosols and rainwater. Therefore, the contribution of the oxidised biogenic components to the SO_4^{2-} pool in rainfall may result in a more negative $\delta^{18}OSO_4^{2-}$ signature than that of marine $\delta^{18}OSO_4^{2-}$.

SO_2 in the atmosphere will rapidly equilibrate isotopically with water vapour or the liquid water phase. The isotopic signature of equilibrated SO_2, therefore, will depend entirely on the $\delta^{18}O$ of associated water or water vapour, and the equilibrium fractionation factor. Further modification occurs to the $\delta^{18}O$ of SO_2 when it oxidises to SO_4^{2-}. The final $\delta^{18}OSO_4^{2-}$ value depends on the mechanism by which SO_2 oxidises to SO_4^{2-}, such as oxidation in the presence or the absence of aqueous-phase water and the type of catalyst (Holt et al., 1981, 1983).

Anthropogenic SO_2 is associated with industrial activities which produce SO_2 from power plants and the burning of fossil fuel. The SO_2 produced by these activities may oxidise to SO_4^{2-} in the atmosphere. The important product of this source is primary sulphate which has a an enriched $\delta^{18}OSO_4^{2-}$ composition (~ +40 ‰ - Holt and Kumar, 1984). The contribution of this source to the sulphate pool in the atmosphere is insignificant in the Murray Basin.

Regardless of the mechanisms and type of catalyst which drive the oxidation reactions of SO_2, the majority of previous studies observed that the variation in the $\delta^{18}OSO_4^{2-}$ in rainfall correlated with $\delta\ ^{18}OH_2O$ variations in atmospheric water vapor and rainfall (Cortecci and Longinelli, 1970; Holt et al., 1981,1982). This indicates that the sulphate in rainfall is formed predominantly by the oxidation of SO_2 in the aqueous phase. In contrast, the oxygen isotope ratio in the atmospheric aerosol sulphate varies randomly with the seasons (Holt et al., 1981,1982).

In summary, it can be inferred that the $\delta^{18}OSO_4^{2-}$ values of rainfall in coastal areas not affected by industrial activities will be similar to the values of rainfall (+9.6 ‰) that originate mainly from sea spray. Because the $\delta^{18}OSO_4^{2-}$ composition derived from oxidation of SO_2 (produced from oxidation of biogenic sulphur compounds) is depleted in ^{18}O compared with $\delta^{18}OSO_4^{2-}$ of sea spray, the increased contribution of this source further inland slightly decrease the $\delta^{18}OSO_4^{2-}$ value in rainfall.

4.3 Results

The results of $\delta\ ^{34}S$ and $\delta^{18}OSO_4^{2-}$ analysis as well as the SO_4^{2-} and Cl^- concentrations of groundwater from the Murray and Renmark Group aquifers is shown in Table 4.1 and 4.2. The spatial distribution of the SO_4^{2-}/Cl^- ratio in the Murray Group Aquifer is shown in Fig 4.1. The SO_4^{2-}/Cl^- ratios were used to normalise any effects of evaporation and evapotranspiration so that changes to the SO_4^{2-}/Cl^- ratio will be

Table 4.1 The $\delta^{34}S$ and $\delta^{18}O$ of dissolved sulphate in groundwater from the Murray Group Aquifer. The registered number with (*) is the Victorian Sinclair Knight Merz (groundwater data base GDB numbers) and Registered Bore number of the Australian Department of Mines and Energy. The results of Cl^- and SO_4^{2-} are quoted in milligrams per litre. $\delta^{34}S$ and $\delta^{18}O$ are expressed in per mil notation relative to standard CTD (Canyon Diablo Triolite) and SMOW (Standard Mean Ocean Water) respectively.

Well Reg. No.	well ID.	Cl^- (mg/l)	SO_4^{2-} (mg/l)	SO_4^{2-}/Cl^-	$\delta^{34}S$ (‰,CTD)	$\delta^{18}O_{SO_4}$ (‰, SMOW)
61922*	M1	116	20.3	0.17		
61930*	M2	506	63.6	0.13		
77850*	M3	589	72.9	0.12		
111321*	M4	486	48.9	0.10		
67829*	M5	322	29.7	0.09		
51846*	M6	531	80.1	0.15	20.8	
92808*	M7	363	56.1	0.15	19.8	
50946*	M8	166	26.8	0.16	19.4	
60610*	M9	141	17.1	0.12	20.0	
79530*	M10	286	39.0	0.14	18.6	
48559*	M11	850	207.0	0.24	17.5	
60436*	M12	511	86.1	0.17	17.7	
84741*	M13	270	25.1	0.09		
75651*	M14	342	52.2	0.15	17.2	
75365*	M15	633	105.6	0.17		
75351*	M16	517	89.7	0.17		
60450*	M17	621	88.8	0.14	14.1	
79655*	M18	848	67.8	0.08	15.8	
58079*	M19	587	99.6	0.17	15.7	
98297*	M20	307	79.5	0.26	9.2	
103369*	M21	213	30.3	0.14		
98254*	M22	253	51.3	0.20	11.2	
49951*	M23	428	85.5	0.20		
49952*	M24	225	50.7	0.23		
49950*	M25	228	57.0	0.25		
66477*	M26	457	71.1	0.16	11.2	
54642*	M27	239	99.3	0.42	4.7	
54636*	M28	268	166.5	0.62		
82220*	M29	429	99.9	0.23	13.2	
61571*	M30	540	140.7	0.26	6.8	
65758*	M31	302	86.1	0.29	8.5	
77199*	M32	441	87.3	0.20		
7026-113	M33	219	50.7	0.23	13.1	8.6
7026-110	M34	305	44.4	0.15	14.5	9.1
7027-566	M35	297	48.0	0.16	10.0	
7027-650	M36	190	41.4	0.22	4.6	
7027-606	M37	221	107.1	0.48	1.0	
7027-592	M38	205	91.5	0.45	0.3	4.8
7027-597	M39	227	58.8	0.26	13.2	7.5
7027-669	M40	323	72.6	0.22	14.6	

Table 4.1 Contd.

Well Reg. No.	well ID.	Cl^- (mg/l)	SO_4^{2-} (mg/l)	SO_4^{2-}/Cl^-	$\delta^{34}S$ (‰,CTD)	$\delta^{18}OSO_4$ (‰, SMOW)
7027-602	M41	319	89.7	0.28	12.4	7.8
7027-405	M42	514	89.7	0.17	14.9	
7027-586	M43	521	112.8	0.22	14.8	5.3
7027-579	M44	347	87.6	0.25	6.6	
6827-1536	M45	890	186.3	0.21	11.7	7.0
7026-120	M46	976	222.6	0.23	6.1	7.1
6927-591	M47	429	108.0	0.25	10.1	5.7
6927-644	M48	905	188.7	0.21	11.5	7.1
6927-590	M49	867	181.8	0.21	12.5	6.8
6927-588	M50	864	180.3	0.21	14.2	5.8
6927-601	M51	514	91.8	0.18	12.3	
6928-567	M52	600	190.2	0.32	7.0	8.0
6928-411	M53	742	196.5	0.26	11.6	7.0
6928-49	M54	669	190.2	0.28	9.1	8.4
6928-260	M55	418	103.8	0.25	9.9	
7028-503	M56	807	224.4	0.28	6.9	
7025-422	M57	1016	202.5	0.20	5.8	
6928-477	M58	1523	414	0.27	11.7	
6928-27	M59	1499	366	0.24	10.3	
6828-112	M60	1239	289	0.23	11.9	
6928-528	M61	2129	375	0.18	15.3	
6928-424	M62	2560	654	0.26	17.7	
6929-154	M63	2579	495	0.19	18.6	7.2
6929-169	M64	2522	612	0.24	18.4	7.4
6928-2	M65	3114	426	0.14	13.6	
49677*	M66	880	122	0.14	7.0	
64363*	M67	3590	456	0.13	21.0	
6929-356	M68	8894	474	0.05	38.7	
85570*	M69	9617	1299	0.14	27.0	
81833*	M70	10310	753	0.07	24.6	
86775*	M71	12030	705	0.06	35.2	
6929-705	M72	10720	1128	0.11	28.5	
6929-700	M73	9480	714	0.08	35.1	
6929-711	M74	10520	666	0.06	37.4	
6929-712	M75	11180	702	0.06	36.7	
6929-710	M76	13010	858	0.07	35.2	
6929-702	M77	11830	843	0.07	32.2	15.6
6929-701	M78	12270	1044	0.09	29.6	
6929-684	M79	12860	1260	0.10	28.1	
6929-651	M80	12830	1074	0.08	27.4	
6929-682	M81	12430	1434	0.12	25.4	
6929-685	M82	12520	1692	0.14	24.6	
6929-686	M83	12380	1332	0.11	26.3	
6929-687	M84	11900	1053	0.09		
6929-689	M85	10800	1002	0.09	33.3	
6929-691	M86	10500	870	0.08	33.8	
6929-692	M87	9213	843	0.09	33.8	

Table 4.1 Contd.

Well Reg. No.	well ID.	Cl^- (mg/l)	SO_4^{2-} (mg/l)	SO_4^{2-}/Cl^-	$\delta^{34}S$ (‰,CTD)	$\delta^{18}OSO_4$ (‰, SMOW)
6929-693	M88	7267	642	0.09	32.4	
6929-1046	M89	11910	2289	0.19	25.3	16.6
6929-1041	M90	9294	1500	0.16	26.7	
6929-1082	M91	11840	1794	0.15	26.5	

Table 4.2 The $\delta^{34}S$ and $\delta^{18}OSO_4^{2-}$ of groundwater from the Renmark Group Aquifer. The results of chemical ions are quoted in milligrams per litre. The $\delta^{34}S$ and $\delta^{18}O$ are expressed in per mil notation relative to standard CTD (Canyon Diablo Troilite) and SMOW (Standard Mean Ocean Water respectively. f refers to fraction of residual sulphate in groundwater. SI refers to saturation state of groundwater with respect to pyrite.

Well Reg. No.	Well ID.	Cl^- (mg/l)	SO_4^{2-} (mg/l)	H_2S (mg/l)	Total Fe (mg/l)	SO_4^{2-}/Cl^-	f	$\delta^{34}S$ (‰, CTD)	$\delta^{18}OSO_4$ (‰, SMOW)	SI Pyrite
67847*	R1	342	86			0.09	0.42	32.1		
60623*	R2	170	20.4			0.12	0.55	21.7		
75669*	R3	450	97.8			0.22	0.99	21.0		
48554*	R4	897	115.9			0.13	0.59	29.0		
58111*	R5	803	172			0.21	0.97	20.0		
60475*	R6	897	184.6			0.21	0.93	17.0		
7026-112	R7	300	54.9	ND	0.13	0.18	0.83	14.9	11.6	8
7026-111	R8	221	41.1	ND	0.02	0.19	0.85	19.0	11.8	
66476*	R9	527	31.2			0.06	0.27	51.0		
7027-585	R10	415	50.7	<1	0.07	0.12	0.56	38.5	13.4	
6928-542	R11	544	32.4	3	0.5	0.06	0.27	56.4	15.3	10
6927-588	R12	380	66.9	ND	0.03	0.18	0.8	17.3	14.2	
6827-1530	R13	702	99.6	2.5	<0.02	0.14	0.64	34.3	18.0	
6929-423	R14	1301	116.8	1.5	0.33	0.09	0.41	51.8	15.0	10
7028-469	R15	2356	188.5	5	<0.02	0.08	0.36	36.7	15.9	
49676*	R16	2194	248.8	2.5		0.11	0.52	24.2		
109458*	R17	2279	324			0.14	0.65	26.0		
6929-760	R18	8223	432	1	0.13	0.05	0.24	39.0		
6829-992	R19	8297	1233	1	0.33	0.15	0.68	26.4	15.8	9
81832*	R20	10780	7656	1.5		0.07	0.32	34.3		
104800*	R21	10340	741	1.5		0.07	0.33	32.0		10
86774*	R22	11940	1143	2	0.34	0.10	0.44	35.2		

indicative of a net addition or removal of SO_4^{2-} in the atmosphere and/or modification of the SO_4^{2-} concentration due to geochemical and/or biogeochemical processes in the aquifer. The groundwater collected from the south and southeastern part of the study area has a SO_4^{2-}/Cl^- ratio of ~ 0.16, which is slightly higher than the marine ratio of 0.14. The SO_4^{2-}/Cl^- ratio increases along the hydraulic gradient to the north and northwest. The highest value of SO_4^{2-}/Cl^- is 0.62. This occurs to the north of Big Desert in Victoria and north of Ngarkat Conservation Park in South Australia near Pinnaroo (Fig. 4.1). Further inland and to the far north and north-west, the SO_4^{2-}/Cl^- ratio decreases to values of 0.08.

Fig. 4.2 shows the distribution of $\delta^{34}S$ in the Murray Group Aquifer. The $\delta^{34}S$ value in the south and south-east is ~ +20 ‰, and systematically decreases toward the north and north-west, where $\delta^{34}S$ values are ~ +0.3 ‰ north of the Big Desert and Ngarkat Conservation Park near Pinnaroo. The large area of low $\delta^{34}S$ corresponds to a high SO_4^{2}/Cl^- ratio of ~ 0.5. Further north and north east the $\delta^{34}S$ values increase to +38.7 ‰.

The SO_4^{2}/Cl^- ratios for groundwater of the Renmark Group Aquifer range from 0.22 to 0.06 and $\delta^{34}S$ values range from +14.9 ‰ to +56.4 ‰ (Table 4.2). A general trend is observed between $\delta^{34}S$ values and SO_4^{2}/Cl^- ratio, with more enriched $\delta^{34}S$ values corresponding to a relatively lower SO_4^{2}/Cl^- ratio (Fig. 4.3).

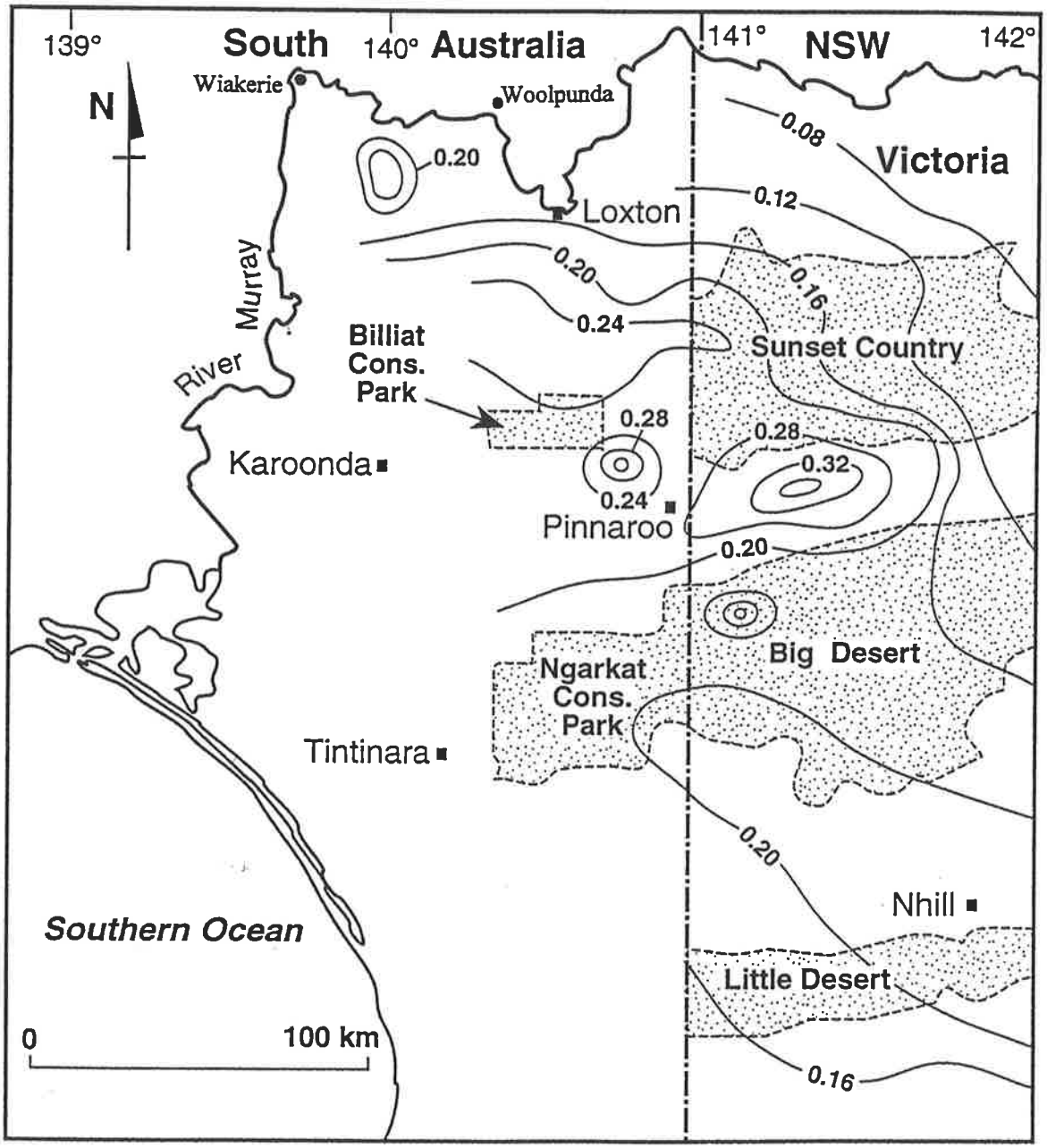

Fig. 4.1 Spatial distribution of SO_4^{2-}/Cl^- in the Murray Group Aquifer. Note that groundwaters that have the highest SO_4^{2-}/Cl^- ratio are located in the central part of the study area north and northwest of Big Desert.

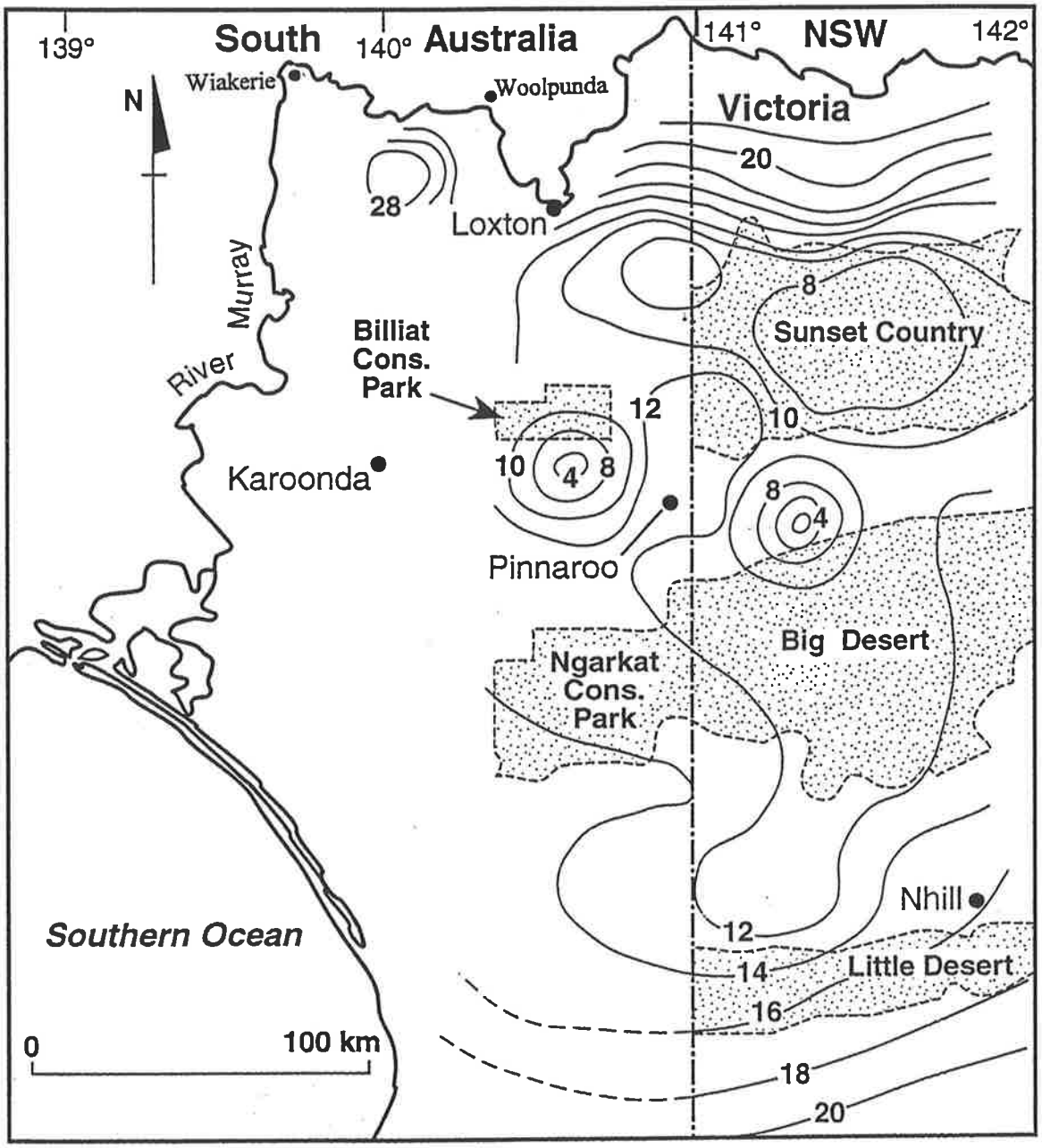

Fig. 4.2 Spatial distribution of $\delta^{34}S$ expressed as per mil notation relative to CTD in the Murray Group Aquifer.

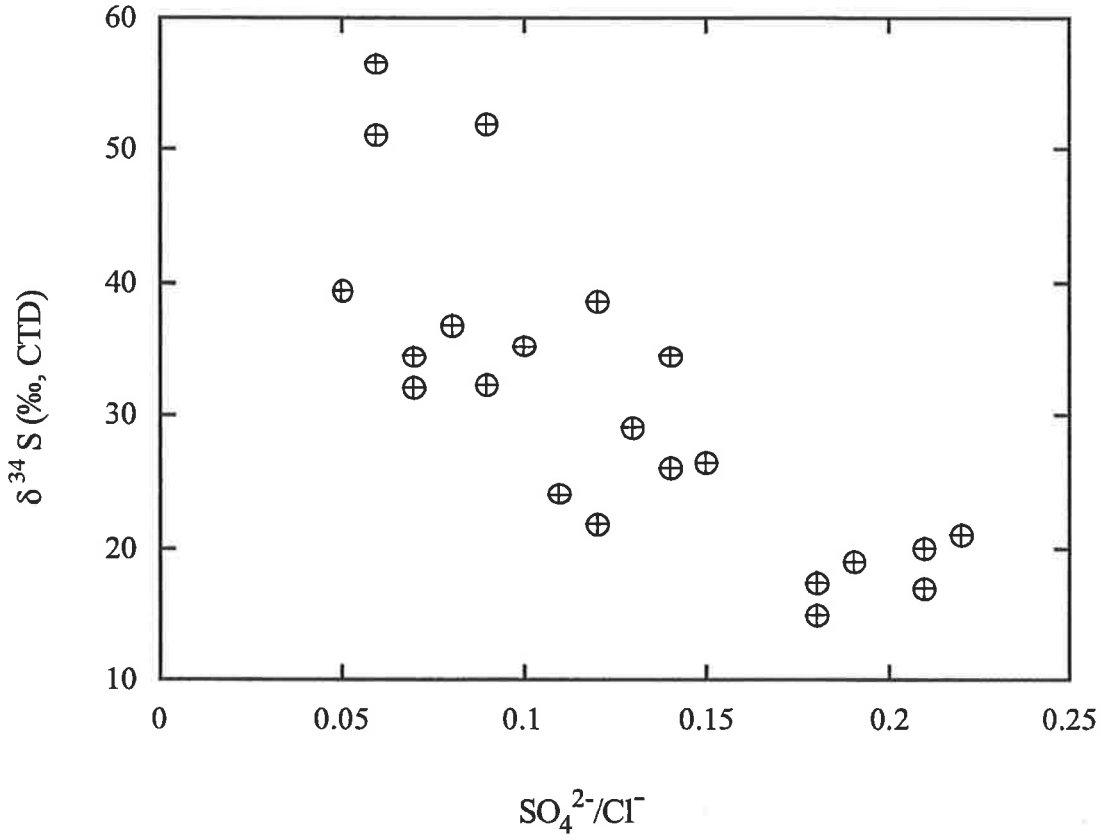

Fig. 4.3 $\delta^{34}S$ value vs. SO_4^{2-}/Cl^- ratio in the Renmark Group Aquifer. Note that the relatively depleted $\delta^{34}S$ values correspond to a higher SO_4^{2-}/Cl^- ratio.

Groundwater samples that have $\delta^{34}S$ value similar to marine $\delta^{34}S$ values of +21 ‰ also have an average SO_4^{2-}/Cl^- ratio of 0.2 which is slightly higher than the marine ratio of 0.14. This indicates little or no modification of SO_4^{2-} concentration in the aquifer. Deviation from the marine SO_4^{2-}/Cl^- ratio to a lower value is due to the removal of SO_4^{2-} by bacterial reduction. Sulphate reduction is implied by the presence of dissolved sulphide in the groundwater from the northern part of the study area (Table 4.2). Oxidation of organic carbon, which serves as the energy source for the bacteria, may be provided by thin beds of lignitic carbon that are present in the Renmark Group Aquifer matrix. Hence, there are favorable conditions for sulphate reduction in this aquifer.

The $\delta^{18}OSO_4^{2-}$ values in the Murray Group Aquifer range from +4.8 ‰ to +9.1 ‰ in the south and central part. These groundwaters are more depleted in ^{18}O compared to the $\delta^{18}OSO_4^{2-}$ values of groundwater from the north and north-east near the River Murray, which have $\delta^{18}OSO_4^{2-}$ values of > +15 ‰ (wells adjacent to the River Murray). The $\delta^{18}OSO_4^{2-}$ values in the Renmark Group Aquifer are generally more enriched than the Murray Group Aquifer and range from +11.6 ‰ to +18 ‰ (Table 4.1, 4.2).

4.4 Discussion

4.4.1 SO_4^{2-}/Cl^- ratio and $\delta^{34}S$ profiles below the water table from the Murray Group Aquifer

Groundwater from the Murray Group Aquifer was sampled from bores and wells that were characterised by different screen intervals depending on the type of bores/wells. Some of these bores/wells were open to the entire aquifer thickness ~ 90m (e.g. M72 to M91), and the others were mainly open to the top 2 to 50 m of the aquifer thickness.

The chemical composition and the concentration of total dissolved ions may vary with depth below the water table due to heterogeneity of aquifers and the stratification of groundwater (Toth, 1983). In order to determine the effect of sampling interval on the chemical and isotopic composition of the groundwater from the Murray Group Aquifer, Cl^- and SO_4^{2-} concentrations as well as $\delta^{34}S$ composition were analysed in

groundwater samples from discrete intervals below the water table (Table 4.3). The location of the bores (MH1, MH2, MH3) is shown in Fig. 2.1.

Table 4.3 The SO_4^{2-}/Cl^- ratio and $\delta^{34}S$ composition in groundwater from discrete depth below the water table of the Murray Group Aquifer. The depth below water table is expressed in metres. The results of Cl^- and SO_4^{2-} are quoted in milligram per litre. The $\delta^{34}S$ is expressed in per mil notation relative to standard CTD (Canyon Diablo Triolite). WT Depth in the third column stands for depth of water table below the surface.

	Depth (m)	WT Depth	Cl^-	SO_4^{2-}	SO_4^{2-}/Cl^-	$\delta^{34}S$
			mg/l			‰(CTD)
MH1		28.2				
	33		874	200.7	0.23	6.8
	36		874	202.5	0.23	6.8
	39		839	200.7	0.24	6.4
	48		817	192.3	0.24	6.7
	57		853	196.5	0.23	6.2
	66		879	205.2	0.23	6.6
MH2		63.8				
	72		386	85.2	0.22	14.6
	75		377	80.4	0.21	14.3
	78		354	79.2	0.22	14.8
	87		366	80.4	0.22	14.5
	90		323	72.6	0.22	14.6
	93		299	65.7	0.22	14.1
	102		298	69.9	0.23	14.1
MH3		68.3				
	84		320	62.4	0.20	12.9
	87		321	59.1	0.18	12.3
	90		300	59.7	0.20	12.1
	99		310	59.7	0.19	12.0
	108		342	64.8	0.19	12.3
	114		341	65.1	0.19	12.3

The concentrations of Cl^- and SO_4^{2-} in MH2 and MH3 from the sampled intervals are similar, and range from 298 mg/l to 377mg/l and 59.1 mg/l to 85.2 mg/l respectively. The concentrations of Cl^- and SO_4^{2-} in groundwater from MH1 down gradient are relatively higher and range from 817mg/l to 879mg/l and 192.3mg/l to 205.2 mg/l respectively (Table 4.3). There is no systematic change in the concentration of both ions (i.e. decrease or increase with the depth below the water table). However the change in concentration of SO_4^{2-} corresponds to the similar change in the

concentration of Cl^-. Consequently the SO_4^{2-}/Cl^- remains fairly constant with depth below the water table (Fig 4.4).

The change in both ions with similar increments in a depth profile may suggest that the variation in Cl^- and SO_4^{2-} concentrations is due to the evapoconcentration effect prior to recharge. The higher rate of evapoconcentration increases the overall concentration of the dissolved ions of water recharging the aquifer without altering ion/Cl^- ratio. A relatively constant SO_4^{2-}/Cl^- ratio of groundwater with depth suggests that the sampling methodology of the groundwater from the Murray Group Aquifer (i.e. groundwater obtained from various depth of the aquifer) may effect the overall concentration of the dissolved ions, however it has a minimum effect on the ions/Cl^- ratio. Therefore, the observed spatial variation in SO_4^{2-}/Cl^- ratio of the Murray Group Aquifer (Fig 4.1) is not an artefact of sampling methodology.

This is also true for the $\delta^{34}S$ values measured from the three bores below the water table (Fig.4.4). The $\delta^{34}S$ profile shows a slight variation, which is not related to the sampling depth below the water table (i.e. systematic change with depth). The $\delta^{34}S$ values for the groundwater samples vary only by 0.5 ‰ and never exceed 0.8 ‰ in any given profile. Given the analytical error of ± 0.2 for $\delta^{34}S$ measurement, the relatively small variation from different depths is not significant, particularly when the observed spatial difference in $\delta^{34}S$ values between the groundwater sampled along the gradient in Zone A is up to 20 ‰ and in Zone B is up to 35 ‰.

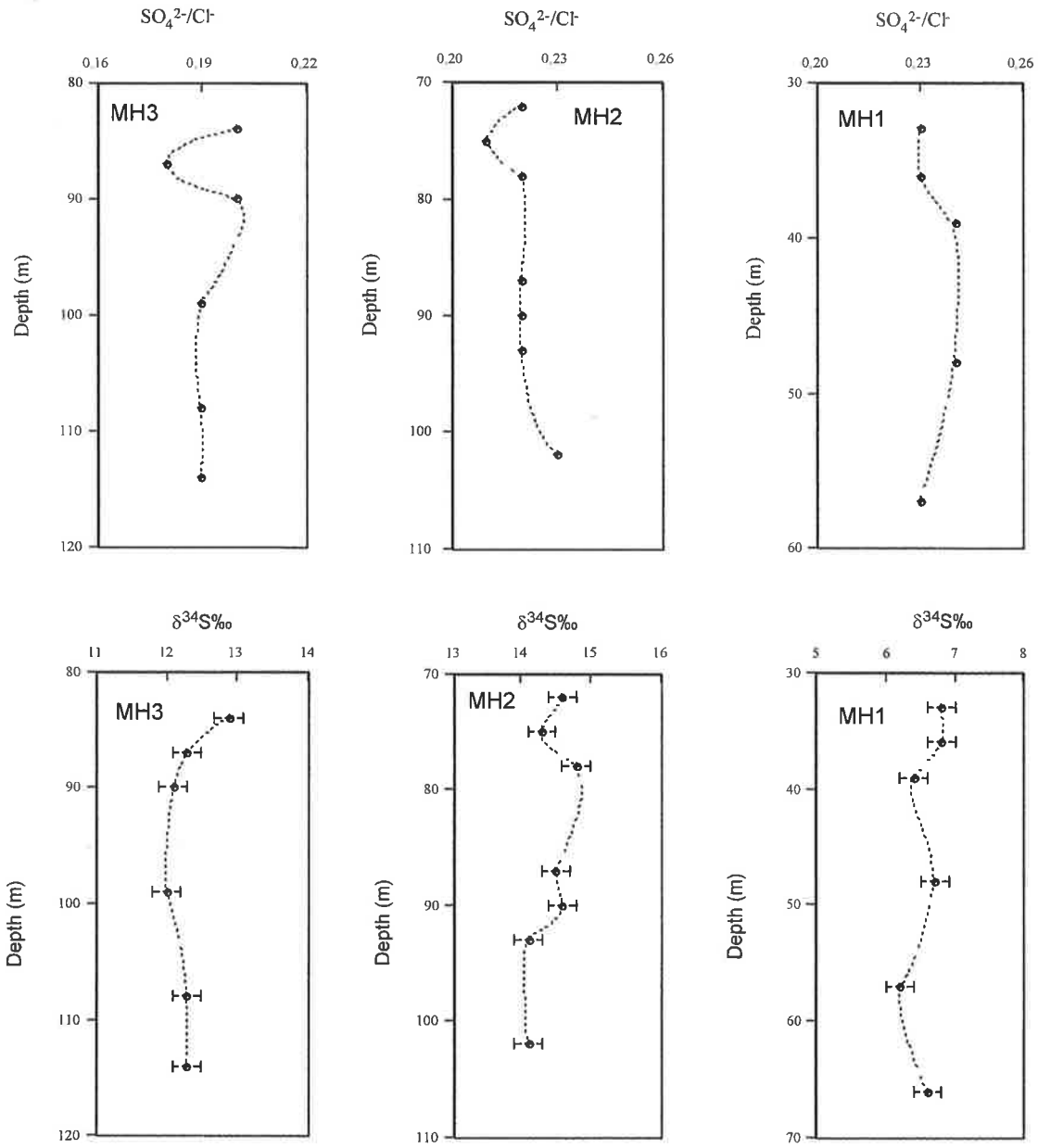

Fig. 4.4 Profiles of SO_4^{2-}/Cl^- ratio and $\delta^{34}S$ composition of the three boreholes from the Murray Group Aquifer. The error bars on the $\delta^{34}S$ profile represent analytical error of ± 0.2 for the $\delta^{34}S$.

The profiles in fig 4.4 show no significant variation in either SO_4^{2-}/Cl^- ratio or in $\delta^{34}S$ values below the water table in the Murray Group Aquifer. The large spatial differences in both SO_4^{2-}/Cl^- ratio and $\delta^{34}S$ values (Fig 4.1 and 4.2) therefore must be due to chemical and/or physical processes occurring in the aquifer.

4.4.2 Spatial distribution of $\delta^{34}S$ in the Murray Group Aquifer

Groundwater from the Murray Group Aquifer can be divided into two zones according to $\delta^{34}S$ values and hydraulic head distribution; (1) Zone A, which represents groundwater from the south and central parts of the study area that are unaffected by mixing with the Renmark Group Aquifer; (2) Zone B, which represents groundwater from the northern part of the study area near the River Murray. The groundwater in this part may be influenced by upward leakage from the Renmark Group Aquifer as indicated by the positive hydraulic head difference between groundwater in the Renmark and Murray Group aquifers (Fig. 1.5).

4.4.2.1 $\delta^{34}S$ of the Murray Group Aquifer in Zone A

Groundwater in the south and south-east part of the study area (Zone A) shows an increase in SO_4^{2-}/Cl^- ratio and decrease in $\delta^{34}S$ values along the hydraulic gradient. The SO_4^{2-}/Cl^- ratio in the Renmark Group Aquifer in Zone A is always less than that in the Murray Group Aquifer. Thus, the source of extra SO_4^{2-} in the Murray Group Aquifer in Zone A is not from the Renmark Group Aquifer through upward leakage. There must therefore, be other sources of dissolved SO_4^{2-} in the Murray Group Aquifer.

Groundwaters in the Murray Group Aquifer that have $\delta^{34}S$ values of ~ +20 ‰ suggest that the SO_4^{2-} concentrations are dominated by input from marine aerosols. Any contribution from wind blown gypsum particles from the playa lakes to the north-east

of the study area, with $\delta^{34}S$ values from +14.2 ‰ to +20.5 ‰ (Schmid, 1985; Jacobson 1988; Chivas et al., 1991) is not likely to be a significant source of SO_4^{2-} along the hydraulic gradient, because the $\delta^{34}S$ values of SO_4^{2-} in the groundwater decrease systematically towards the central part of the basin (Fig. 4.2). Groundwater in the central part has the lowest $\delta^{34}S$ values (+0.3 ‰ and +1 ‰ - Table 4.1). If wind blown gypsum was a dominant factor in increasing SO_4^{2-} concentration, the wells in the central part, which are closer to the playa lakes, would have higher $\delta^{34}S$ values than the wells in the basin margin in the south and south-east of the study area.

Groundwater in the Murray Group Aquifer is undersaturated with respect to gypsum. Therefore, gypsum dissolution from the aquifer matrix is not likely to produce the extra sulphate in groundwater. However, this does not rule out dissolution of gypsum in the soil and the unsaturated zone. This is also unlikely because the $\delta^{34}S$ values of gypsum in the Australian continent are dominated by marine $\delta^{34}S$ ranging from +14 ‰ to +20 ‰ (Chivas et al., 1991). These values are much higher than the $\delta^{34}S$ observed in some of the groundwaters in the Murray Group Aquifer.

Pyrite oxidation will also increase SO_4^{2-} concentrations, but decrease $\delta^{34}S$ values and increase acidity. The reaction may proceed either by the direct oxidation of pyrite exposed to air or water (Eq. 4.1), or by the reduction of ferric iron via Eq. 4.3 - 4.5 below (Stumm and Morgan, 1981):

$$FeS_2 + 7/2\ O_2 + H_2O \rightarrow Fe^{2+} + 2SO_4^{2-} + 2H^+ \quad (4.2)$$

$$Fe^{2+} + 1/4O_2 + H^+ \rightarrow Fe^{3+} + 1/2H_2O \quad (4.3)$$

$$Fe^{3+} + 3H_2O \rightarrow Fe(OH)_3 + 3H^+ \quad (4.4)$$

$$FeS_2 + 14Fe^{+3} + 8H_2O \rightarrow 15Fe^{2+} + 2SO_4^{2-} + 16H^+ \quad (4.5)$$

Fe^{2+} produced via Eq. 4.5 may re-enter the reaction cycle again via reaction Eq. 4.3.

The production of acidity via pyrite oxidation may then result in the dissolution of calcite. This can be quantitatively tested via mass balance/mass transfer calculations. The oxidation of pyrite along the hydraulic gradient from the basin margin to the central part was modeled to account for the increase of SO_4^{2-} concentration, using computer code PHREEQM, (Nienhuis et al., 1991). Two wells were selected; one in the southwestern margin to represent recharge water in the south, well M9, and the second well in the central part with lowest $\delta^{34}S$ value at well M37 (Fig 3.1). The effect of pyrite oxidation on the evolution of groundwater was carried out by an irreversible reaction of pyrite with oxygen (pO_2= 0.2 atm.). The pH was buffered by equilibrium with calcite, and total iron in solution was controlled by goethite equilibrium and the pe calculated as a function of the oxidation reaction. Chemical composition, pH, pe and mass transfer were calculated for 10 steps of addition of O_2, until the concentration of the SO_4^{2-} in the groundwater was equal to that measured at well M37 (The detailed input data for the pyrite oxidation model is given in Appendix 2).

Oxidation of 0.25 mmol/l of pyrite would be needed to account for the observed 0.5 mmol/l increase in SO_4^{2-} concentration between well M9 and M37. This should correspond to an increase in Ca^{2+} concentration to 2.55 mmol/l via calcite dissolution,

and a decrease in pH from 7.37 to 7.1. No increase in Ca^{2+} concentration in groundwater from the south to the central part of the study area is observed, indicating that pyrite oxidation does not contribute to the observed increase in SO_4^{2-} concentration in the Murray Group Aquifer. This finding was further supported by a petrographic study of cutting specimens of five drill holes in the Murray Group Aquifer. These specimens show no evidence of pyrite or any sulphide minerals in the aquifer matrix.

The most likely explanation for the observed increases of both dissolved SO_4^{2-} concentrations and SO_4^{2-}/Cl^- ratios in the Murray Group Aquifer further inland is an increase in the contribution of biogenic SO_4^{2-} in the rainfall recharging the aquifer. The $\delta^{34}S$ values of the groundwater decrease from ~ +20 ‰ (i.e. similar to marine SO_4^{2-} and approach those of biogenic SO_4^{2-} ~ 0 ‰). Figure 4.5 shows that water at one end of the spectrum has SO_4^{2-}/Cl^- ~ 0.14 and has a marine $\delta^{34}S$ signature of ~ +20 ‰. The other end of the spectrum represents biogenic sulphur with relatively high SO_4^{2-}/Cl^- and a $\delta^{34}S$ signature of ~ 0 ‰. Samples that have higher SO_4^{2-}/Cl^- (exceeding 0.14), generally have lower and decreasing $\delta^{34}S$ values depending on the contribution from sea-spray.

All the samples collected from the Murray Group Aquifer in the south and central part of the basin scatter between marine and biogenic $\delta^{34}S$ values. If mixing between a distinctly biogenic source and a marine source of sulphate were the sole factor in controlling the SO_4^{2-}/Cl^- and $\delta^{34}S$ in the Murray Group Aquifer, the data in Fig 4.5

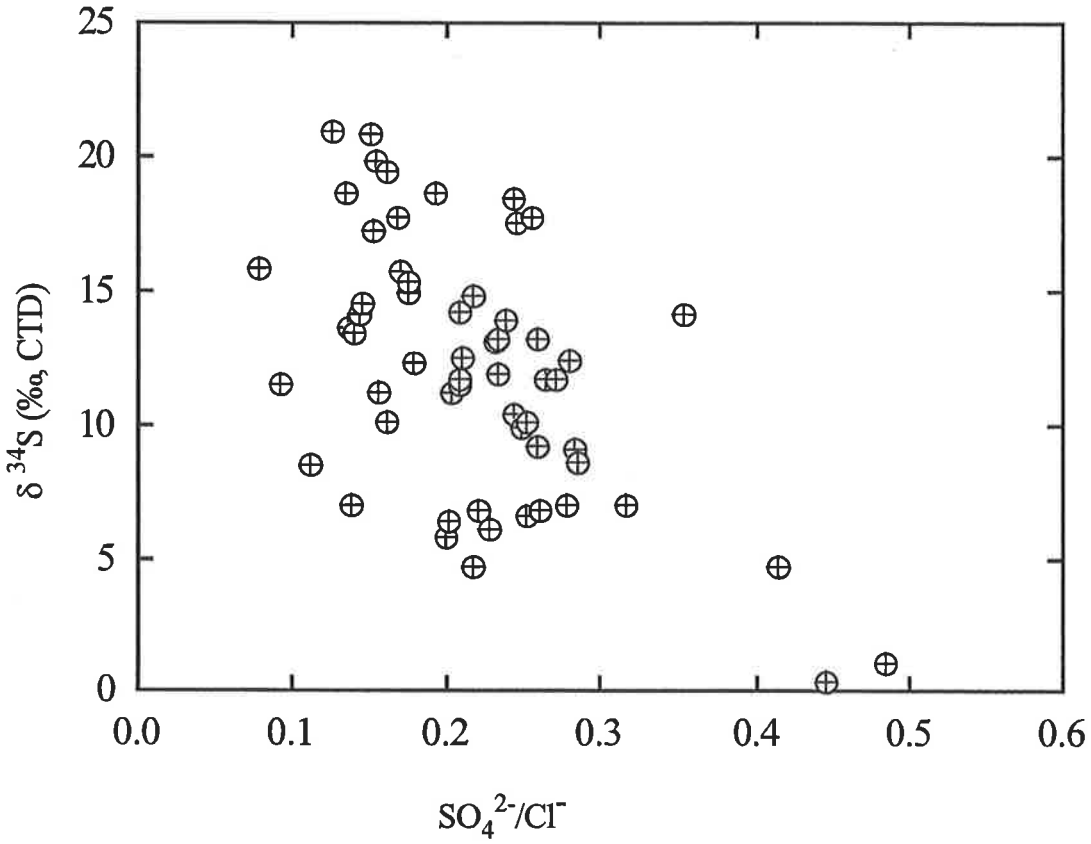

Fig. 4.5 $\delta^{34}S$ vs. SO_4^{2-}/Cl^- ratio in the Murray Group Aquifer from the south and central part of the study area.

would fall on a straight line. One possible mechanism that may be responsible for the scatter of the data is mineralisation of organic sulphur in the soil zone (Mayer et al., 1991). This would cause an increase in the sulphate concentration and the SO_4^{2-}/Cl^- ratio without a significant change in $\delta^{34}S$ values (fractionation during oxidation is ~ +1 ‰; Norman, 1994). The amount of mineralised organic sulphur in the soil zone and its contribution to the sulphate pool in groundwater depend on the recharge rate and the concentration of organic sulphur present in the soil zone. The contribution of organic sulphur to the sulphate pool in the Murray Group Aquifer is estimated by $\delta^{18}OSO_4^{2-}$ mass balance calculations and is discussed in detail in section (4.4.4).

The spatial variation of SO_4^{2-}/Cl^- and $\delta^{34}S$ values, and their relationship in groundwater from the south and central parts the Murray Group Aquifer suggest that: (1) the $\delta^{34}S$ of dissolved sulphate in groundwater from the Murray Group Aquifer generally conserves its isotopic signature as precipitation infiltrates through the soil zone; (2) processes such as dissolution of gypsum, oxidation of pyrite, or reduction of SO_4^{2-} in the groundwater are not significant; (3) contribution of wind blown gypsum particles from the playa lakes is not a significant source for sulphate; and (4) vertical input of SO_4^{2-} via local recharge is more significant compared with that derived from lateral flow.

4.4.2.2 $\delta^{34}S$ of the Murray Group Aquifer in Zone B

SO_4^{2-}/Cl^- ratios of the Murray Group Aquifer in the northern part of the study area (Zone B) decrease from 0.5 in the Big Desert to values as low as 0.05 at Woolpunda, 20 km south of the River Murray (Fig 4.1). At the same time sulphate $\delta^{34}S$ values increase from +0.3 ‰ to a maximum value of +38.7 ‰ at Woolpunda. The $\delta^{34}S$ value of groundwater in well M68 located in the centre of the Woolpunda groundwater mound, is almost identical to the Renmark Group Aquifer (R18) at the same location ($\delta^{34}S$= +39 ‰). The similarity of the $\delta^{34}S$ and SO_4^{2-}/Cl^- in the two aquifers is an indication of the high degree of upward leakage in this part of the study area. Previous studies conducted at the Woolpunda site (Herczeg et al., 1989; Cook et al., 1992) support the conclusion that the groundwater mound at Woolpunda is due to upward leakage from the Renmark Group Aquifer. The reason for the high degree of mixing at

the Woolpunda site could be due to a large hydraulic head difference between the two aquifers (~25m), resulting in a high potential for upward leakage from the Renmark Group Aquifer. Telfer (1990) documents a thinning of the Renmark Group Aquifer beds from ~ 400m to ~100m at this site due to the Hamley Fault which could be responsible for upward diversion of groundwater to the Murray Group Aquifer. The hydraulic head distribution between the Renmark and Murray Group aquifers (Chapter 1, Fig. 1.5) indicates that the hydraulic potential for upward leakage increases from the central part of the study area to the north and north east. As upward leakage from the Renmark Group Aquifer proceeds, the $\delta^{34}S$ signature should increase in the groundwater in the Murray Group Aquifer. However, this is not observed at all of the wells sampled adjacent to the River Murray (M72 to M91). The $\delta^{34}S$ values of groundwater from these wells range from +25.3 ‰ to +37.4 ‰, and are higher than the observed $\delta^{34}S$ value in the Renmark Group Aquifer (R19 - Table 4.2). A plot of $\delta^{34}S$ versus SO_4^{2-}/Cl^- in groundwater for the Murray Group Aquifer wells adjacent to the River Murray at Woolpunda and Waikerie show a strong inverse correlation (Fig. 4.6). This is most probably the result of sulphate reduction, where low redox conditions may be induced by mixing with the anaerobic groundwater from the Renmark Group Aquifer. That is, the reducing conditions induced on the Murray Group Aquifer following upward leakage result in relatively more enriched $\delta^{34}S$ values compared to groundwater in the Renmark Group Aquifer.

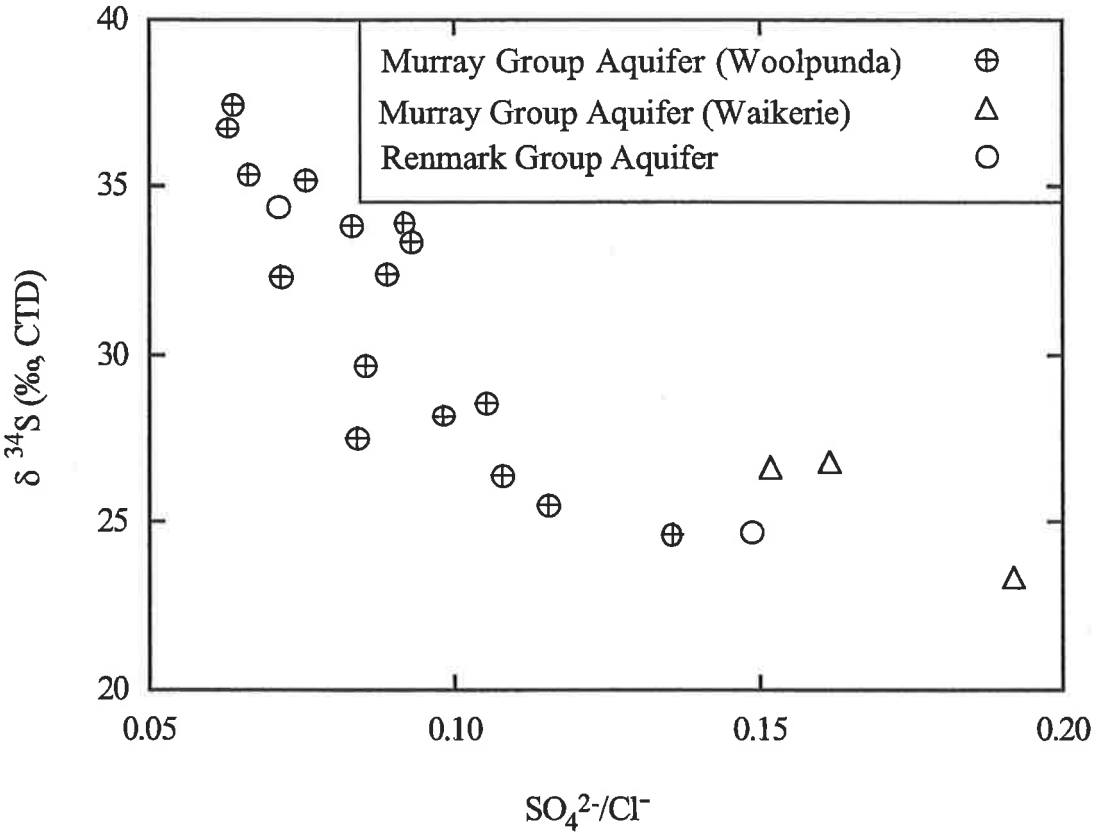

Fig. 4.6 $\delta^{34}S$ vs. SO_4^{2-}/Cl^- ratio in the Murray and Renmark Group aquifers for the wells adjacent to the River Murray in the northern part of the study area.

The sulphate concentration in groundwater from the Murray Group Aquifer at Waikerie and Woolpunda ranges from 642 to 2289 mg/l. Six of these wells have sulphate concentrations higher than the groundwater of the Renmark Group Aquifer (i.e. 1233 mg/l). This suggests addition of SO_4^{2-} to the groundwater of the Murray Group Aquifer by processes other than upward leakage from the Renmark Group Aquifer. Because the SO_4^{2-}/Cl^- ratio increases with increase in SO_4^{2-} concentration (Fig .4.7), there is a net addition of SO_4^{2-} to the Murray Group Aquifer. The increase in SO_4^{2-} concentration may be due to addition of sulphate to the Murray Group Aquifer by dissolution of gypsum as water percolates through the unsaturated zone.

Gypsum has been reported in exposures along the River Murray cliffs near the study area (Jack, 1921; King, 1951).

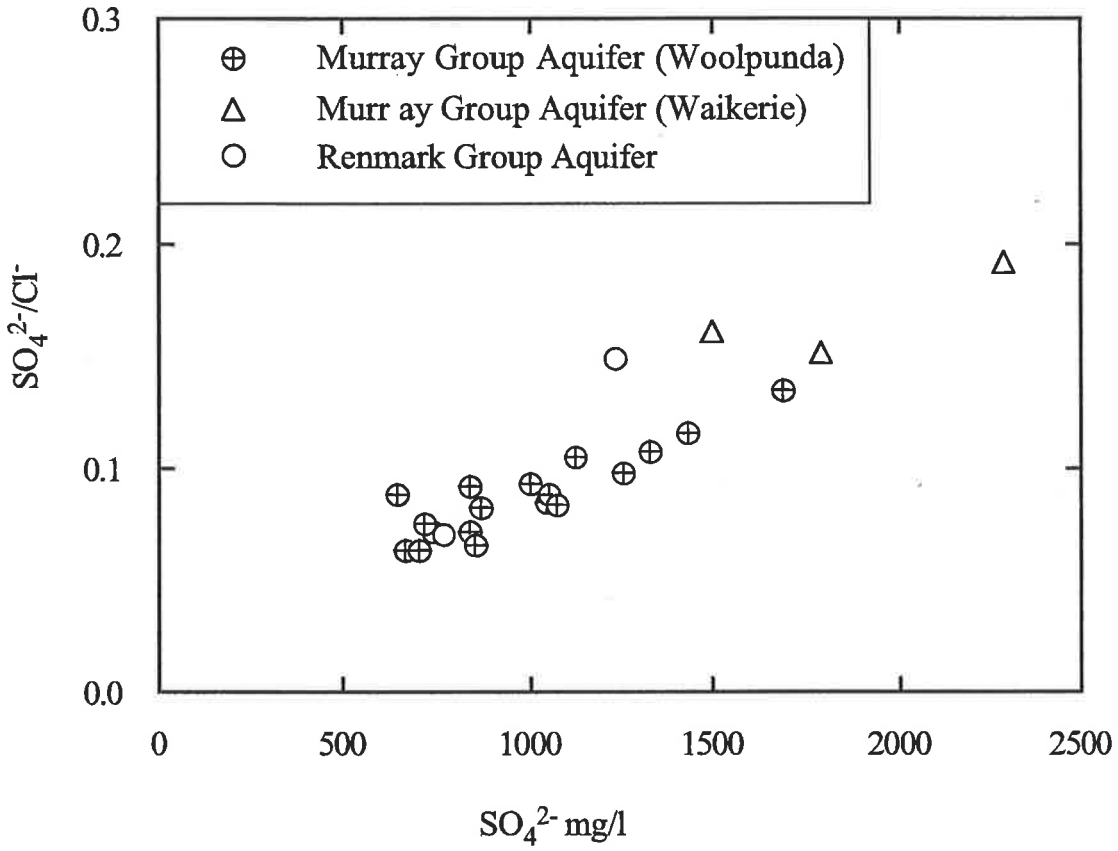

Fig. 4.7 SO_4^{2-}/Cl^- ratio vs. SO_4^{2-} concentration from wells adjacent to the River Murray in the Murray and Renmark Group aquifers.

Gypsum dissolution may increase the dissolved SO_4^{2-} and Ca^{2+} concentrations in groundwater according to Eq. 4.6,

$$CaSO_4.2H_2O \rightarrow Ca^{2+} + SO_4^{2-} + 2H_2O \quad K = 10^{-4.602} \text{ at } 25^\circ C \qquad (4.6)$$

As dissolution of gypsum progresses, the molar proportion of Ca^{2+} to SO_4^{2-} increase is 1:1. If the increase of dissolved SO_4^{2-} and Ca^{2+} in groundwater at Woolpunda and

Waikerie was mainly from gypsum dissolution, their molar concentration should increase in equal proportions. Fig. 4.8 shows that the groundwater at Woolpunda and Waikerie represents two distinct waters with different chemical characteristics.

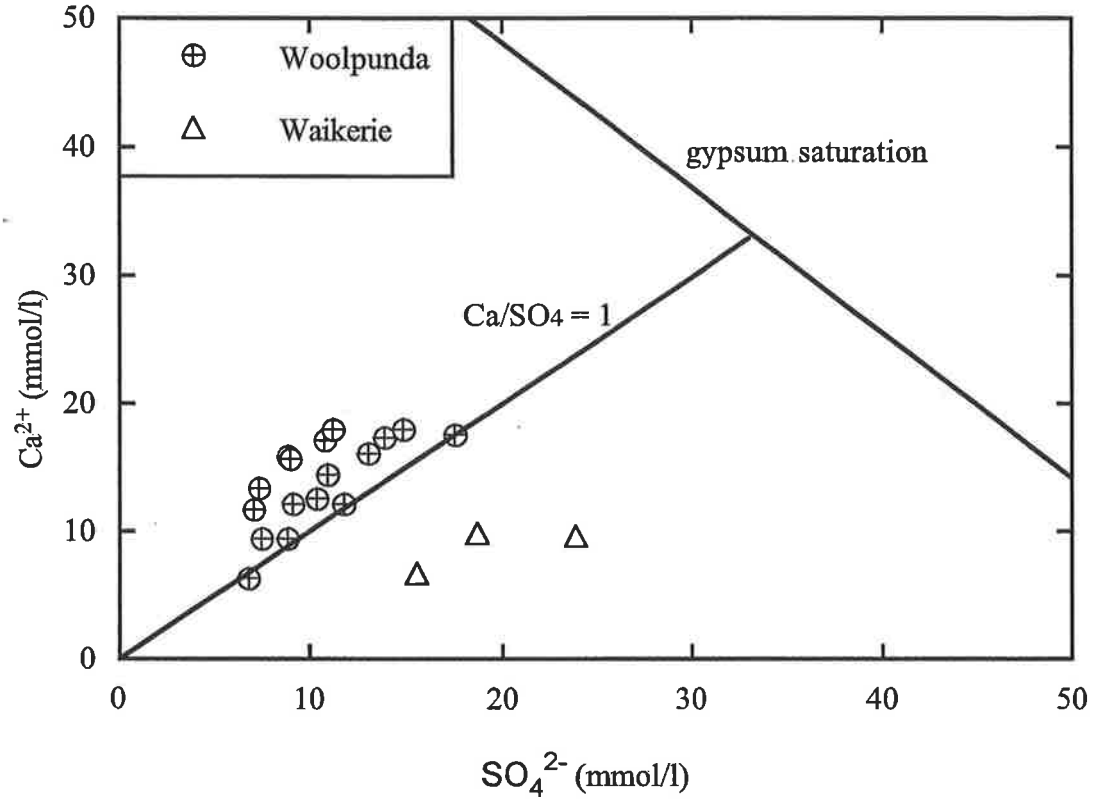

Fig. 4.8 Ca^{2+} vs. SO_4^{2-} molar concentrations in the Murray Group Aquifer at Woolpunda and Waikerie. The groundwater from Woolpunda site is characterised by higher Ca concentration due to bacterial sulphate reduction.

The molar SO_4^{2-}/Ca^{2+} ratio of groundwater at Waikerie is > 1, suggesting that gypsum dissolution is not the main factor in the increase of SO_4^{2-} concentrations in these groundwaters. The increase in SO_4^{2-} concentration in the Woolpunda wells, on the other hand, corresponds to an increase in the Ca^{2+} concentration but not in 1:1 ratio. Most of the data fall to the left of the 1:1 ratio line suggesting removal of SO_4^{2-} from the system, which results in an increase in the Ca^{2+}/SO_4^{2-} ratio. Only three (M81,M82

and M83) of the 17 groundwater samples at Woolpunda fall on the 1:1 ratio line indicating that sulphate removal by bacterial sulphate reduction following upward leakage from the Renmark Group Aquifer is not significant. Therefore, the $\delta^{34}S$ value for these wells can be calculated for the three groundwater samples via chemical and mass balance equations to check whether the SO_4^{2-} concentration in the Murray Group Aquifer was derived from a combination of upward leakage from the Renmark Group Aquifer and gypsum dissolution during recharge.

The $\delta^{34}S$ values reported for gypsum from the South Australia and the Victorian playa lakes ranges from +14.2 ‰ to +20.5 ‰ (Schmid, 1985; Jacobson 1988; Chivas et al., 1991). Assuming the average $\delta^{34}S$ values of +18 ‰ for gypsum, and $\delta^{34}S$ value of the groundwater in the Renmark Group Aquifer of +26.4 ‰ at this specific location, the $\delta^{34}S$ value of the groundwater in the Murray Group Aquifer can be estimated by the following mass balance equation:

$$\{\delta^{34}S\ (SO_4^{2-})\}_M = \{\delta^{34}S\ (SO_4^{2-})\}_R + \{\delta^{34}S_g\ (SO_4^{2-})\}_{M\text{-}R} \qquad (4.7)$$

where $\delta^{34}S$ and (SO_4^{2-}) are the sulphur isotopic composition and sulphate concentration respectively, and subscripts M and R refer to the Murray and Renmark Group aquifers, $\delta^{34}S$ is sulphur isotopic composition of gypsum in the unsaturated zone, and $(SO_4^{2-})_{M\text{-}R}$ is the difference in SO_4^{2-} concentration between the Murray and Renmark Group aquifers.

The results of calculated $\delta^{34}S$ values for the three wells at Woolpunda are presented in Table 4.3, and are similar to the observed $\delta^{34}S$ value. This is further evidence that the increase of the SO_4^{2-} concentration in the groundwater in this part of the basin is due to gypsum dissolution.

In summary, the variation in sulphate concentration and the relatively enriched $\delta^{34}S$ in the Murray Group Aquifer at the Woolpunda site could be due to a combination of three processes: (1) gypsum dissolution during local recharge; (2) upward leakage from the Renmark Aquifer; and (3) bacterial sulphate reduction.

Table 4.4 The observed and calculated $\delta^{34}S$ values obtained via a chemical and isotopic mass balance equation for three wells at the Woolpunda site.

	SO_4^{2-} mg/l	Observed δ^{34} ‰ (CTD)	Calculated $\delta^{34}S$ ‰ (CTD)
Renmark Group Aquifer			
R19	1233	26.4	
Murray Group Aquifer			
M81	1434	25.4	25.2
M82	1692	24.6	24.1
M83	1332	26.3	25.7

4.4.3 $\delta^{34}S$ in the Renmark Group Aquifer

The Redox potential (Eh) measurements for the confined Renmark Group Aquifer are generally < -80mV which indicates that the groundwaters are oxygen free.

Groundwaters from the south and south-east (i.e. upgradient) are more oxidising (Eh ~ -80 mV) compared to groundwaters further north and north-west near the River Murray (Eh ~ -400 mV). The relatively more positive Eh values in the upgradient part of the Renmark Group Aquifer are associated with recharge water from the Dundas Plateau in Victoria. The low redox potential and the presence of significant amount of organic matter in the Renmark Group sediments (2.95% by weight) provides an ideal environment for bacterial sulphate reduction (Thode, 1991). Most of the groundwater samples from the Renmark Group Aquifer have $\delta^{34}S$ values higher than marine $\delta^{34}S$ of +21 ‰ indicating bacterial sulphate reduction. $\delta^{34}S$ values of up to +56 ‰ were measured in groundwaters at Zone B in the northern part of the study area.

According to the bacterial sulphate reduction (Eq 4.1), each mole of sulphate reduced produces one mole of sulphide. The dominant sulphide species (H_2S & HS^-) in groundwater is determined by pH. Because the dissociation constant of H_2S is ($pK_{25°C}$= 6.96), and the pH of groundwater ranges from 7 to 8.7, the dominant sulphur species in the Renmark Group Aquifer is HS^-. The sulphide produced from the reduction reaction is scavenged by dissolved Fe^{+2}, and precipitates initially as amorphous FeS. As the solubility of pyrite is low ($pK_{25°C}$ = -18.6 - Stumm and Morgan, 1996), trace amounts of sulphide are sufficient to precipitate pyrite in the presence of Fe^{2+}.

The saturation index (SI) with respect to pyrite was calculated with the computer program WATEQ within the NETPATH package (Plummer et al., 1991), for water samples from the Renmark Group Aquifer (Table 4.2). The groundwater from these wells is over saturated with respect to pyrite. Test runs were carried out for groundwater from well R14 (Fig. 3.1) to determine the minimum amount of H_2S required to achieve pyrite saturation in the presence of 0.02 mg/l Fe^{2+} (the detection limit for Fe^{2+} concentration by the Atomic Absorption method). The result indicates that $1.3X10^{-5}$ mg/l of sulphide is sufficient for equilibrium with respect to pyrite. The calculated concentration of H_2S is well below the detection limit, (the threshold odour concentration of H_2S in water is between $2.5x10^{-5}$ and $2.5x10^{-4}$ mg/l). Therefore, pyrite saturation could be achieved in the Renmark Group Aquifer without detecting the presence of H_2S or Fe^{2+}. However, several wells in the Renmark Group Aquifer contain measurable amounts of H_2S (Table 2.4). Therefore, it can be concluded that there is insufficient dissolved iron to remove all the dissolved sulphide or the concentration of sulphide and iron is controlled by other forms of sulphide minerals such as amorphous iron sulphide.

Sulphide produced during sulphate reduction is always depleted in ^{34}S due to the kinetically more favored ^{32}S reactivity facilitated by bacteria (Nakai and Jensen, 1964). Although the concentration of organic matter in the Renmark Group Aquifer is high in places up to 3% weight, the rate of the reduction reaction is controlled by the amount of labile organic matter, not the total concentration of particulate organic matter. The reactivity of organic matter decreases with time, due to the consumption of the more

labile proportion with early flushing of the aquifer. In addition to the amount of organic matter, the rate of reduction depends on the abundance of sulphate. The decrease in reactivity of organic matter will result in lower rates of SO_4^{2-} reduction. Lower reaction rates may correspond to an increase in the enrichment factor between residual sulphate and produced sulphides (Harrison and Thode, 1958; Kaplan and Rittenberg, 1964). In the presence of abundant sulphate, the reduction will proceed until all available organic matter is consumed.

The enrichment factor of $\delta^{34}S$ in the Renmark Group Aquifer between SO_4^{2-} and H_2S can be calculated using the method described by Strebel et al. (1990), where in a closed system such as the Renmark Group Aquifer, the reaction follows a Rayleigh-type distillation process. Isotopic enrichment of the reactant (SO_4^{2-}) can be described by the relationship:

$$\delta_R = \delta_I + \varepsilon \ln f \qquad (4.8)$$

where δ_R and δ_I are the initial and residual $\delta^{34}S$ values, respectively, ε is the isotopic enrichment factor, and f is the fraction of initial SO_4^{2-} remaining. The enrichment factor can be obtained from the slope of the regression line fitted to the semi-log plot of $\delta^{34}S$

versus *f* (Fig. 4.9). In this case, *f* has been determined relative to the highest observed

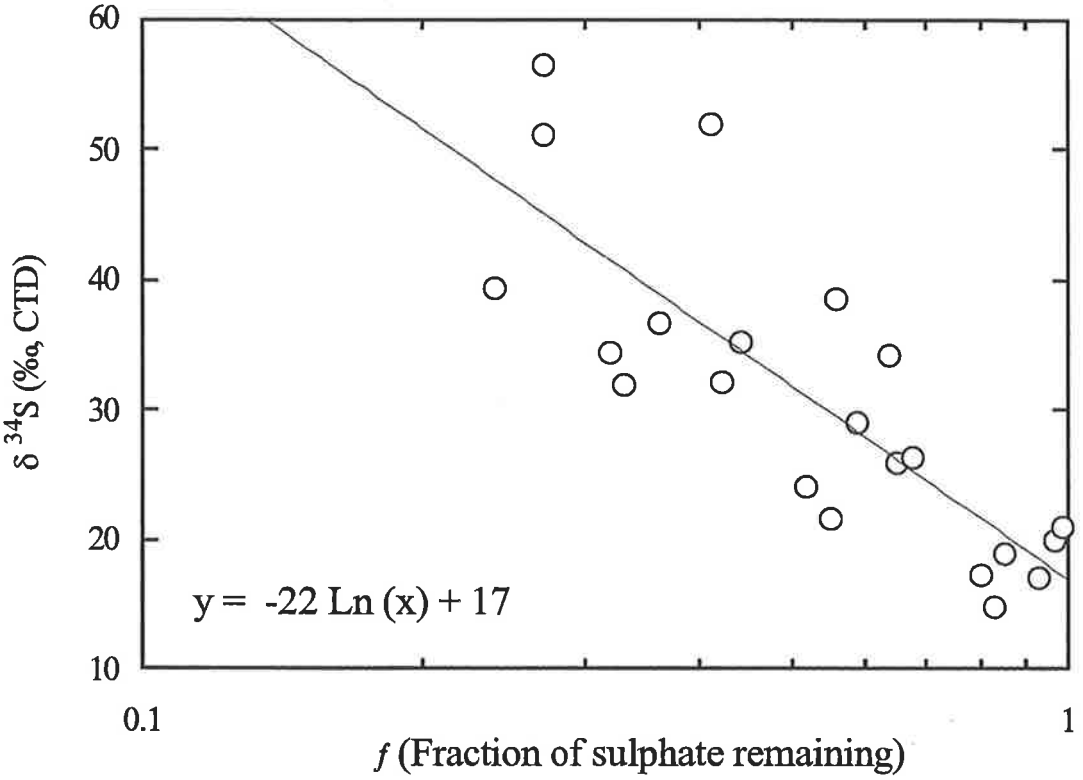

Fig. 4.9 $\delta^{34}S$ vs. the fraction of sulphate remaining (*f*) as a result of bacterial sulphate reduction in the Renmark Group Aquifer.

SO_4^{2-}/Cl^- ratio in the groundwater ($SO_4^{2-}/Cl^- = 0.22$). The 0.22 ratio is assumed to represent the initial input. The rest of the groundwater SO_4^{2-}/Cl^- ratios were divided by the initial value to determine the fraction of sulphate remaining for each sample. The regression line shows a correlation coefficient r^2 of (-0.62) between $\delta^{34}S$ and *f* and an enrichment factor of ~ -22 ‰ ± 6.5 (90% confidence interval). The enrichment factor (ε) estimated in this study is similar to the kinetic fractionation factor of -22 ‰ measured in laboratory experiments by Harrison and Thode (1958). A smaller enrichment factor of -9.7 ‰ was observed by Strebel et al. (1990), for the Fuhberger

Aquifer in Germany and -15.5 ‰ by Robertson and Schiff (1994) for groundwaters at Sturgeon Falls, Ontario, Canada. They attributed the small enrichment factor to low concentrations of organic matter and SO_4^{2-} in these aquifers.

Although laboratory experiments generally have shown that ε during bacterial sulphate reduction is close to the kinetic fractionation factor, some of the experiments produced ε values of up to 62 ‰ (Harrison and Thode, 1958; Kaplan and Rittenberg, 1964; Nakai and Jensen, 1964; Mizutani and Rafter, 1973). High enrichment factors are also observed in natural environments such as the Black Sea (Vinogradov et al., 1962), the coast of California (Kaplan et al., 1963), Madison Aquifer, USA (Busby et al., 1991) and a carbonate aquifer in Florida (Rye et al., 1980).

Many hypotheses have been proposed to explain the wide variation in the observed enrichment factor. Some of these hypotheses relate a higher enrichment to the conditions of the experimental conditions such as temperature, concentration of sulphate and the type of electron donor (Kemp and Thode, 1968) or factors relating to the mechanisms and the pathways by which sulphate reduction occurs (Rees et al., 1973). Another suggestion is that these high ε values are probably due to the establishment of the isotopic equilibrium between the sulphate and sulphide (Rye et al., 1980). However, Thode (1991) stated that there is no evidence of isotopic exchange between sulphate and sulphide at ambient temperatures, and that the time required to establish equilibrium may be long even on geological time scales.

The enrichment factor in this study is much lower than the equilibrium fractionation of ~74 ‰ (Tudge and Thode, 1950), despite the long residence time of >40,000 yr. of groundwater in the Renmark Group Aquifer. Therefore, it is concluded that the fractionation of 22 ‰ represents the dominance of kinetic fractionation which is caused by the unidirectional biochemical reaction. There is no evidence that the equilibrium enrichment factor has influenced the $\delta^{34}S$ value during sulphate reduction in the Renmark Group Aquifer.

4.4.4 $\delta^{18}OSO_4^{2-}$ in the Murray Group Aquifer

The $\delta^{18}OSO_4^{2-}$ values of groundwater from the Murray and Renmark Group aquifers are shown in Table 4.1 and 4.2. The $\delta^{18}OSO_4^{2-}$ values for the Murray Group Aquifer in the south and central part of the study area range from +4.8 ‰ to +9 ‰ . These values are less than the marine aerosol $\delta^{18}OSO_4^{2-}$ value of ~ +9.6 ‰ (Lloyd, 1967, 1968). Although no analysis of rainfall samples was conducted in this study, $\delta^{18}OSO_4^{2-}$ values measured in other investigations indicate that $\delta^{18}OSO_4^{2-}$ values for rainfall that are not affected by industrial activities averages ~ +10 ‰ (Mizutani and Rafter, 1969b; Holt, 1986; Caron, 1986; Norman, 1991; Van Stempvoort and Krouse, 1992).

Water that percolates through the soil zone to the groundwater has been observed to be depleted in $^{18}OSO_4^{2-}$ compared with local rainfall (Holt, 1986; Caron, 1986). Thus, it is expected that the $\delta^{18}OSO_4^{2-}$ values for the Murray Group Aquifer would be lower than

the anticipated value for rainfall (~ +10 ‰). Therefore, low $\delta^{18}OSO_4^{2-}$ values observed in groundwater of the Murray Group Aquifer are not the result of addition of depleted $\delta^{18}OSO_4^{2-}$ via pyrite oxidation. Earlier discussion of the $\delta^{34}S$ showed that oxidation of pyrite in the soil zone is not significant (section 4.5.1). The $\delta^{18}OSO_4^{2-}$ value also does not change by sorption or retention of sulphate in the soil zone (Van Stempvoort et al., 1990).

Isotopic exchange between the oxygen in sulphate molecules and the oxygen atoms in the water molecule cannot account for low $\delta^{18}OSO_4^{2-}$ compared to rainfall $\delta^{18}OSO_4^{2-}$ values, because this process is too slow. Lloyd (1968) concluded that the time required for almost complete exchange between $\delta^{18}OH_2O$ and $\delta^{18}OSO_4^{2-}$ at a temperature of 25 C° and a pH = 7 is ~10,000 years. Chiba and Sakai (1985) suggested that equilibrium times are > 100,000 years. The high uncertainties in these estimates eliminates any quantitative assessment of the importance of $\delta^{18}O$ exchange between water and sulphate. However, the $\delta^{18}O$ data of groundwater and sulphate suggest that the equilibrium fractionation factor which ranges from ~28 ‰ to 32 ‰ at 25C° (Muzituni and Rafter, 1969 b; Lloyd, 1968) has not been achieved, despite the long residence time of groundwater of >40,000 years.

The process more likely to cause the observed depletion of $\delta^{18}OSO_4^{2-}$ in groundwater is mineralisation of organic sulphur within the soil zone which results in 2 ‰ to 9 ‰ depletion relative to atmospheric precipitation (Van Everdingen et al., 1982; Holt and

Kumar, 1986; Mayer et al., 1991; Van Everdingen and Krouse, 1992; Mayer et al., 1995). Sulphate in groundwater consists of the atmospheric derived sulphate accompanying recharge water, and sulphate from mineralisation of organic sulphur in the soil zone.

Estimates of the proportion of sulphate contribution from mineralisation of organic sulphur to the groundwater can be made by the mass balance (Eq. 4.7). During the mineralisation process, the organic sulphur in the soil zone acquires oxygen from both dissolved oxygen and H_2O molecules according to the relationship (Lloyd, 1968):

$$\delta^{18}OSO_4^{2-} = X(\delta_{H2O} + \varepsilon_{H2O}) + (1-X)(\delta_{O2} + \varepsilon_{O2}) \qquad (4.7)$$

where X is the fraction of ^{18}O atoms from water during the formation of sulphate; ε_{H2O} and ε_{O2} are the equilibrium fractionation factors between oxygen attached to water molecules and dissolved oxygen with respect to oxygen atoms in sulphate molecules; δ_{H2O} and δ_{O2} are the $\delta^{18}O$ of the water and dissolved oxygen respectively.

Using values of X= 0.68, and $\varepsilon_{H2O} = 0$ ‰, $\varepsilon_{O2} = -8.7$ ‰ given by Lloyd (1968) and $\delta_{H2O} = -5.5$ ‰ for groundwater from the Murray Group Aquifer and, assuming that the dissolved oxygen has the same value as that of O_2 in atmosphere ($\delta_{O2} = +24.5$ ‰ Kroopnick and Craig, 1972), the calculated contribution from mineralisation of organic sulphur to the sulphate pool in groundwater ranges from 20% to 30%. These numbers are only rough estimates for the sulphate contribution from oxidation of organic sulphur to the groundwater.

The $\delta^{18}OSO_4^{2-}$ data above suggest that the vertical input of sulphate via local recharge may be an important source of sulphate in the Murray Group Aquifer. Once SO_4^{2-} reaches the saturated zone, no change in the $\delta^{18}OSO_4^{2-}$ values of sulphate occurs unless there is addition of SO_4^{2-} from oxidation of sulphide minerals or dissolution of sulphate minerals. Because the aquifer in the south and central part of the study area is free of sulphate or sulphide minerals, the change in observed $\delta^{18}OSO_4^{2-}$ must be due to addition of SO_4^{2-} via mineralisation of organic sulphur in soil zone during local recharge. This conclusion is also substantiated by $\delta^{34}S$ values which show that the variability of the SO_4^{2-}/Cl^- ratio and $\delta^{34}S$ values is caused by vertical input of the sulphate via local recharge to the Murray Group Aquifer (section 4.5.1.1).

4.4.5 $\delta^{18}OSO_4^{2-}$ in the Renmark Group Aquifer

The $\delta^{18}OSO_4^{2-}$ values for the Renmark Group Aquifer are more enriched compared to those of the Murray Group Aquifer, and range from +11.6 ‰ to +18 ‰. The SO_4^{2-}/Cl^- ratios range from 0.2 to 0.08 and are also lower than the Murray Group Aquifer which range from 0.14 to 0.5 (Fig. 4.10). As mentioned in section 4.5.2 the relatively low SO_4^{2-}/Cl^- ratios in the Renmark Group Aquifer are most probably caused by the removal of SO_4^{2-} by bacterial sulphate reduction.

The $\delta^{18}OSO_4^{2-}$ values in the Renmark Group Aquifer appear to be independent of $\delta^{34}S$ (Fig. 4.11). Because bacteria preferentially metabolise both light oxygen and sulphur

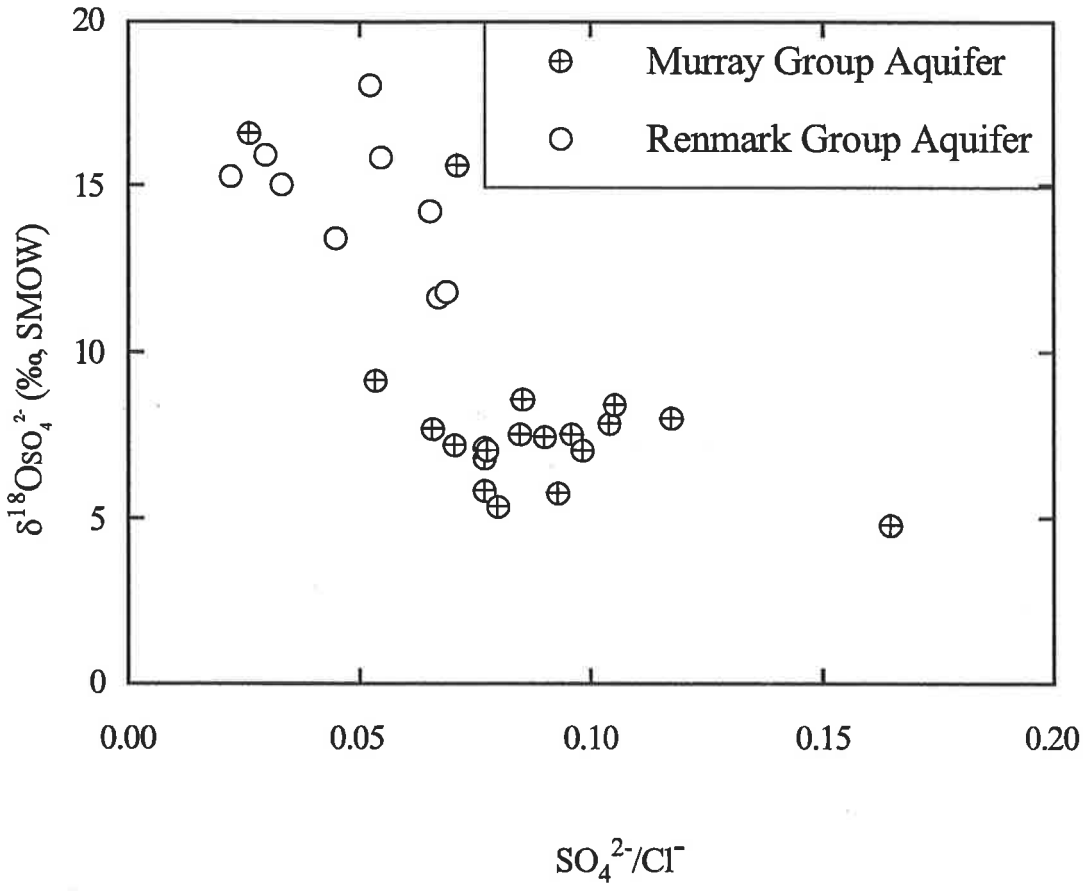

Fig. 4.10 $\delta^{18}OSO_4^{2-}$ vs. SO_4^{2-}/Cl^- ratio in the Murray and Renmark Group aquifers. The relatively enriched $\delta^{18}OSO_4^{2-}$ values in the Renmark Group Aquifer are caused by bacterial sulphate reduction.

(^{16}O and ^{32}S) of dissolved sulphate, more positive values of $\delta^{18}OSO_4^{2-}$ and $\delta^{34}S$ for the remaining sulphate can be expected. However, in both field observations and laboratory experiments, the $\delta^{34}S$ enrichment is not always accompanied by a corresponding $\delta^{18}OSO_4^{2-}$ enrichment (Mizutani and Rafter, 1973; Fritz et al., 1989). Their studies concluded that while the fractionation factor for $\delta^{34}S$ does not change during sulphate reduction, the $\delta^{18}OSO_4^{2-}$ of residual sulphate is modified by oxygen exchange between SO_4^{2-} and H_2O through the intermediate steps (sulphate-enzyme complexes and water) during sulphate reduction. Therefore, the $\delta^{18}OSO_4^{2-}$ of residual

sulphate depends on the $\delta^{18}O$ composition of the associated water, as well as the rate of reaction.

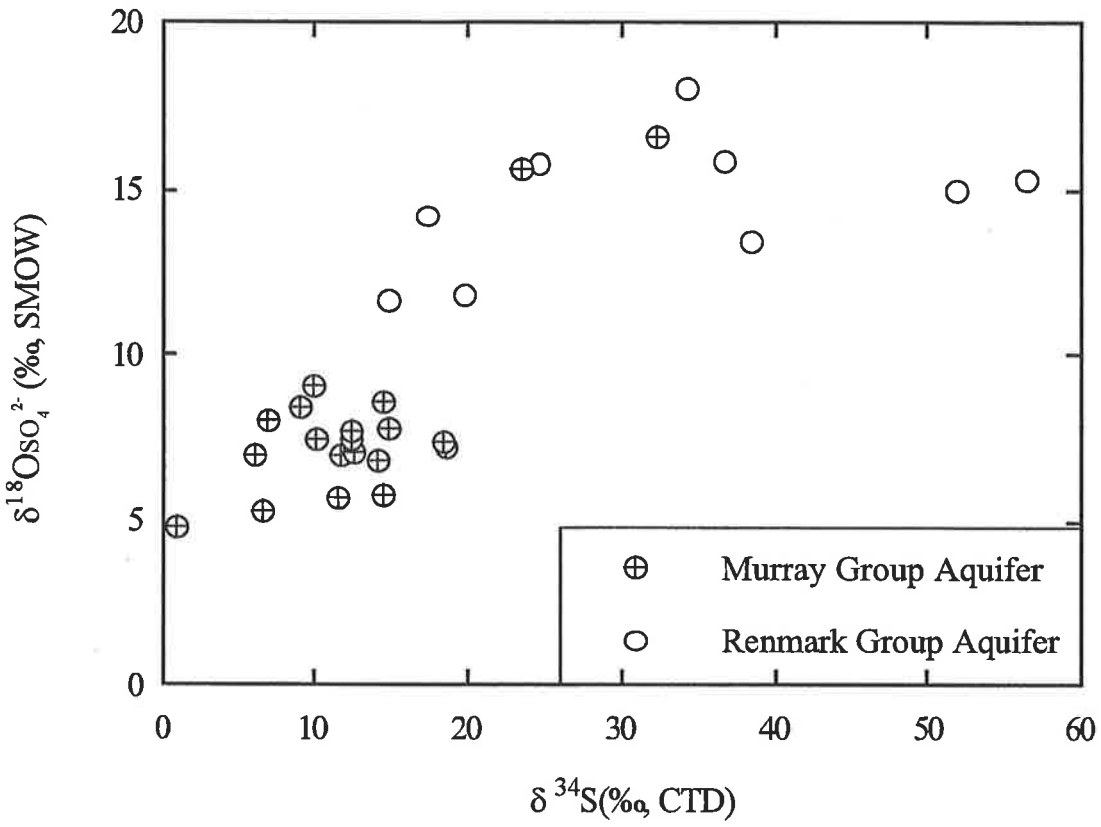

Fig. 4.11 The $\delta^{34}S$ and $\delta^{18}OSO_4^{2-}$ relationship in the Murray and Renmark Group aquifers. Both $\delta^{34}S$ and $\delta^{18}OSO_4^{2-}$ values of dissolved sulphate in the Murray Group Aquifer are depleted in heavy isotopes compared with the groundwater in the Renmark Group Aquifer.

Fritz et al. (1989) estimated a fractionation factor of ~ 25 ‰ at 30°C for $\delta^{18}O$ between residual sulphate and associated water. $\delta^{18}OH_2O$ values in groundwater from the Renmark Group Aquifer range from -6 ‰ to -3.5 ‰. Therefore the expected $\delta^{18}OSO_4^{2-}$ value for groundwater using a fractionation factor obtained by Fritz et al. (1989) would range from +19 ‰ to +22 ‰. However, the observed $\delta^{18}OSO_4^{2-}$ values for groundwater

samples affected by sulphate reduction (enriched in $\delta^{34}S$) are +13 ‰ to +18 ‰. The experiment carried out by Fritz et al. (1989) had abundant nutrient and SO_4^{2-} concentrations, and was conducted over a relatively short time period. In contrast, groundwater in the Renmark Group Aquifer has a long residence time (>40,000 years) and is more typical of slower natural processes. Although the $\delta^{18}OSO_4^{2-}$ data clearly indicates that an exchange process is important during bacterial sulphate reduction at low temperature, fractionation may be lower than that measured in laboratory experiments.

4.5 Summary and Conclusions

The range of $\delta^{18}O$ and $\delta^{34}S$ compositions of dissolved sulphate in the Murray and Renmark Group aquifers are caused by different redox conditions and differences in sources of SO_4^{2-}. Therefore, a mixing zone between the two aquifers can be identified when the values of $\delta^{18}O$ and $\delta^{34}S$ are plotted as a function of SO_4^{2-}/Cl^- for all the samples from both aquifers. Fig. 4.10 and Fig. 4.12 show that the $\delta^{34}S$ and $\delta^{18}OSO_4^{2-}$ of the Murray and Renmark Group aquifers fall between a range of two end members.

The groundwater of the Renmark Group Aquifer is more enriched in ^{34}S and $^{18}OSO_4^{2-}$ compared to that in the Murray Group Aquifer. The $\delta^{34}S$ and $\delta^{18}OSO_4^{2-}$ values falling between the two end members represent areas with a potential for mixing. The majority of these wells are located in the northern part of the study area. The upward leakage

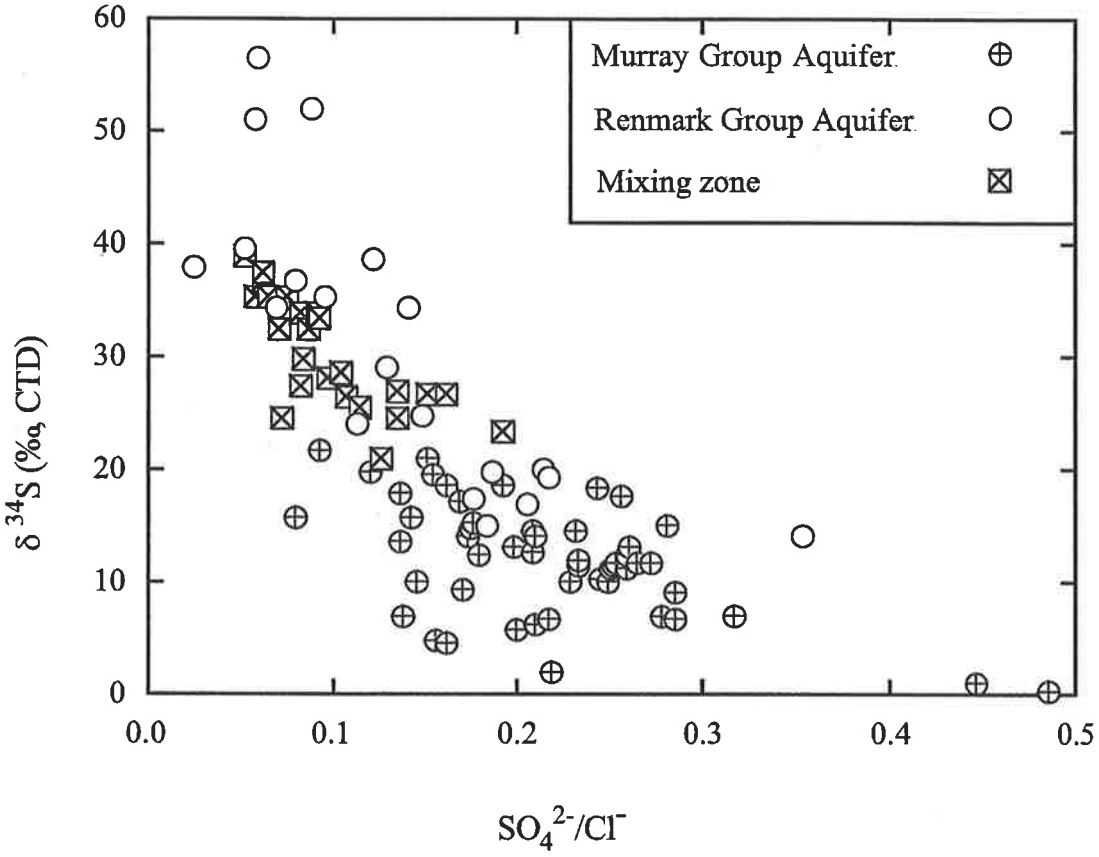

Fig. 4.12 The $\delta^{34}S$ values vs. SO_4^{2-}/Cl^- ratio of groundwater in the Murray and Renmark Group aquifers. The data for the mixing zone fall between the data of the groundwater from the Murray and Renmark Group aquifers.

from the Renmark Group Aquifer near the River Murray can be identified (Fig. 4.10, 4.12), where groundwater of the Murray Group Aquifer displays similar $\delta^{18}OSO_4^{2-}$ values to those of the Renmark Group Aquifer. The relationship between $\delta^{34}S$ values and Cl^- concentrations of groundwater also shows two distinct groups of data (Fig. 4.13). Groundwaters from the Murray Group aquifer that have a relatively high Cl^- and located to the northern part of the have relatively enriched $\delta^{34}S$ values.

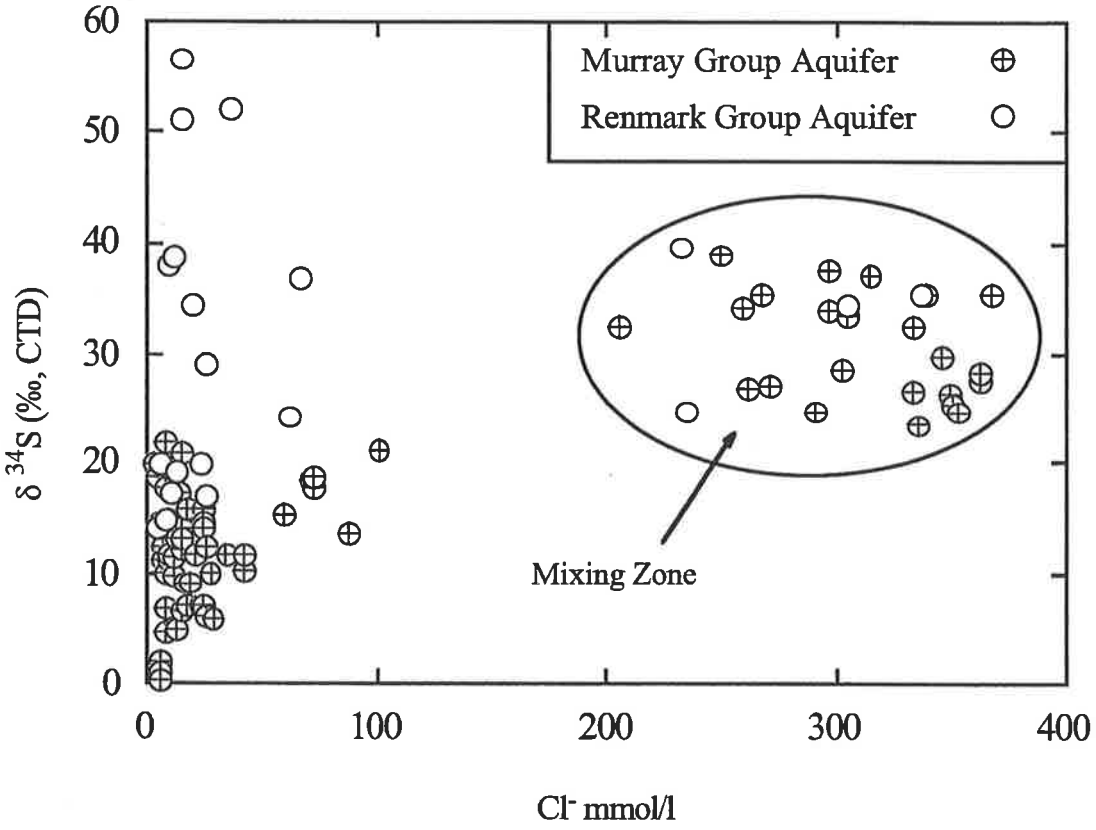

Fig. 4.13 $\delta^{34}S$ value vs. Cl^- concentration in mmol/l of the groundwater from the Murray and Renmark Group aquifers. The relatively high Cl^- concentrations and enriched $\delta^{34}S$ value in the northern part of the study area are caused by upward leakage from the Renmark Group Aquifer.

It is apparent therefore that the hydraulic head distribution has a major effect on Cl^- concentration and subsequently on the water quality in the Murray Group Aquifer. The highest Cl^- concentration (> 7500 mg/l) in the Murray Group Aquifer coincides with areas of similar Cl^- concentration in the Renmark Group Aquifer, where there is high potential for upward leakage, (head difference >15m) from the Renmark Group Aquifer.

The distribution of the SO_4^{2-}/Cl^-, $\delta^{34}S$ and $\delta^{18}OSO_4^{2-}$ values suggest that:

1. Sulphate in groundwater from the Murray Group Aquifer originates primarily from rainfall. Further modification and increase in the sulphate concentration in the down gradient part of the study area occurs due to mixing with the Renmark Group Aquifer, through upward leakage. Dissolution of gypsum in the unsaturated zone near the River Murray increases the concentration of sulphate above that measured in the Renmark Group Aquifer;

2. The relatively enriched $\delta^{34}S$ values and low sulphate concentration in the groundwater from the Renmark Group Aquifer is due to the removal of sulphate through sulphate reduction. The enrichment factor between residual SO_4^{2-} and H_2S produced during bacterial sulphate reduction of 22 ‰ is identical to the kinetic fractionation factor, indicating the dominance of kinetic processes in this natural environment;

3. The spatial distribution of the $\delta^{34}S$ and SO_4^{2-}/Cl^- ratio suggests that vertical input of sulphate into the Murray Group Aquifer through local recharge is the dominant process relative to recharge at the basin margins, followed by lateral flow. This finding was also supported by the 4 ‰ variation of $\delta^{18}OSO_4^{2-}$ values in the Murray Group Aquifer, indicating that this variation is a result of the groundwater originating from local recharge percolating through the soil zone in different parts of the study area. As the mineralisation of organic sulphur is not uniform and depends on many factors, the final

$\delta^{18}OSO_4^{2-}$ varies depending on the amount of organic sulphur contribution to the sulphate pool in groundwater.

4. Inter-aquifer mixing locations can be identified from $\delta^{34}S$ and $\delta^{18}OSO_4^{2-}$ values. The high $\delta^{34}S$ value in the Murray Group Aquifer near the River Murray is caused primarily by upward leakage from the Renmark Group Aquifer. Quantifying the fraction of mixing between the two aquifers is not possible by $\delta^{34}S$ isotopes due to the variation of $\delta^{34}S$ values because of further sulphate reduction occurs in the Murray Group Aquifer.

CHAPTER 5

$^{87}Sr/^{86}Sr$ ratio as an indicator of carbonate mineral dissolution and inter-aquifer mixing

5.1 Introduction

Interactions between carbonate minerals and groundwater in limestone aquifers may play an important role in the composition and evolution of groundwater chemistry. Because Sr^{2+} ions can replace Ca^{2+} ions in carbonate minerals (Faure, 1986), Sr^{2+} concentrations and $^{87}Sr/^{86}Sr$ ratio in groundwater can be used to identify the source of Sr^{2+} and the extent of carbonate mineral-groundwater interactions (Stueber et al., 1984, 1993; McNutt et al., 1984, 1987, 1990; Collerson et al., 1988).

Furthermore, carbonate mineral reactions with groundwater can reduce the ^{14}C concentration of groundwater independently of radiometric decay by adding "dead" carbon into solution. To correct groundwater ^{14}C concentration for this dilution effect, the precise nature of these reactions must be known. Groundwater in carbonate aquifers, particularly in large basins in arid and semi-arid regions, often has a long residence time. Therefore, equilibrium may be established between carbonate minerals and groundwater. Reactions involving these minerals may occur by the mechanism

known as incongruent dissolution i.e. dissolution of one phase and concomitant reprecipitation of a second carbonate minerals. In aquifers containing calcite with different Mg concentrations, incongruent dissolution involves dissolution of high Mg-calcite and concurrent precipitation of low Mg-calcite (Hanshaw and Back, 1979). The association of Sr^{2+} ions with Ca^{2+} ions in carbonate minerals and their similar chemistry therefore can be useful in providing information on the nature of these reactions and in determining their effect on ^{14}C activities in groundwater.

In the previous chapter the use of stable isotopes of dissolved sulphate ($\delta^{34}S$ and $\delta^{18}O$) as physical tracers to discern mixing between the Murray Group and Renmark Group aquifers was examined. However, the "pure" $\delta^{34}S$ and $\delta^{18}OSO_4^{2-}$ composition of the Murray Group Aquifer could not be explicitly identified due to the possibility of sulphate reduction after mixing. Hence the resulting isotopic character of the mixture through upward leakage from the Renmark Group Aquifer could not be interpreted with respect to the original end-members by application of a two-component mixing model. This problem may be eliminated by using concentration and isotopic ratio of dissolved Sr^{2+} in both aquifers. Because the dissolved Sr^{2+} ions are not affected by redox conditions of the groundwater in the Murray Group Aquifer, their concentration and isotopic ratios of the resulting mixture are preserved, and can be used to calculate the proportion of upward leakage from the Renmark Group Aquifer, by applying mixing equations (Faure, 1986).

The main objectives of this chapter are:

1. to examine the usefulness of strontium isotopes ($^{87}Sr/^{86}Sr$) as a quantitative physical groundwater mixing tracer to validate the $\delta^{34}S$ and $\delta^{18}OSO_4^{2-}$ isotopes results;
2. to assess the extent and types of chemical reactions occurring between carbonate minerals and groundwater in the unconfined Murray Group Aquifer, and to elucidate the affect of these reactions on overall groundwater chemistry.
3. to determine the importance of carbonate-water interaction when calculating ^{14}C ages of groundwater in the Murray Group Aquifer.

5.2 Background

Strontium is an ubiquitous minor element in the earth's crust. Its concentration in common rock types is typically a few hundred parts per million (Turekian and Kulp, 1956). The ionic radius of Sr^{2+} (1.13 Å) is similar to that of Ca^{2+} (0.99 Å) and therefore Sr^{2+} can replace Ca^{2+} in many Ca bearing minerals (e.g. carbonates and plagioclase). The concentration of Sr^{2+} in Ca-bearing minerals is higher than in K-bearing minerals (e.g. mica and K-feldspar). Thus, Sr^{2+} concentrations and isotopic ratios can be used as geochemical tracers to assist in determining the origin and conditions of diagenesis of carbonate rocks and minerals (Baker et al., 1982).

The Sr^{2+} concentration in carbonate minerals varies over time due to diagenesis after precipitation. As groundwater flows through a marine carbonate aquifer, geochemical processes such as dissolution and recrystallisation occur. Aragonite and high Mg-calcite convert to a more stable form of low-Mg-calcite (Hanshaw and Back, 1979). Because Sr^{2+} ions fit more readily in the orthorhombic aragonite structure than the rhombohedral calcite structure, Sr^{2+} is partially rejected from the recrystallisation materials. The observed increase of Sr^{2+} content in groundwater along inferred flow paths in carbonate aquifers has been thought to result from this process (Plummer et al., 1976; Hanshaw and Back, 1979).

Strontium has four stable isotopes ^{84}Sr (0.55%), ^{86}Sr (9.86%), ^{88}Sr (82.59%) and ^{87}Sr(6.99%). $^{87}Sr/^{86}Sr$ ratios vary in minerals over a wide range from ~ 0.700 to ~1.000, depending on their age and initial Sr^{2+} and Rb^{2+} concentration. While the ^{84}Sr, ^{86}Sr, ^{88}Sr isotopes do not change in abundance with time, ^{87}Sr increases with time as a result of its production from the radioactive decay of ^{87}Rb, with a half life of $4.9x10^{10}$ years. Therefore, the ^{87}Sr pool is derived from two different sources: (1) non-radiogenic ^{87}Sr which is formed in the cosmos at the same time as other Sr^{2+} isotopes, and (2) radiogenic ^{87}Sr which is formed due to radioactive decay of ^{87}Rb. The relative amount of these two sources of ^{87}Sr to the total Sr^{2+} pool determines the final $^{87}Sr/^{86}Sr$ ratio of minerals.

Rubidium ions have a similar ionic radius to potassium, and can replace potassium ions in K-bearing minerals. The high Rb^{2+}/ Sr^{2+} ratio in K-bearing minerals results in greater

radiogenic ^{87}Sr production, causing a relatively higher $^{87}Sr/^{86}Sr$ ratio than minerals with a low Rb^{2+}/ Sr^{2+} ratio. Ca-bearing minerals generally have a lower Rb^{2+}/ Sr^{2+} ratio. Hence, their $^{87}Sr/^{86}Sr$ ratio is lower than that in the K-bearing minerals. Figure 5.1 shows the evolution of $^{87}Sr/^{86}Sr$ values for three minerals with initial Rb^{2+}/ Sr^{2+} ratios of 30, 10, 1 respectively, each with an initial $^{87}Sr/^{86}Sr$ of 0.704. Each of the three minerals will have different $^{87}Sr/^{86}Sr$ ratios, depending on the initial Rb^{2+}/ Sr^{2+} and the elapsed time as ^{87}Rb decays to ^{87}Sr.

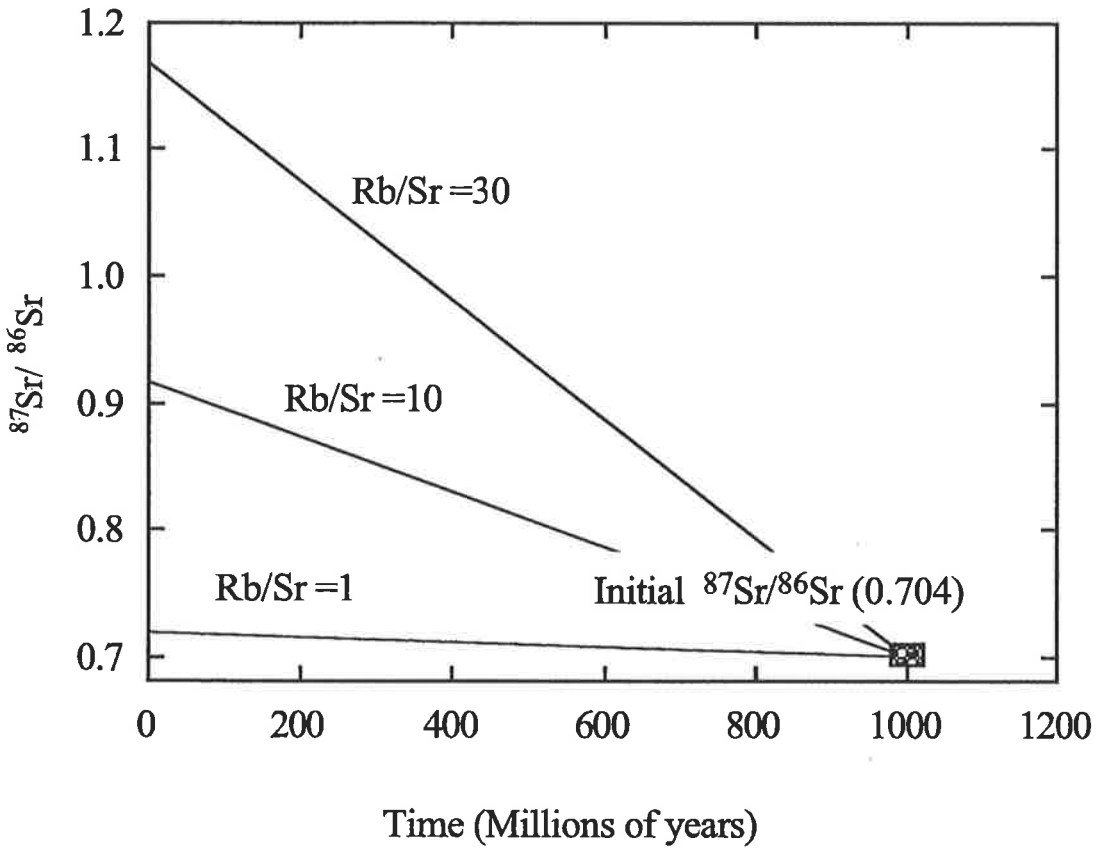

Fig 5.1 The $^{87}Sr/^{86}Sr$ evolution diagram, based on three hypothetical minerals formed 1000 million years ago. Each had the same initial $^{87}Sr/^{86}Sr$ ratio of 0.704 but different Rb/Sr contents. Over time their $^{87}Sr/^{86}Sr$ ratios change due to ^{87}Rb decay.

Strontium ions in marine carbonate minerals are derived from dissolved Sr^{2+} in sea water. The Sr^{2+} concentration and $^{87}Sr/^{86}Sr$ ratio in sea water has varied systematically over time due to changes in fluxes of Sr^{2+} from various rivers draining the continents, as well as input from hydrothermal vent waters. The $^{87}Sr/^{86}Sr$ ratio of sea water has fluctuated between 0.7068 and 0.7092 over the last 600 million years (Burke et al., 1982; Hess et al., 1986). Rivers supply more radiogenic Sr^{2+} than hydrothermal fluids due to the weathering of various continental formations (Krishnaswami et al., 1992). The $^{87}Sr/^{86}Sr$ ratio of carbonate minerals formed in marine environments has an identical $^{87}Sr/^{86}Sr$ ratio to that of sea water at the time of deposition (Faure, 1986). The $^{87}Sr/^{86}Sr$ ratio for the Miocene carbonates of the Murray Group Aquifer range from 0.7082 to 0.7090 (Hodell, 1991).

Strontium dissolved in rainfall is derived from aerosol sea spray and wind blown dust from the interior of the continent. Aerosols composed of sea salt have a marine $^{87}Sr/^{86}Sr$ ratio and are typically several micrometers in diameter (Georgii, 1978). These aerosols are removed from the atmosphere by rainfall and dry fallout. Therefore the $^{87}Sr/^{86}Sr$ ratio of rainfall near the coast approximates the present day ocean $^{87}Sr/^{86}Sr$ ratio (~ 0.7092-Burke et al., 1982; Hodell et al., 1990). Rapid removal of these aerosols in coastal regions by rainfall causes a decrease in their contribution to the Sr^{2+} pool in the atmosphere further inland (Graustein, 1987). Wind blown dust further inland, contributes significant amounts of alkali earth elements, including Sr^{2+}, to rainfall. Previous studies found that at least 50% of Sr^{2+} in rainfall further inland is derived from the weathering of soil minerals (Seimbill et al., 1988; Herut et al., 1993). Seimbill et al.

(1988) have found that the major component of Sr^{2+} in rainfall in Paris, France, is derived from dissolution of limestone present in soil dust. Herut et al. (1993) derived an analytical equation to quantify the contribution of Sr^{2+} from various sources to the Sr^{2+} pool in rainfall in Israel, and concluded that > 50% of Sr^{2+} is derived from recent marine minerals and mineral dust eroded from rock outcrops and soil. Simpson and Herczeg (1994) studied the transport of marine chloride in precipitation in the Murray Basin and concluded that 50% of Cl^- ions were derived from continental dust resulting in high Ca^{2+}/Na^+ ratios of rainfall. It is likely that Sr^{2+} ions further inland in the study area also exhibit similar behaviour and may also be derived from similar sources.

Strontium dissolved in groundwater is initially derived from rainfall followed by dissolution of minerals in the unsaturated and saturated zone. Although in some surface waters the flux of atmospherically derived strontium may exceed the flux from mineral dissolution (Graustein and Armstrong, 1983), the latter usually is the larger source by a factor of ten or more (Brass 1976), especially in groundwater. Therefore the $^{87}Sr/^{86}Sr$ ratio in groundwater is more likely to reflect the $^{87}Sr/^{86}Sr$ ratio of the minerals in the soil and aquifer matrix, rather than the initial Sr^{2+} input from the rainfall. Given that various minerals in a rock have different $^{87}Sr/^{86}Sr$ ratios, the $^{87}Sr/^{86}Sr$ ratio of water in contact with the rock will probably differ from that of the bulk rock because of differences in the rates at which different minerals release strontium. The relative rate depends on mineral solubility and the chemical environment in the soil and aquifer matrix (Bullen et al., 1996). The $^{87}Sr/^{86}Sr$ ratio released into solution may be higher (Goldich and Gast, 1966) or lower (Brass, 1975) than that of the bulk rock. However

Jones and Faure (1978) found that the observed $^{87}Sr/^{86}Sr$ ratio in runoff is usually similar to the isotopic composition of the host whole rock.

The strontium isotopes in groundwater, unlike light isotopes, are not affected by mass fractionation. The $^{87}Sr/^{86}Sr$ ratio, therefore, reflects the relative contribution of Sr^{2+} from different minerals that are in contact with groundwater, as well as evapo-concentration of dissolved Sr^{2+} in rainfall.

A schematic diagram for the possible sources of Sr^{2+} in the Murray and Renmark Group aquifer is shown in Fig. 5.2. Because the Murray Group Aquifer consists of carbonate minerals of Tertiary age, the $^{87}Sr/^{86}Sr$ ratio of groundwater should approach that of the carbonate minerals, providing the groundwater and carbonate rocks have reached chemical and isotopic equilibrium. In contrast, the Renmark Group Aquifer consists of Paleocene continental deposits which originated from much older rocks than the Tertiary carbonates. Therefore $^{87}Sr/^{86}Sr$ ratios of groundwater from the Renmark Group Aquifer reflect the more radiogenic silicate minerals. Thus, groundwater in this aquifer will have a $^{87}Sr/^{86}Sr$ ratio higher than in the Murray Group Aquifer (e.g. > 0.7092). The distinct $^{87}Sr/^{86}Sr$ ratio of groundwater in the two aquifer systems may permit the identification of mixing zones and allow mixing proportions to be calculated.

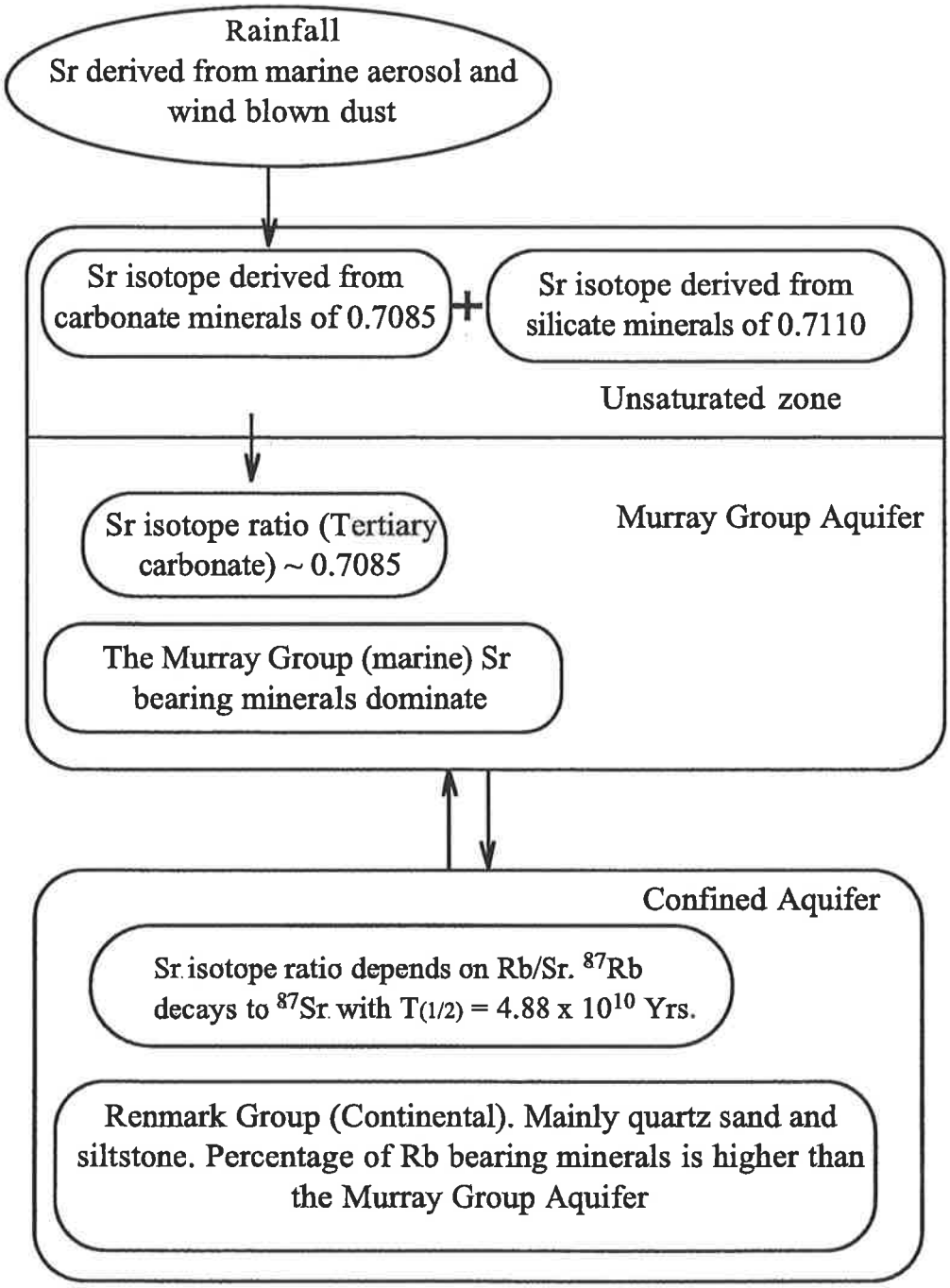

Fig. 5.2 Schematic diagram showing various sources of Sr^{2+} in the Murray Group and Renmark Group aquifers.

5.3 Previous Studies

A considerable amount of work has been done involving Sr^{2+} isotopes in various aspects of surface and groundwater hydrology. These include: the estimation of atmospheric transport of Sr^{2+} and the weathering budget in watersheds (Graustein and Armstrong, 1983; Aberg et al., 1989; Wickman and Jacks, 1992); investigation of geochemical cycles of Sr^{2+} in sea water, and the causes for variation of its $^{87}Sr/^{86}Sr$ ratio over geological time (Brass, 1975, 1976; Burke et al., 1982; Hodell et al., 1990; Hodell et al., 1991); investigation of the origin of brines in shield environments (McNutt, 1987; McNutt et al., 1984, 1987, 1990); study of the evolution and migration of brines in sedimentary basins, and brines associated with oil fields (Chaudhuri, 1978, Sass and Starinsky 1979; Starinsky et al., 1983; Stueber et al., 1984; Chaudhuri et al., 1987, Chaudhuri and Clauer, 1993) and the study of the conditions of diagenesis of carbonate rocks and minerals (Baker et al., 1982; James et al., 1993). Despite the investigations employing $^{87}Sr/^{86}Sr$ in groundwater in saline waters, few studies have been conducted on the use of $^{87}Sr/^{86}Sr$ as a tracer in fresh or brackish groundwaters. For example, Jorgensen and Martin (1995) have successfully used $^{87}Sr/^{86}Sr$ ratios as mixing tracers to delineate the origin of saline groundwater in the east coast of Jutland in Denmark. Collerson et al. (1988) found that the $^{87}Sr/^{86}Sr$ ratio evolves towards more radiogenic $^{87}Sr/^{86}Sr$ ratios along the inferred flow lines in the Great Artesian Basin in Australia. Negrel et al. (1997) also used the $^{87}Sr/^{86}Sr$ ratios as a mixing tracer, and studied the effect of mineral water interaction on groundwater chemistry of the Massif Central, in France.

5.4 Results

5.4.1 Geochemical and $^{87}Sr/^{86}Sr$ ratio of rock samples

Calcium concentrations in the bulk rock samples from four drillholes into the Murray Group Aquifer range from 574± 91 mmol/kg to 867± 110 mmol/kg, and Sr^{2+} concentrations range from 3.41± 0.24 to5.31± 0.8 mmol/kg respectively. These values are much higher than the corresponding mean Ca^{2+} and Sr^{2+} concentration from the Renmark Group Aquifer which range from 82±35 to 232 ± 54 mmol/kg, and from 1.6±0.2 to 2.5 ± 0.34 mmol/kg respectively. Higher Ca^{2+} and Sr^{2+} concentrations in the Murray Group Aquifer, are due to the fact that the aquifer matrix mainly consists of carbonate minerals which have higher Ca^{2+} and Sr^{2+} concentrations than silicate minerals.

$^{87}Sr/^{86}Sr$ values for the carbonate component, silicate minerals, and the bulk aquifer rocks of the Murray Group and Renmark Group are presented in Table 5.1. The $^{87}Sr/^{86}Sr$ value of the whole rock in the Murray Group Aquifer represents the amount weighted average $^{87}Sr/^{86}Sr$ value of all minerals forming the aquifer rocks. The $^{87}Sr/^{86}Sr$ ratio in calcite ranges from 0.7084 to 0.7087, whereas the $^{87}Sr/^{86}Sr$ ratio in residual silicates ranges from 0.7101 to 0.7111.

Variation of $^{87}Sr/^{86}Sr$ ratios of the carbonate component in the Murray Group Aquifer (Table 5.1) could be due to the increase in age down the drillhole, thus representing

TABLE 5.1 $^{87}Sr/^{86}Sr$ isotope ratio and Sr^{2+} concentration of aquifer matrix from the Murray Group and Renmark Group aquifer. The registered bore number is the South Australian Department of Mines and Energy registered number. The Sr^{2+} concentration in groundwater is in milligrams per litre and its concentration in rock samples is in mmol/kg. Errors for $^{87}Sr/^{86}Sr$ ratio are 2σ mean and apply to the last decimal place.

Well ID	Depth from surface (m)	Sr Conc. in groundwater mg/l	Sr Conc. in calcite (mmol/kg)	Sr Conc. in silicates (mmol/kg)	$^{87}Sr/^{86}Sr$ in calcite	$^{87}Sr/^{86}Sr$ silicates	$^{87}Sr/^{86}Sr$ in bulk rock
Murray Group Aquifer							
6929-423	84	5.50	1.71	0.25	0.70847±6	0.71014±10	0.70869±11
6929-423	64	4.81			0.70843±5	0.71021± 5	0.70878± 7
6928-542	88	1.18	2.75	0.68	0.70884±4	0.71102±11	0.70890± 8
6927-588	88	1.12	3.44	0.72	0.70863±6	0.71134± 7	0.70917± 4
6927-48	86	1.43			0.70863±4	0.71186± 5	0.70913± 3
7027-586	88	1.20			0.70879±8	0.71185±11	0.70911± 8
7026-111	122	0.96	2.29	0.46	0.70865±6	0.71271± 6	0.70934± 6
7026-113	88	0.99	3.24	0.57	0.70862±5	0.71112± 4	0.70907± 7
Renmark Group Aquifer							
7026-111	214	0.53			0.70842±7	0.71402± 7	0.70934± 4
6927-588	204	0.50			0.70841±7	0.71236± 8	0.70924± 7
7027-585	220	0.40			0.70872±8	0.71185± 5	0.70919± 8
7026-112	220	0.59	1.19	0.22	0.70824±7	0.71402±15	0.70917± 7
6928-542	220	0.04			0.70842±6	0.71214±22	0.70946± 6
6929-423	220	0.58			0.70908±9	0.72015±21	0.70998± 8

variations in the $^{87}Sr/^{86}Sr$ ratio of sea water during the Tertiary period. The observed $^{87}Sr/^{86}Sr$ ratios of the carbonates in the Murray Group Aquifer matrix are consistent with the Tertiary age carbonate $^{87}Sr/^{86}Sr$ ratio, which range from 0.7082 to 0.7090 throughout the Miocene (Hodell, 1991).

The $^{87}Sr/^{86}Sr$ values for carbonate in the Renmark Group Aquifer are more variable than the Murray Group carbonates and range from 0.7082 to 0.7090. Carbonate minerals in the Renmark Group Aquifer originate from two different sources:

1. allochthonous carbonate minerals older than Tertiary carbonates, deposited with the original Renmark Group continental deposit. The $^{87}Sr/^{86}Sr$ ratio of this component depends on the age of the carbonate minerals.
2. calcite precipitated from the groundwater. $^{87}Sr/^{86}Sr$ values of this component are similar to the groundwater $^{87}Sr/^{86}Sr$ ratio, and vary as a function of distance down gradient.

The $^{87}Sr/^{86}Sr$ ratios for silicate minerals (plagioclase and clay minerals) are more radiogenic than the $^{87}Sr/^{86}Sr$ ratios of carbonate minerals in both aquifers. The $^{87}Sr/^{86}Sr$ ratio of silicate minerals in the Murray Group Aquifer range from 0.7102 to 0.7127 and is less radiogenic than the $^{87}Sr/^{86}Sr$ ratio of silicates in the Renmark Group Aquifer, which range from 0.7118 to 0.7140.

Table 5.2 Mean strontium and calcium concentration from the Murray Group and Renmark Group core cuttings in four drill holes. Registered number is the abbreviated Registered Bore number of South Australian Department of Mines and Energy. Concentration of Sr^{2+} and Ca^{2+} are expressed in mmol/kg.

Well ID	No. of samples (n)	Sr^{2+} mmol/kg	Ca^{2+} mmol/kg	Sr/Ca x 1000
Murray Group Aquifer				
7026-113	5	3.4 ± 0.2	850 ± 0.3	4.0 ± 0.3
7026-111	5	2.6 ± 0.2	570 ± 91	5.0 ± 0.7
6927-588	7	5.0 ± 0.5	720 ± 15	5.0 ± 0.6
6928-567	8	5.3 ± 0.8	870 ± 110	6.0 ± 1.0
Renmark Group Aquifer				
7026-112	4	1.6 ± 0.2	130 ± 38	13 ± 4.0
6927-110	4	2.5 ± 0.3	230 ± 54	9 ± 0.9
6927-587	5	3.0 ± 0.9	130 ± 11	10 ± 4.0
6928-542	4	1.7 ± 0.6	80 ± 35	20 ± 4.0

The carbon-13 composition ($\delta^{13}C$) of carbonates for 17 specimens collected from cuttings and cores of 4 drill holes from the Murray Group Aquifer matrix ranged from -2.2‰ to 2.4 ‰ relative to PDB ($\bar{X}$= 0.8, n = 17). The $\delta^{13}C$ values of carbonate minerals in the Murray Group Aquifer are similar to those of biogenic carbonates in the geologically equivalent Gambier Limestone in the Otway Basin, South Australia (James et al., 1993).

5.4.2 Results of the $^{87}Sr/^{86}Sr$ ratio of groundwater

Concentrations of dissolved Ca^{2+} and Sr^{2+} in the Murray Group Aquifer range from 0.58mmol/l to 17.6 mmol/l and from 2µmol/l to 793µmol/l respectively. Concentration of Ca^{2+} and Sr^{2+} in the Renmark Group Aquifer are lower and range from 0.18 mmol/l to 15.14 mmol/l and 0.5µmol/l to 383µmol/l (Table 5.3).

Table 5.3. $^{87}Sr/^{86}Sr$ ratio, $\delta^{13}C$ and Sr^{2+}, Ca^{2+} concentration in the groundwater from the Murray and Renmark Group aquifers. The registered number with (*) is the Victorian Sinclair Knight Merz (groundwater data base number), and the abbreviated Registered Bore number of the South Australian Department of Mines and Energy, e.g. (6929-423). Sr^{2+} and Ca^{2+} concentrations are expressed in mmol/l, and Sr^{2+}/Ca^{2+} is the molar ratio. The $\delta^{13}C$ is the carbon-13 composition of the DIC (CO_2, HCO_3^-, CO_3^{-2}) expressed in per mil notation relative to standard PDB. Errors for the $^{87}Sr/^{86}Sr$ ratio are 2σ mean and apply to the last decimal place.

Well Reg. No.	Well ID.	Ca^{2+} (mmol/l)	Sr^{2+} (μmol/l)	Sr^{2+}/Ca^{2+} (molar ratio)	$^{87}Sr/^{86}Sr$	$\delta^{13}C$ (‰, PDB)
Murray Group Aquifer						
69122*	M1	0.94	15	0.015		
61930*	M2	1.28	52	0.040	0.70865± 4	
77850*	M3	2.32	19	0.008	0.70876± 4	
111321*	M4	2.72	14	0.005		
67829*	M5	1.66	9	0.005	0.70923± 8	
51846*	M6	2.03	14	0.007	0.70923± 10	-5.9
92808*	M7	1.78	16	0.009	0.70891± 6	-4.2
50946*	M8	1.80	13	0.007		-3.9
60610*	M9	1.19	10	0.008	0.70899± 5	-6.4
79530*	M10	1.87	13	0.007	0.70915± 7	-5.7
60436*	M12	2.11	24	0.011	0.70909± 6	-3.7
84741*	M13	1.96	21	0.011	0.70899± 4	-2.9
75651*	M14	1.74	20	0.012	0.70924± 11	-3.4
75365*	M15	2.31	40	0.017		
75351*	M16	2.05	34	0.017		
60450*	M17	1.82	24	0.013	0.70924± 7	-4.6
58079*	M19	1.63	9	0.005	0.70972± 5	-9.2
98297*	M20	1.47	19	0.013	0.70892± 4	-1.5
103369*	M21	1.55	6	0.004	0.70931± 6	
98254*	M22	1.44	14	0.010	0.70903± 8	-3.3
49951*	M23	0.96	11	0.012	0.70931± 4	
49952*	M24	0.58	9	0.015	0.70915± 7	
49950*	M25	0.58	9	0.015	0.70910± 5	
66477*	M26	2.09	13	0.006		-9.8
54642*	M27	1.31	10	0.008	0.70896± 5	-3.1
54636*	M28	1.43	11	0.008	0.70897± 6	
61571*	M30	1.33	21	0.016	0.70888± 3	-0.8
65758*	M31	1.39	13	0.009		
77199*	M32	1.51	19	0.012		
7026-113	M33	1.12	11	0.010	0.70888± 4	-1.6
7026-110	M34	1.42	11	0.008	0.70903± 15	-3.7
7027-566	M35	1.61	11	0.006	0.70951± 17	-7.1
7027-650	M36	1.37	6	0.004		-4.7
7027-606	M37	1.43	14	0.010		-2.8
7027-592	M38	1.15	12	0.010	0.70894± 11	-3.3
7027-597	M39	1.02	6	0.006	0.70932± 4	-5.6
7027-669	M40	0.66	2	0.003		-5.6
7027-602	M41	1.05	6	0.006	0.70927± 7	-5.6
7027-405	M42	1.16	5	0.004	0.70986± 7	-7.9
7027-586	M43	1.34	14	0.010	0.70921± 4	-6.8

Table 5.3 Contd.

Well Reg. No.	Well ID.	Ca^{2+} (mmol/l)	Sr^{2+} (μmol/l)	Sr^{2+}/Ca^{2+} (molar ratio)	$^{87}Sr/^{86}Sr$	$\delta^{13}C$ (‰, PDB)
7027-579	M44	1.73	9	0.005	0.70912± 7	-4.9
6827-1536	M45	1.55	23	0.015	0.70906± 5	-4.2
7026-120	M46	1.62	16	0.010	0.70924± 8	-6.1
6927-591	M47	1.26	21	0.016	0.70880± 5	-5.8
6927-644	M48	1.92	17	0.009		-5.3
6927-590	M49	1.87	16	0.009	0.70935± 19	-5.4
6927-588	M50	2.01	13	0.006	0.70951± 9	-5.4
6927-601	M51	1.40	10	0.007	0.70933± 4	-7.5
6928-567	M52	1.08	14	0.012	0.70903± 9	-5.5
6928-411	M53	1.62	15	0.009	0.70911± 8	-7.5
6928-49	M54	1.22	26	0.021	0.70884± 6	-5.4
6928-260	M55	1.10	11	0.010	0.70911± 4	-5.9
7025-422	M57	2.03	34	0.016	0.70916± 5	-7.6
6928-477	M58	1.71	53	0.031		-6.1
6928-27	M59	1.80	56	0.031		-6.8
6828-112	M60	1.52	44	0.029	0.70871± 7	-4.4
6928-528	M61	1.63	70	0.043	0.70865± 7	-5.0
6928-424	M62	1.66	73	0.044	0.70868± 9	
6929-154	M63	1.16	55	0.047	0.70866± 4	
6929-169	M64	1.45	63	0.043	0.70866± 4	-7.5
6928-2	M65	2.08	102	0.049	0.70870± 5	-8.0
49677*	M66	1.06	25	0.024	0.70896± 4	-1.0
64363*	M67	1.28	34	0.026	0.70882± 4	-2.7
6929-356	M68	10.08	188	0.019	0.71122± 4	
85570*	M69	5.66	287	0.050	0.70868± 9	-3.7
81833*	M70	10.43	793	0.076	0.70850± 7	-7.5
86775*	M71	11.15	770	0.069	0.70851± 4	
6929-700	M73	9.43	216	0.023	0.70985± 9	
6929-711	M74	11.78	220	0.019	0.71062± 6	
6929-712	M75	13.45	237	0.017	0.71107± 4	
6929-710	M76	15.54	271	0.017	0.71104± 8	
6929-702	M77	15.82	253	0.016	0.70975± 7	
6929-701	M78	17.17	268	0.015	0.71117± 4	
6929-684	M79	16.14	277	0.017	0.71114±10	
6929-651	M80	17.89	277	0.015	0.71090± 5	
6929-682	M81	17.94	277	0.015	0.71072± 6	
6929-685	M82	17.61	284	0.016	0.71004± 7	
6929-686	M83	17.27	293	0.017	0.70991± 4	
6929-687	M84	14.42	279	0.019	0.71018± 9	
6929-689	M85	12.55	226	0.018	0.71023± 22	
6929-691	M86	12.03	221	0.018	0.71011± 4	
6929-692	M87	9.33	178	0.019	0.71015± 8	
6929-693	M88	6.34	146	0.023	0.70881± 8	
6929-1046	M89	9.58	225	0.023	0.70963± 8	
6929-1041	M90	6.59	180	0.027	0.70942± 4	
6929-1082	M91	9.83	293	0.030	0.70915± 10	
Renmark Group Aquifer						
67847*	R1	0.87	9	0.010	0.70933± 7	
60623*	R2	0.43	11	0.026	0.70895± 9	
48554*	R3	0.72	8	0.010		
75669*	R4	1.61	14	0.009		

Table 5.3 Contd.

Well Reg. No.	Well ID.	Ca^{2+} (mmol/l)	Sr^{2+} (µmol/l)	Sr^{2+}/Ca^{2+} (molar ratio)	$^{87}Sr/^{86}Sr$	$\delta^{13}C$ (‰, PDB)
58111*	R5	1.41	13	0.009	0.70939± 8	
7026-112	R7	1.41	6	0.005	0.70969± 3	
7026-111	R8	1.28	6	0.005	0.70969± 6	
66476*	R9	0.31	5	0.016	0.70985± 8	
7027-585	R10	0.35	5	0.013	0.70956±11	
6927-588	R11	0.98	6	0.006		
6928-542	R12	0.16	0.5	0.003	0.70926± 4	
6827-1530	R13	0.18	1	0.006	0.70950± 3	
6929-423	R14	0.44	7	0.016	0.70948± 4	
49676*	R15	1.73	37	0.021	0.71111±12	
7028-469	R16	0.09	33	0.356	0.71092± 8	
109458*	R17	1.53	35	0.023		
6929-760	R18	8.83	159	0.018	0.71122± 5	
6829-992	R19	7.14	148	0.021	0.71084± 8	
81832*	R20	11.63	310	0.027	0.71108± 9	
104800*	R21	13.45	383	0.021	0.71167± 4	
86774*	R22	15.14	282	0.018	0.71192± 6	

The $^{87}Sr/^{86}Sr$ ratio in groundwater from the Murray Group Aquifer ranges from 0.7084 to 0.7112. Based on the Sr^{2+} concentrations, groundwater in the Murray Group Aquifer is divided into two groups (Fig. 5.3). The $^{87}Sr/^{86}Sr$ ratio of groundwater of the first group tends to decrease with an increase in Sr^{2+} concentration, approaching a value of 0.7085 which is equivalent to the average $^{87}Sr/^{86}Sr$ ratio of Tertiary age carbonate. Groundwaters of this group are located to the south and central part of the study area (Zone A). The $^{87}Sr/^{86}Sr$ ratios of the second group are independent of Sr^{2+} concentration and range from 0.7088 to 0.7112 with a Sr^{2+} concentration of 146µmol/l to 293µmol/l. Groundwaters of this group are located in the northern part of the study area near the River Murray (Zone B).

The $^{87}Sr/^{86}Sr$ ratios of groundwater in the Renmark Group Aquifer in Zone B are greater than the present day ocean $^{87}Sr/^{86}Sr$ ratio of 0.7092, and generally higher than that observed for the Murray Group Aquifer. However, in the south and southeastern part of the study area (Zone A) there is no clear distinction between the $^{87}Sr/^{86}Sr$ ratios in the Murray and Renmark Group aquifers. The highest $^{87}Sr/^{86}Sr$ value in the Renmark Group Aquifer is 0.7112, at well R18 located in the centre of the Woolpunda groundwater mound in Zone B (Fig. 1.2).

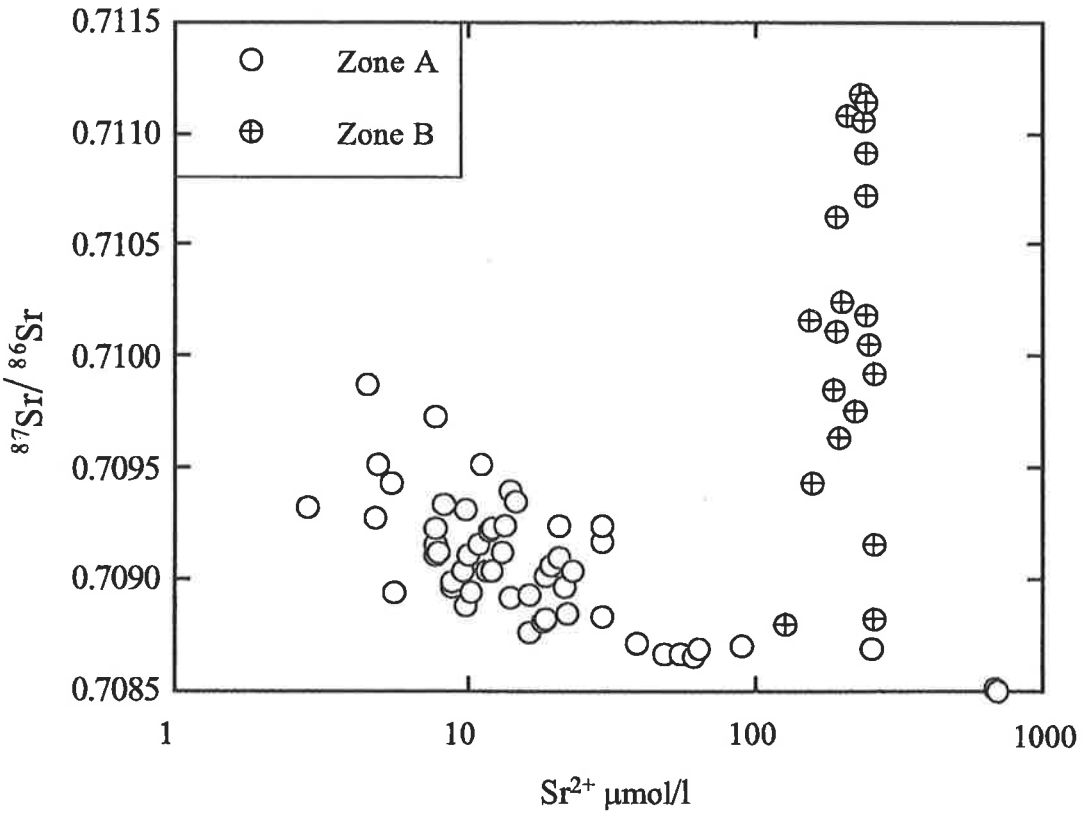

Fig. 5.3. The $^{87}Sr/^{86}Sr$ ratio vs. Sr^{2+} concentration of groundwater from the Murray Group Aquifer. The data is divided into two distinct groups. The $^{87}Sr/^{86}Sr$ ratio of groundwaters from the south and central part of the study area (Zone A) decrease with increase in Sr^{2+} concentration. Groundwaters that have a relatively high $^{87}Sr/^{86}Sr$ ratio are located to the northern part of the study area (Zone B).

5.5 Discussion

5.5.1 $^{87}Sr/^{86}Sr$ of groundwater of the Murray Group Aquifer (Zone A)

5.5.1.1 The variation of Sr^{2+}/Ca^{2+} and $^{87}Sr/^{86}Sr$ ratios with depth below the water table

Changes in the concentration of major ions and $^{87}Sr/^{86}Sr$ ratio of the unconfined Murray Group Aquifer may be related to the sampling interval below the water table. Generally, groundwater in regional unconfined aquifers is characterised by three flow regimes; local, intermediate and regional. These flow regimes may have different chemical composition and concentrations of major ions depending on many factors as discussed in chapters 2 and 3. The type of the flow regime that prevails at a specific sampling interval therefore may control the concentration and chemical composition of groundwater. Determining whether the spatial variation of Sr^{2+}/Ca^{2+} and $^{87}Sr/^{86}Sr$ ratios are due to hydrochemical and/or physical processes, or whether it is an artefact of sampling methodology, is essential for the discussion of Sr^{2+}/Ca^{2+} and $^{87}Sr/^{86}Sr$ ratios in the following sections.

Groundwater from various depths below the water table of the Murray Group Aquifer were obtained from three boreholes along the hydraulic gradient (Fig. 2.1). The depth to the water table from the surface in the bores MH3, MH2 and MH1 were 68.3m, 63.8m and 28.3m respectively. The sites were selected along the hydraulic gradient due to the difference in the concentration of the major ions and depth to the water table in the boreholes.

The results of Sr^{2+}/Ca^{2+} and $^{87}Sr/^{86}Sr$ ratios of the groundwater from discrete intervals below the water table in boreholes (MH1, MH2, MH3) are presented in the following table:

Table 5.4. $^{87}Sr/^{86}Sr$ ratio and Sr^{2+} and Ca^{2+} concentrations in the groundwater from discrete intervals below the water table in the Murray Group Aquifer. Sr^{2+} and Ca^{2+} concentrations are expressed in mmol/l, and Sr^{2+}/Ca^{2+} is the molar ratio. Errors for the $^{87}Sr/^{86}Sr$ ratio are 2σ mean and apply to the last decimal place.

Depth (m)	Ca^{2+}	Sr^{2+} (mmol/l)	Ca^{2+}/Sr^{2+}	$^{87}Sr/^{86}Sr$	Error
MH1					
33	1.17	0.016	0.014	0.70922	±4
36	0.46	0.006	0.015	0.70924	±3
39	1.15	0.017	0.015	0.70924	±6
48	1.29	0.020	0.016	0.70926	±5
57	1.47	0.019	0.013	0.70922	±4
66	1.40	0.020	0.015	0.70924	±4
MH2					
72	0.66	0.007	0.011	0.70890	±3
75	0.73	0.005	0.007	0.70890	±3
78	0.61	0.005	0.008	0.70895	±4
87	0.88	0.006	0.007	0.70892	±3
93	0.85	0.006	0.007	0.70895	±4
102	1.00	0.008	0.008	0.70892	±5
MH3					
84	1.47	0.013	0.009	0.70898	±5
87	1.57	0.013	0.008	0.70900	±3
90	1.42	0.012	0.008	0.70900	±3
99	1.21	0.013	0.011	0.70899	±3
108	1.30	0.012	0.009	0.70898	±5
114	1.32	0.011	0.008	0.70898	±4

The depth profiles (Fig.5.4) for the boreholes indicate that there are no significant variations in both Sr^{2+}/Ca^{2+} and $^{87}Sr/^{86}Sr$ ratios with depth. The variation in Sr^{2+} concentration is smaller than the analytical uncertainty. This is also true for the $^{87}Sr/^{86}Sr$ ratio which remains relatively constant below the water table. The slight variation of

Sr^{2+}/Ca^{2+} ratio below the water table may indicate that the concentration of both Sr^{2+} and Ca^{2+} ions in the Murray Group Aquifer is controlled by calcite equilibrium. These results suggest that although the sampling interval may slightly affect the Sr^{2+}/Ca^{2+} ratio, it does not have a significant effect on the $^{87}Sr/^{86}Sr$ ratio.

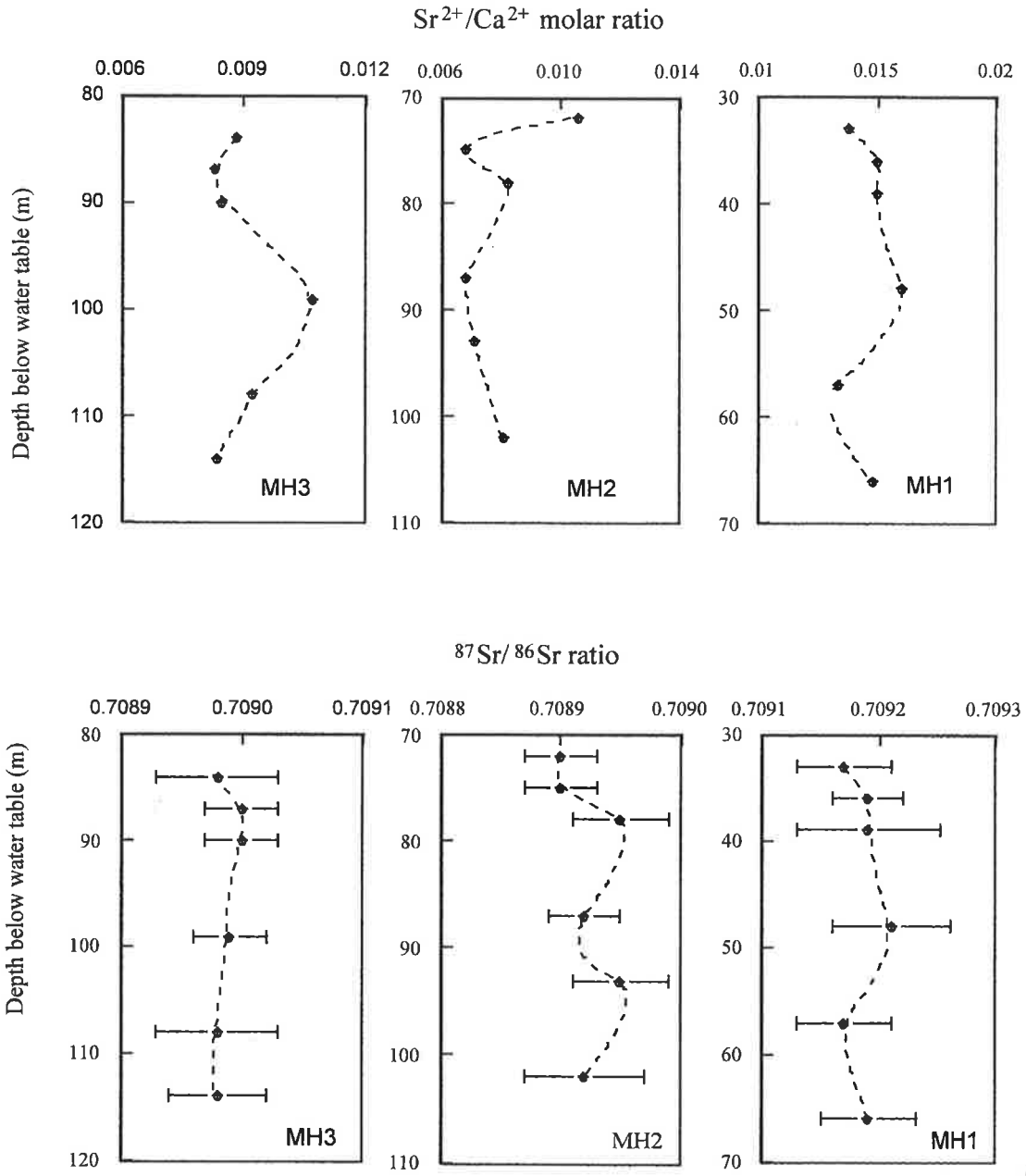

Fig. 5.4 Profiles of Sr^{2+}/Ca^{2+} and $^{87}Sr/^{86}Sr$ ratio measured in discrete intervals below the water table in the Murray Group Aquifer.

5.5.1.2 Sources of dissolved Sr^{2+} in groundwater

Dissolved Sr^{2+} in groundwater from the Murray Group Aquifer is derived from two sources; (1) initial Sr^{2+} concentration in rainfall, and (2) Sr^{2+} derived from dissolution of minerals in the unsaturated and saturated zones. The concentration of Sr^{2+} in rainfall in the study area is unknown. Several measurements of Sr^{2+} concentration in rainfall from various parts of the world show Sr^{2+} concentrations are generally low and can vary over two orders of magnitude from 2×10^{-3} to 3×10^{-1} mg/l (Seimbille et al., 1988; Herut et al., 1993; Bullen et al., 1996). The much higher Sr^{2+} concentrations in groundwater are controlled mainly by; (1) evapotranspiration and (2) mineral dissolution that results in addition of Sr^{2+} to the water.

Brass (1976) found that the Sr^{2+} dissolved in surface water is derived from dissolution of minerals and is the larger source by a factor of ten or more, relative to the initial Sr^{2+} in rainfall. Regardless of the initial concentration of Sr^{2+} in rainfall, evapotranspiration prior to recharge will increase the Sr^{2+} concentration above that of rainfall. Although evapotranspiration does not change the $^{87}Sr/^{86}Sr$ ratio of groundwater, mineral dissolution modifies the $^{87}Sr/^{86}Sr$ ratio depending on the $^{87}Sr/^{86}Sr$ ratio in the minerals reacting with the soil water or groundwater. Therefore, the change of the $^{87}Sr/^{86}Sr$ ratio in groundwater from that of rainfall is only dependent on the rock $^{87}Sr/^{86}Sr$ ratio, and the extent of the groundwater-mineral reactions. If no dissolution of aquifer rocks occurs, the $^{87}Sr/^{86}Sr$ ratio in the groundwater should resemble that of $^{87}Sr/^{86}Sr$ in rainfall.

Groundwaters from the Murray Group Aquifer which have a low Sr^{2+} concentration display relatively more radiogenic $^{87}Sr/^{86}Sr$ ratios compared to groundwater with a higher Sr^{2+} concentration (Fig. 5.5).

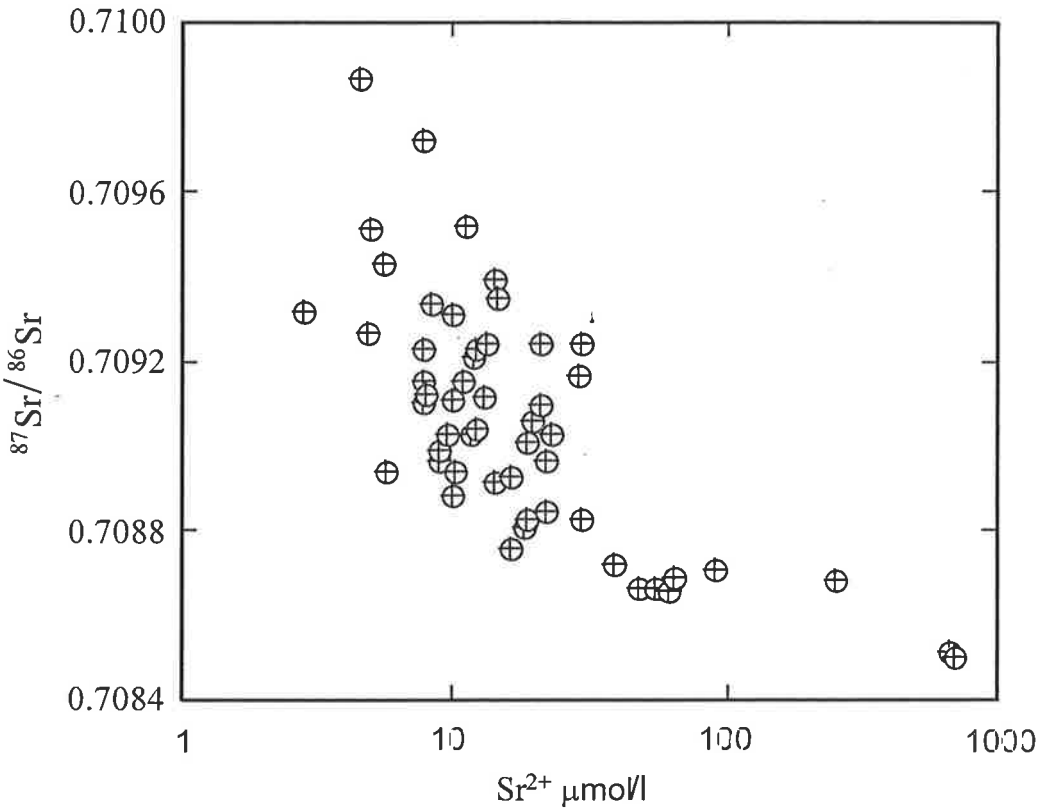

Fig. 5.5 The $^{87}Sr/^{86}Sr$ ratio vs. Sr^{2+} concentration in the Murray Group Aquifer from Zone A. Groundwaters that have a low Sr^{2+} concentration are more radiogenic than groundwaters that have a higher Sr^{2+} concentration.

The distribution of $^{87}Sr/^{86}Sr$ ratios and Sr^{2+} concentration in the Murray Group Aquifer from the south and central part of the study area (Zone A) may be explained by mixing between the two end members; (1) water that derives Sr^{2+} from carbonate minerals having an average Tertiary age $^{87}Sr/^{86}Sr$ ratio of ~ 0.7085, and (2) water that derives Sr^{2+} from silicates with a $^{87}Sr/^{86}Sr$ ratio of ~ 0.7110. The observed $^{87}Sr/^{86}Sr$ ratio in

groundwater represents a mixture of these two end members depending on the contributions of each to the groundwater.

Dissolution of carbonate minerals in the Murray Group Aquifer can initially occur as a result of reaction with soil water charged with high pCO_2 in the soil zone ($\sim 10^{-1.5}$ to $10^{-2.5}$ atm. - Dighton and Allison, 1985). This results in an increase of Ca^{2+}, Mg^{2+} and Sr^{2+} concentration relative to infiltrating rainfall and a change in the Sr^{2+}/Ca^{2+} ratio, depending on the Sr^{2+}/Ca^{2+} ratio in the carbonate minerals and in the initial soil water.

The Sr^{2+}/Ca^{2+} molar ratio in groundwater of the Murray Group Aquifer progressively increases from 4×10^{-3} to 8×10^{-2} with a decrease in the $^{87}Sr/^{86}Sr$ ratio (Fig. 5.6). The Sr^{2+}/Ca^{2+} ratio in carbonate and silicate minerals from the aquifer matrix in the Murray Group Aquifer is $\cong 5 \times 10^{-3}$ (Table 5.2) and is significantly lower than the Sr^{2+}/Ca^{2+} ratio in most of the groundwaters. It appears, therefore, that congruent dissolution of carbonate and/or dissolution of silicate minerals alone cannot explain the high Sr^{2+}/Ca^{2+} ratio in the groundwaters of the Murray Group Aquifer. The possible mechanisms that can result in the observed $^{87}Sr/^{86}Sr$ and Sr^{2+}/Ca^{2+} ratio relationship are; (1) addition of recharge water having a relatively high Sr^{2+}/Ca^{2+} ratio relative to laterally flowing groundwater, and (2) incongruent dissolution of carbonate minerals.

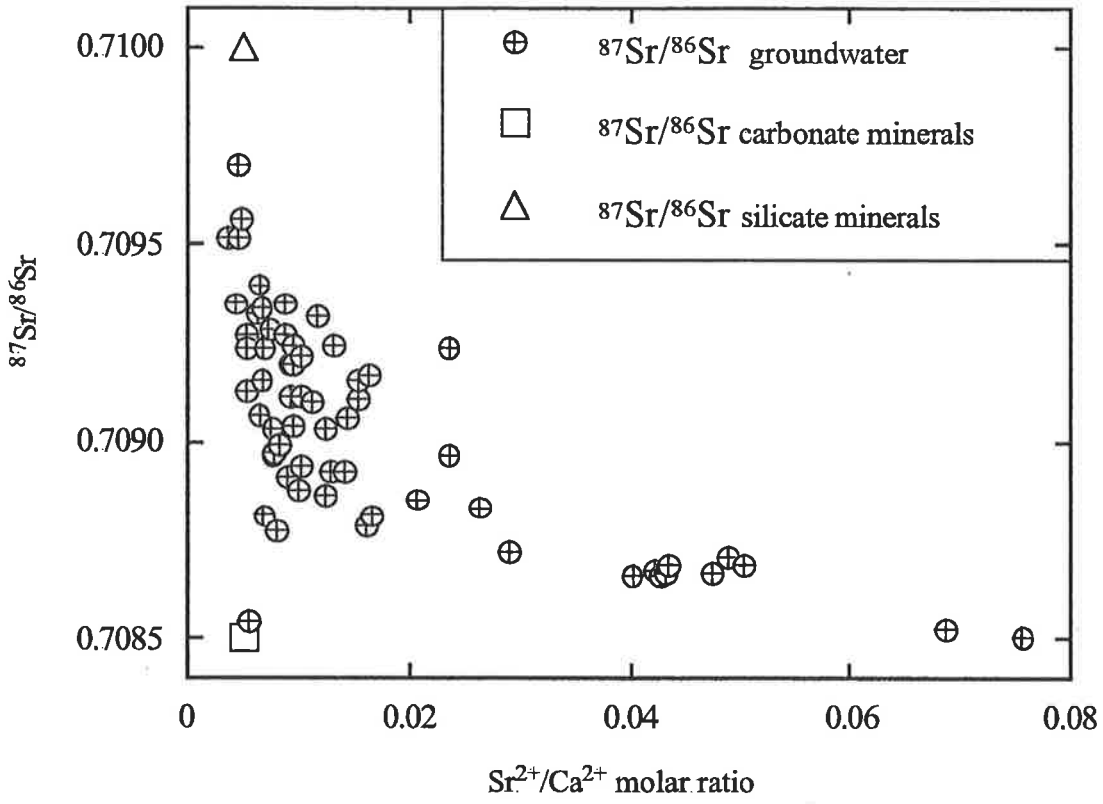

Fig. 5.6 $^{87}Sr/^{86}Sr$ vs. Sr^{2+}/Ca^{2+} ratio in the groundwater and in the aquifer matrix from the Murray Group Aquifer. Note that the Sr^{2+}/Ca^{2+} ratio for the groundwaters that have relatively more radiogenic $^{87}Sr/^{86}Sr$ ratio fall between the carbonate and silicate minerals.

5.5.1.2.1 Addition of recharge water to groundwater

Chloride concentrations and $\delta^{34}S$ and $\delta^{18}OSO_4^{2-}$ composition in the Murray Group Aquifer indicated the importance of contribution of dissolved salt via local recharge relative to the dissolved salt derived from laterally flowing groundwater in modifying the chemical composition of the groundwater. Therefore, the variation in Sr^{2+}/Ca^{2+} and $^{87}Sr/^{86}Sr$ ratios in groundwater of the Murray Group Aquifer may also be caused by addition of local recharge to a laterally flowing groundwater. The Sr^{2+}/Ca^{2+} and $^{87}Sr/^{86}Sr$ ratio for the two end members can be obtained from Fig. 5.5. Laterally flowing

groundwater will be represented by a low Sr^{2+}/Ca^{2+} ratio range of 0.005 to 0.01, similar to that of the groundwater in the south and south-east of Zone A at the basin margin. Local recharge, on the other hand, is represented by a higher Sr^{2+}/Ca^{2+} ratio of 0.075 similar to groundwater from the northern part of Zone A (Well M70). The combination of evapotranspiration and calcite precipitation from the soil water results in the relatively high Sr^{2+}/Ca^{2+} ratio in soil water recharging the aquifer.

It has already been established that evapotranspiration is responsible for the increase of major ion concentrations in soil water (chapter 3). Furthermore, it has been proposed that the Ca^{2+} concentration in soil water is controlled by calcite equilibrium at the early stages of evapotranspiration (Herczeg and Lyons, 1991). The initial Sr^{2+}/Ca^{2+} ratio in soil water at the early stages of transpiration is preserved and remains unchanged until the water reaches calcite equilibrium. When the water loss exceeds calcite saturation the ratio starts to increase due to the removal of Ca^{2+} by calcite precipitation.

Considering the Cl^- concentration in the unsaturated zone as an indicator of the extent in which water is transpired and concentrated, the amount of water lost in the unsaturated zone from the central and northern part of the study area is about 99.9%, assuming an average Cl^- concentration of 6,000 mg/l in the soil water (Cook et al., 1992). Herczeg and Lyons (1991) estimated the amount of water loss in order to reach calcite equilibrium from various starting solutions in the Murray Basin. In the case of rainwater, they found that calcite equilibrium is achieved after approximately 70% loss of initial water. This is much lower than the value obtained for total water loss in the

unsaturated zone in the study area (99.9%). Therefore, it is concluded that calcite equilibrium in the unsaturated zone has been reached, and further transpiration beyond calcite equilibrium consequently causes the high Sr^{2+}/Ca^{2+} ratio in recharge water in the unsaturated zone.

The effect of the addition of local recharge to laterally flowing groundwater on Sr^{2+}/Ca^{2+} and $^{87}Sr/^{86}Sr$ ratios was carried out using the computer code PHREEQM, and the problem was treated as a titration of one end member (groundwater), by another end member (local recharge). PHREEQM was used because it takes into account the effect of ion speciation during titration on Ca^{2+} and Sr^{2+} concentrations. The $^{87}Sr/^{86}Sr$ ratio and Ca^{2+} and Sr^{2+} concentrations, after incremental addition of water from local recharge to the groundwater, were calculated using the mass balance equations as follows:

$$\frac{Sr}{Ca} = \frac{XSr_1 + (1-X)Sr_2}{XCa_1 + (1-X)Ca_2} \qquad (1)$$

$$\frac{^{87}Sr}{^{86}Sr} = \frac{X\left(\frac{^{87}Sr}{^{86}Sr} \times Sr_1\right)_1 + (1-X)\left(\frac{^{87}Sr}{^{86}Sr} \times Sr_2\right)_2}{(Sr_1 + Sr_2)} \qquad (2)$$

where the Sr/Ca and $^{87}Sr/^{86}Sr$ ratios represent values of the final solution , Sr_1, Sr_2 and Ca_1, Ca_2 are concentrations in the first and second end member respectively, $\left(\frac{^{87}Sr}{^{86}Sr}\right)_1$ and $\left(\frac{^{87}Sr}{^{86}Sr}\right)_2$ are isotope ratios in the first and second end member respectively, and X is the fraction of second end member (0.001) added to the first end member. The evolution of Sr^{2+}/Ca^{2+} and $^{87}Sr/^{86}Sr$ ratios in the Murray Group Aquifer was calculated by progressive addition of the local recharge water, represented by well (M70), to fresh

groundwater at the basin margin, represented by well (M4). Because the observed Sr^{2+}/Ca^{2+} ratios of groundwater at the basin margin varies from 0.004 to 0.01 (Fig. 5.6), the model was run twice, using two different initial Sr^{2+}/Ca^{2+} ratios of 0.001 and 0.01 for the second end member (laterally flowing groundwater), by changing the concentration of Sr^{2+} from 14 μmol/l to 7μmol/l in the groundwater.

The results of the mixing model are shown in Fig. 5.7. Groundwater in the Murray Group Aquifer generally falls between the two modeled curves, each representing different initial Sr^{2+}/Ca^{2+} ratios. These results indicate that the $^{87}Sr/^{86}Sr$ ratio, and the Sr^{2+}, Ca^{2+} concentrations in the groundwater of the Murray Group Aquifer could have evolved through the addition of Sr^{2+} with a $^{87}Sr/^{86}Sr$ ratio of 0.7085 to laterally flowing groundwater with the $^{87}Sr/^{86}Sr$ ratio observed in groundwater at the basin margin in the south and south-east.

However, the addition or mixing between two waters in equilibrium with calcite, can result in a mixture that may be either undersaturated (Thrailkill, 1968) or supersaturated with respect to calcite (Wigley, 1973), depending on the chemical composition, pH, temperature and proportion of the two end-members represented in the final solution. This is mainly caused by redistribution of the carbonate species in the mixture (Wigley and Plummer, 1976). The addition of soil water via local recharge to the groundwater, will also have a direct effect on Sr^{2+}/Ca^{2+} and $^{87}Sr/^{86}Sr$ ratios. If the mixture is under saturated with respect to calcite, more calcite will be dissolved from the carbonate Murray Group matrix, resulting in change of the Sr^{2+}/Ca^{2+} and $^{87}Sr/^{86}Sr$

ratios. On the other hand, if the mixture was over-saturated, calcite will precipitate from the mixture, removing Ca^{2+} ions causing an increase in the Sr^{2+}/Ca^{2+} ratio. Therefore, it is essential to incorporate a calcite equilibrium condition in the titration model in order to simulate as accurately as possible the conditions under which addition of soil water via local recharge proceeds in the Murray Group Aquifer.

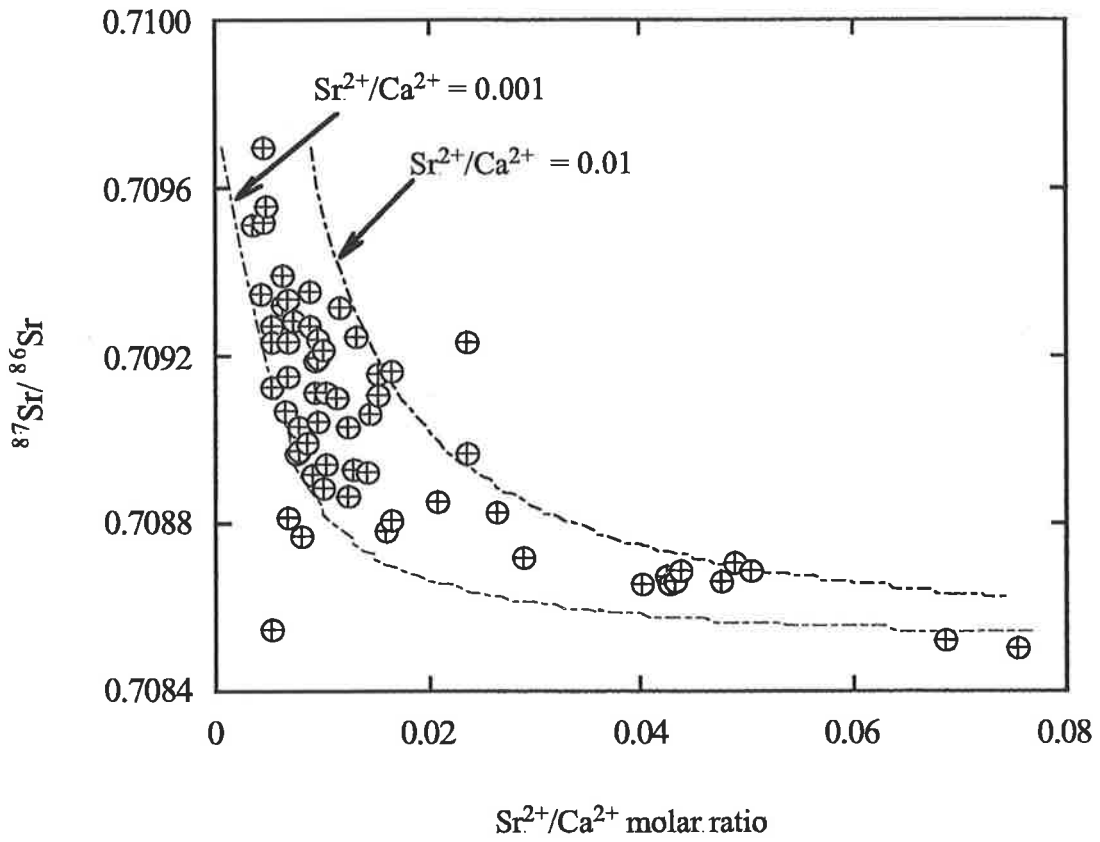

Fig. 5.7 The dashed curves represent the computed variation of $^{87}Sr/^{86}Sr$ and Sr^{2+}/Ca^{2+} ratios in groundwater as a result of progressive addition of incremental amounts of soil water to laterally flowing groundwater. The crossed circles represent the measured $^{87}Sr/^{86}Sr$ and Sr^{2+}/Ca^{2+} ratios in groundwater from Zone A.

5.5.1.2.2 Addition of recharge water to groundwater and equilibrium with calcite

Addition of soil water that is in equilibrium with respect to calcite to laterally flowing groundwater in incremental steps was carried out using PHREEQM and the final solution in each step was equilibrated with calcite. The amount of Ca^{2+} and Sr^{2+} removed or added by precipitation or dissolution of calcite was calculated as follows:

1. soil water and laterally flowing groundwater represented by chemical composition of well M70 and M4 were equilibrated with respect to calcite;
2. soil water was added in 0.001 fraction to laterally flowing groundwater and Ca^{2+} and Sr^{2+} concentrations were obtained from the final solution after each incremental step;
3. the difference in Ca^{2+} and Sr^{2+} concentrations were calculated after the final solution was equilibrated with respect to calcite;
4. the amount of Ca^{2+} removed by calcite precipitation when the final solution was oversaturated with respect to calcite was calculated by subtracting the Ca^{2+} concentration after equilibrium with calcite from Ca^{2+} concentration before equilibrium with calcite. The amount of Sr^{2+} removed from solution was calculated by multiplying the fraction of Ca^{2+} removed during calcite precipitation by Sr^{2+} concentration in the final solution, and the result was multiplied by the Sr^{2+} distribution coefficient of 5.7×10^{-2} (Katz et al., 1972). Detail input data for one step of the model is presented in the Appendix 3.

The results of the model are shown in Fig. 5.8. The modeled curves are identical to the curves obtained in the previous model (addition of soil water to laterally flowing groundwater without equilibrium with calcite), and suggest that the calcite saturation state of the final solution has no effect on the evolution of Sr^{2+}/Ca^{2+} and $^{87}Sr/^{86}Sr$ ratios

in the Murray Group Aquifer. This is probably due to the addition of relatively small amounts of soil water to a large volume of ground water in each step, resulting in a very small shift from equilibrium with respect to calcite. Subsequently, the amounts of Ca^{2+} and Sr^{2+} removed due to this process are insignificant compared to their amounts in the final solution.

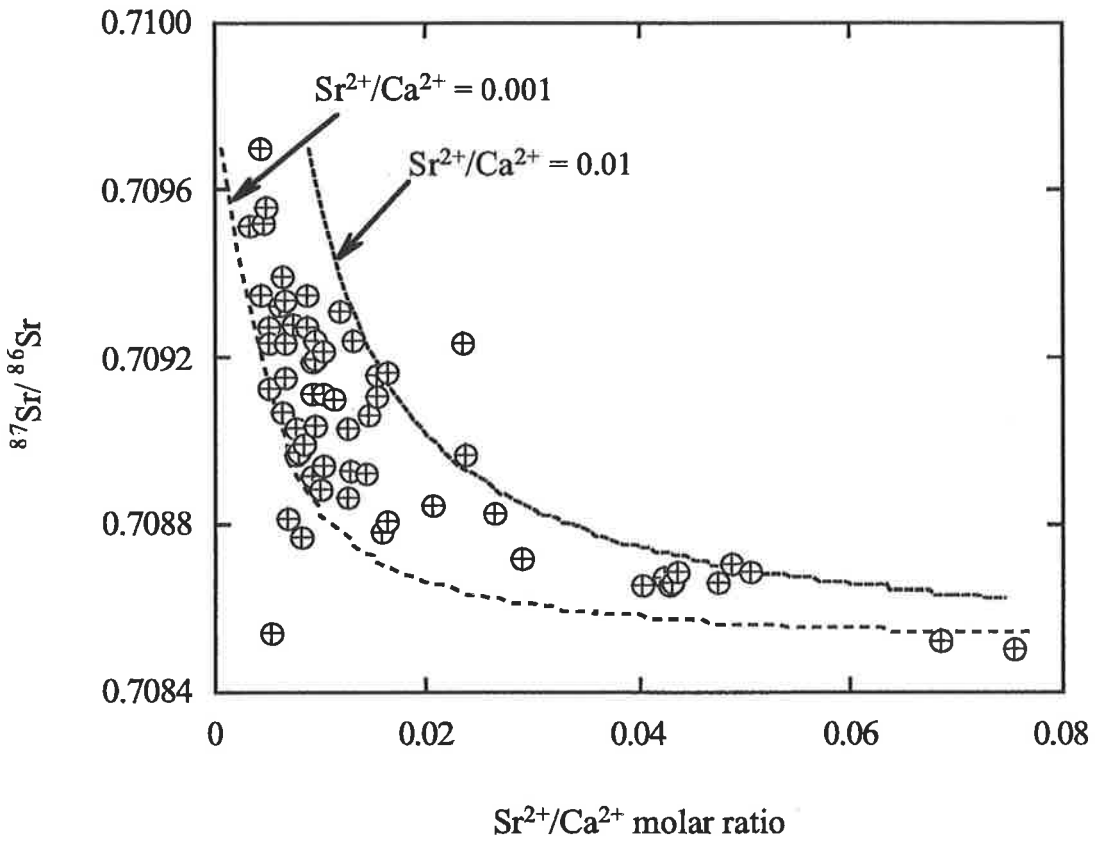

Fig. 5.8 The computed variation of the $^{87}Sr/^{86}Sr$ and Sr^{2+}/Ca^{2+} ratios of the groundwater as a result of the addition of recharge water to laterally flowing groundwater followed by equilibrium with calcite.

The result of the model indicates that the $^{87}Sr/^{86}Sr$ ratio, and Sr^{2+} and Ca^{2+} concentrations in the groundwater of the Murray Group Aquifer could have evolved through the addition of soil water to laterally flowing groundwater, possibly under calcite equilibrium conditions. The model is also consistent with the results obtained

from the $\delta^{34}S$ data and the major ion chemistry in the Murray Group Aquifer, suggesting that the addition of local recharge to the unconfined Murray Group Aquifer, over a large aerial extent is an important process.

5.5.1.2.3 Incongruent dissolution of carbonate minerals

The carbonate minerals that form the carbonate aquifers contain at least trace amounts of all components present in sea water from which they were precipitated (Tucker and Wright, 1990). Magnesium is a major component and strontium is a minor component of sea water both of which coprecipitate with calcium in carbonate minerals (e.g. calcite). The concentration of Mg, which ranges from ~2 to ~ 16 mole percent $MgCO_3$ in calcite, affects its solubility behavior (Tucker and Wright, 1990; Morse and Mackenzie, 1990). Generally high Mg-calcite is characterised by higher solubility relative to low Mg-calcite (Plummer and Mackenzie, 1974). High Mg-calcite dissolves incongruently when it comes in contact with Mg-poor groundwater, releasing Mg and Sr^{2+} into the groundwater. During this process, the concentration of Mg^{2+} increases relative to Ca^{2+}, and the magnitude of increase in the Mg^{2+}/Ca^{2+} and Sr^{2+}/Ca^{2+} ratios in the groundwater depends on the concentration of Mg^{2+} and Sr^{2+} of carbonate minerals and the extent of reaction (i.e. how far away from equilibrium it was in the first place).

The increase in Sr^{2+} concentration in groundwater during incongruent dissolution is due to its low partition coefficient for calcite (5.7×10^{-2}-Katz et al., 1972) that is the affinity of Sr^{2+} to remain in groundwater is higher than it's affinity to coprecipitate

with calcite (Pingitore and Eastman, 1986). Therefore, the amount of added Sr^{2+} due to dissolution of calcite is always higher than the amount of Sr^{2+} removed from groundwater as a result of an equivalent amount of calcite precipitation. Because the change in Ca^{2+} concentration during incongruent dissolution of carbonates is small (Wigley et al.,, 1978), net addition of Sr^{2+} to groundwater results in an increase in the Sr^{2+}/Ca^{2+} ratio.

Incongruent dissolution of Mg-calcite progressively modifies the $^{87}Sr/^{86}Sr$ ratio in groundwater, towards a value closely resembling that of the mineral dissolved. This process occurs in two steps; (1) dissolution of carbonate minerals, causing addition of Sr^{2+} to groundwater and subsequent modification of the $^{87}Sr/^{86}Sr$ ratio, and (2) reprecipitation of carbonate minerals, causing removal of Sr^{2+} from the groundwater without altering the $^{87}Sr/^{86}Sr$ ratio.

Starinsky et al. (1983) presented a model for the incongruent dissolution of Mg-calcite to explain the Sr^{2+}/Ca^{2+} and $^{87}Sr/^{86}Sr$ ratios in oilfield brines, and suggested that the final $^{87}Sr/^{86}Sr$ ratio of the brine depends exclusively on the $^{87}Sr/^{86}Sr$ of the reacting minerals. The assumptions made for the mathematical treatment of this model were:

1. incongruent dissolution will not affect the concentration of Ca in groundwater. That is the amount of Ca^{2+} added by Mg-calcite dissolution is equal to the amount of Ca removed by calcite precipitation;
2. incongruent dissolution occurs in a closed system and the amount of Ca^{2+} in the aquifer rock is much greater than that in groundwater.

From these two assumptions the change in Sr^{2+}/Ca^{2+} and $^{87}Sr/^{86}Sr$ ratios is mathematically treated by conservation of Ca^{2+} mass in the system. The final equation used to determine the $^{87}Sr/^{86}Sr$ ratio of the final groundwater during the dissolution reprecipitation reaction according to Starinsky et al. (1983) is :

$$(\frac{^{87}Sr}{^{86}Sr})_L = \frac{(\frac{Sr}{Ca})_{Li}(\frac{^{87}Sr}{^{86}Sr})_{Li}\exp(-K^C_{Sr}.(\frac{Ca_S}{Ca_L})) + \frac{1}{K^C_{Sr}}(\frac{Sr}{Ca})_R(\frac{^{87}Sr}{^{86}Sr})_R(1-\exp(-K^C_{Sr}(\frac{Ca_S}{Ca_L})))}{(\frac{Sr}{Ca})_{Li}\exp(-K^C_{Sr}.(\frac{Ca_S}{Ca_L})) + \frac{1}{K^C_{Sr}}(\frac{Sr}{Ca})_R(\frac{^{87}Sr}{^{86}Sr})_R(1-\exp(-K^C_{Sr}(\frac{Ca_S}{Ca_L}))} \quad (5.3)$$

Where $(\frac{^{87}Sr}{^{86}Sr})_L$ and $(\frac{^{87}Sr}{^{86}Sr})_R$ are the isotopic ratios of groundwater and carbonate rocks respectively, the $(\frac{Sr}{Ca})_{Li}$ and $(\frac{Sr}{Ca})_R$ are initial ratios in groundwater and carbonate rocks before incongruent dissolution, the $(\frac{Ca_S}{Ca_L})$ is the ratio of the amount of Ca^{2+} released by dissolution of carbonate rocks to its amount in the initial solution (i.e. reaction progress), and the K^C_{Sr} is the partition coefficient of Sr^{2+} between calcite and water.

The input data in Eq. 5.3 for $^{87}Sr/^{86}Sr$ ratio of groundwater of the Murray Group Aquifer and carbonate minerals from the aquifer matrix are 0.7097 and 0.7085 (Table 5.1) respectively. The Sr^{2+}/Ca^{2+} ratio in the carbonate rocks of the Murray Group Aquifer matrix is (5×10^{-3}, n = 25) (Table 5.2). Two initial Sr^{2+}/Ca^{2+} ratios of 0.01 and 0.001 were used for groundwater similar to the initial Sr^{2+}/Ca^{2+} value in the two previous models. The two curves in Fig. 5.9 represent theoretical $^{87}Sr/^{86}Sr$ and Sr^{2+}/Ca^{2+} ratio evolution during incongruent dissolution of carbonate minerals in the Murray Group Aquifer. The observed data of groundwater from the Murray Group

Aquifer fall between the two theoretical curves suggesting that incongruent dissolution of carbonate minerals may explain the current Sr^{2+}/Ca^{2+} and $^{87}Sr/^{86}Sr$ ratio evolution in groundwater from the Murray Group Aquifer. The Mg^{2+}/Ca^{2+} and $^{87}Sr/^{86}Sr$ ratios relationship (Fig 5.10) suggests that dissolution of carbonates results in the addition of Mg^{2+} relative to Ca^{2+}, and relatively low $^{87}Sr/^{86}Sr$ ratio to groundwater.

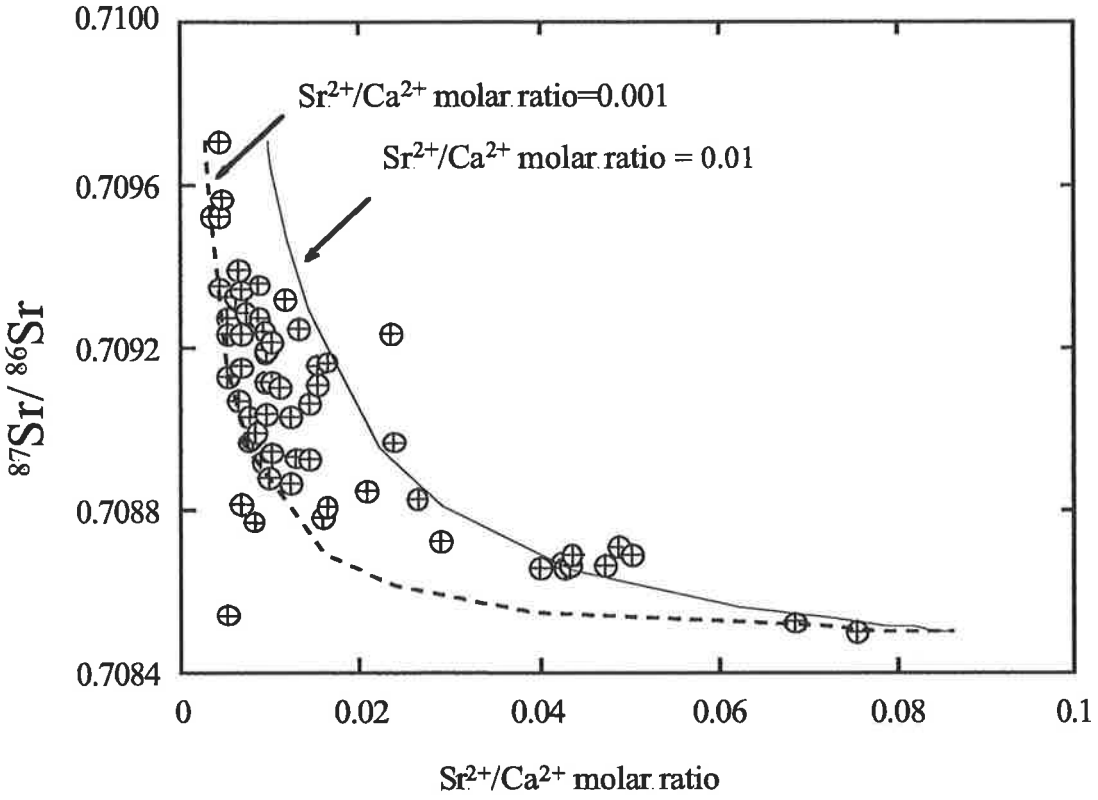

Fig. 5.9 The computed variation of $^{87}Sr/^{86}Sr$ and Sr^{2+}/Ca^{2+} ratios during incongruent dissolution of carbonate minerals according to the Starinsky et al. (1983) analytical model with different initial Sr^{2+}/Ca^{2+} ratio in groundwater. Also shown are data from the Murray Group Aquifer.

Thus, the evolution of the $^{87}Sr/^{86}Sr$ ratio in the Murray Group Aquifer could be caused by the addition of soil water to laterally flowing groundwater under calcite equilibrium conditions or incongruent dissolution of carbonates in the aquifer, or a combination of both processes. In order to determine the most likely process responsible for the

current Sr^{2+}/Ca^{2+} and $^{87}Sr/^{86}Sr$ ratio distribution in the Murray Group Aquifer, the $\delta^{13}C$ content of the total dissolved inorganic carbon (TDIC) is also used as a constraint to evaluate the importance of each of the above mentioned processes.

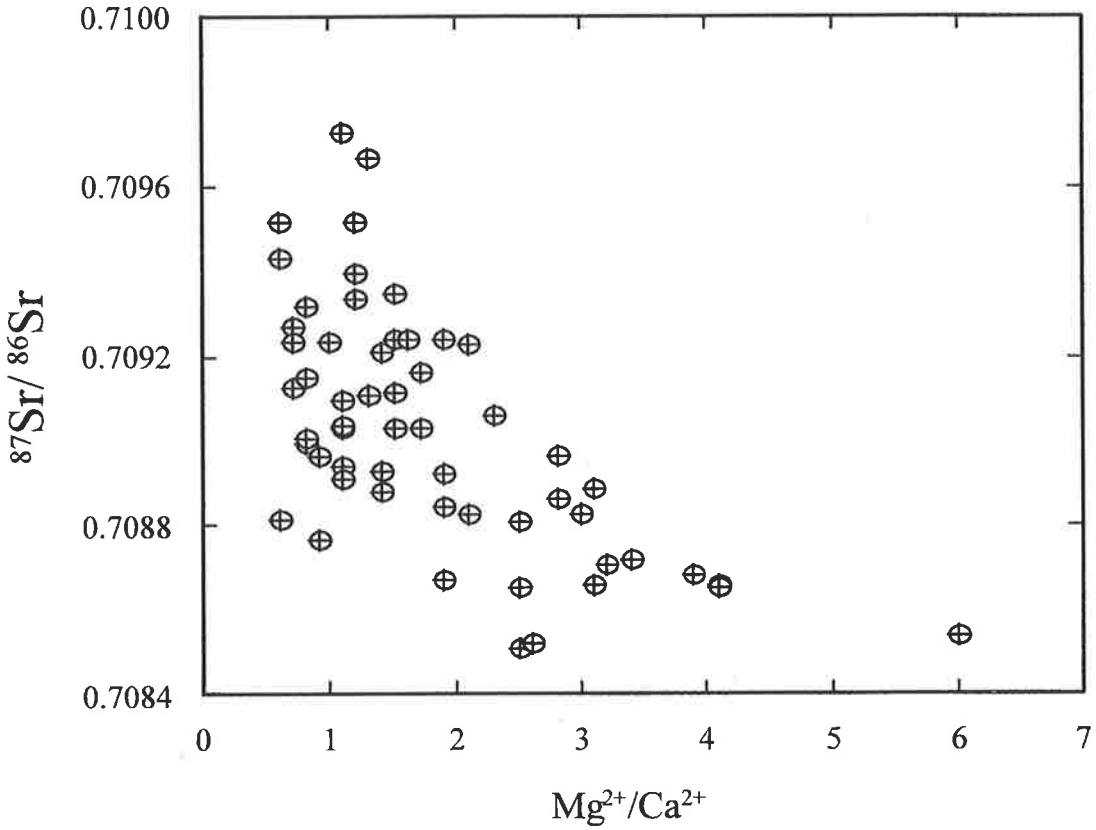

Fig. 5.10 The Mg^{2+}/Ca^{2+} and $^{87}Sr/^{86}Sr$ ratio relationship in the Murray Group Aquifer. The higher Mg^{2+}/Ca^{2+} ratio corresponds to the relatively less radiogenic $^{87}Sr/^{86}Sr$ ratio.

5.5.1.4 Constraints on incongruent dissolution of carbonates imposed by $\delta^{13}C$

Incongruent dissolution of carbonate minerals in the Murray Group Aquifer would alter the initial $\delta^{13}C$ composition of the groundwater by continuously adding a relatively enriched source of ^{13}C. In this case, the $\delta^{13}C_{TDIC}$ (Total dissolved inorganic carbon) will not only reflect the carbonate mineral source, but also the isotopic fractionation during

calcite precipitation. Hence, the $\delta^{13}C_{TDIC}$ of the groundwater would become progressively enriched towards the $\delta^{13}C$ of carbonates in the Murray Group Aquifer. Addition of soil water to laterally flowing groundwater on the other hand, could not account for $\delta^{13}C_{TDIC}$ values > -6‰ (Table 5.3).

The $\delta^{13}C$ value of total dissolved inorganic carbon (TDIC = $CO_{2\,aq}$, HCO_3^-, CO_3^{2-}) of groundwater is controlled primarily by; (1) the $\delta^{13}C$ of CO_2 produced by respiration of plants and microbial oxidation of organic matter in the soil zone, which dissolve in soil water, (2) subsequent interaction with carbonate minerals in the unsaturated zone, and (3) once in the saturated zone, addition of CO_2 by microbial degradation of organic matter, and congruent and incongruent dissolution of carbonate minerals. The $\delta^{13}C$ of CO_2 produced in the soil zone in the study area ranges from ~ -22 to -20‰ (Dighton and Allison, 1985; Leaney et al, 1986), and $\delta^{13}C$ of the carbonate minerals in the Murray Group Aquifer were measured, and range from 2.4 ‰ to -2.2‰ ($\bar{X}$= 0.8, n = 17).

The $\delta^{13}C_{TDIC}$ of the final solution when addition of soil water to the laterally flowing groundwater occurs depends on the $\delta^{13}C$ composition and pH of soil CO_2. Under open system condition (open to soil CO_2) and neutral pH, the $\delta^{13}C$ of soil CO_2 re-equilibrates with the dissolved CO_2, and the $\delta^{13}C_{TDIC}$ in groundwater will reflect the $\delta^{13}C$ of soil CO_2 and the equilibrium fractionation value between soil CO_2 and dissolved

CO_2 in groundwater (Deines et al., 1974). In this case, the $\delta^{13}C_{TDIC}$ in the mixture would range from -14‰ to -12 ‰, which is the sum of the $\delta^{13}C_{TDIC}$ in the soil (-22‰ to -20‰) and the equilibrium fractionation factor of 7.85‰. However, after the final solution is isolated from soil CO_2 in the saturated zone, the groundwater may be further enriched by carbonate dissolution in the aquifer, according to the equation below:

$$CaCO_3 + CO_2 + H_2O \leftrightarrow Ca^{2+} + 2HCO_3 \qquad (4)$$

The $\delta^{13}C_{TDIC}$ of the groundwater following calcite dissolution would range from -6.8 ‰ to -5.6 ‰ assuming average $\delta^{13}C$ for carbonate minerals of 0.8‰ (n = 17). The measured $\delta^{13}C_{TDIC}$ data of groundwater in the Murray Group Aquifer ranges from -10.6‰ to -1.5‰ (Table 5.3) and the majority has $\delta^{13}C_{TDIC}$ values more enriched than -5.6‰ which cannot be accounted for by the addition of soil water to the laterally flowing groundwater or by calcite dissolution in the aquifer.

Smith et al. (1975) showed that continuous dissolution and precipitation of carbonate minerals within the London Basin Aquifer is responsible for the enrichment of $\delta^{13}C_{TDIC}$ from -13‰ to -1‰ over an 8km distance of flow path. Wigley (1976) and Wigley et al. (1978, 1979) presented a more quantitative discussion on the evolution of $\delta^{13}C_{TDIC}$ in groundwater with special emphasis on incongruent dissolution and dedolomitisation. During incongruent dissolution of Mg-calcite, the $\delta^{13}C_{TDIC}$ will not only increasingly reflect the Mg-calcite source, but is also affected by isotopic fractionation during low

Mg-calcite precipitation. As noted in the previous section, the dissolved Sr^{2+} will acquire the carbonate mineral $^{87}Sr/^{86}Sr$ ratio with progressive addition of Sr^{2+} to groundwater from dissolution of carbonate minerals.

The $^{87}Sr/^{86}Sr$ ratio vs. $\delta^{13}C_{TDIC}$ relationship (Fig. 5.11) shows that there is a general trend of enrichment in $\delta^{13}C_{TDIC}$ of dissolved CO_2 with a decrease in the $^{87}Sr/^{86}Sr$ ratio. The more enriched $\delta^{13}C_{TDIC}$ groundwater corresponds to less radiogenic $^{87}Sr/^{86}Sr$ ratios which are similar to that of the carbonate $^{87}Sr/^{86}Sr$ ratio (Table 5.1).

The progressive enrichment of $\delta^{13}C_{TDIC}$, combined with a decrease of the $^{87}Sr/^{86}Sr$ ratio approaching the carbonate minerals $^{87}Sr/^{86}Sr$ ratio only occurs as a result of incongruent dissolution of carbonate minerals. The $\delta^{13}C_{TDIC}$, data and the relationship with the $^{87}Sr/^{86}Sr$ ratios, provides further evidence that incongruent dissolution of carbonates may play a significant role in modifying the Ca^{2+}, Mg^{2+}, Sr^{2+} concentrations and $^{87}Sr/^{86}Sr$ ratios in the Murray Group Aquifer. Incongruent dissolution of carbonates can also explain the enriched $\delta^{13}C$ values observed in the groundwater.

The results obtained for each of the models, namely, (1) the addition of soil water to the laterally flowing groundwater and, (2) incongruent dissolution of carbonate minerals, can adequately explain the current $^{87}Sr/^{86}Sr$ and Sr^{2+}/Ca^{2+} ratio distribution in the Murray Group Aquifer. The addition of soil waters with different Cl^- concentrations (depending on evapoconcentration rate) via local recharge to the

groundwater is evidenced by the unsystematic distribution of Cl^- concentration and the model presented for $\delta^{34}S$ distribution in the Murray Group Aquifer. The occurrence of

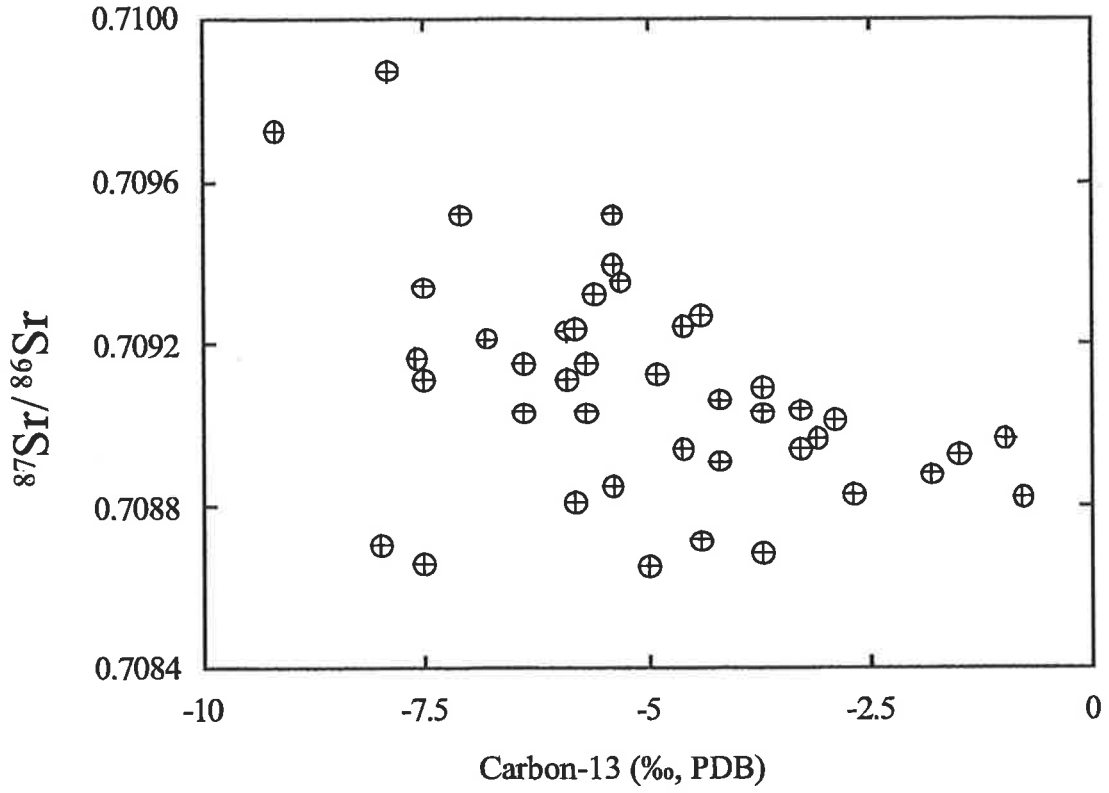

Fig. 5.11 Carbon-13 vs. $^{87}Sr/^{86}Sr$ ratios in groundwater from the Murray Group Aquifer. Groundwater with a more enriched $\delta^{13}C_{TDIC}$ composition, generally has a less radiogenic $^{87}Sr/^{86}Sr$ ratio.

incongruent dissolution of the carbonate minerals in the aquifer, on the other hand, is supported by the Mg/Ca and $\delta^{13}C$ value relationship with $^{87}Sr/^{86}Sr$ ratio of groundwater. Therefore, both processes may be occurring in the Murray Group Aquifer together causing the current distribution of $^{87}Sr/^{86}Sr$ and Sr^{2+}/Ca^{2+} ratio.

5.5.2 $^{87}Sr/^{86}Sr$ of groundwater from the Renmark Group Aquifer

The $^{87}Sr/^{86}Sr$ versus Sr^{2+}/Ca^{2+} relationship for the Renmark Group Aquifer (Fig 5.12), displays two distinct groups; (1) $^{87}Sr/^{86}Sr$ ratio ranging from 0.7089 to 0.7097, similar to that of modern sea water, with a Sr^{2+}/Ca^{2+} ratio ranging from 0.005 to 0.025, and (2) a more radiogenic $^{87}Sr/^{86}Sr$ ratio, ranging from 0.7108 to 0.7111 with a Sr^{2+}/Ca^{2+} ratio > 0.016.

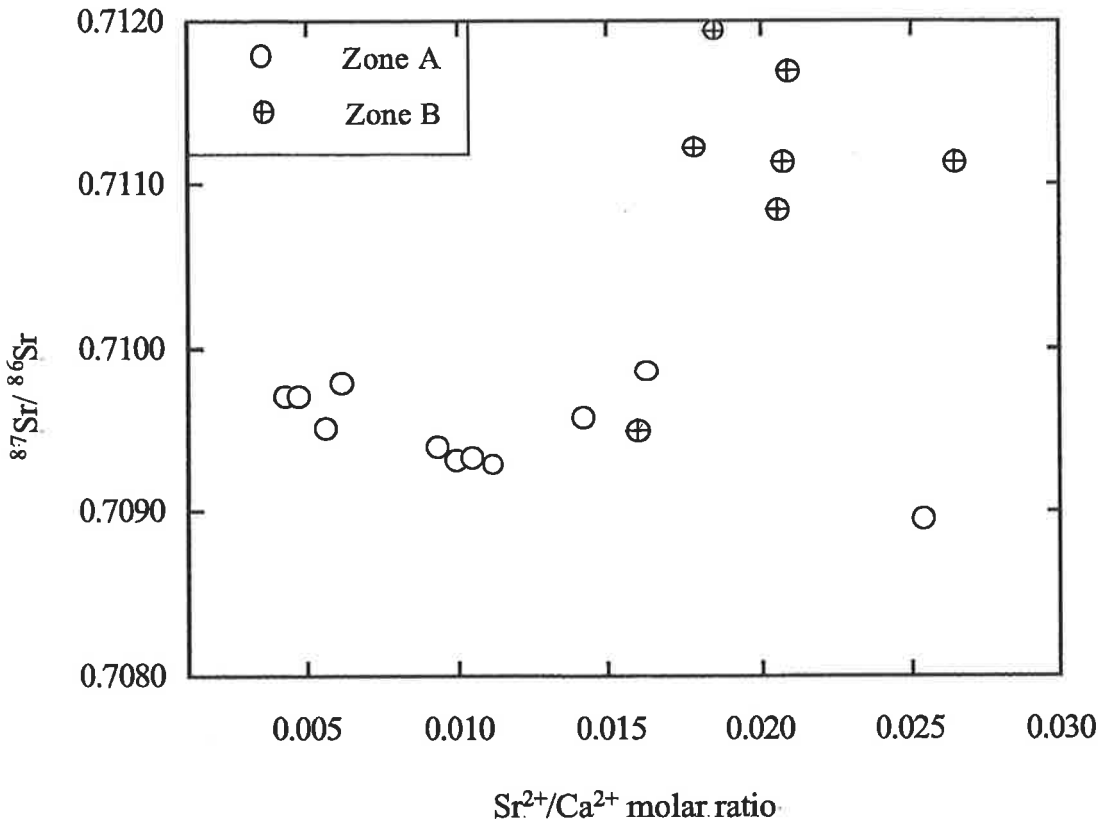

Fig. 5.12 $^{87}Sr/^{86}Sr$ vs. Sr^{2+}/Ca^{2+} ratio of groundwater from the Renmark Group Aquifer. The data display two distinct groups of groundwater. Groundwater with a more radiogenic $^{87}Sr/^{86}Sr$ ratio is from the north, and groundwater with a relatively less radiogenic $^{87}Sr/^{86}Sr$ ratio is from the south and central part of the study area.

The difference between the $^{87}Sr/^{86}Sr$ ratios of the two groups is probably an indication of the different recharge areas (i.e. different aquifer mineralogy) for different parts of

the Renmark Group Aquifer. The groundwater from the first group is located to the south and central part of the study area (Zone A) which is recharged from the south and south-east in the Dundas Plateau in Victoria. The second group is located to the northern part of the study area in Zone B near the River Murray. The $^{87}Sr/^{86}Sr$ and Sr^{2+}/Ca^{2+} ratio supports the hypothesis presented by Evans and Kellett (1989) that groundwater in the Renmark Group Aquifer in the northern part of the study area has originated from the Riverine Province ~ 400 km northeast of the study area compared with the groundwater recharged from the Dundas Plateau in Victoria, south of the study area.

A plot of the $^{87}Sr/^{86}Sr$ ratio versus Cl^- concentration for the Renmark Group Aquifer (Fig. 5.13) also shows two different groups. Groundwater that is located to the northern part of the study area is more saline and radiogenic compared with the groundwater located to the south and central part of the study area.

5.5.3 $^{87}Sr/^{86}Sr$ as a tracer for groundwater mixing

The $^{87}Sr/^{86}Sr$ ratio of groundwater in the Murray Group Aquifer in the north and northeastern part of the study area (Zone B) is considerably enriched in ^{87}Sr compared to the $^{87}Sr/^{86}Sr$ ratio in Zone A (Fig. 5.2) and markedly higher from that of the carbonate rocks (Table 5.1). The $^{87}Sr/^{86}Sr$ value of groundwater in well M68 is higher than the bulk $^{87}Sr/^{86}Sr$ ratio for the rock samples from the Murray Group Aquifer (Table 5.1). Groundwater will acquire more radiogenic $^{87}Sr/^{86}Sr$ ratio than the bulk rock

only if the Sr^{2+} comes exclusively from silicate minerals. This is unlikely to occur because carbonate minerals are much more abundant in the Murray Group matrix and more reactive than silicate minerals (Appelo and Postma, 1993).

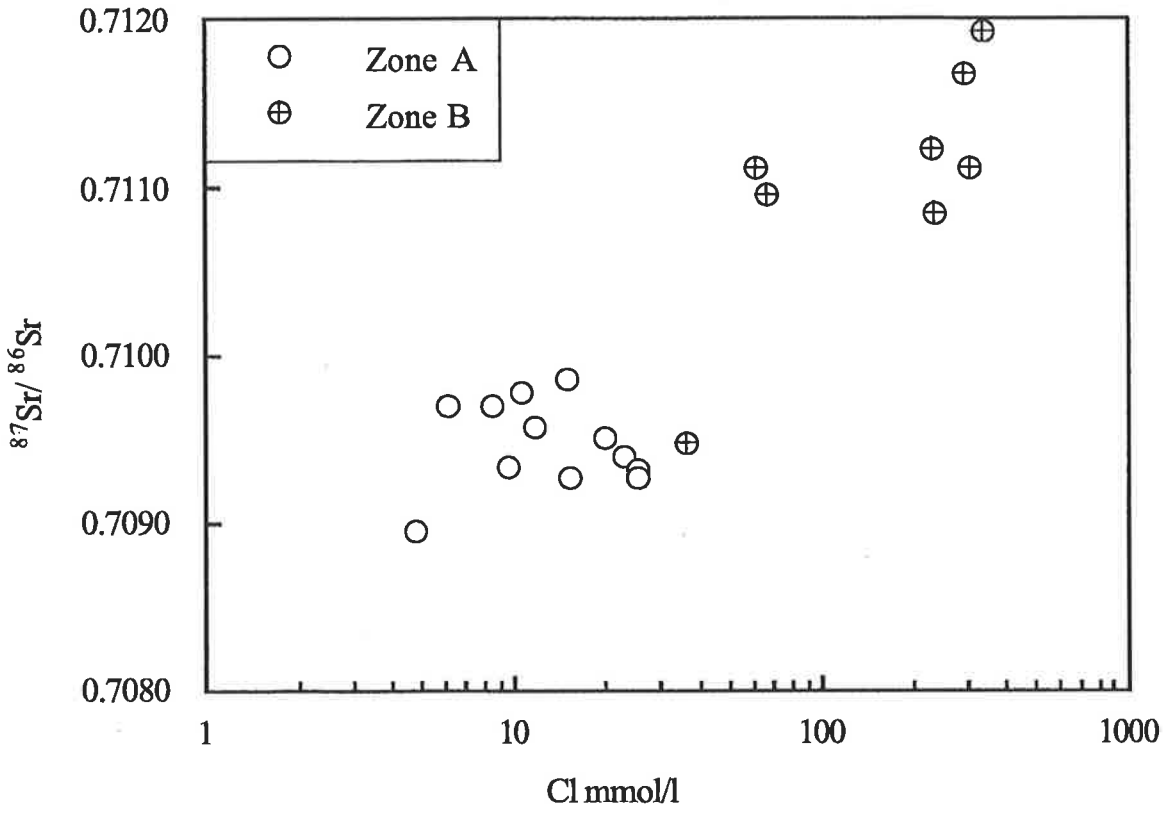

Fig. 5.13 $^{87}Sr/^{86}Sr$ ratio vs. Cl^- concentration of groundwaters from the Renmark Group Aquifer.

The $^{87}Sr/^{86}Sr$ ratio of the Renmark Group Aquifer at the same location of M68 has an identical value to that of the Murray Group Aquifer (R18-Table 5.3). Therefore the more enriched $^{87}Sr/^{86}Sr$ ratio in the groundwater at well M68 is probably due to the addition of more radiogenic Sr^{2+} via groundwater from the Renmark Group Aquifer through upward leakage. Stable isotope and hydrochemical data (Herczeg et al., 1989;

Cook et al., 1991) also suggested that the groundwater in this part of the study area is derived from upward leakage from the Renmark Group Aquifer.

In order to estimate the mixing proportions the $^{87}Sr/^{86}Sr$ ratio and Sr^{2+} concentrations of the respective end members need to be defined. The first end member is groundwater in the Renmark Group Aquifer in the wells adjacent to the River Murray where $^{87}Sr/^{86}Sr$ ratios range from 0.71085 to 0.71122. The second end member is groundwater in the Murray Group Aquifer which is not influenced by mixing and is in chemical and isotopic equilibrium with carbonate minerals. The $^{87}Sr/^{86}Sr$ ratios for this end member is similar to that of the carbonate minerals (0.7085). Groundwater from the Murray Group Aquifer wells adjacent to the River Murray that are influenced by mixing have $^{87}Sr/^{86}Sr$ ratios that range from 0.70881 to 0.71117.

The isotope systematics of two component mixtures have been described in detail by Faure (1986). By plotting $^{87}Sr/^{86}Sr$ ratio vs. $1/Sr^{2+}$ of the groundwaters, the proportion of mixing between the respective two end members can be estimated. If groundwater in the Murray Group Aquifer resulted from the two components mixing, each having different $^{87}Sr/^{86}Sr$ ratios and Sr^{2+} concentrations, then the groundwater data plotted in $^{87}Sr/^{86}Sr$ vs. $1/Sr^{2+}$ space must fall on a straight line. However, the $^{87}Sr/^{86}Sr$ and $1/Sr^{2+}$ ratio for groundwater in the Murray Group Aquifer for Zone B appear to represent mixing between three end members (Fig. 5.14). The third end member probably represents local recharge and its importance in contributing significant amount of

dissolved salt relative to laterally flowing groundwater was highlighted in previous sections.

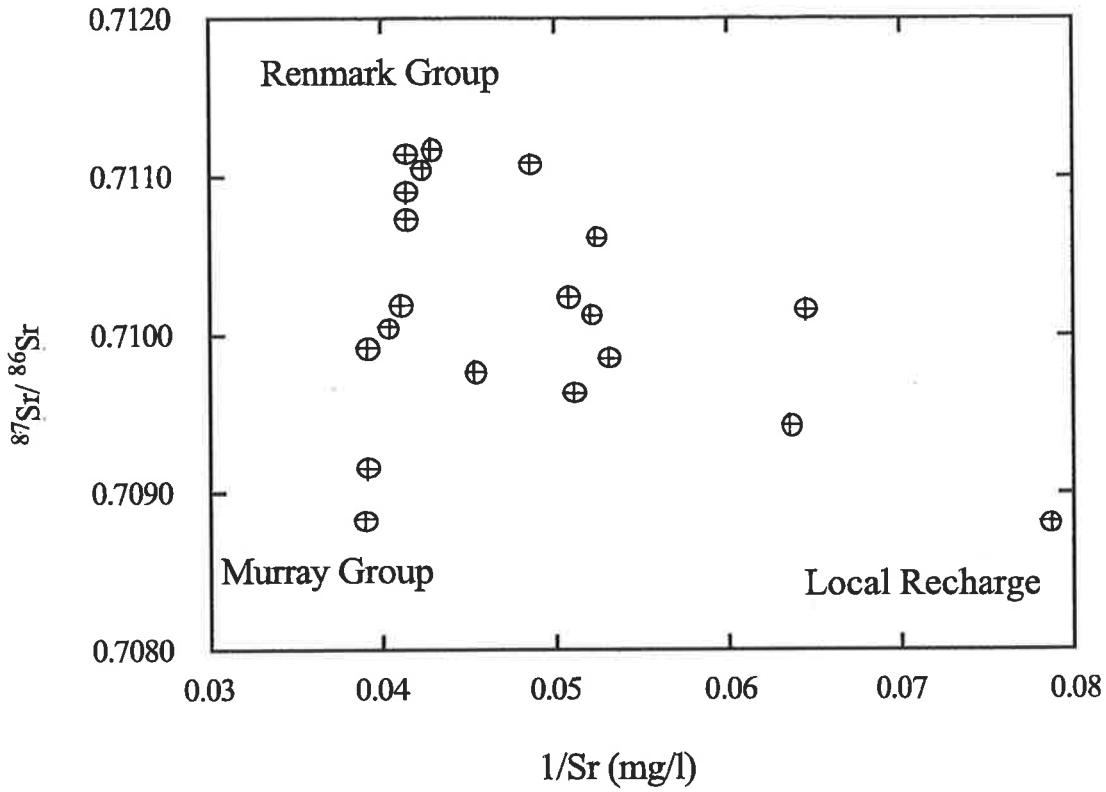

Fig. 5.14 Measured $^{87}Sr/^{86}Sr$ ratio vs. reciprocals of strontium concentration in the Murray Group Aquifer from Zone B. The plot shows mixing between three end members, local recharge, upward leakage from the Renmark Group Aquifer and groundwater from the Murray Group Aquifer.

The proportion of mixing of the three end members can be calculated from a set of mass and isotopic balance equations as follows:

$$Sr^{2+} = A\ Sr^{2+}_{M} + B\ Sr^{2+}_{R} + C\ Sr^{2+}_{L} \quad (5.5)$$

$$(Sr^{2+}.\ ^{87}Sr/^{86}Sr) = (A\ Sr^{2+}.\ ^{87}Sr/^{86}Sr)_{M} + (B\ Sr^{2+}.\ ^{87}Sr/^{86}S)_{R} + (C\ Sr^{2+}.\ ^{87}Sr/^{86}Sr)_{L} \quad (5.6)$$

$$1 = A + B + C \quad (5.7)$$

where Sr^{2+} and $^{87}Sr/^{86}Sr$ are the concentrations and isotopic ratios in the final solution. The $(Sr^{2+}.\ ^{87}Sr/^{86}Sr)_{M}$, $(Sr^{2+}.\ ^{87}Sr/^{86}S)_{R}$ and $(Sr^{2+}.\ ^{87}Sr/^{86}Sr)_{L}$ are the concentrations and

isotopic ratios of Sr^{2+} in the three end members: the Murray Group Aquifer (M), Renmark Group Aquifer (R), and local recharge (L) respectively. A, B, and C are the proportion of each of three proposed end members to the final solution.

The $^{87}Sr/^{86}Sr$ data as a function of mixing fraction of three components in the Murray Group Aquifer is plotted in Fig (5.15). The two diagonal lines represent (a) addition of groundwater from the Renmark Group Aquifer through upward leakage and (b) addition of soil water via local recharge to the Murray Group Aquifer.

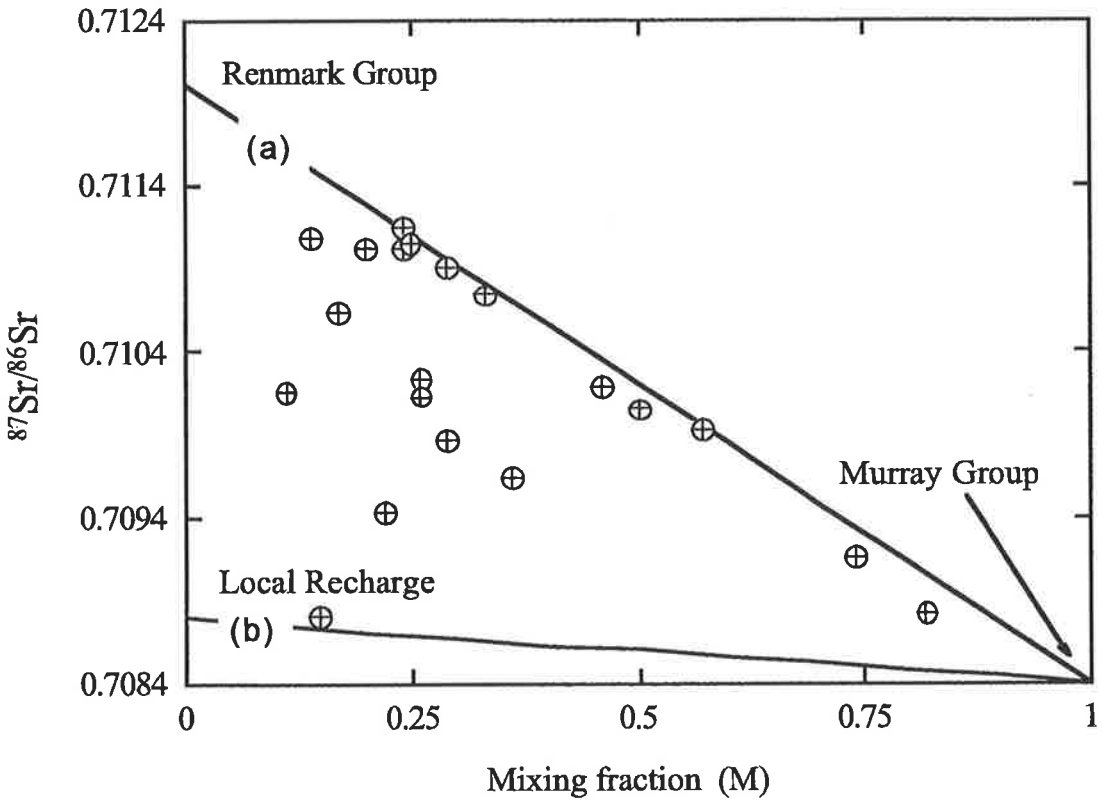

Fig. 5.15 Model of the $^{87}Sr/^{86}Sr$ ratio in the Murray Group Aquifer from the northern part of the study area. The two straight lines represent mixing between groundwater from the Murray Group Aquifer with the soil water via local recharge and with groundwater from the Renmark Group Aquifer via upward leakage respectively.

The results suggest that although most of the data falls on or parallel to a mixing line between the Murray and Renmark Group aquifers, the apparent contribution of Sr^{2+} from soil water, via local recharge, to the Sr^{2+} pool in groundwater at some of the wells is as significant as the contribution through upward leakage from the Renmark Group Aquifer.

Further evidence for the importance of local recharge is that there is measurable ^{14}C activity in the Murray Group Aquifer in the northern part of the study area. Groundwater in the Murray Group Aquifer flowing laterally from the south-eastern margin of the basin would be devoid of measurable ^{14}C content after about 40 km, assuming a velocity of groundwater of ~ 1m/year (Barnett, 1989). Groundwater in the Renmark Group Aquifer also does not contain measurable ^{14}C in the northern part of the study area. Mixing of these two end members would result in groundwater also devoid of ^{14}C. The measured ^{14}C activities therefore, must be introduced to the groundwater in the Murray Group Aquifer through local recharge. The ^{14}C concentrations in both aquifers is discussed in detail in Chapter 6.

5.6 Conclusions

Groundwater $^{87}Sr/^{86}Sr$ ratios, in combination with Sr^{2+}/Ca^{2+}, and Mg^{2+}/Ca^{2+} ratios as well as $\delta^{13}C$, provide constraints on the nature of carbonate mineral-groundwater reactions in the carbonate rich Murray Group Aquifer. The main findings are:

1. The $^{87}Sr/^{86}Sr$ ratios in groundwater from the south and central part of the study area are controlled by the dissolution of carbonate as soil water percolates through the unsaturated zone, and mixes with laterally flowing groundwater. A model of $^{87}Sr/^{86}Sr$ and Sr^{2+}/Ca^{2+} ratio variations shows that incongruent dissolution of carbonate minerals in the aquifer is also important. This conclusion is further supported by $\delta^{13}C$ data, in that TDIC becomes progressively more enriched in ^{13}C as the $^{87}Sr/^{86}Sr$ ratio decreases towards the ratios exhibited by carbonates in the aquifer matrix.

2. Groundwater from the Murray Group Aquifer in the northern part of the study area, near the River Murray has a more radiogenic $^{87}Sr/^{86}Sr$ ratio compared with that in the south and central parts of the study area. Sr^{2+} concentrations and $^{87}Sr/^{86}Sr$ ratios of the groundwater in this part is most likely dominated by mixing with more radiogenic groundwater from the silicate rich Renmark Group Aquifer, through upward leakage and local recharge, rather than interaction with carbonate minerals.

3. Groundwater in the Renmark Group Aquifer can also be divided into two groups according to the $^{87}Sr/^{86}Sr$ and Sr^{2+}/Ca^{2+} ratio, (1) groundwater in the south that has a relatively low $^{87}Sr/^{86}Sr$ ratio and low Cl^- concentration, and (2) groundwater in the north and north-east that has more radiogenic values and higher Cl^- concentrations. Therefore, the $^{87}Sr/^{86}Sr$ data support the hypothesis presented by Kellett and Evans (1989) that groundwater in the north has a different recharge area and is originated in the Riverine Province 400 km northeast of the study area.

CHAPTER 6

Carbon-13 and Radiocarbon

6.1 Introduction

The use of radiocarbon (^{14}C) activity in groundwater has been an integral part of many hydrological investigations for establishing flow patterns and age estimates of groundwater (Smith et al., 1975, 1976; Downing, 1977) and has provided information on past climatic conditions in regional groundwater basins (Hotzl et al., 1980; Edmunds and Walton, 1980). However, the majority of previous studies have used ^{14}C dating in the confined aquifers assuming that the dominant transport mechanism is lateral flow which can be approximated to that of a piston flow (e.g. Love et al., 1994). In those situations groundwater residence time and velocity can be estimated by sampling water on an inferred flow line. In contrast, unconfined aquifers receive recharge throughout their spatial exposure resulting in the mixing of waters of different ^{14}C concentrations. As a consequence, ^{14}C dating of groundwater is more complex than in confined aquifers. The ^{14}C dating method, therefore, cannot be used unless the potential end members that contribute to groundwater budget are identified (Hufen et al., 1974; Verhagen et al., 1974).

In previous chapters, the $\delta^{34}S$ and $^{86}Sr/^{87}Sr$ isotope data highlighted the significance of local recharge to the Murray Group Aquifer. However, interpretation of these isotopes can only provide semi-quantitative information on the amount of water derived from local recharge. Unlike $\delta^{34}S$ and $^{86}Sr/^{87}Sr$ isotopes, the ^{14}C activity, can be used as a quantitative tracer to estimate recharge rates (Edmunds and Wright, 1979) to the Murray Group Aquifer, and also to verify sulphur and strontium isotope data.

The groundwater velocity of the Murray Group Aquifer is ~ 1m/year (Barnett, 1989), the ^{14}C activity of groundwater emanating from the basin margin at the south and southeast would be <1 pmc after travelling ~ 40 km further inland. Therefore, any ^{14}C activity > 1 pmc measured in groundwater from the central and northern parts of the study area must be due to the introduction of modern ^{14}C via local recharge. Accordingly, the amount of ^{14}C measured in groundwater beyond the 40km limit from the basin margin would be a function of the amount of the local recharge added to the Murray Group Aquifer.

Identifying the chemical reactions which occur in groundwater, particularly in carbonate aquifers that affect total dissolved inorganic carbon (TDIC) and in turn modify the ^{14}C concentration is a pre-requisite in the correction of ^{14}C activities to estimate groundwater residence time (Ingerson and Pearson, 1964). These reactions include dissolution of soil CO_2 in soil water percolating through the unsaturated zone, congruent and incongruent dissolution of carbonate minerals in the Murray Group Aquifer. These reactions were identified using strontium isotopes (chapter 5). This

chapter examines the effect of inter-aquifer mixing and carbonate minerals-solution reactions on ^{14}C concentration to provide better estimates of groundwater ^{14}C age.

The main objectives of this chapter are:

1. to use ^{14}C data as a tracer in order to verify the main conclusions obtained from the previous chapters for the importance of dissolved salt and water derived from local recharge throughout the Murray Group Aquifer relative to that derived from laterally flowing groundwater;
2. to correct measured ^{14}C data for reactions occurring in the aquifer and estimate groundwater residence time;
3. to convert groundwater residence time to estimate recharge rates in various parts of the study area.

6.2 Background

^{14}C is produced in the upper atmosphere by cosmic ray interactions with ^{14}N (Libby, 1965). ^{14}C is oxidised to CO_2 and mixes with atmospheric CO_2. The ^{14}C of atmospheric CO_2 is then introduced into surface and groundwater. The most important mechanism of ^{14}C introduction to groundwater is via production of the CO_2 by respiration and the decay of plants in the soil zone. Because CO_2 produced in the soil

zone is introduced to the plants from atmospheric CO_2, it has a similar ^{14}C activity to that of the atmosphere.

The anthropogenic addition of CO_2 into the atmosphere by the burning of fossil fuels since the 1800's and the addition of ^{14}C via nuclear bomb tests after 1953, have changed the ^{14}C activity of the atmosphere (Fontes, 1983). However, the effect of these processes is only important when dealing with relatively young groundwaters (i.e. <150 years). Apart from the temporary increase of ^{14}C activity due to bomb tests, the ^{14}C activity of atmospheric CO_2 generally is assumed to be constant, due to the steady state between cosmic production, decay, and transformation to other forms of carbon (dissolved CO_2 in water and photosynthesis).

The assumption of the constant ^{14}C concentration of the atmospheric CO_2 and constant initial ^{14}C input has a practical advantage in dating groundwaters. The radioactive decay of ^{14}C produces ^{14}N which can escape or mix with common nitrogen. Therefore, it is impossible to estimate the amount of radiogenic nitrogen produced exclusively by ^{14}C decay. Thus, the conventional radioactive decay equation which relates the amount of secondary element produced via radioactive decay of the parent element can not be strictly applied to ^{14}C dating.

Assuming that the initial ^{14}C activity (Ao) can be accurately determined, it is possible to estimate the time since the groundwater was isolated from atmospheric CO_2 by using the decay equation :

$$A = Ao\ e^{-\lambda t} \qquad (6.1)$$

where A and Ao are the measured ^{14}C activity at the present time, and the initial ^{14}C activity respectively and λ is the ^{14}C decay constant (1.7×10^{-4} yr^{-1}).

Because the relationship between the remaining ^{14}C activity and its age is exponential, the estimated age of groundwater derived from a mean ^{14}C concentration of a mixture of two components will not represent the real age of the mixture. For example, if two waters mix in equal amounts with ^{14}C activities of 80pmc and 20 pmc (per cent modern carbon) respectively, the age of each water calculated from the decay equation would be 1844 years and 13305 years respectively. The mean age of the mixture of these two end members would be 7574 years. However, if the age of the mixture was calculated from the mean of their ^{14}C concentrations (i.e. 50 pmc), the mean age of the mixture would be 5730 yr. which is about 1700 yr. younger than the real age of the mixture. Therefore, large errors can result in the determination of the ages of groundwater that originates from the mixing of various sources or consist of components of different ages. The relative errors increase with the increase in the mean age of the mixture and can be significantly higher than the errors that arise by the correction models (Evans et al., 1978).

The most problematic parameter in interpreting ^{14}C activities is the estimation of initial ^{14}C activity of the water at the time of recharge. The measured ^{14}C activities of groundwater must be corrected for the addition of dead carbon by congruent and

incongruent dissolution of carbonate minerals, oxidation of old organic matters (e.g. lignite) and possibly methanogenesis.

A number of models have been developed for the interpretation of ^{14}C activity and age adjustments for systems which are open and closed to soil CO_2 (Wigley, 1975; Reardon and Fritz, 1978; Wigley et al., 1978; Fontes and Garnier, 1979). The open and closed system conditions have been explained by Garrels and Christ (1965), and Langmuir (1971). Under open system conditions, groundwater- aquifer matrix reactions occur in the presence of an infinite CO_2 reservoir, whereas, under closed system conditions, the reactions occur in isolation of a soil CO_2 reservoir. These conditions are often realised in nature. For example, open system conditions could be applied to soil zone processes and closed system conditions could be applied to the geochemical processes taking place in confined aquifers (Wigley, 1975).

Under open system conditions, the ^{14}C activity of soil water is directly related to the ^{14}C activity of soil CO_2 and the equilibrium fractionation factor. Exchange between different phases such as CO_2 gas, dissolved carbon species ($CO_{2(aq)}$, HCO_3^- and CO_3^{2-}), and solid carbonate in unsaturated zone can lead to fractionation of carbon isotopes between phases and between dissolved carbon species. Theoretical and experimental studies (Urey, 1947; Craig, 1954) confirm that the isotopic fractionation is approximately twice as large for ^{14}C as it is for ^{13}C i.e.

$$\varepsilon\ ^{14}C = 2.3 \times \varepsilon\ ^{13}C \qquad (6.2)$$

The fractionation factors for ^{13}C between carbon phases and dissolved species in groundwater are given in Deines et al. (1974). For example, equilibrium fractionation of ^{13}C between dissolved HCO_3^- and gas CO_2 at 25°C and pH = 7 is 7.85‰. However, because the ^{14}C activities are expressed in % rather than ‰, the equilibrium fractionation of ^{14}C between HCO_3^- and gas CO_2 at 25 °C is

$$\frac{2x7.85}{10} = 1.6\% \qquad (6.3)$$

The ^{14}C activity of soil water in equilibrium with soil CO_2 will be slightly enriched relative to soil CO_2 gas and can be calculated from the following equation (Mook, 1980):

$$A_R = A_g + (HCO_3^- \varepsilon_{g\text{-}HCO3\text{-}} + CO_3^{2-} \varepsilon_{g\text{-}CO32\text{-}} + CO_{2(aq)} . \varepsilon_{g\text{-}CO2(Aq)})/C_T \qquad (6.4)$$

where A_R and A_g denote the ^{14}C activity in soil water and in soil CO_2 respectively, HCO_3^-, CO_3^{2-} and $CO_{2(aq)}$ are the fraction of dissolved carbon species in soil water, the $\varepsilon_{g\text{-}HCO3\text{-}}$, $\varepsilon_{g\text{-}CO32\text{-}}$, and $\varepsilon_{g\text{-}H2CO3}$ are the ^{14}C fractionation factors between soil gas CO_2 and dissolved carbon species in the soil water, and C_T is the TDIC in soil water. Sometimes Eq. 6.4 is applied in a simplified way, for example assuming the pH of recharge water reacting with carbonate minerals ranges between 7 to 8, the dissolved carbon species would be mainly in the form of bicarbonate. Hence equation (4) in this case reduces to:

$$A_R = A_g + \varepsilon_{g\text{-}HCO3\text{-}} \qquad (6.5)$$

Assuming the ^{14}C activity of soil gas CO_2 is 100 pmc, the ^{14}C activity of recharge water would be 101.6pmc. The assumption that the pH of soil water ranges from 7 to 8 is reasonable given observation in recharge areas of other carbonate aquifers (Jacobson and Langmuir, 1970; Reardon et al., 1980).

If carbonate minerals are dissolved in the soil water, the ^{14}C activity of HCO_3^- added to the solution will be 50pmc due to the addition of carbon devoid of ^{14}C, according to stoichiometry of the carbonate dissolution reactions as follows:

$$CO_2 + H_2O + CaCO_3 = Ca^{2+} + 2HCO_3^- \quad (6.6)$$

If the soil water remains in the unsaturated zone after carbonate dissolution, dissolved HCO_3^- re-equilibrates with soil CO_2 and ^{14}C activity approaches that of the soil CO_2 plus the fractionation factor according to equation (6.4). On the other hand, if soil water reaches the water table before re-equilibration with soil CO_2, ^{14}C activity will be lower than the equilibrium value with soil CO_2 and in this case the closed system condition applies to the unsaturated zone.

Reardon et al. (1980) showed that the equilibrium between HCO_3^- dissolved in soil water and soil CO_2 is a function of the rate of soil gas diffusion to the water table and carbonate mineral dissolution. Equilibrium is often not achieved, particularly in temperate regions with high recharge rates when voids in the unsaturated zone are partially filled with water. Retention of CO_2 and $^{14}CO_2$ on carbonate minerals has been observed in the unsaturated zone causing a decrease of ^{14}C activity of soil water from that of the equilibrium value (Striegl and Armstrong, 1990). The above mentioned studies suggest that even in open system conditions, equilibrium with soil CO_2 cannot be assumed if the residence time of soil water in the unsaturated zone is relatively short compared with the time required for the diffusion of soil CO_2 to the water table.

Once soil water reaches the water table and is isolated from the soil CO_2 reservoir,

congruent and incongruent dissolution of carbonate minerals causes a decrease of the ^{14}C activity of groundwater. Therefore an essential factor in estimating residence time of groundwater is to account for the affect of these reactions that decrease the ^{14}C activity independent of radioactive decay by using appropriate correction models (Fontes and Garnier, 1979; Fontes, 1983). The corrected ^{14}C age then can be used to estimate recharge rates.

6.3 Results

$\delta^{13}C_{TDIC}$ values for groundwater in the Murray Group Aquifer range from -20.8‰ to 0.8‰ and ^{14}C activities range from less than 1pmc to about 21pmc, with the majority of samples having a ^{14}C activity < 1pmc (Table 6.1).

Table 6.1 Carbonate chemistry and $\delta^{13}C$ and ^{14}C concentrations of groundwater from the Murray and Renmark Group aquifers. The carbonate species were calculated by the computer code PHREEQM from pH, alkalinity and major ion data (Table 3.3) and expressed in mmole units. $\delta^{13}C$ composition is expressed in ‰ relative to PDB. The observed and adjusted ^{14}C activities are expressed in per cent modern carbon.

Well Reg. No.	Well ID	Depth of screen from water table (m)	$CO_2(aq)$	HCO_3^-	$\delta^{13}C_{TDIC}$	Measured ^{14}C	Adjusted ^{14}C
			(mmol/l)		(‰,PDB)	(pmc)	
51846	M6	19.8	1.5	5.8	-5.90	6	
92808	M7	37.5	0.8	4.9	-4.20	9.6	43.9
50946	M8	47.5	1.6	4.8	-3.90	9.2	51.1
60610	M9	76.4	0.3	4.0	-6.40		
79530	M10	10.0	0.4	4.6	-5.70	13.6	33.1
60436	M12	44.1	0.6	5.6	-3.70	2.4	15.5
84741	M13	60.0	0.4	5.0	-2.90	10.8	
75651	M14	42.6	0.3	4.9	-3.40	5.5	47.4
60450	M17	50.1	0.3	4.8	-4.60	4.6	17.1
79655	M18	73.0	0.2	2.7	-5.90	0	
58079	M19	81.6	0.2	4.2	-9.20	19.6	22.8
98297	M20	24.2	0.3	5.4	-1.50	8.8	

Table 6.1 Contd.

Well Reg. No.	Well ID	Depth of screen from water table (m)	CO_2(aq) (mmol/l)	HCO_3^- (mmol/l)	$\delta^{13}C_{TDIC}$ (‰,PDB)	Measured ^{14}C (pmc)	Adjusted ^{14}C (pmc)
98254	M22	50.3	0.2	4.8	-3.30	4	38.7
54642	M27	95.5	0.3	3.8	-3.10	0	
82220	M29	68.0	0.8	8.1	-5.70	16.6	40.4
61571	M30	154.6	0.1	4.2	-0.80	3.3	
7026-113	M33	32.5	0.2	4.2	-1.60	3.6	
7026-110	M34	34.5	0.2	3.5	-3.70	5.8	37.5
7027-566	M35	11.6	0.4	4.2	-7.10	0	
7027-650	M36	74.5	0.3	4.1	-4.70	0	
7027-606	M37	20.8	0.4	5.2	-2.80	0	
7027-592	M38	26.5	0.3	4.6	-3.30	0	
7027-597	M39	45.4	0.2	3.6	-4.60	0	
7027-602	M41	31.8	0.2	4.5	-3.70	0	
7027-405	M42	71.0	0.3	4.8	-7.90	6.2	8.9
7027-586	M43	64.4	0.2	3.8	-6.80	3.2	5.8
7027-579	M44	61.0	0.3	3.6	-4.90	2.2	7.1
6827-1536	M45	35.5	0.9	7.6	-4.20	4.5	20.6
7026-120	M46	38.5	0.5	6.5	-6.14	0	
6927-591	M47	20.5	1.2	7.3	-5.80	10	23.6
6927-644	M48	39.0	0.3	4.6	-7.60	0	
6927-590	M49	47.0	0.2	4.2	-5.30	8	22.3
6927-588	M50	36.6		4.1	-5.40	6.5	17.5
6927-601	M51	31.0	0.4	4.2	-7.50	0	
6928-567	M52	32.3	0.3	6.3	-5.50	0	
6928-411	M53	4.7	0.7	5.9	-7.50	0	
6928-49	M54	1.8	0.9	7.2	-5.44	6.9	18.3
6928-260	M55	22.6	0.3	4.7	-5.90	0	
7028-503	M56	15.3	0.8	8.0	-5.80	0	
7025-422	M57	1.2	0.5	5.9	-7.60	0	
64363	M67	105.4	0.4	8.5	-2.70	15.1	
6928-477	M58	8.2	0.7	8.9	-6.10	7.9	17.1
6928-27	M59	11.6	0.9	8.1	-6.80	3.8	6.9
6828-112	M60	1.3	1.5	10.2	-4.40	12.8	52.4
6928-528	M61	7.4	1.8	12.4	-5.00	10	31.2
6929-154	M63	3.4	1.4	12.6	-7.50	20.3	31.7
6928-2	M65	28.1	1.3	10.7	-8.00	0	
49677	M66	55.5		5.3	-1.00	0	
64363	M67	105.4	0.4	8.5	-2.70	15.1	
6929-356	M68	18.9	2.3	7.6	-14.10	15.1	
6929-700	M73	45.7	2.2	5.3	-10.10	0	
6929-711	M74	40.7	2.3	5.4	-14.23	3.4	
6929-712	M75	36.0	2.6	4.8	-16.50	9.3	
6929-710	M76	46.6	2.5	4.4	-17.50	21.1	
6929-702	M77	32.8	2.2	4.6	-18.32	9.2	
6929-701	M78	32.5	2.1	4.7	-20.20	3.1	
6929-684	M79	36.0	1.8	4.1	-20.82	11.3	
6929-651	M80	37.0	1.8	4.1	-19.46	7.5	
6929-682	M81	40.0	1.8	3.8	-19.04	5	
6929-685	M82	45.0	1.4	4.1	-18.17	6.6	
6929-686	M83	41.0	1.7	5.3	-19.59	3.8	
6929-687	M84	41.0	2.2	6.4	-19.40	4.9	
6929-689	M85	39.0	2.0	6.8	-16.00	4.1	

Table 6.1 Contd.

Well Reg. No.	Well ID	Depth of screen from water table (m)	CO_2(aq) (mmol/l)	HCO_3^- (mmol/l)	$\delta^{13}C_{TDIC}$ (‰,PDB)	Measured ^{14}C (pmc)	Adjusted ^{14}C (pmc)
6929-691	M86	44.0	2.3	6.7	-11.64	8.9	
6929-692	M87	43.0	2.4	7.3	-12.40	9.6	
6929-693	M88	42.0	2.4	7.8	-12.40	0	
6929-1082	M91	49.0	2.3	7.3	-6.39	4.4	
6929-1041	M90	42.7	1.7	8.2			
6929-1046	M89	42.0	2.4	7.8	-8.50	5.5	
Renmark Group Aquife							
67847	R1		0.06	2.7	-11.11	0	
75669	R4		0.20	5.3	-6.20	0	
58111	R5		0.01	2.9	-3.90	0	
7026-112	R7		0.21	3.9	-4.00	0	
7026-111	R8		0.12	3.9	-4.80	0	
7027-585	R10		0.15	5.9	-8.90	0	
6927-588	R11		0.13	4.5	-9.10	0	
6928-542	R12		0.15	10.5	-12.00	0	
6827-1530	R13		0.41	9.9	-11.50	0	
6929-423	R14		0.37	10.8	-12.70	0	
49676	R15		0.9	6.4	-13.10	0	
7028-469	R16		0.06	3.8	-14.20	0	
6929-760	R18		1.2	7.9	-18.10	0	
6829-992	R19		0.51	6.0	-14.10	0	
81832	R20		0.92	6.9	-20.23	0	
86774	R22		0.09	5.6	-21.65	0	
Rb1	R23			5.6	-19.10	0	

Groundwaters sampled from the Renmark Group Aquifer are all devoid of ^{14}C.

Groundwater of the Murray Group Aquifer is divided into two distinct groups based on the $\delta^{13}C_{TDIC}$ values and HCO_3^- concentrations (Fig. 6.1). The $\delta^{13}C_{TDIC}$ values for the first group range from -0.8 to -9.2‰ and the HCO_3^- concentrations range from 3.8 mmole/l to 12.6 mmole/l. Groundwater samples of this group are from the south and central part of the study area (Zone A). $\delta^{13}C_{TDIC}$ values of the second group of samples range from -8.5 to -20.8‰ and their HCO_3^- concentrations range 4.1mmole/l to 7.8 mmole/l. These groundwater samples are located to the north of the study area in Zone B. $\delta^{13}C_{TDIC}$ of groundwaters in the Renmark Group Aquifer from Zone B

generally have more depleted $\delta^{13}C_{TDIC}$ compared with groundwater in Zone A and range from -14.1‰ to -21.65‰ and from -3.9‰ to -13.1‰ respectively.

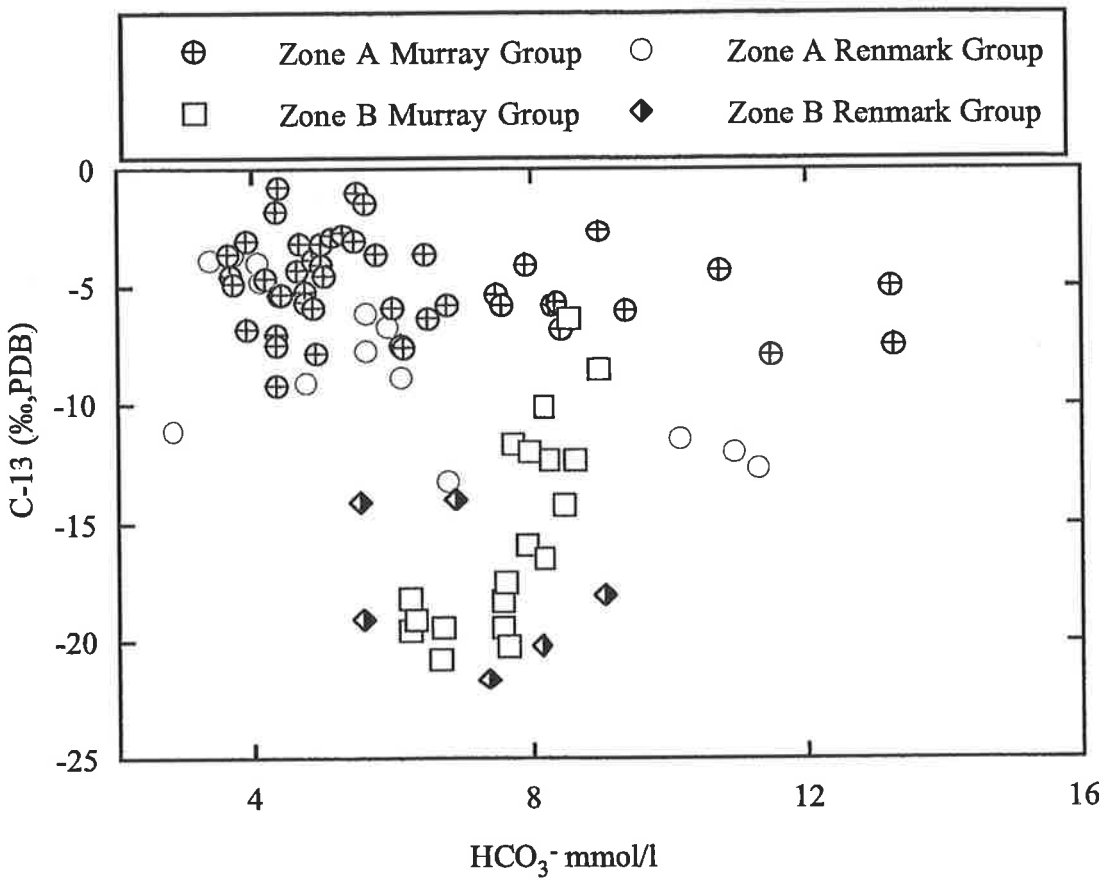

Fig. 6.1 $\delta^{13}C_{TDIC}$ composition vs. the HCO_3 concentrations of groundwater in the Murray and Renmark Group aquifers. The $\delta^{13}C_{TDIC}$ value in Zone B is relatively depleted compared with $\delta^{13}C_{TDIC}$ in Zone A.

6.4 Discussion

6.4.1 Controls on $\delta^{13}C_{TDIC}$ of the Murray Group Aquifer (Zone A)

Evolution of $\delta^{13}C_{TDIC}$ of groundwater could occur either in isolation from the soil CO_2

reservoir or in contact with the soil CO_2 reservoir. Equilibrium will be established between the $\delta^{13}C_{TDIC}$ of groundwater and the $\delta^{13}C$ of soil CO_2 if groundwater is in contact with soil CO_2. The $\delta^{13}C_{TDIC}$ value of groundwater in the Murray Group Aquifer in equilibrium with soil CO_2 ($\delta^{13}C$ -17‰ to -21‰ Dighton and Allison, 1985) can be calculated by carbon mass balance (Mook, 1980), as follows:

$$C_T.\ (\delta^{13}C_{soil\ CO2} + \delta^{13}C_{TDIC}) = a\varepsilon_{a\text{-}g} + b\varepsilon_{b\text{-}g} + c\varepsilon_{c\text{-}g} \qquad (6.7)$$

where C_T is the total dissolved inorganic carbon; $\delta^{13}C_{soil\ CO2}$ and $\delta^{13}C_{TDIC}$ are the ^{13}C content of soil CO_2 and total dissolved inorganic carbon; a, b, c are the mole fraction of $CO_{2(aq)}$, HCO_3^- and CO_3^{2-} respectively, and $\varepsilon_{a\text{-}g}$, $\varepsilon_{b\text{-}g}$, $\varepsilon_{c\text{-}g}$ are the fractionation factors between carbonate species ($CO_{2(aq)}$, HCO_3^- and CO_3^{2-}) and CO_2 gas (Deines et al., 1974). The calculated $\delta^{13}C_{TDIC}$ values range from -9.5 to -11.8‰. These $\delta^{13}C_{TDIC}$ values are depleted in ^{13}C compared to the observed $\delta^{13}C_{TDIC}$ values of the groundwater in Zone A (Table 6.1), indicating that the $\delta^{13}C_{TDIC}$ of groundwater in the Murray Group Aquifer evolved under a closed or partially closed system (in isolation from soil CO_2) conditions.

Carbonate dissolution may cause the relatively enriched $\delta^{13}C_{TDIC}$ of groundwater in the Murray Group Aquifer. The stoichiometry of the carbonate dissolution reaction Eq. 6.6 suggests that $\delta^{13}C_{TDIC}$ should range from -8.1 to -10.1 if mixing between soil gas and the addition of $\delta^{13}C$ = 0.8‰ was dominant (Ingerson and Pearson, 1964). $\delta^{13}C_{TDIC}$ values observed for the majority of groundwater samples in the Murray Group Aquifer

from Zone A range from -9.2 ‰ to -0.8‰ and are too enriched in ^{13}C to be derived from congruent dissolution of carbonate minerals alone (Table 6.1).

Enrichment of $\delta^{13}C_{TDIC}$ in groundwater may be caused by the continuous dissolution and reprecipitation of carbonate minerals in the Murray Group Aquifer matrix (Smith, 1975). This process, known as incongruent dissolution, was inferred from $^{87}Sr/^{86}Sr$ and $\delta^{13}C_{TDIC}$ relationships (Chapter 5). The schematic diagram depicting the effect of incongruent dissolution of carbonate on the $\delta^{13}C_{TDIC}$ and ^{14}C of groundwater is shown in Fig. 6.2.

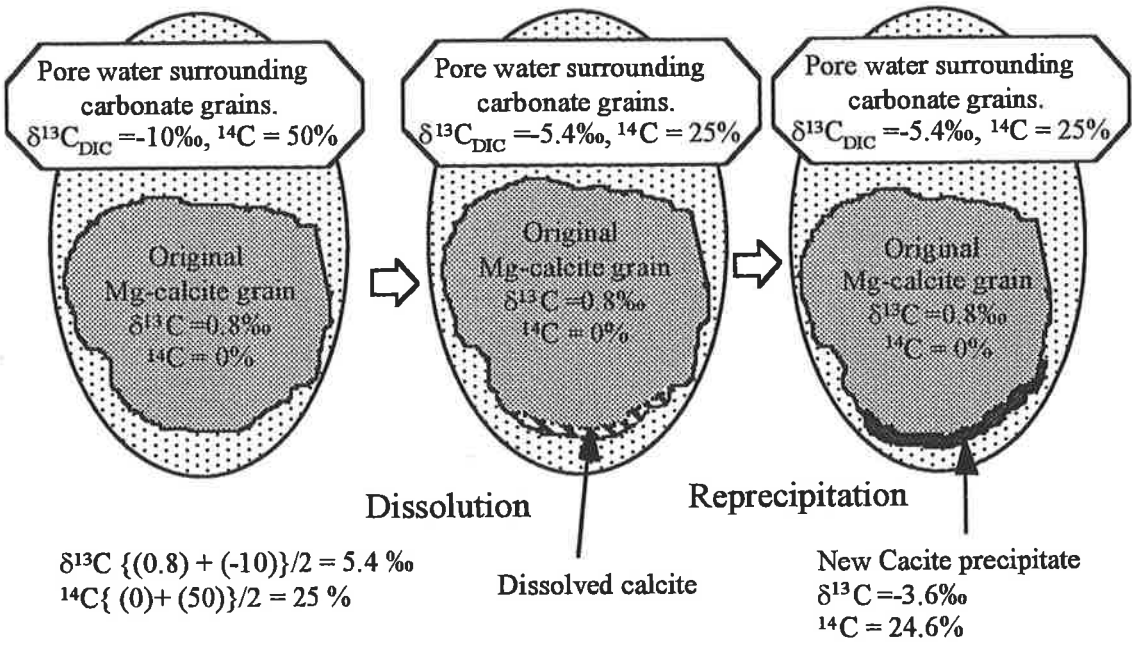

Fig. 6.2 Schematic diagram showing the effect of incongruent dissolution of carbonate minerals on $\delta^{13}C$ composition and ^{14}C activity of groundwater. The $\delta^{13}C$ composition and ^{14}C activity of groundwater approaches that of the carbonate minerals by continuous addition of enriched ^{13}C and dead carbon to the groundwater.

Incongruent dissolution of carbonates occurs in two steps; (1) dissolution of carbonate minerals causing the addition of relatively enriched $\delta^{13}C$ and carbon devoid of ^{14}C to groundwater and, (2) reprecipitation of more stable carbonate minerals causing removal of carbonate from groundwater.

6.4.2 Adjustment of ^{14}C data of the Murray Group Aquifer (Zone A)

The ^{14}C of the added soil water via local recharge is modified by congruent and incongruent dissolution of carbonate minerals in the Murray Group Aquifer as discussed in section 6.4.1. Therefore, the effect of the addition of dead carbon by dissolution of carbonate minerals should be taken into account in estimating the correct ages of groundwater. The correction of the measured ^{14}C activity can be accomplished by adopting the approach described by Ingerson and Pearson (1964) and Wigley et al., (1978, 1979). The Ingerson and Pearson (1964) model considers dilution of ^{14}C activity with dead carbon derived from the dissolution of carbonate minerals in the unsaturated zone. The result of this model used as input for the Wigley et al. (1978, 1979) model, which considers the affect of incongruent dissolution of carbonate minerals in the saturated zone. Reprecipitation of calcite during incongruent dissolution in the saturated zone in the Wigley et al. (1978, 1979) model is assumed to occur in equilibrium with dissolved carbonate species in the groundwater. It is assumed that the dissolved carbonate minerals are part of the original carbonate components in the Murray Group matrix, and not carbonate minerals that have been precipitated from

groundwater. It is also assumed that the amount of carbonate dissolved is equal to the amount of carbonate precipitated from the groundwater.

The carbonate dissolution reaction in the unsaturated zone was estimated via the following equation (Ingerson and Pearson, 1964):

$$\delta^{13}C - \delta^{13}C_R = (\delta^{13}C_o - \delta^{13}C_R)\,X \qquad (6.9)$$

where $\delta^{13}C$, is the ^{13}C content of total dissolved carbonate in the water sample; $\delta^{13}C_o$ and $\delta^{13}C_R$ are the $^{13}C/^{12}C$ content at the beginning of incongruent dissolution and of carbonate minerals respectively, and the X parameter is the adjustment factor required for the estimation of $^{14}C_o$ activities in the water samples. A $\delta^{13}C$ value of -19‰ was taken as the average value representing soil CO_2 in the study area (Dighton and Allison, 1985; Leaney and Allison, 1986). The average $\delta^{13}C$ value measured for carbonate minerals of the Murray Group is 0.8‰. The activities of the carbonate species were obtained from the computer code PHREEQM and the 'X' parameter for the congruent dissolution reaction is calculated from HCO_3 and $CO_{2(aq)}$ concentrations for each groundwater sample via the equation below:

$$X = \frac{mCO_2(aq) + 0.5mHCO_3^-}{mCO_2(aq) + mHCO_3^-} \qquad (6.10)$$

where $mCO_2(aq)$ and $mHCO_3^-$ are the molar concentration of dissolved carbon species in groundwater. The X value for the groundwater samples calculated from Eq. 6.10 ranges from 0.51 to 0.62. Based on these X values, the $\delta^{13}C_{TDIC}$ and ^{14}C activity at the end of congruent dissolution according to Eq. 6. 9 were calculated and range from -11.2‰ to -10.3‰ and from 61pmc to 52pmc respectively. For example the $\delta^{13}C$ content for groundwater of well M7 would be:

$$\delta^{13}C = 0.6\ (-19 - 0.8) + 0.8 = -11.08 \qquad (6.11)$$

And, if the Ao activity of soil CO_2 is 100pmc, the initial ^{14}C activity at the beginning of incongruent dissolution of carbonate would be:

$$A = Ao\ .\ X \qquad (6.12)$$

$A = 100 \times 0.61 = 61$pmc.

The $\delta^{13}C$ and ^{14}C values used in the incongruent dissolution model (Wigley et al., 1978,1979) were as follows:

$$\beta\delta^{13}C - \delta^{13}C_R + \varepsilon/\Gamma = (\beta\ \delta^{13}C_o - \delta^{13}C_R + \varepsilon/\Gamma)\ X \qquad (6.13)$$

where

$\beta = 1 + (\alpha - 1/\Gamma)$;

$\Gamma = 1$ and is the ratio of dissolving to precipitating carbonate; $\delta^{13}C$ is the ^{13}C content of total dissolved carbonate in the water sample ; $\delta^{13}C_o$ and $\delta^{13}C_R$ are the $^{13}C/^{12}C$ ratio of groundwater at the beginning of incongruent dissolution and of carbonate minerals respectively; ε is the fractionation factor between dissolved and precipitating carbonates; X is the adjustment factor.

The $\delta^{13}C$ values for groundwater at the beginning of incongruent dissolution of carbonate minerals were calculated from Eq. 6.10 and average -11.8‰. The $\delta^{13}C_R$ value for carbonate minerals is 0.8‰. The fractionation factor (ε) of 2.5‰ between precipitated calcite and dissolved carbon species was calculated by expressions given by Deines et al. (1974).

Progressive dissolution and precipitation of carbonates results in the $\delta^{13}C_{TDIC}$ of groundwater approaching a constant value of $\delta^{13}C_R - \varepsilon/\Gamma$ in Eq. 6.13. When the $\delta^{13}C_{TDIC}$ of groundwater approaches ($\delta^{13}C_R - \varepsilon/\Gamma$), the ^{14}C activity of the groundwater will approach zero. For example, using 2.5‰ for the fractionation between dissolved and precipitated carbonate and 0.8‰ for the $\delta^{13}C$ value of carbonate minerals, the $\delta^{13}C$ limiting value is -1.7‰. Groundwaters that have $\delta^{13}C$ more positive than -1.7‰, are beyond the limiting $\delta^{13}C$ value where the initial ^{14}C approaches zero, and the $^{14}C_o$ value for these groundwaters cannot be determined from Eq. 6.13. Groundwater samples with ^{14}C concentrations < 2 pmc and also those with $\delta^{13}C_{TDIC}$ more positive than - 1.7‰ were therefore excluded from the correction model.

The adjusted ^{14}C activities for groundwater samples of the Murray Group Aquifer are presented in Table 6.1 and range from 5.1pmc to 51pmc. The variation of ^{14}C values is probably due to the variation in recharge rates and decay of ^{14}C in the saturated zone. The estimation of the recharge rate from the adjusted ^{14}C values in the Murray Group Aquifer is discussed below.

6.4.3 Estimation of recharge rates from radiocarbon data for the Murray Group Aquifer (Zone A)

Mixing of local recharge that has relatively high ^{14}C activity and laterally flowing groundwater devoid of ^{14}C occurs via advection and/or diffusion. Generally the

advection is the dominant process of mixing when the recharge rate is 1mm > a^{-1} (Walker and Cook, 1991). Therefore, the depth of groundwater sampled from the water table is critical in assessing the adjusted ^{14}C activity data and recharge estimate in the Murray Group Aquifer.

Vogel (1966) and Bredenkamp and Vogel (1970) presented a model for quantification of recharge rates from the groundwater ^{14}C activity. Their model describes movement of ^{14}C derived from recharge coupled with radioactive decay. The schematic diagram of decay and transport of ^{14}C of groundwater in an unconfined aquifer according to this model is presented in Fig. 6.3. The decay profile varies depending on the recharge rate. The relatively high recharge rates cause faster mixing with laterally flowing groundwater. Therefore, their respective profiles will be steeper than the profiles corresponding to lower recharge rates. The transport mechanism of ^{14}C in the Bredenkamp and Vogel (1970) model is assumed to be only by advection. However Walker and Cook (1991) argued that in arid and semi-arid regions where recharge rates are <0.1mm a^{-1}, diffusion of ^{14}C in groundwater may be an important transport mechanism in the saturated zone. They incorporated the diffusion equation to the former model (mixing via advection) to account for transport of ^{14}C in saturated zone. The ^{14}C concentration as a function of depth according to Walker and Cook (1991) model is given by:

$$C = C_0\{\cosh [(1-z^*) (D^*_T)]\}\{\cosh [(D^*_T) - 0.5]\}^{-1} \qquad 6.14$$

where C_0 is the initial ^{14}C concentration of groundwater, C is its concentration at depth Z below the water table, D^*_T is despersion coefficient and expressed as:

$D^*_T = D_0 \theta \tau$

where D_0 is the diffusion coefficient for carbonate in solution ($\sim 1.2 \times 10^{-9}$ $m^2 s^{-1}$), θ is porosity of the aquifer and τ is the tortuosity.

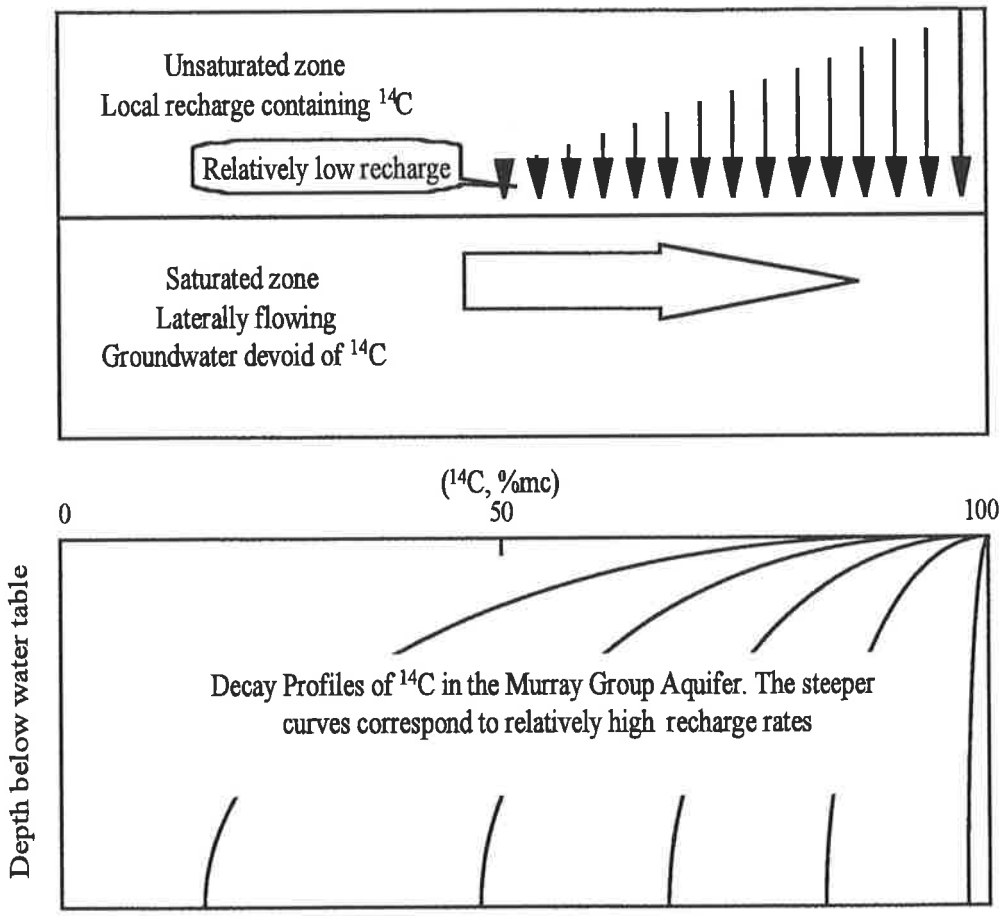

Fig. 6.3. Schematic diagram showing mixing of water derived from local recharge and laterally flowing groundwater. The concentration of ^{14}C in the groundwater is a function of the recharge rate and radioactive decay. The higher recharge rates result in steeper ^{14}C profile.

The Walker and Cook (1991) model requires an input of initial ^{14}C activity of local recharge and aquifer porosity and thickness. Generally, the saturated thickness of the Murray Group Aquifer decreases in the northern part of the study area near the River Murray as the potentiometric level decreases. The saturated thickness in the north and central part of the study area is between 60m and 100m (Reed, 1980; Barnett, 1983) and in the south is higher and range between 80m to 120m. The average value of 100m was used for the saturated aquifer thickness for the south and central part of the study area (i.e. Zone A). Porosity of the Murray Group Aquifer has been measured as 0.25 (Barnett, 1983) and there appears to be no significant variation with depth.

Using these values for the aquifer parameters and the lowest initial ^{14}C activity (51pmc) for local recharge water calculated from the correction models, the calculated ^{14}C activity as a function of depth below the water table for various recharge rates is shown in Fig. 6.4. Using this graph, recharge rates estimated from ^{14}C data range from <0.1 to 20 mm a^{-1}. Groundwater located to the south and southeast of Zone A is characterised by higher recharge rates, ranging from 1mm a^{-1} to ~ 20 mm a^{-1} while groundwater from the northern part of Zone A is characterised by lower recharge ranging from 1mm a^{-1} to values < 0.01mm a^{-1}. Higher recharge rates in the south and south east part of the study area were also elucidated by Leaney et al. (1994, 1995) based on Cl^- mass balance. They attributed higher recharge rates in this part of the study area to relatively higher rainfall of ~ 650mm a^{-1} versus 250mm a^{-1} in the north and northeast part of the study area.

Four groundwater samples that were sampled from depths of 0.5 to 15m below the water table have a corrected ^{14}C activity of < 40pmc, and two samples from just below the water table having ^{14}C < 1pmc fall out of the range of the decay profiles shown in Fig 6.4. The lowest ^{14}C activity obtained for the groundwater samples by the model considering the dissolution of carbonate minerals was 51pmc. Therefore groundwater sampled from the water table should have a minimum value of 51pmc unless other processes occurring in the unsaturated zone cause further dilution of the ^{14}C activity of soil water before it reaches the water table.

Several previous studies have also reported a lower than expected ^{14}C activity of soil water, particularly in the deep unsaturated zone in semi-arid regions (Thorstenson et al., 1983; Tyler et al., 1996). However, the causes for these low values is unknown.

The possible explanation for this phenomena could be dilution of the ^{14}C of soil water by CO_2 produced by the oxidation of old organic matter devoid of ^{14}C in the unsaturated zone. The second possible explanation is that incongruent dissolution of carbonates could be occurring in the unsaturated zone. Thus, causing an apparent depletion of the ^{14}C of soil water. There is no isotopic data from the unsaturated zone in the study area to evaluate either of these explanations. The interpretation of lower than expected ^{14}C activity of some groundwater samples must therefore await further research into processes more likely to control ^{14}C in the unsaturated zone of the Murray Group Aquifer.

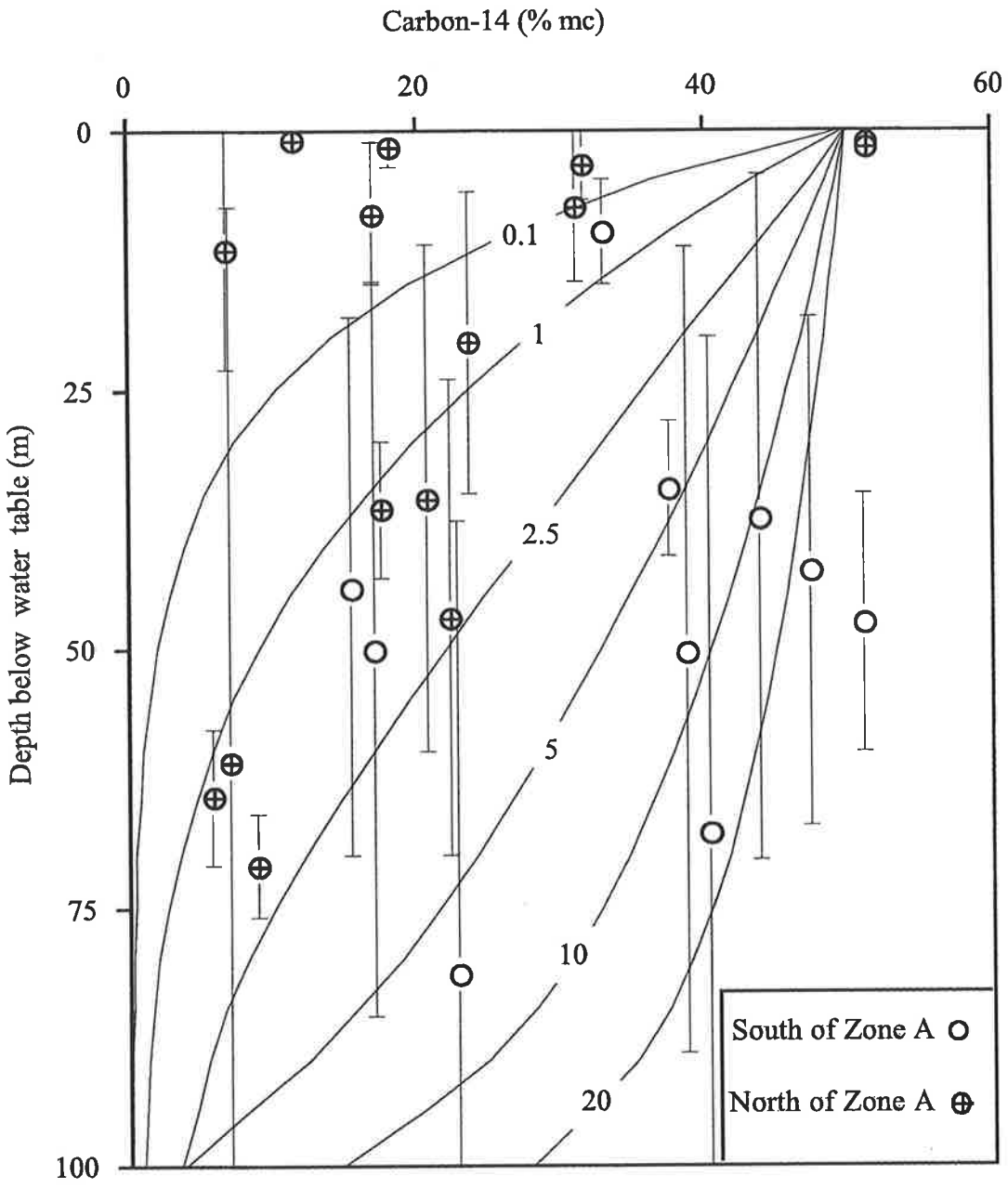

Fig 6.4 The adjusted ^{14}C data of the Murray Group Aquifer plotted with respect to depth below the water table. The error bars represent the depth of the screened intervals. The curves represent decay profiles of the ^{14}C for various recharge rates expressed in mm a^{-1}. The crossed circles represent groundwater from north part of Zone A, whereas the white circles represent groundwater in the southern part of Zone A.

6.4.4 Controls on $\delta\ ^{13}C_{TDIC}$ of the Murray Group Aquifer (Zone B)

Most of the groundwater samples from the Murray Group Aquifer in Zone B have $\delta^{13}C_{TDIC} < -14‰$ (Table 6.1). The depleted $\delta^{13}C_{TDIC}$ values can only be caused by the addition of a carbon source that is depleted in ^{13}C. Sulphur isotope data for the groundwater of both aquifers in Zone B suggests the occurrence of sulphate reduction. Bacterial sulphate reduction in groundwater results in the production of HCO_3, causing the addition of HCO_3 depleted in ^{13}C via the following reaction:

$$SO_4^{2-} + 2CH_2O \rightarrow H_2S^{\uparrow} + HCO_3^- \qquad (6.14)$$

There is no data available on the $\delta^{13}C$ composition of organic matter within the Murray Group Aquifers. However, the $\delta^{13}C$ reported for organic matter in continental and marine deposits ranges from ~ -17 ‰ to ~ -30‰ (Deines, 1980). Assuming the $\delta^{13}C$ for the organic matter has a similar range of values, the production of HCO_3^- with these depleted $\delta^{13}C$ values could explain the observed depleted $\delta^{13}C_{TDIC}$ of groundwater in the Murray Group Aquifer (Table 6.1).

The sulphur and strontium isotope data also suggests significant upward leakage from the Renmark Group Aquifer to the Murray Group Aquifer in Zone B near the River Murray. The $\delta^{13}C_{TDIC}$ of groundwater from the Renmark Group Aquifer in Zone B ranges from -14‰ to -21.6‰. Mixing of groundwater with these depleted $\delta^{13}C_{TDIC}$ water through upward leakage could be the second process that causes the depleted $\delta^{13}C_{TDIC}$ values in the Murray Group Aquifer.

6.4.5 Processes affecting ^{14}C activity of the Murray Group Aquifer (Zone B)

The measured ^{14}C activity of groundwater from the Murray Group Aquifer in Zone B ranges from 0pmc to 21pmc (Table 6.1). This variation may be caused by two competing processes; (1) variation in the recharge rate which adds water containing modern carbon to the groundwater, and (2) variation in the rate of upward leakage from the Renmark Group Aquifer which adds water devoid of ^{14}C to the Murray Group Aquifer. The higher ^{14}C activity of groundwater may indicate higher recharge rates compared with leakage from the Renmark Group Aquifer.

Mixing of groundwater devoid of ^{14}C with groundwater containing measurable amounts of ^{14}C, results in a mixture with an indeterminate age. This occurs because groundwater that contains no measurable ^{14}C could have any age > 40,000 years (practical limit of groundwater ^{14}C dating). Calculation of the age of mixture of two waters that have measurable ^{14}C from their mean ^{14}C activity also result in a large errors for age estimate. The effect of mixing of such groundwaters is schematically shown in Fig (6.5).

The age of mixture of modern and 40,000 year old water calculated from the mixing equation is represented by a solid line. The age of the same mixture was calculated by the radiocarbon decay equation from the mean ^{14}C activity of the two waters and is represented by a solid curve. It is apparent from Fig. 6.5 that the error associated with the age calculated from the mean activity of the end members in some cases is greater

than the real age of the mixture. Accordingly upward leakage of groundwater devoid of ^{14}C from the Renmark Group Aquifer in Zone B with groundwater containing measurable amounts of ^{14}C of the Murray Group Aquifer results in groundwater with an indeterminate age. Therefore, the ^{14}C activity of groundwater of the Murray Group Aquifer can only be used qualitatively to highlight the significance of local recharge to the Murray Group Aquifer in this part of the study area.

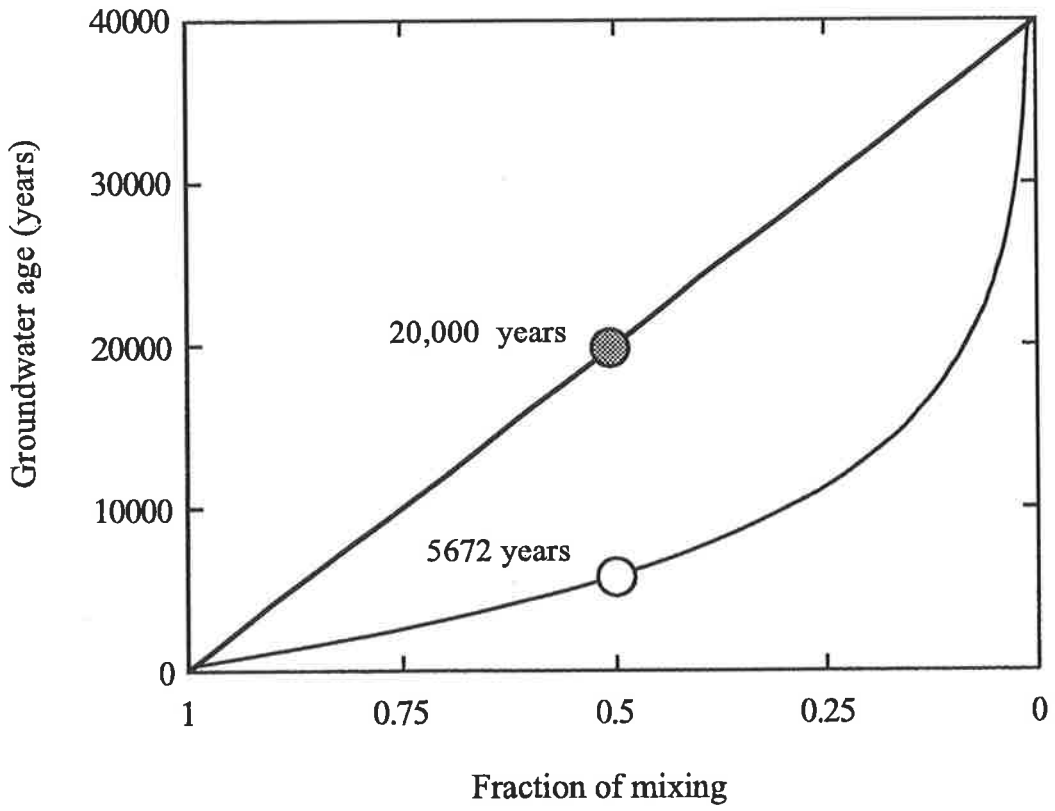

Fig. 6.5. Relationship between mixing proportion of groundwaters with different ^{14}C activity and age of the final solution. The two circles represent ages of a final solution that results from mixing of modern water (0 age) and 40,000 years old in the same proportion. The age of the mixture calculated by two component mixing equation (gray circle) is three times higher than the age calculated from the mean ^{14}C activity of the two waters by the decay equation (Eq.6.1) (white circle).

6.5 Conclusions

Information provided by ^{14}C data of the groundwater in the Murray and Renmark Group aquifers contributes significantly to the main theme of this study and suggests that:

1. Local recharge is the only source of measurable ^{14}C concentration in the Murray Group Aquifer. This conclusion supports previous conceptual models obtained from the chemical and isotopic composition of groundwater in the Murray Group Aquifer indicating the significance of local recharge relative to lateral flow.

2. In addition to radiocarbon decay, congruent and incongruent dissolution of carbonate minerals in the Murray Group Aquifer is the primary cause for apparent dilution of the ^{14}C activity of groundwater. Based on the geochemical correction models, measured ^{14}C data was adjusted for the effect of the above mentioned processes and recharge rates were estimated in various parts of the study area.

3. Recharge rates in the south and southeastern part of Zone A range from 1 mm a^{-1} to 20 mm a^{-1} and are higher than estimated recharge rates in the northern part which are <1mm^{-1}. The higher recharge rates in the south and southeast corroborate those estimated by Leaney et al. (1995, 1996) using Cl^- mass balance.

4. Mixing of groundwater of the Renmark Group Aquifer devoid in ^{14}C via upward leakage with the Murray Group Aquifer containing ^{14}C, results in a mixture with

indeterminate age. However, the variation of ^{14}C activity for groundwater of the Murray Group Aquifer in Zone B suggests the significance of two competing processes, namely local recharge and upward leakage from the Renmark Group Aquifer.

CHAPTER 7

Concluding Remarks

7.1 Regional groundwater chemistry

In the semi-arid southwestern Murray Basin, where potential evaporation exceeds precipitation, the small fraction of precipitation that contributes to groundwater recharge is concentrated in the soil zone and can produce highly saline recharge water. Introduction of the highly saline recharge water to the groundwater particularly, in the northern part of the study area, causes the current chemical composition and salinity in the Murray Group Aquifer. Mixing of saline groundwater from the Renmark Group Aquifer through upward leakage also plays a major role in the current distribution of major ions and contributes to the increase in salinity of the Murray Group Aquifer in the north and northeastern part of the study area.

Rock-water interaction in groundwaters which have a residence time of > 40,000 years can also be a factor in modifying the chemical composition of groundwater along the inferred flow lines in the Murray and Renmark Group Aquifers. Generally the long residence time is caused by the low relief and the low groundwater hydraulic gradient, which in turn provide sufficient contact time for aquifer minerals-groundwater reactions.

Quantifying the above mentioned long term processes is not possible by conventional hydrological and hydrochemical investigations. For example, chemical composition and stable isotopes of water molecules in both aquifers are similar, and although they can be used as primary investigation tools to provide information on distribution of major chemical ions and the sources of water molecules in groundwater. They are not useful as groundwater mixing tracers in the Murray Basin. Therefore, this thesis explored the usefulness of alternative environmental isotopes such as $\delta^{34}S$ and $\delta^{18}O$ of dissolved sulphate and $^{87}Sr/^{86}Sr$ ratio of dissolved strontium in groundwater as tracers of inter-aquifer mixing and rock water interaction in the semi-arid region of the southeastern Murray Basin.

7.2 $\delta^{34}S$ and $\delta^{18}OSO_4^{2-}$

The $\delta^{34}S$ and $\delta^{18}O$ composition of dissolved sulphate primarily depends on the sources of sulphate and the redox condition of groundwater. Because the redox conditions and mineralogy within the Murray and Renmark Group aquifers are different, the $\delta^{34}S$ and $\delta^{18}O$ of dissolved sulphate in the groundwater in each of the aquifers also exhibits different $\delta^{34}S$ and $\delta^{18}OSO_4^{2-}$ signatures. In the highly reducing Renmark Group Aquifer, both $\delta^{34}S$ and $\delta^{18}O$ of residual dissolved sulphates are relatively enriched due to bacterial sulphate reduction. In contrast, the $\delta^{34}S$ and $\delta^{18}OSO_4^{2-}$ values in the relatively aerobic Murray Group Aquifer are dominated by sulphate having $\delta^{34}S$ and $\delta^{18}OSO_4^{2-}$ values similar to atmospheric aerosol isotope values, plus the mineralisation of organic sulphur from the soil zone during recharge. These distinctive signatures are

used as tools in identifying upward leakage from the Renmark Group Aquifer, as well as the relative importance of vertical input of sulphate via diffuse local recharge.

In the absence of significant anthropogenic emission of sulphur to the atmosphere, the measured $\delta^{34}S$ isotope of dissolved sulphate in groundwater from the Murray Group Aquifer generally reflects the original $\delta^{34}S$ of the rainfall that recharges the aquifer. Therefore, in the absence of sulphate minerals (e.g. gypsum) in the aquifer matrix, the $\delta^{34}S$ of dissolved sulphate in aerobic aquifers can be an effective tool in revealing information on rainfall patterns over relatively long periods of time. Previous investigations (Chivas, 1991) in Western Australia also found that the $\delta^{34}S$ of gypsum precipitated from surface waters reflects the $\delta^{34}S$ of sulphate pool in rainfall over a regional scale.

$\delta^{34}S$ and $\delta^{18}OSO_4^{2}$ composition in the Murray and Renmark Group aquifers from the northern part of the study area suggests the occurrence of upward leakage south of the River Murray. However, the amount of upward leakage from the Renmark Group Aquifer could not be quantified because the $\delta^{34}S$ and $\delta^{18}OSO_4^{2-}$ composition of the Murray Group Aquifer could not be explicitly identified due to possible sulphate reduction after mixing. Hence the resulting isotopic character of the mixture through upward leakage from the Renmark Group Aquifer could not be interpreted with respect to the original end-members by application of the two-component mixing model.

7.3 $^{87}Sr/^{86}Sr$ ratio

Because strontium ions can substitute for Ca ions in carbonate minerals, their concentration and isotopic signature in groundwater from the carbonate Murray Group Aquifer can be used to identify the source of Sr and the extent of water-rock interactions. The relatively long groundwater residence time provides ideal environments for chemical and isotopic equilibrium between the carbonate Murray Group Aquifer matrix and groundwater. Furthermore, unlike $\delta^{34}S$ and $\delta^{18}OSO_4^{2-}$ isotopes of dissolved sulphate, the $^{87}Sr/^{86}Sr$ ratios of groundwater are not affected by the redox conditions of the groundwater. Therefore, the distinct $^{87}Sr/^{86}Sr$ ratio of the groundwater in chemical and isotopic equilibrium with carbonate rocks in the Murray Group Aquifer is successfully used to estimate upward leakage from the Renmark Group Aquifer.

The $^{87}Sr/^{86}Sr$ ratio revealed that in addition to the upward leakage of groundwater from the Renmark Group Aquifer, significant amounts of water from the Murray Group Aquifer in the northern part of the study area are derived from local recharge. This observation could not be corroborated by $\delta^{34}S$ and $\delta^{18}OSO_4^{2-}$ composition because the $\delta^{34}S$ and $\delta^{18}OSO_4^{2-}$ signature of local recharge following mixing with laterally flowing groundwater were altered by bacterial sulphate reduction in the Murray Group Aquifer. However, introduction of local recharge to groundwater in the northern part of the study area was supported by measurable amounts of ^{14}C.

7.4 Carbonate-solution interaction

$^{87}Sr/^{86}Sr$ ratios of groundwater from the Murray Group Aquifer in the south and central part of the study suggest that dissolution of carbonate minerals occurs as soil water percolates through the unsaturated zone. A model of the $^{87}Sr/^{86}Sr$ and Sr/Ca ratio relationship also suggests the occurrence of incongruent dissolution of carbonate minerals following the addition of local recharge to the laterally flowing groundwater. This conclusion is further supported by $\delta^{13}C$ data, in that total inorganic carbon dissolved in groundwater becomes progressively more enriched in ^{13}C as the $^{87}Sr/^{86}Sr$ ratio decreases towards that of carbonates in the aquifer matrix.

Dissolution of carbonate minerals has a direct effect on ^{14}C content of groundwater due to the addition of dead carbon from the aquifer matrix that causes dilution of the ^{14}C content. The measured ^{14}C data therefore, was adjusted to account for congruent and incongruent reactions using appropriate models. The adjusted ^{14}C data then was converted to estimate recharge rates in the south and central part of the study area, using the model presented by Walker and Cook (1991). The ^{14}C age estimation for groundwater of the Murray Group Aquifer in the northern part of the study area (mixing zone) was not possible because of upward leakage of groundwater from the Renmark Group Aquifer that is devoid of ^{14}C. The measurable amount of ^{14}C in the Murray Group Aquifer results in a mixture with indeterminate water age.

Finally, this thesis has highlighted the effectiveness of the application of multiple isotopic techniques in identifying long-term processes that affect the chemical

composition of groundwater in semi arid regions. The application of strontium, sulphur, oxygen, and carbon isotopes are useful because they integrate the spatial and temporal variability of large-scale heterogeneous aquifers. They also provide an insight into the temporal variation of the physical and chemical processes that occur in the aquifer in the context of solute concentration and transport.

Conventional hydrogeological investigations, which deal with aquifer characteristics and present day water level measurements alone, are not adequate in quantifying the effect of these processes on the current distribution of major chemical ions and groundwater salinity. The information obtained from the isotopes also has major management implications because it provides information on important parameters such as recharge rates, source and origin of solutes, groundwater residence time, etc....

For example, some of the models developed in the study area with important management implications were; (i) the models showing spatial distribution of groundwater salinity caused by natural processes over long periods of time that were not induced by human activities, (ii) Quantification of the extent of inter-aquifer mixing (one of the major sources of salinity in the Murray Group Aquifer in the northern part of the study area) and, (iii) Estimation of groundwater residence time and recharge rate to the Murray Group Aquifer.

Furthermore, study has contributed towards a better understanding of how the systematic of various isotopic techniques work in regional aquifers of semi-arid environments, and has also demonstrated the added value of the information obtained from the isotopes in redefining and validating the conventional hydrological model of the study area.

Appendix 1

Results of XRD analysis

The results of XRD analysis of the rock samples taken from cuttings of drill holes (M33, M34, M50, M52, M64) penetrating the Murray and Renmark Group Aquifers are shown according to their depth from the surface. The 2θ angle increases from left to right on the horizontal scale and the intensity of the diffracted peaks above the background is given by the vertical scale. The major peaks corresponding to the dominant minerals in the rock samples are also shown for each spectrum.

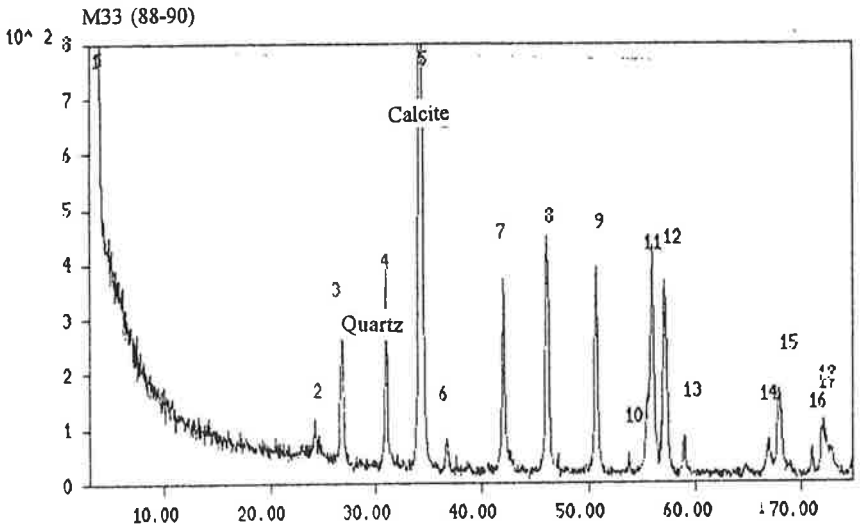
M33 (88-90)
10^ 2
Calcite
Quartz
10.00
20.00
30.00
40.00
50.00
60.00
70.00

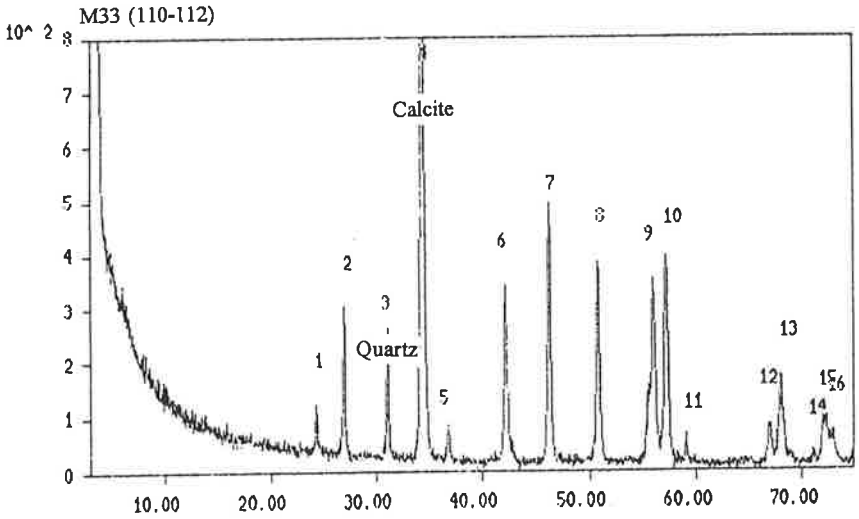
M33 (110-112)
10^ 2
Calcite
Quartz
10.00
20.00
30.00
40.00
50.00
60.00
70.00

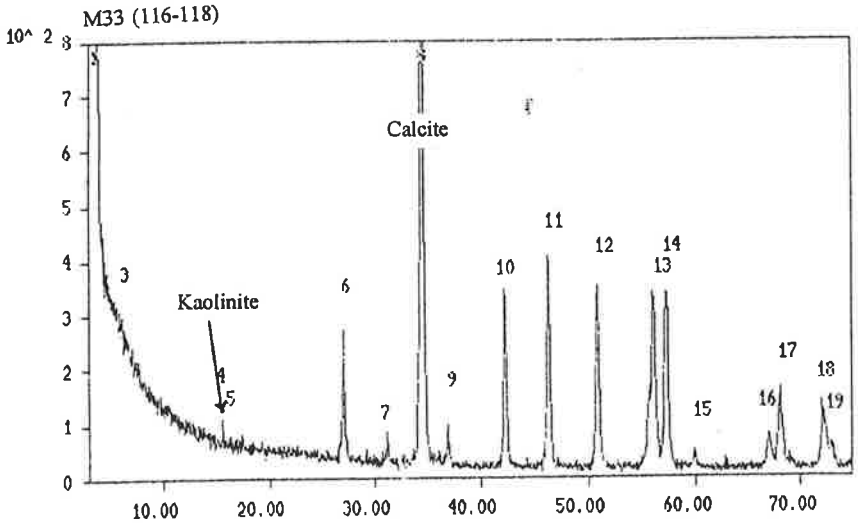
M33 (116-118)
10^ 2
Calcite
Kaolinite
10.00
20.00
30.00
40.00
50.00
60.00
70.00

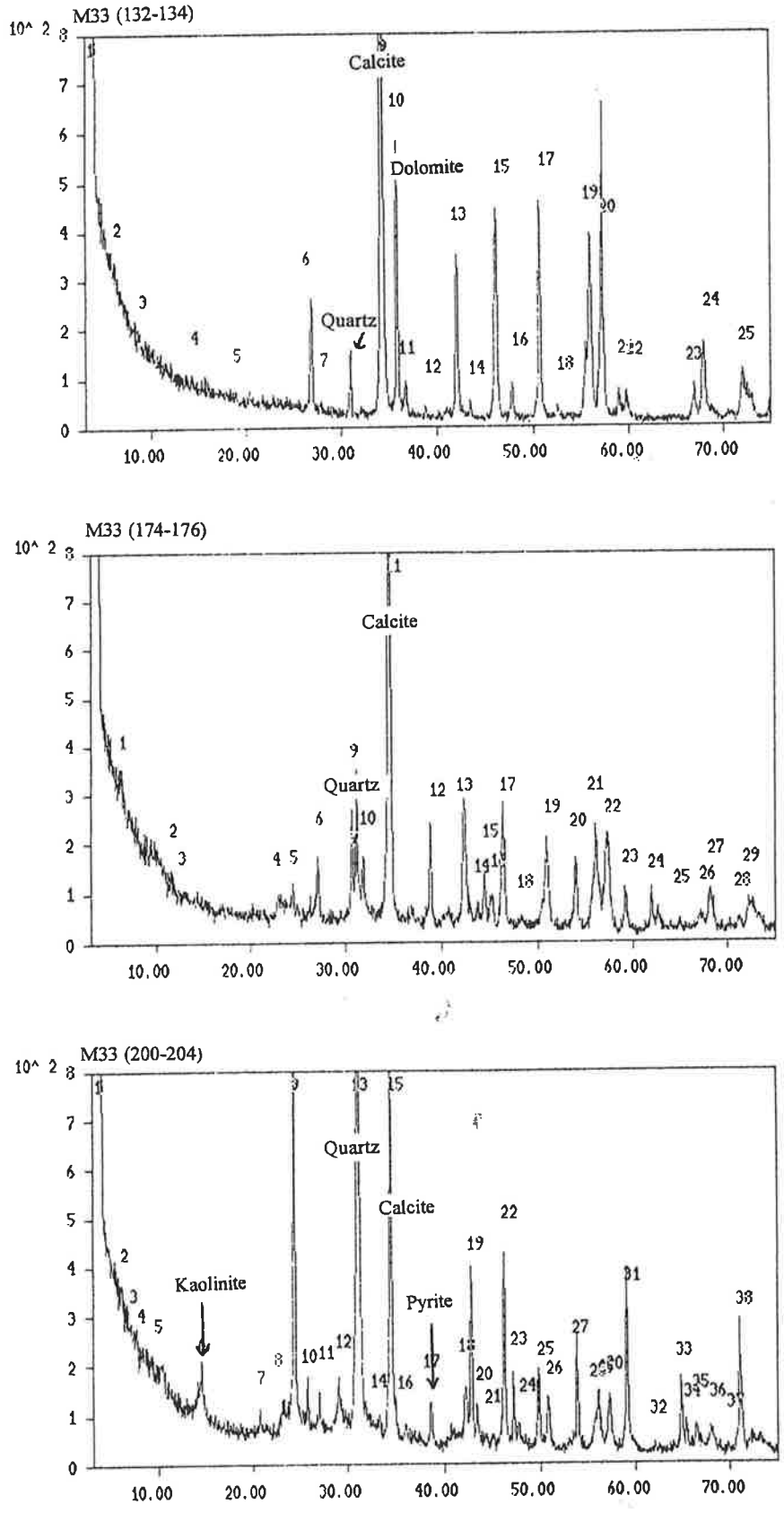
M33 (132-134)
10^ 2
Calcite
Dolomite
Quartz
M33 (174-176)
10^ 2
Calcite
Quartz
M33 (200-204)
10^ 2
Quartz
Calcite
Kaolinite
Pyrite
10.00
20.00
30.00
40.00
50.00
60.00
70.00

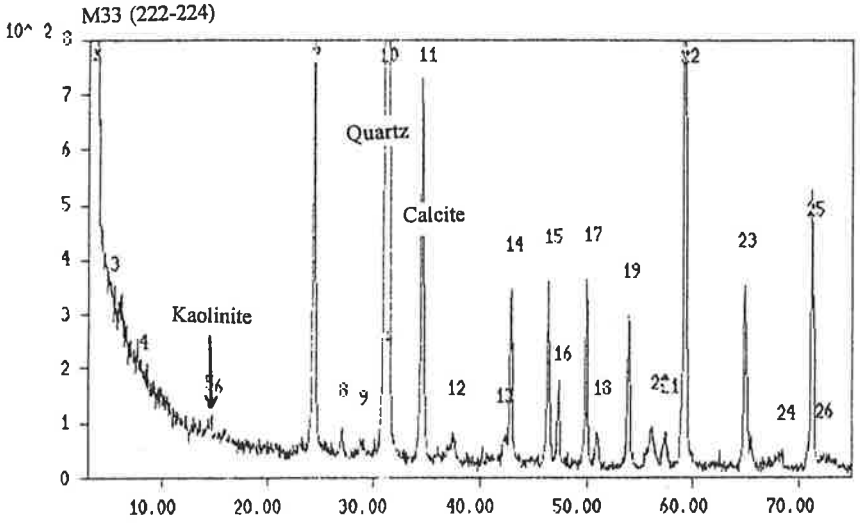
M33 (222-224)
10^ 2
Quartz
Calcite
Kaolinite
10.00
20.00
30.00
40.00
50.00
60.00
70.00

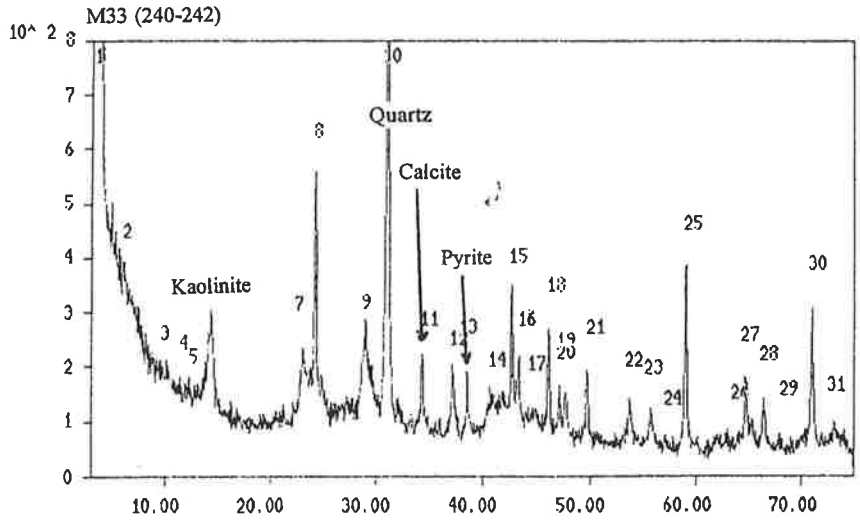
M33 (240-242)
10^ 2
Quartz
Calcite
Pyrite
Kaolinite
10.00
20.00
30.00
40.00
50.00
60.00
70.00

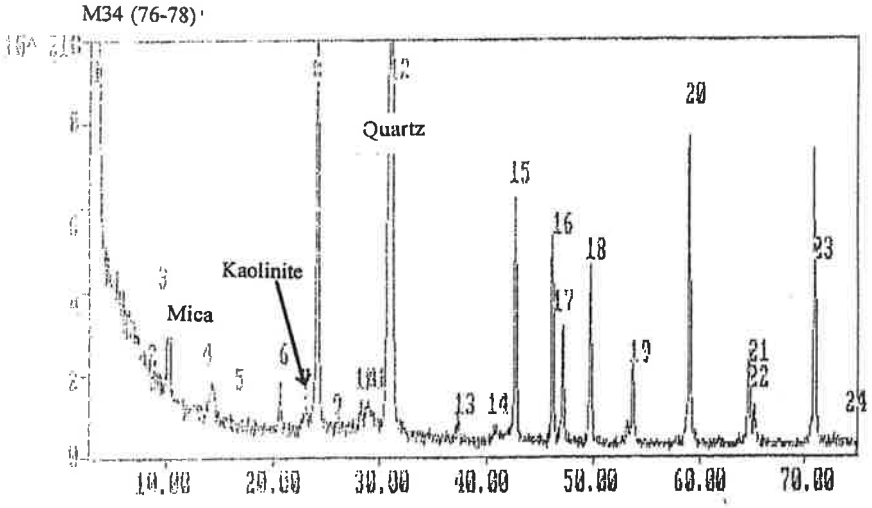
M34 (76-78)
Quartz
Kaolinite
Mica
10.00
20.00
30.00
40.00
50.00
60.00
70.00

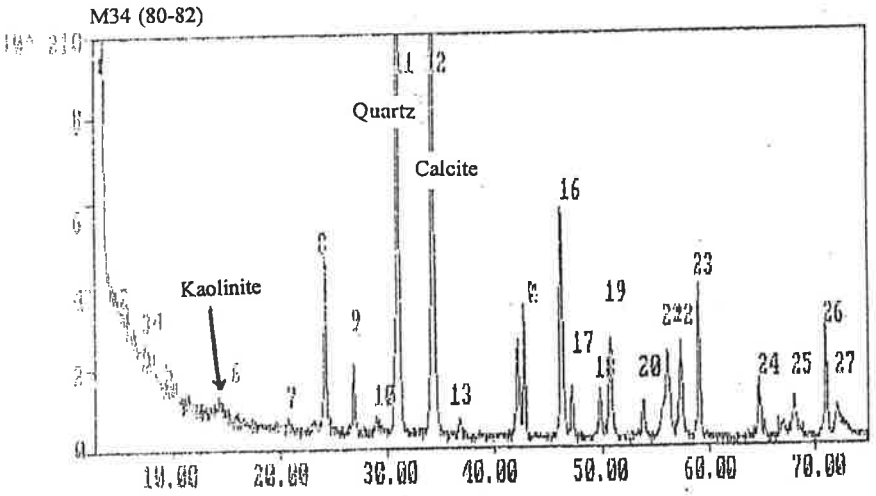
M34 (80-82)
Quartz
Calcite
Kaolinite
10.00
20.00
30.00
40.00
50.00
60.00
70.00

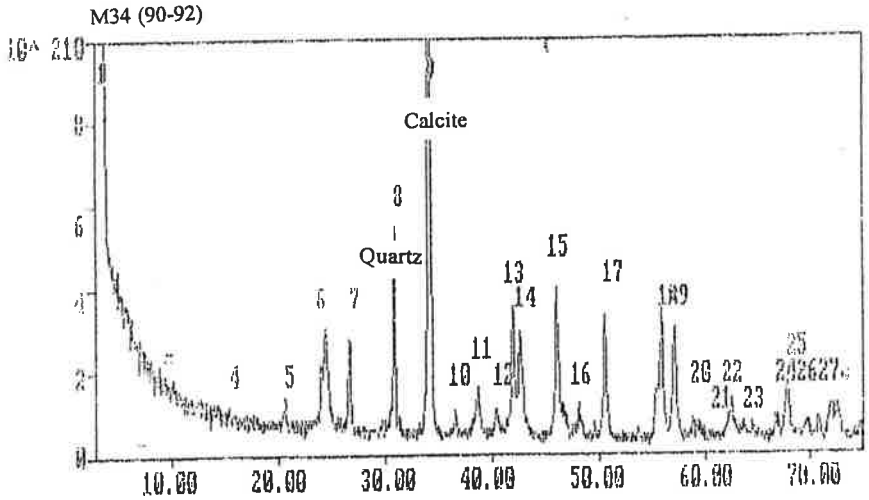
M34 (90-92)
Calcite
Quartz
10.00
20.00
30.00
40.00
50.00
60.00
70.00

M34 (102-104)

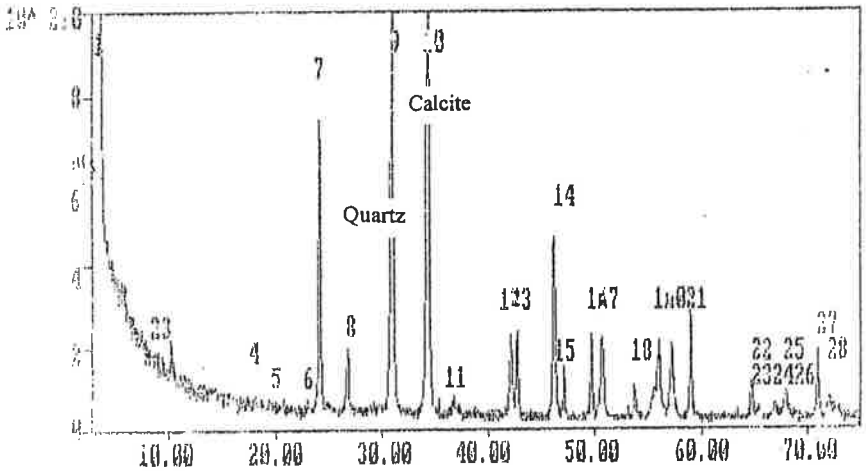

M34 (122-124)

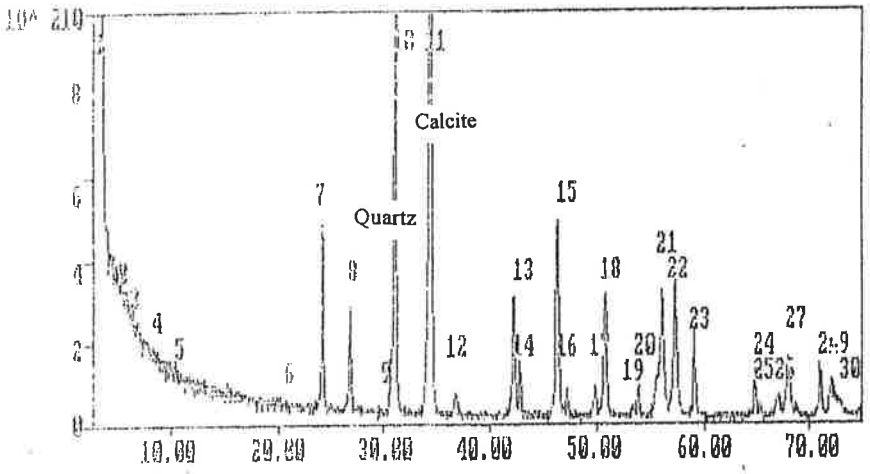

M34 (142-144)

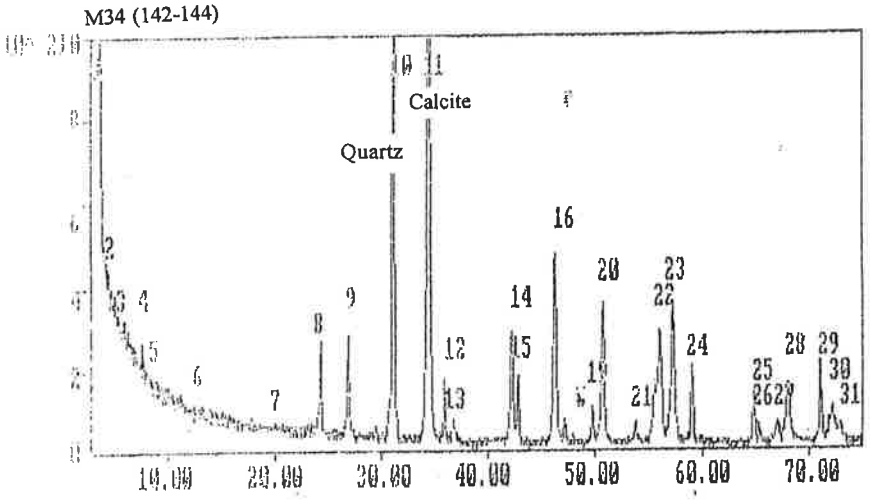

M34 (162-164)

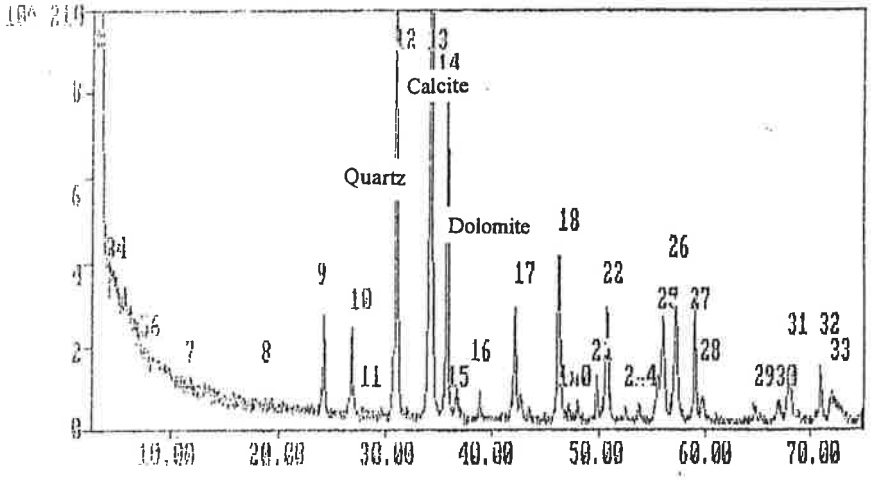

M34 (172-174)

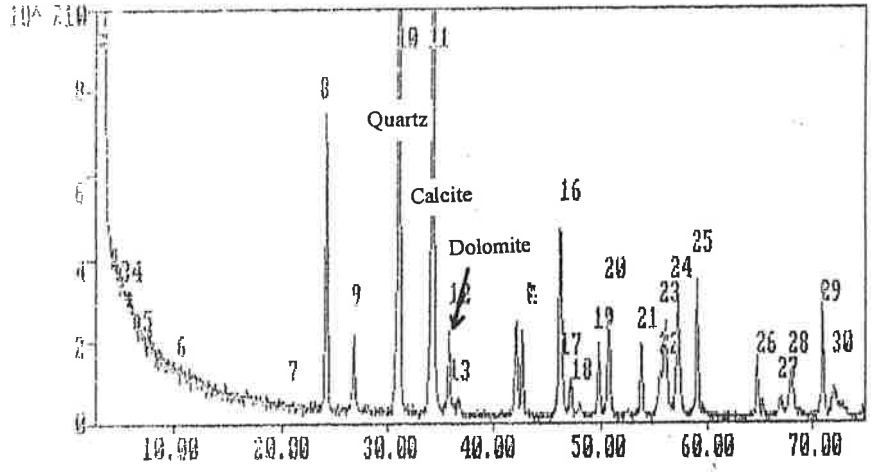

M34 (180-182)

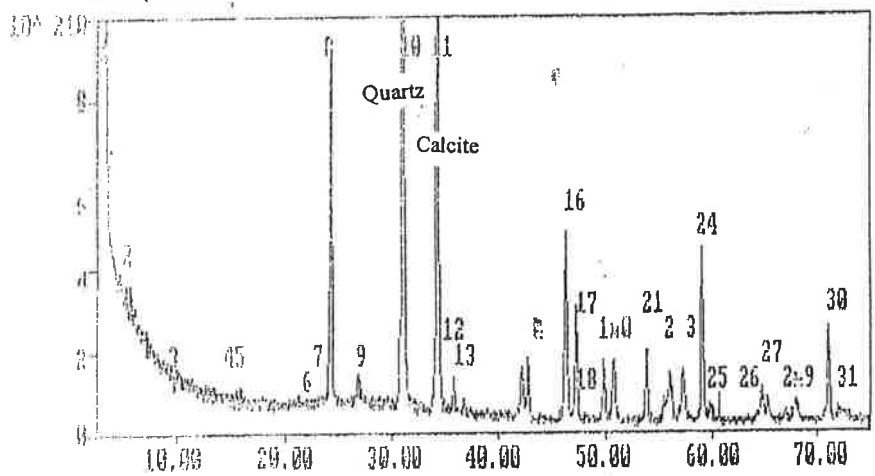

M34 (192-194)

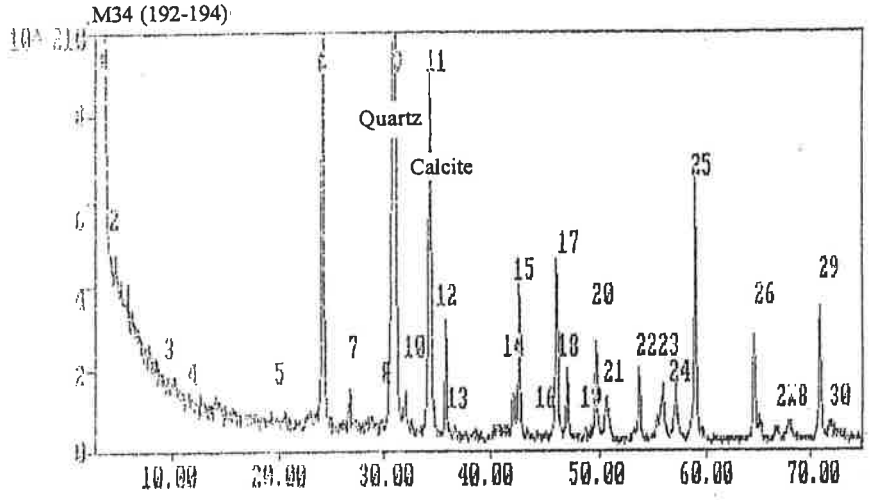

M34 (202-204)

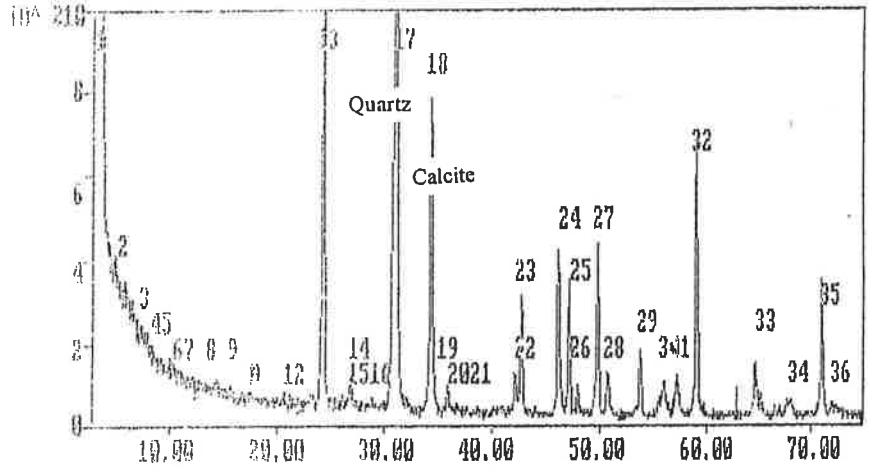

M34 (230-232)

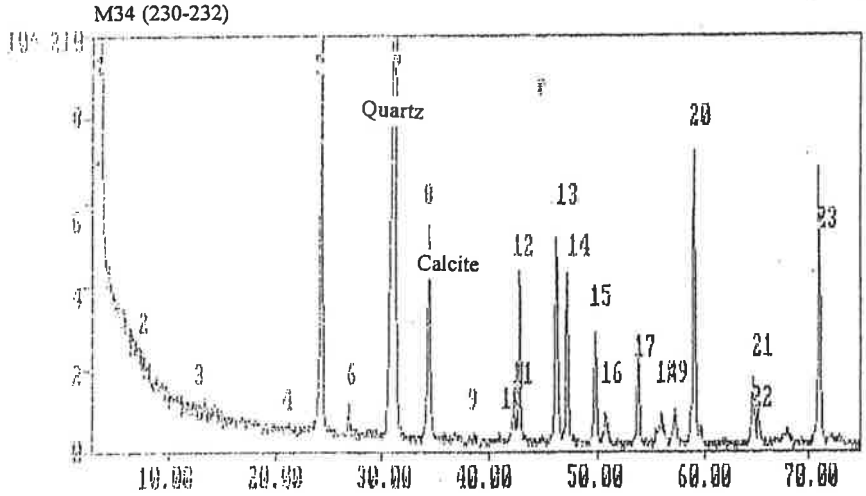

M50 (62-64)

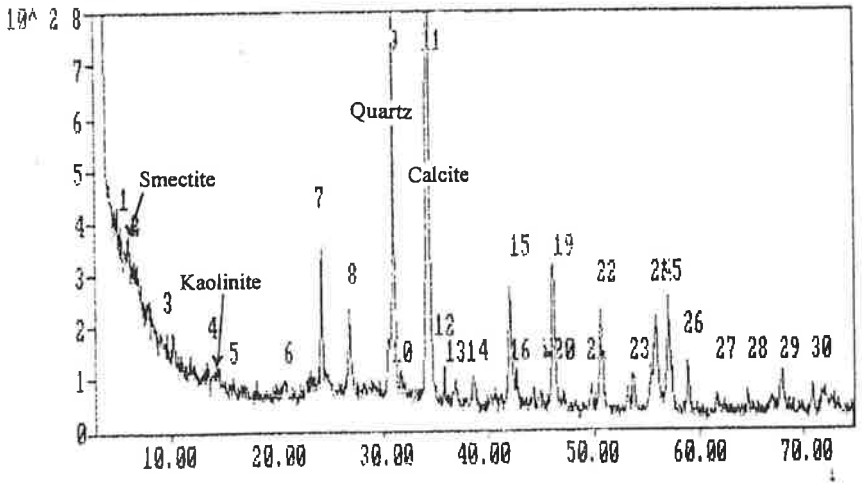

M50 (76-78)

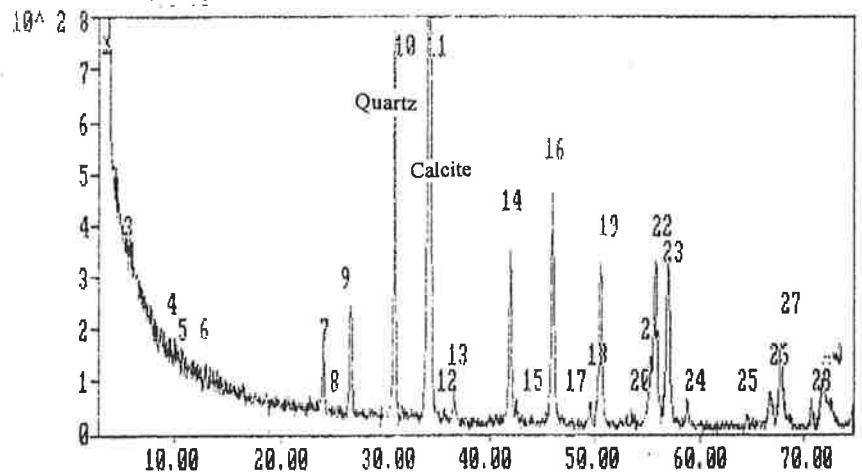

M50 (104-106)

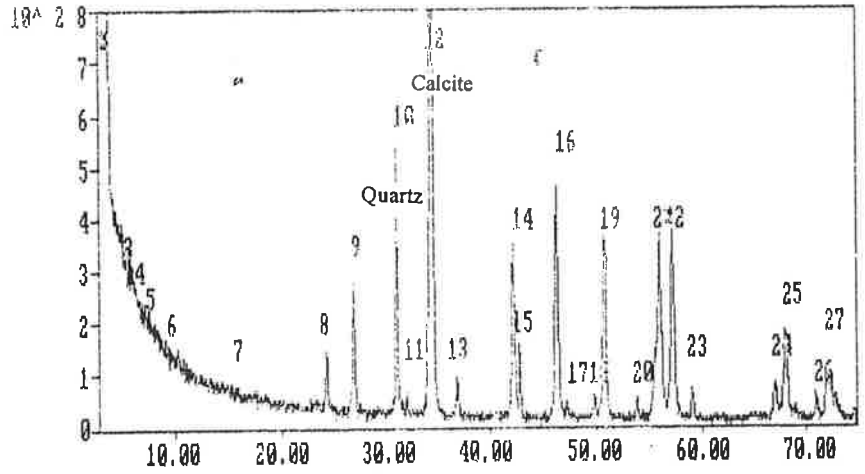

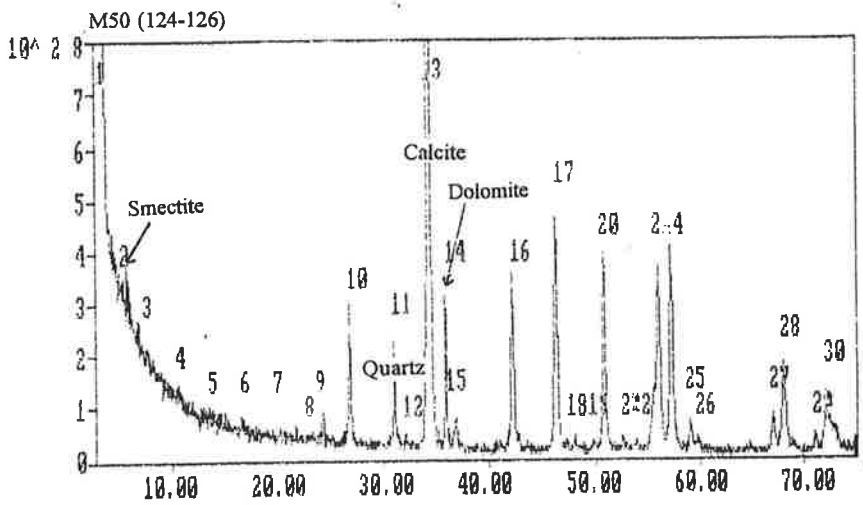
M50 (124-126)
10^ 2
Smectite
Calcite
Dolomite
Quartz
10.00
20.00
30.00
40.00
50.00
60.00
70.00

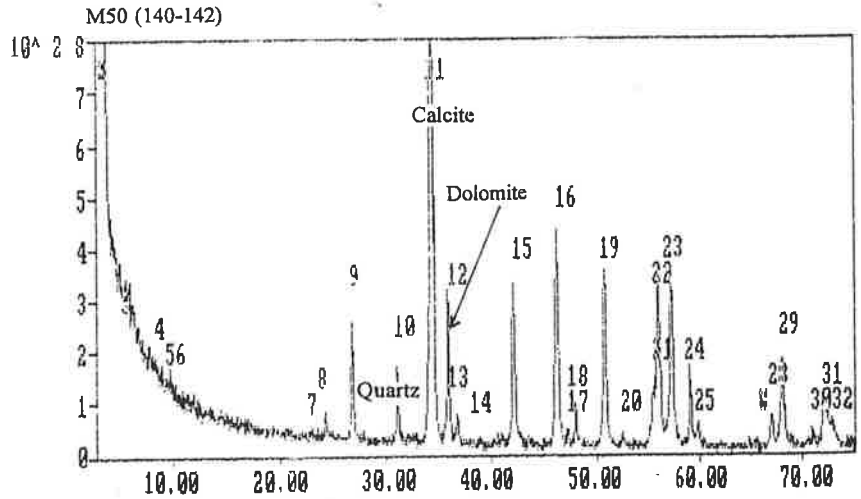
M50 (140-142)
10^ 2
Calcite
Dolomite
Quartz
10.00
20.00
30.00
40.00
50.00
60.00
70.00

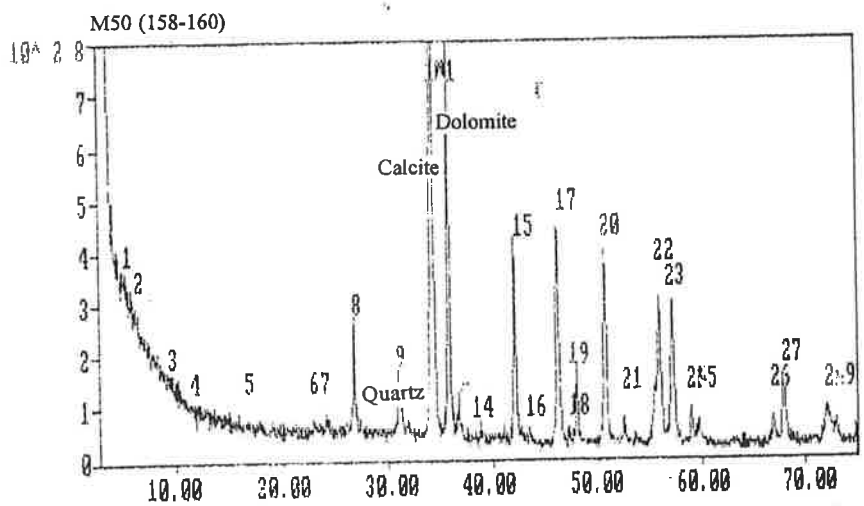
M50 (158-160)
10^ 2
Dolomite
Calcite
Quartz
10.00
20.00
30.00
40.00
50.00
60.00
70.00

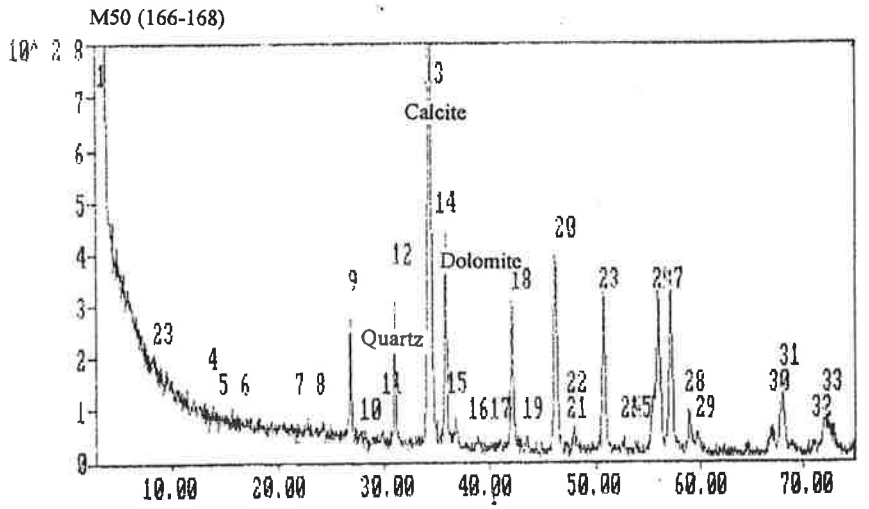
M50 (166-168)
Calcite
Dolomite
Quartz
10.00
20.00
30.00
40.00
50.00
60.00
70.00

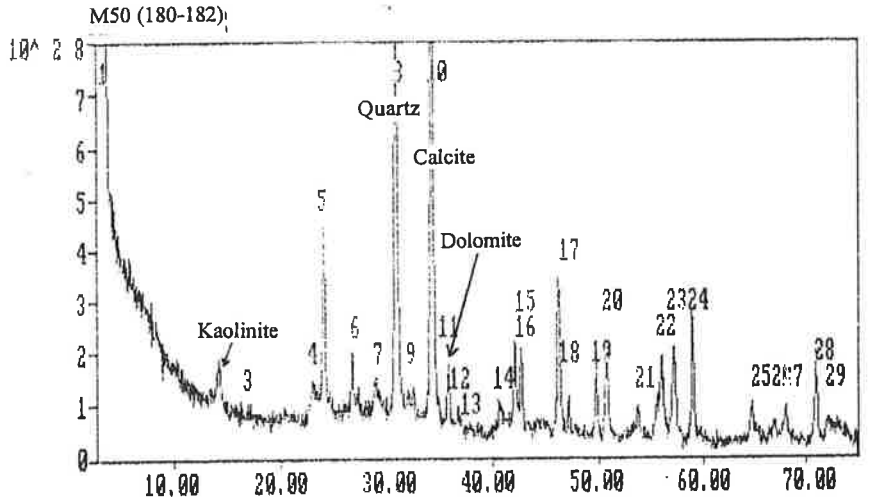
M50 (180-182)
Quartz
Calcite
Dolomite
Kaolinite
10.00
20.00
30.00
40.00
50.00
60.00
70.00

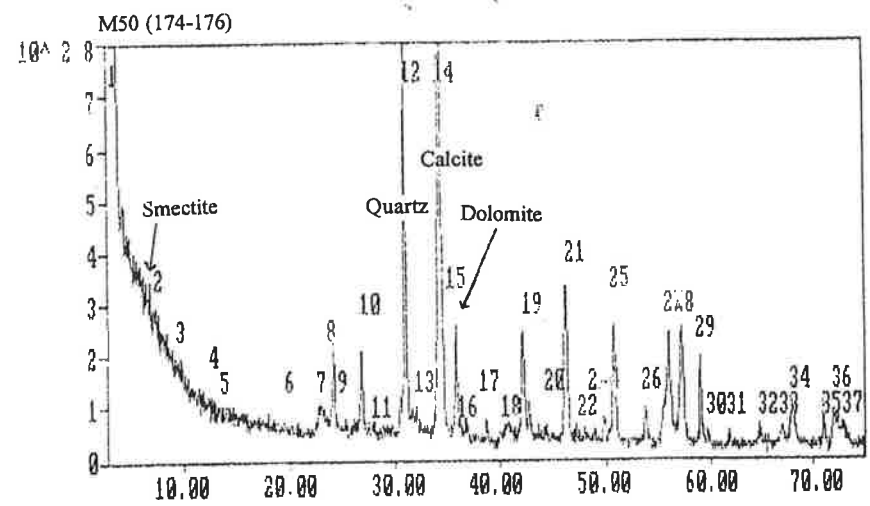
M50 (174-176)
Calcite
Smectite
Quartz
Dolomite
10.00
20.00
30.00
40.00
50.00
60.00
70.00

M50 (194-196)

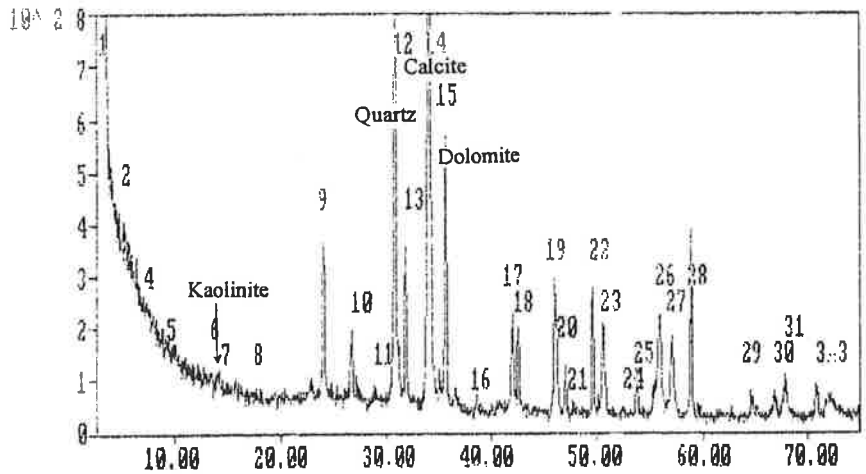

M50 (222-224)

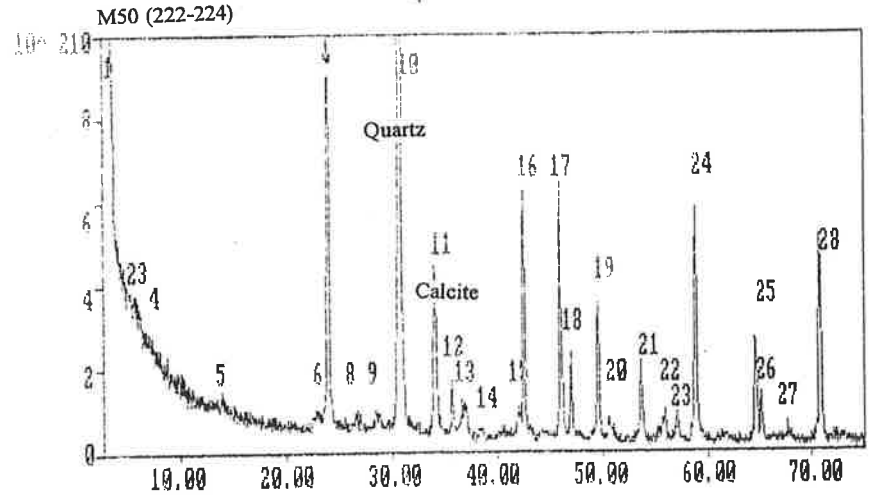

M50 (202-204)

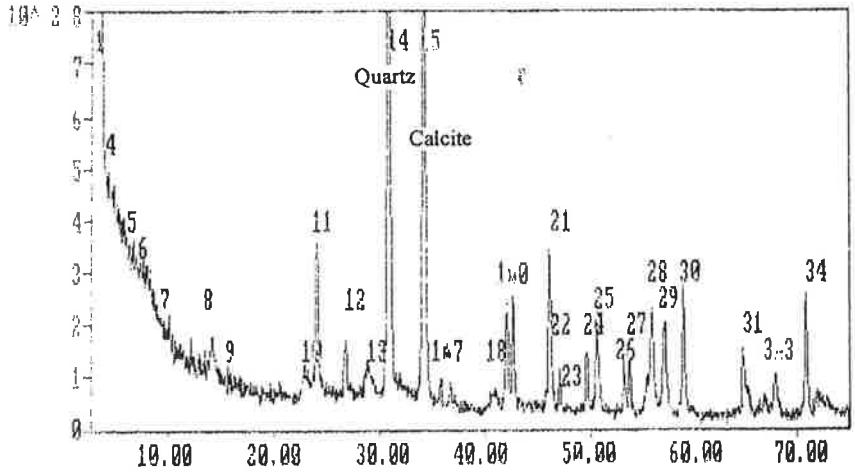

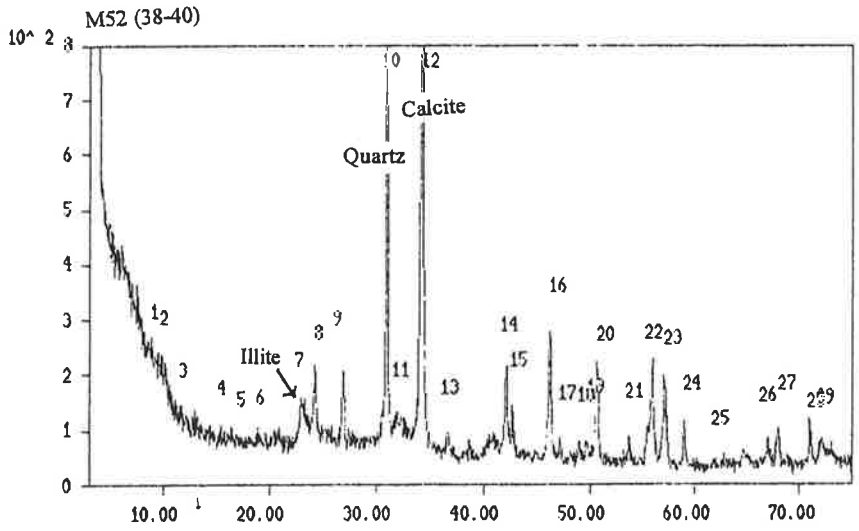
M52 (38-40)
10^ 2
Calcite
Quartz
Illite
10.00
20.00
30.00
40.00
50.00
60.00
70.00

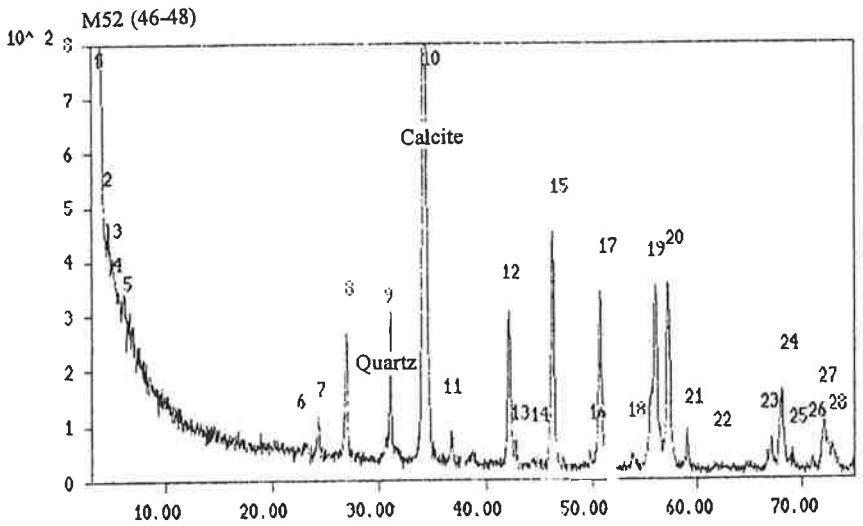
M52 (46-48)
10^ 2
Calcite
Quartz
10.00
20.00
30.00
40.00
50.00
60.00
70.00

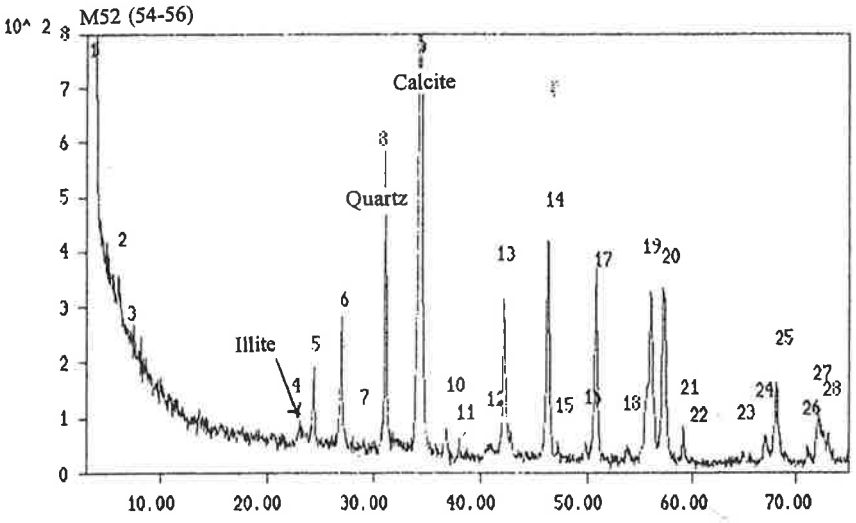
M52 (54-56)
10^ 2
Calcite
Quartz
Illite
10.00
20.00
30.00
40.00
50.00
60.00
70.00

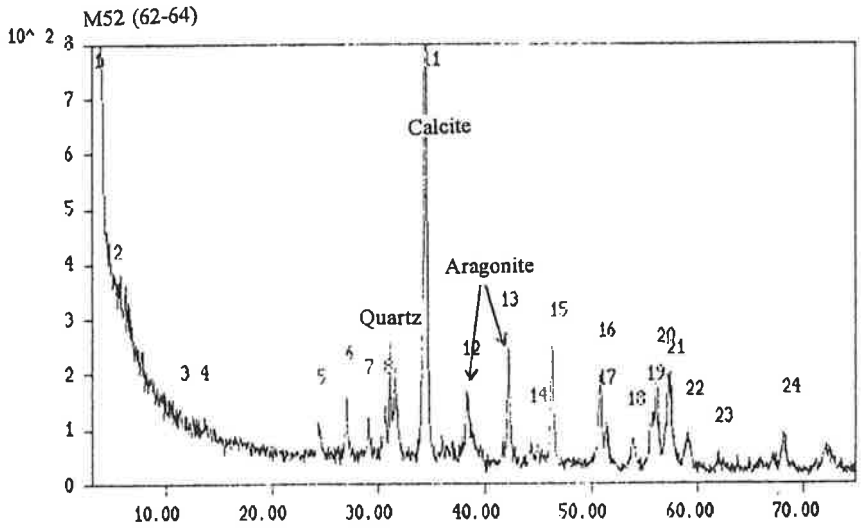
M52 (62-64)
10^ 2
Calcite
Aragonite
Quartz
10.00
20.00
30.00
40.00
50.00
60.00
70.00

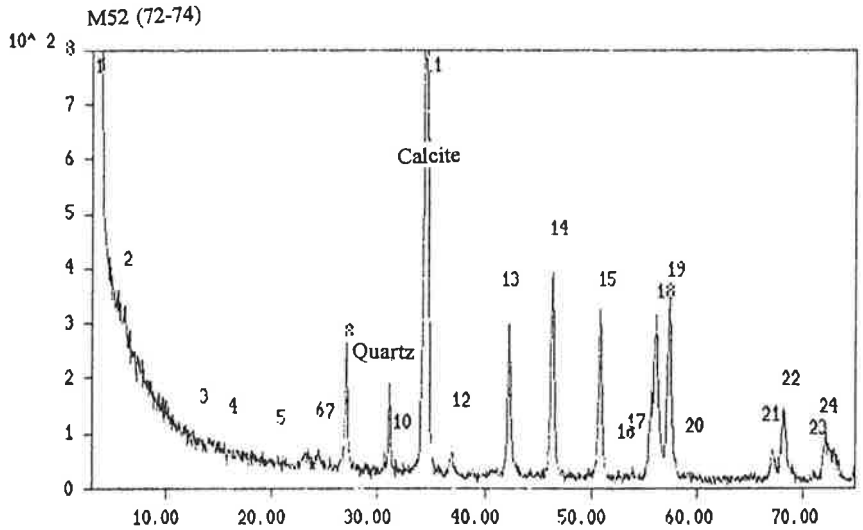
M52 (72-74)
10^ 2
Calcite
Quartz
10.00
20.00
30.00
40.00
50.00
60.00
70.00

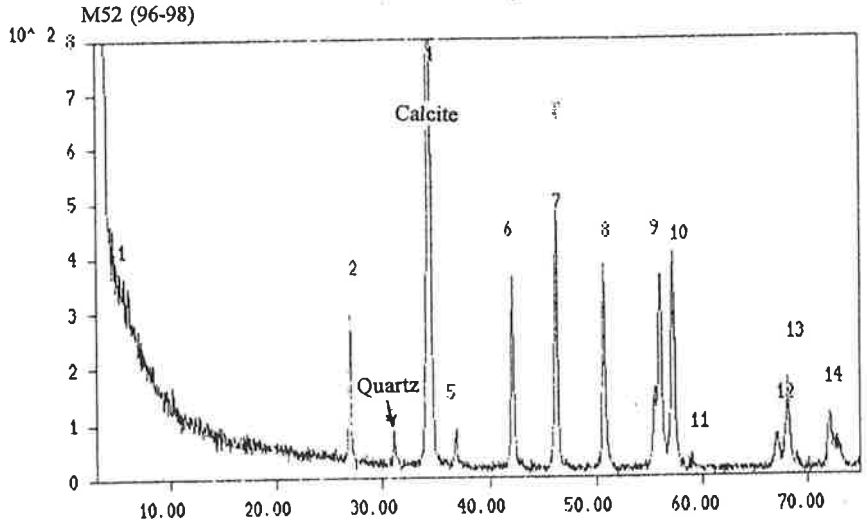
M52 (96-98)
10^ 2
Calcite
Quartz
10.00
20.00
30.00
40.00
50.00
60.00
70.00

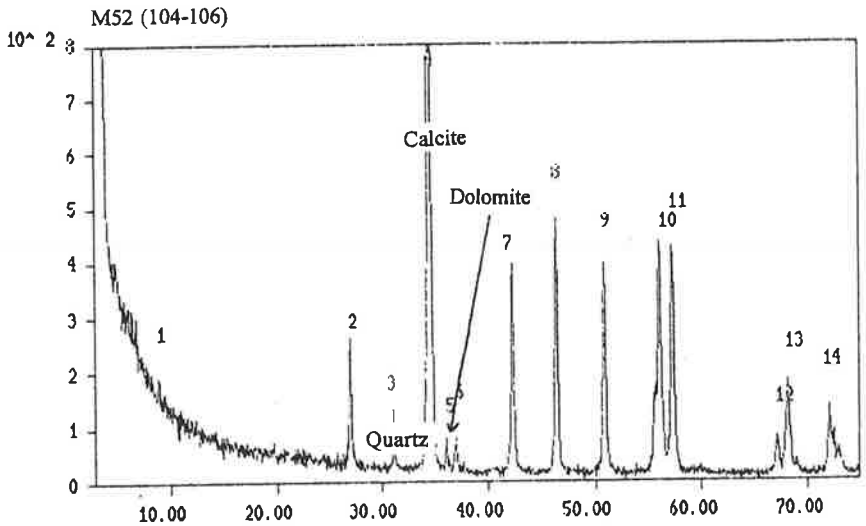
M52 (104-106)
10^ 2
Calcite
Dolomite
Quartz
10.00
20.00
30.00
40.00
50.00
60.00
70.00

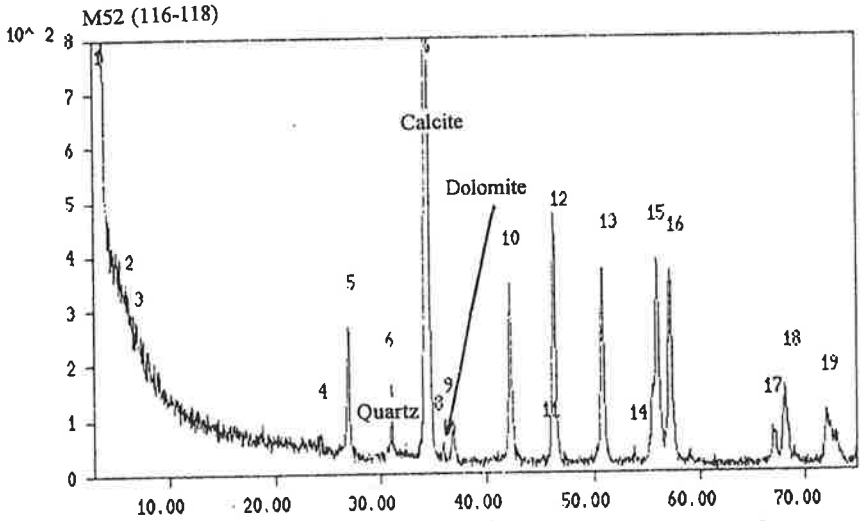
M52 (116-118)
10^ 2
Calcite
Dolomite
Quartz
10.00
20.00
30.00
40.00
50.00
60.00
70.00

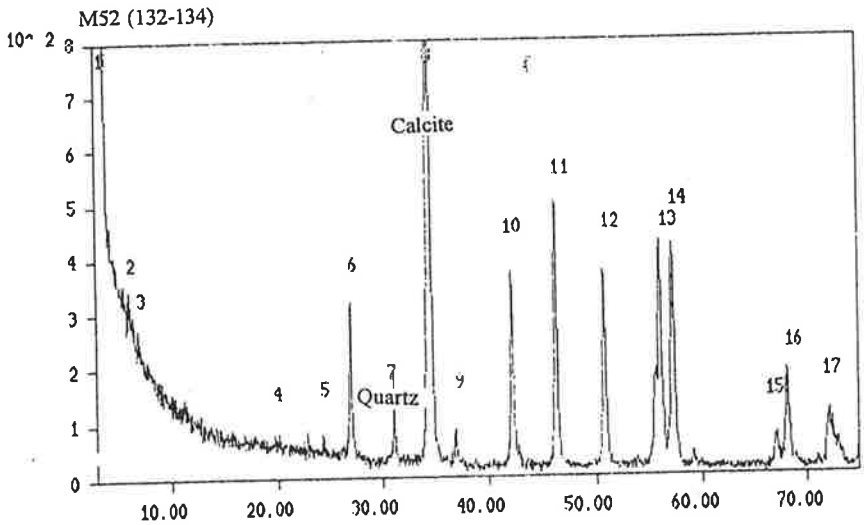
M52 (132-134)
10^ 2
Calcite
Quartz
10.00
20.00
30.00
40.00
50.00
60.00
70.00

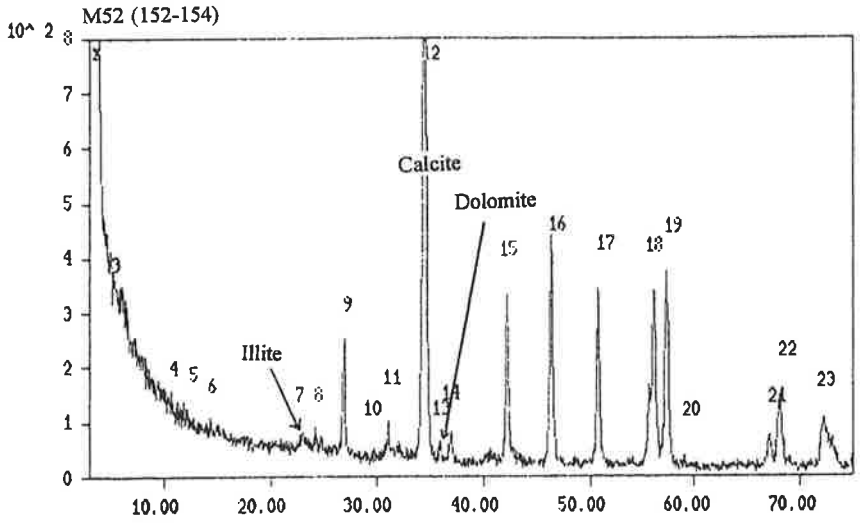
M52 (152-154)
10^ 2
Calcite
Dolomite
Illite
10.00
20.00
30.00
40.00
50.00
60.00
70.00

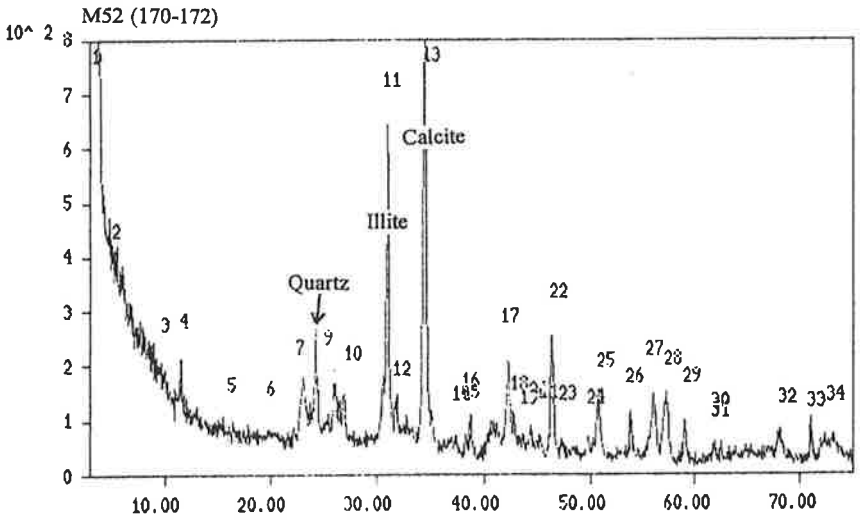
M52 (170-172)
10^ 2
Calcite
Illite
Quartz
10.00
20.00
30.00
40.00
50.00
60.00
70.00

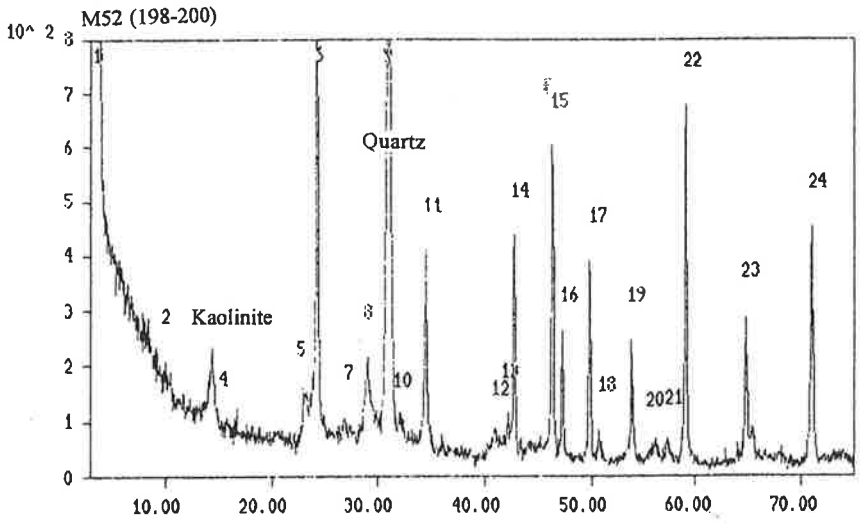
M52 (198-200)
10^ 2
Quartz
Kaolinite
10.00
20.00
30.00
40.00
50.00
60.00
70.00

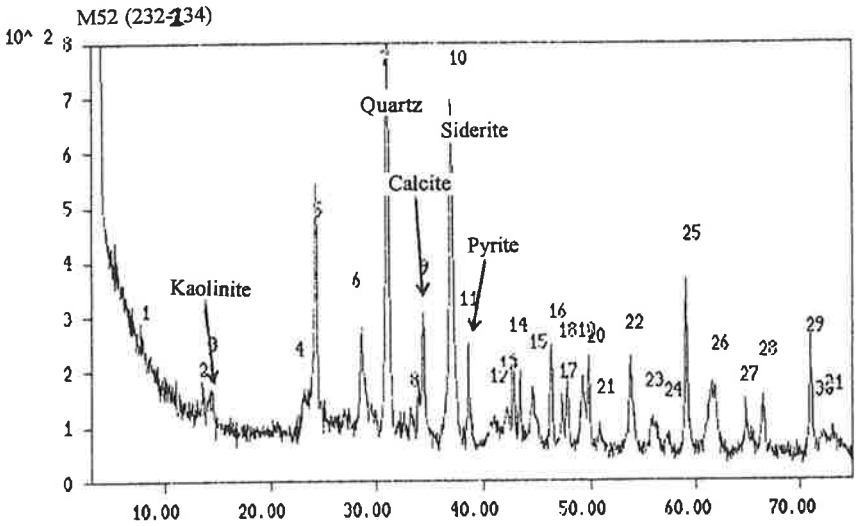
M52 (232-234)
10^ 2
Quartz
Siderite
Calcite
Pyrite
Kaolinite
10.00
20.00
30.00
40.00
50.00
60.00
70.00

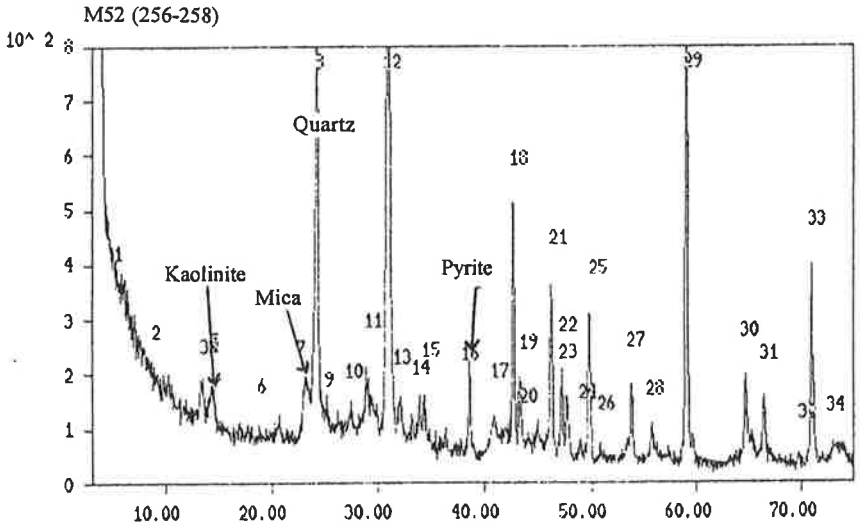
M52 (256-258)
10^ 2
Quartz
Kaolinite
Mica
Pyrite
10.00
20.00
30.00
40.00
50.00
60.00
70.00

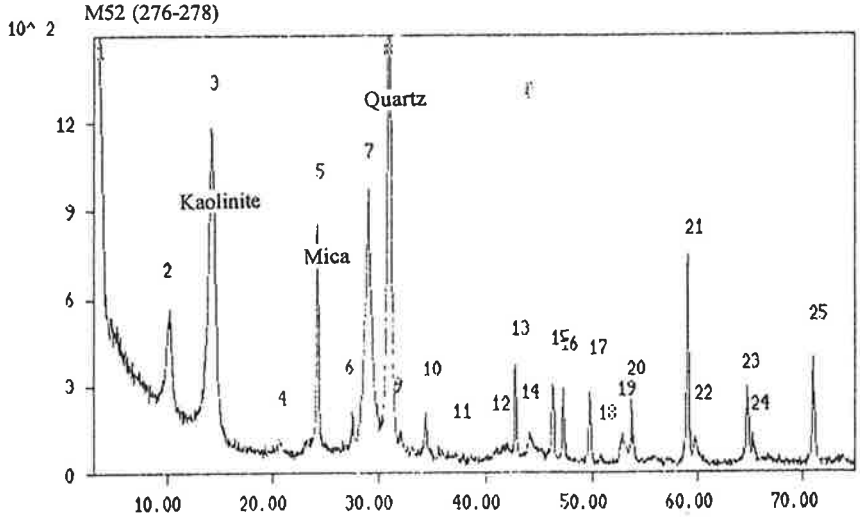
M52 (276-278)
10^ 2
Quartz
Kaolinite
Mica
10.00
20.00
30.00
40.00
50.00
60.00
70.00

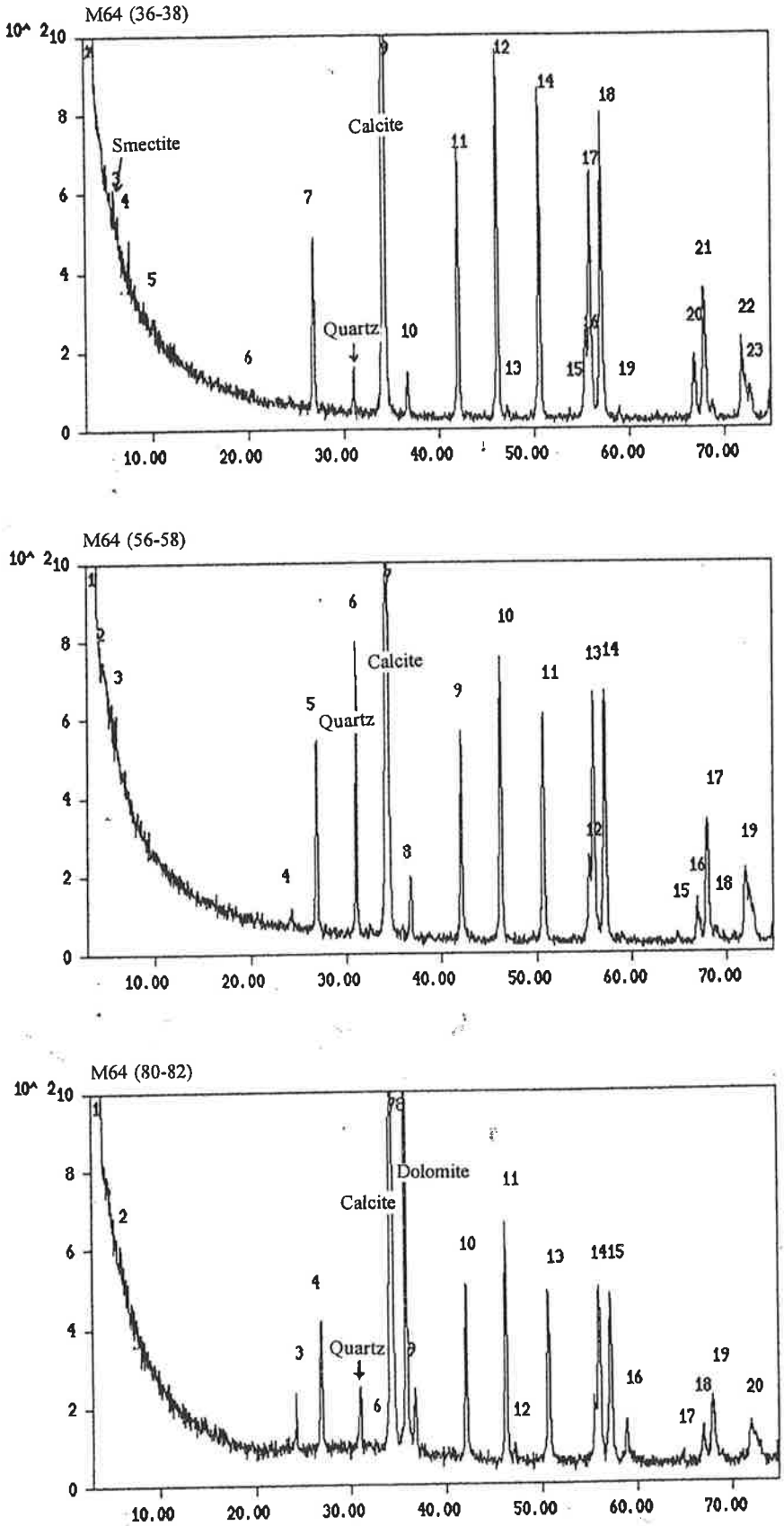
M64 (36-38)
10^ 2 10
Smectite
Calcite
Quartz
M64 (56-58)
10^ 2 10
Calcite
Quartz
M64 (80-82)
10^ 2 10
Dolomite
Calcite
Quartz
10.00
20.00
30.00
40.00
50.00
60.00
70.00

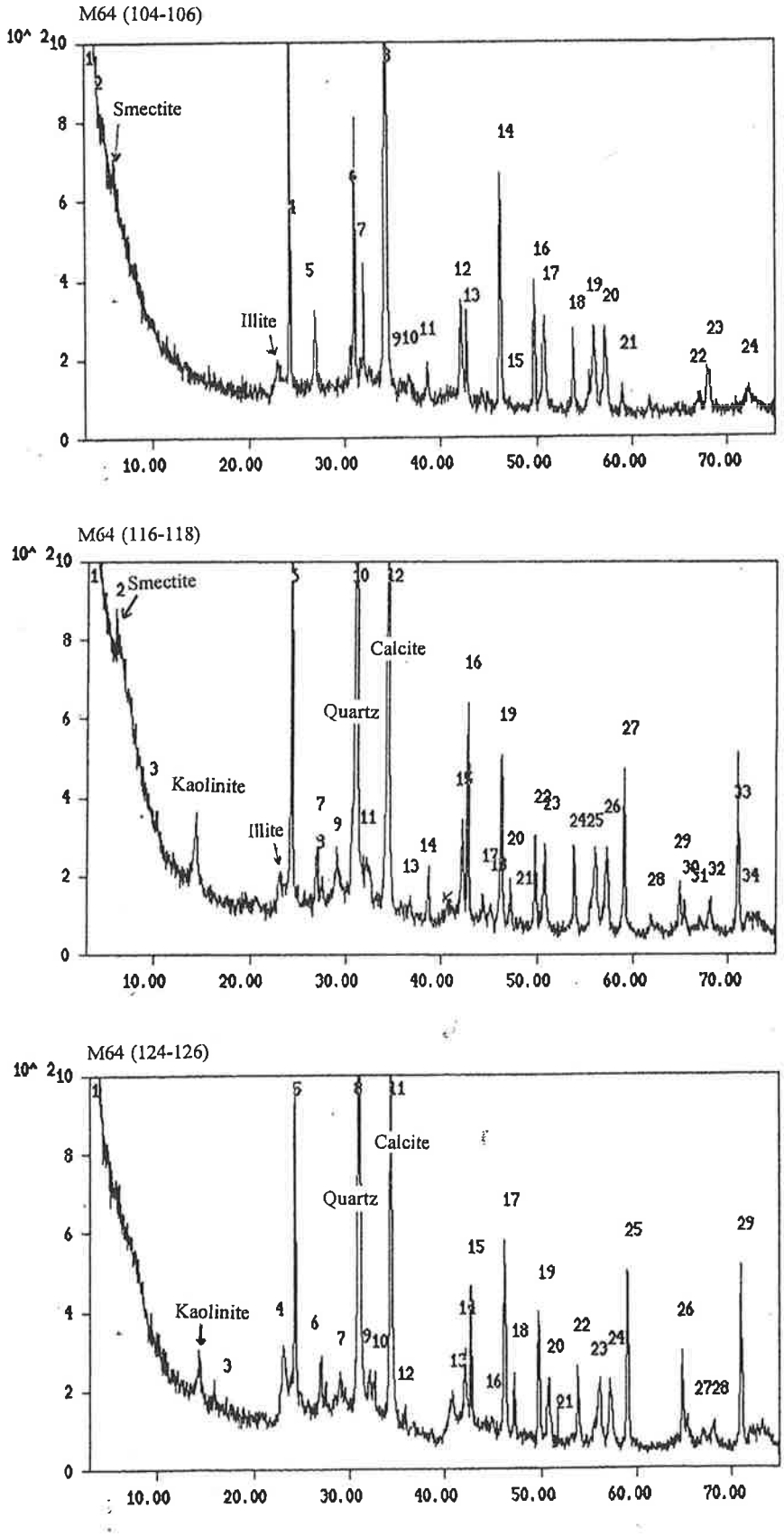
M64 (104-106)
10^ 2
Smectite
Illite
M64 (116-118)
Smectite
Kaolinite
Illite
Quartz
Calcite
M64 (124-126)
Kaolinite
Quartz
Calcite
10.00
20.00
30.00
40.00
50.00
60.00
70.00

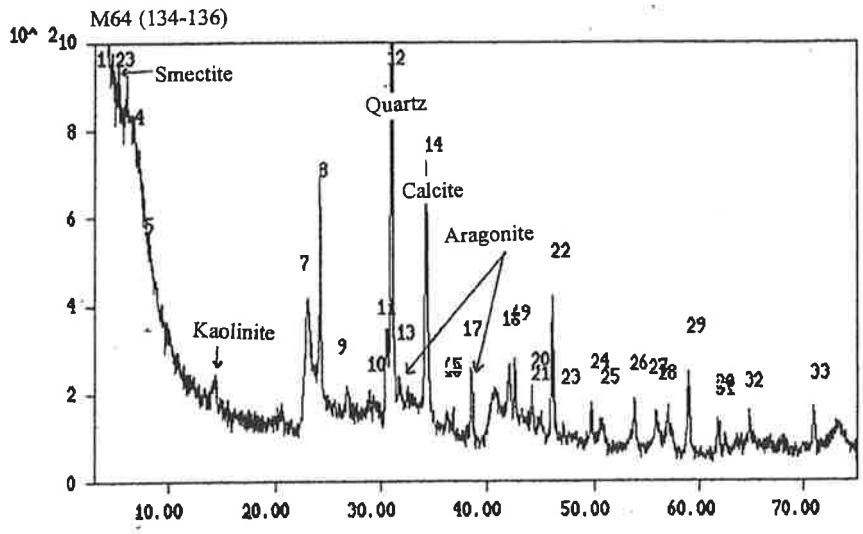
M64 (134-136)
10^ 2
Smectite
Quartz
Calcite
Aragonite
Kaolinite
10.00
20.00
30.00
40.00
50.00
60.00
70.00

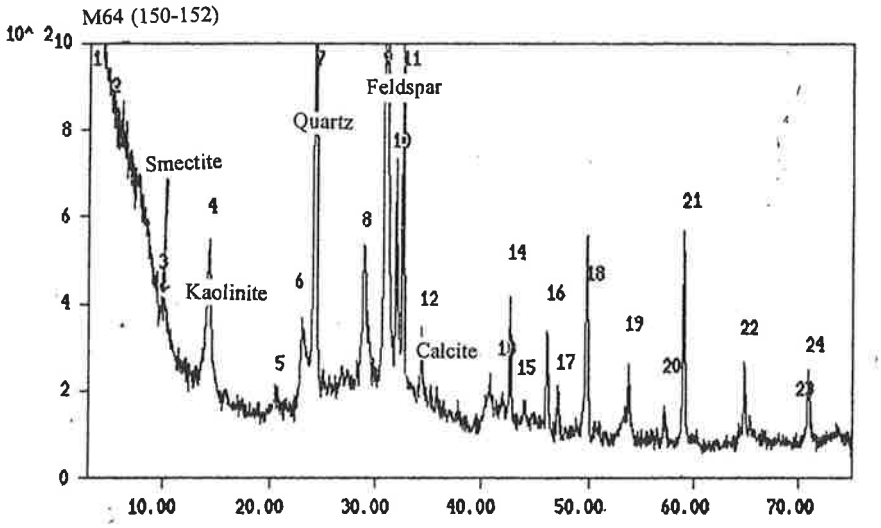
M64 (150-152)
10^ 2
Feldspar
Quartz
Smectite
Kaolinite
Calcite
10.00
20.00
30.00
40.00
50.00
60.00
70.00

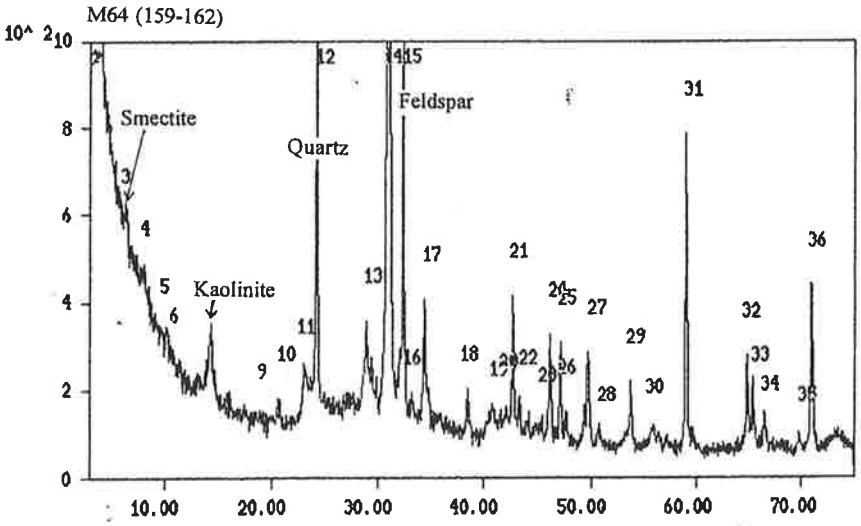
M64 (159-162)
10^ 2
Feldspar
Smectite
Quartz
Kaolinite
10.00
20.00
30.00
40.00
50.00
60.00
70.00

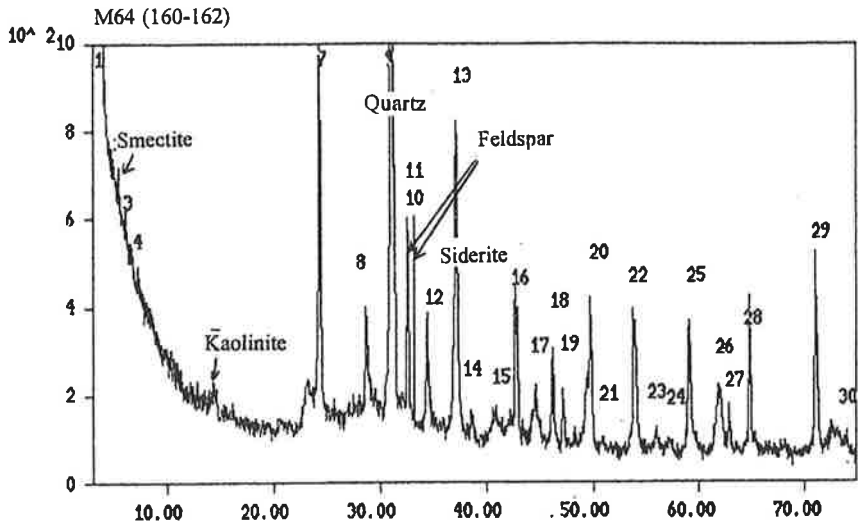
M64 (160-162)
10^ 2
Smectite
Quartz
Feldspar
Siderite
Kaolinite
10.00
20.00
30.00
40.00
50.00
60.00
70.00

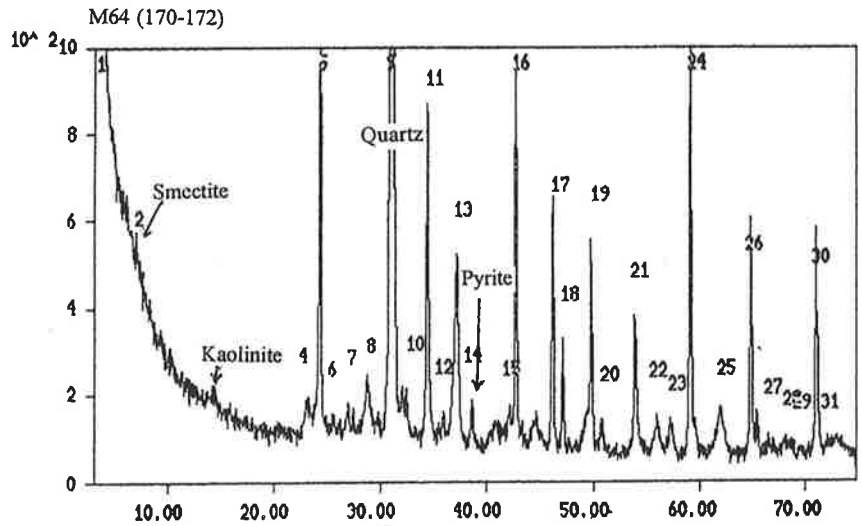
M64 (170-172)
10^ 2
Smectite
Quartz
Pyrite
Kaolinite
10.00
20.00
30.00
40.00
50.00
60.00
70.00

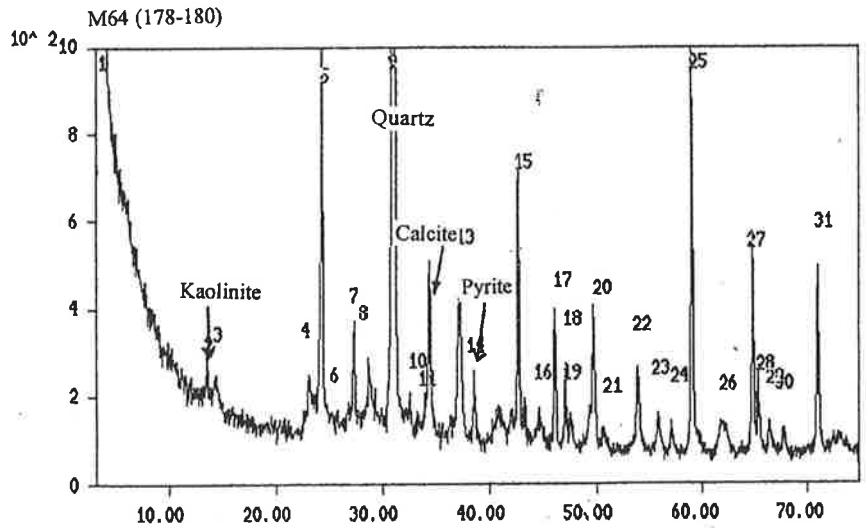
M64 (178-180)
10^ 2
Quartz
Calcite
Pyrite
Kaolinite
10.00
20.00
30.00
40.00
50.00
60.00
70.00

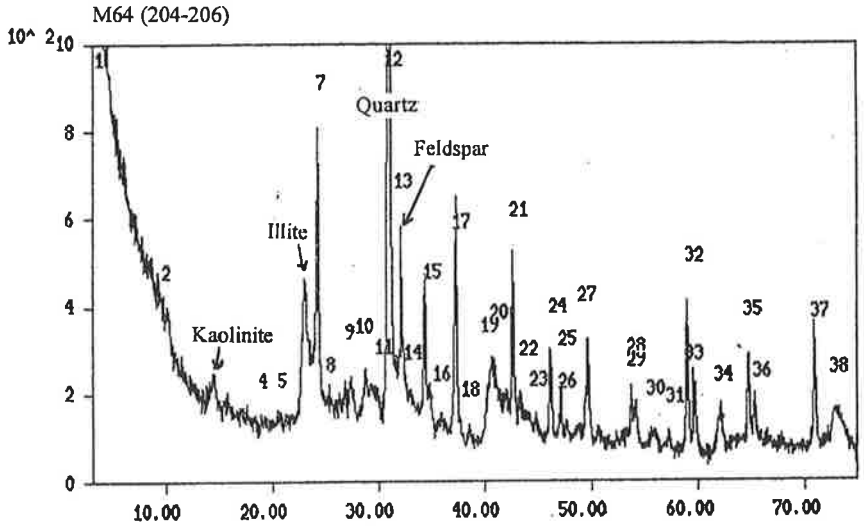
M64 (204-206)
10^ 2
Quartz
Feldspar
Illite
Kaolinite
10.00
20.00
30.00
40.00
50.00
60.00
70.00

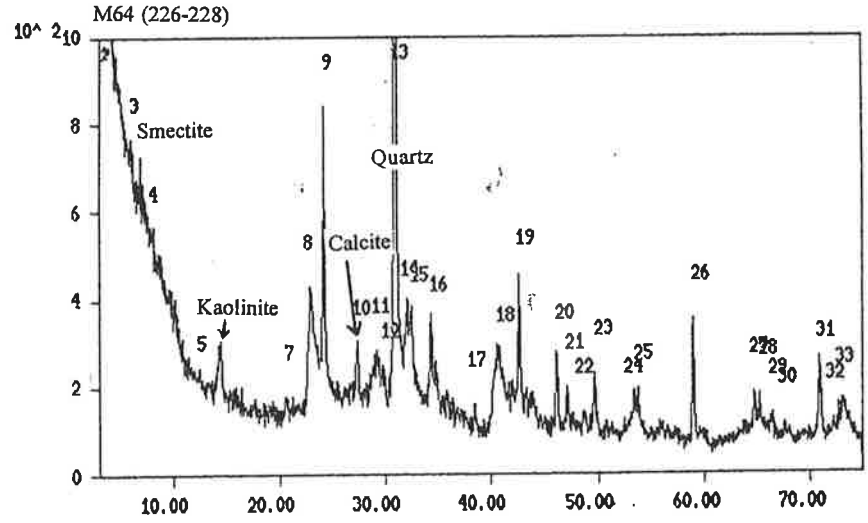
M64 (226-228)
10^ 2
Smectite
Quartz
Calcite
Kaolinite
10.00
20.00
30.00
40.00
50.00
60.00
70.00

Appendix 2

Pyrite oxidation model

The input data for pyrite oxidation model by computer code PHREEQM. The model investigate the increase of sulphate concentration of groundwater from the Murray Group Aquifer by oxidation of pyrite. The starting solution is groundwater from well M9. The pH of solution is buffered by equilibrium with calcite and iron in solution is controlled by goethite equilibrium. The final solution composition, pH and mass transfer are calculated for 0.0. 0.001, 0.0015. 0.002, 0.0025, 0.003, 0.004, 0.0045, 0.005 and 0.01 mmole/kg addition of oxygen.

```
Example
003011000010 1        0.00000
SOLUTION 1
M9
9  15 2       7.48      4.0      19.9       1.0
  4 4.8000E+01   5 2.3700E+01   6 9.5400E+01   7 1.0000E+01  12 1.0800E+00
  13 1.8000E+00  14 1.4100E+02  15 2.5100E+02  16 1.7100E+01
MINERALS
CALCITE   2  4.0      -8.480    -2.297        1        0.00
  15 1.0000E+00   4 1.0000E+00
-171.9065   -.077993    2839.319      71.595
GOETHITE  3  3.0      -1.0                 0        0.00
 115 1.0000E+00   3 2.0000E+00   1-3.0000E+00
PYRITE    4     0.0    -18.48     11.3         0        0.00
   1-2.0000E+00   2-2.0000E+00   8 1.0000E+00  42 2.0000E+00

REACTION
  32   1.000   4.000
STEPS
 0.000E+00 1.000E-03 1.500E-03 2.000E-03 2.500E-03 3.000E-03 4.000E-03
4.500E-03 5.000E-03 1.000E-02
END
```

Appendix 3

The model for the addition of soil water to the laterally flowing groundwater followed by equilibrium with calcite

The input data for the model of addition of soil water to laterally flowing groundwater followed by equilibrium with calcite by computer code PHREEQM. Soil Water represented by groundwater in well M70 is added in incremental steps to laterally flowing groundwater represented by M9. The final solution in each step equilibrated with calcite and the change in Ca and Sr concentration are calculated as discussed in section (5.5.1.2)

```
Example
0000011000 0 0        0
SOLUTION 1
M9
9  15 2       7.48      4.0      19.9       1.0
  4 4.8000E+01   5 2.3700E+01   6 9.5400E+01   7 1.0000E+01  12 1.0800E+00
  13 1.8000E+00  14 1.4100E+02  15 2.5100E+02  16 1.7100E+01
MINERALS
CALCITE   2   4.0      -8.480    -2.297        1        0.00
  15 1.0000E+00   4 1.0000E+00
-171.9065   -.077993    2839.319      71.595

END
Example
0000012000 0 0        0
SOLUTION 2
M70
 9 15 2       7.04      8.0      25.0       1.0
  4 4.1800E+02   5 6.4300E+02   6 5.5430E+03   7 1.2200E+02  12 6.6150E+01
  14 1.0306E+04  15 2.3200E+02  16 7.5300E+02  22 3.2100E+01
MINERALS
```

```
CALCITE   2  4.0      -8.480   -2.297        1        0.00
  15 1.0000E+00   4 1.0000E+00
-171.9065   -.077993   2839.319     71.595

END
Example
00100110001 0        1.00000
MINERALS
CALCITE   2  4.0      -8.480   -2.297        1        0.00
  15 1.0000E+00   4 1.0000E+00
-171.9065   -.077993   2839.319     71.595

STEPS
 9.99E-01

END
```

REFERENCES

Aberg, G., Jacks, G., and Hamilton, P.J. (1989) Weathering rates and $^{87}Sr/^{86}Sr$ ratios: An isotopic approach. *J. Hydrol.*, 109: 65-78.

Allison, G.B. (1982) The relationship between ^{18}O and Deuterium in water in sand columns undergoing evaporation. *J. Hydrol.*, 55: 163-169.

Allison, G.B. (1986) Estimation of groundwater discharge and recharge with special reference to arid areas. Proceedings of the International Conference on Groundwater Systems Under Stress. Australian Water Council Conference Series, No. 13, pp. 231-238.

Allison, G.B. and Hughes, M.W. (1978) The use of environmental chloride and tritium to estimate total recharge to an unconfined aquifer. *Aust. J. Soil. Res.*, 16: 181-195.

Allison, G.B. and Hughes, M.W. (1983) The use of natural tracers as indicators of soil-water movement in a temperate semi-arid region. *J. Hydrol.*, 60: 157-173.

Allison, G.B., Barnes, C. J., Hughes, M.W. and Leaney, F.W. J. (1983) Effect of climate and vegetation on oxygen-18 and deuterium profiles in soils. In: Isotope Hydrology, IAEA, Vienna, Austria, pp. 105-123.

Allison, G.B., Cook, P.G., Barnett, S.R., Walker, G.R., Jolly, I.D., and Hughes, M.W. (1990) Land clearance and river salinisation in the Western Murray Basin, Australia. *J. Hyrol.* 119: 1-20.

Allison, G.B., Stone, W.J. and Hughes, M.W. (1985) Recharge in karst and dune

elements of a semi-arid landscape as indicated by natural isotopes and chloride. *J. Hydrol.*, 76: 1-25.

Anderson, J.W. (1980) Assimilation of inorganic sulfate into cysteine. In: P.K. Stumpf and E.E. Conn, (Editors) The Biochemistry of Plants. Academic Press, New York. Vol. 5, pp. 203-223.

Andreae, M.O., and Jaeschke, W.A. (1992) Exchange of sulphur between biosphere and atmosphere over temperate and tropical regions. In: R.W. Howarth, J.W.B. Stewart, and M.V. Ivanov (Editors) Sulphur Cycling on the Continents. SCOPE 48, pp. 27-66.

Appelo, C.A.J. and Postma, D. (1993) *Geochemistry, Groundwater and Pollution.* Balkema Publishers, Rotterdam, 536 pp.

Arad, A., and Evans, R. (1987) The Hydrogeology, hydrochemistry and environmental isotopes of the Campaspe River aquifer system, north-central Victoria, Australia. *J. Hydrol.*, 95: 63-86.

Back, W. (1960) Origin of hydrochemical facies and groundwater in the Atlantic Coastal Plain. Report XXI, *Int. Geol. Congress*, Nordend. Pt. 1, 87 pp.

Back, W. (1961) Techniques for mapping of hydrochemical facies, *U.S. Geol. Surv. Prof. Papers,* 424-D, pp. 380-382.

Back, W. (1966) Hydrochemical facies and groundwater flow patterns in northern part of the Atlantic Coastal Plain. *U.S. Geol. Surv. Prof. Papers,* 498-A, pp. 1-42.

Back, W. and Hanshaw, B.B. (1965) *Chemical geohydrology.* In V.T. Chow (Editor), Advances in Hydroscience, Academic Press, Inc., New York, 2, pp. 49-109.

Baker P.A., Gieskes J.M., and Elderfield, H. (1982) diagenesis of carbonates in deep-sea sediments - evidence from Sr/Ca ratios and interstitial Sr^{+2} data. *J. Sedim.*

petrol., 52: 71-82.

Baker, M.N., and Horton, R.E. (1936) Historical development of ideas regarding the origin of springs and groundwater, *Trans. Amer. Geophysical Union*, Vol. 17, pp. 395-400.

Barnes, C.J. and Allison, G.B. (1983) The distribution of deuterium and ^{18}O in dry soils. 1. Theory. *J. Hydrol.*, 60: 141-156.

Barnes, C.J. and Allison, G.B. (1988) Tracing of water movement in the unsaturated zone using stable isotope of hydrogen and oxygen. *J. Hydrol.*, 100: 148-176.

Barnett, S.R. (1983) Murray Basin hydrogeological investigation, data assessment-Mallee region. South Australian Department of Mines and Energy, Report No. 83/18.

Barnett, S.R. (1989) The Hydrogeology of the Murray Basin in South Australia with special reference to the alluvium of the River Murray flood plain. MSc. Thesis, Flinders University of South Australia.

Bentley, H.W., Philips, F.M., Davis, S.N., Habermehl, M.A., Airey, P.L., Calf, G.E., Elmore, D., Gove, H. E., and Torgersen, T. (1986) Chlorine 36 dating of very old groundwater: 1. The Great Artesian Basin, Australia. *Water Resour. Res.*, 22: 13, 1991-2001.

Bigeleisen, J., Perlman, M.L., and Prosser, H.C. (1952) Conversion of hydrogenic materials to hydrogen for isotope analysis. *Anal. Chem.*, 24: 8, 1356-1357.

Black, R. (1989) The origin of high sodium bicarbonate waters in the Otway Basin, Victoria, Australia. In: D.L. Miles (Editor) Water-Rock Interaction WRI-6, Proceedings of the 6th International Symposium. Malvern, U.K. Balkema, Rotterdam, pp. 83-85.

Blackburn, G. and Mcleod, S. (1983) Salinity of atmospheric precipitation in the Murray-Darling drainage division, Australia. *Aust. J. Soil. Res.*, 21: 411-434.

Bonython, C.W. (1956) The salt of Lake Eyre-its occurrence in Madigan Gulf and its possible origin. *R. Soc. S. Aust. Trans.*, 79: 66-90.

Bottrell, S.H., Smart, P.L., Whitaker, F., and Raiswell, R. (1991) Geochemistry and isotope systematic of sulphur in the mixing zone of Bahamian blue holes. *Appl. Geochem.*, 6: 97-103.

Bowler, J. (1990) The last 500,000 years. In: N. Mackay, and D. Eastburn (Editors) The Murray, Groundwater and Salinity. Murray Darling Basin Commission, Canberra, Australia, pp. 95-111.

Braitsch, O., (1971) *Salt Deposits, their Origin and Composition.* Springer, New York, 297 pp.

Brass, G.W. (1975) The effect of weathering on the distribution of strontium isotope in weathering profiles. *Geochim. Cosmochim. Acta*, 39: 1647-1654.

Brass, G.W. (1976) The variation of the marine $^{87}Sr/^{86}Sr$ during Phanerozoic time: Interpretation using a flux model. *Geochim. Cosmochim. Acta,* 40: 712-730.

Bredenkamp, D.B., and Vogel, J.C. (1970) Study of a dolomitic aquifer with carbon-14 and tritium. In: Isotope Hydrology, IAEA, Vienna, Austria, pp. 349-372.

Bremner, J.M., and Steele, C.G. (1978). Role of microorganisms in the atmospheric sulfur cycle. *Adv. Mocrob. Ecol.*, 2: 155-201.

Brown, C.M. (1989) Structural and stratigraphic framework of groundwater occurrence and surface discharge in the Murray Group Basin, southeastern Australia. BMR *J. Aust. Geol. Geophys.*, 11: 127-146.

Brown, C.M., and Stephenson, A.E. (1991) Geology of the Murray Basin, southeastern

Australia. Bureau of Mineral Resources, Geology, and Geophysics, BMR Bulletin, 235 pp.

Bullen, T.D., Krabbenhoft, D.P., and Kendall, C. (1996) Kinetic and mineralogic controls on the evolution of groundwater chemistry and $^{87}Sr/^{86}Sr$ in a sandy silicate aquifer, northern Wisconsin, USA. *Geochim. Cosmochim. Acta*, 6: 1807-1821.

Burke, W.H., Denison, R.E., Hetherington, E.A., Koepnick, R.B., Nelson, H.F., and Otto, J.B. (1982) Variation of seawater $^{87}Sr/^{86}Sr$ throughout Phanerozoic time. *Geology,* 10: 516-519.

Busby, J.F, Plummer, L.N., Lee, R.W. and Hanshaw, B.B. (1991) Geochemical evolution of water in the Madison Aquifer in Parts of Montana, South Dakota, and Wyoming. *U.S. Geol. Surv. Prof. Paper* 1273-F, 89 pp.

Calhoun, J.A. and Bates, T.S. (1989) Sulfur isotope ratios. Traces of non-sea-salt sulfate in the remote atmosphere. In: E.S. Saltzman and W.J. Cooper (Editors) Biogenic Sulphate in the Environment. *Amer. Chem. Soc.,* 367-379.

Calhoun, J.A. (1990) Chemical and isotopic methods for understanding the natural marine sulfur cycle. Ph.D. Thesis, University of Washington.

Caron, F., Tessier A., Kramer J.R., Schwarcz H.P., and Rees C.E. (1986) Sulphur and oxygen isotopes of sulphate in precipitation and lake water, Quebec, Canada. *Appl. Geochem.,* 1: 601-606.

Cartwright, B., Merry, R.H. and Tiller, K.G. (1976) Heavy metal contamination of soils around a lead smelter at Port Pirie, South Australia. *Austral. J. Soil. Res.*, 15: 69-81.

Chambers, L.A. Bartley, J.G. and Herczeg, A.L. (1995) Hydrochemical evidence for

surface water recharge to a shallow regional aquifer in northern Victoria, Australia. *J. Hydrol.,* 181: 63-83.

Chambers, L.A., and Trudinger, P.A. (1979) Microbiological fractionation of stable sulfur isotopes: a review and critique. *Geomicrobiol. J.,* 1: 249-293.

Chaudhuri, S., Broedel, V., and Clauer, N. (1987) Strontium isotopic evolution of oil-field waters from carbonate reservoir rocks in Bindley field, central Kansas, USA. *Geochim Cosmochim Acta*, 51: 45-53.

Chaudhuri, S. (1978) Strontium isotopic composition of several oilfield brines from Kansas and Colorado *Geochim Cosmochim Acta*, 42: 329-331.

Chaudhuri, S. and Clauer, N. (1993) Strontium isotopic compositions and potassium and rubidium contents of formation waters in sedimentary basins: Clues to the origin of the solutes. *Geochim Cosmochim Acta*, 57: 429-437.

Chebotarev, I. I. (1955) Metamorphism of natural waters in the crust of weathering. *Geochim. Cosmochim. Acta,* 8: 22-28.

Chiba, H., and Sakai, H. (1985) Oxygen isotope exchange rate between dissolved sulfate and water at hydrothermal temperatures. *Geochim. Cosmochim. Acta*, 49: 993-1000.

Chivas, A.R., Andrew, A.S., Lyons, W.B., Bird, M.I., and Donnelly, T.H. (1991) Isotopic constraints on the origin of salts in Australian Playas. 1. Sulphur. *Palaeogeogr., Palaeoclimatol., Palaeoecol.,* 84: 309-332.

Clauer, N., Frape, S. K., and Fritz, B. (1989) calcite veins of the Stripa (Sweden) as records of the origin of the groundwaters and their interactions with the granitic body. *Geochim. Cosmochim. Acta*, 48: 1777-1781.

Claypool, G.E., Holser, W.T., Kaplan, I.R., Sakai, H., and Zak, I. (1980) The age

curves of sulfur and oxygen isotopes in marine sulfate and their mutual interpretation. *Chem. Geol.*, 28: 199-260.

Coleman, M.L., and Moore, M.P. (1978) Direct reduction of sulfates to sulfur dioxide for isotopic analysis. *Anal. Chem.*, 50: 1594 -1595.

Collerson, K.D., Ullman, W.J., and Torgersen, T. (1988) Groundwaters with unradiogenic $^{87}Sr/^{86}Sr$ ratios in the Great Artesian Basin, Australia. *Geology*, 16: 59-63.

Cook, P.G. and Walker, G.R. (1989) Groundwater recharge in western New South Wales. Centre for Research in Groundwater Processes. Report No. 9.

Cook, P.G., Jolly, I.D., Hughes, M.W., Beech, T.A., and Fiebiger, C.T. (1992) Recharge studies in the western Murray Basin. 5. Results of drilling programs at Maggea, Melevale, Pfeiffers and Boolgun. CSIRO, Technical Memorandum 92/8.

Cook, P.G., Jolly, I.D., Walker, G.R. Allison, G.B. and Leaney, F.W. (1991) Localised recharge in the vicinity of the Woolpunda Groundwater Mound. In: A.K. Kennett-Smith and G.R. Walker (Editors) Point recharge and diffuse discharge in the Murray Geological Basin. CSIRO Division of Water Resources, Australia, Water Resources Series No.7, pp. 44-61.

Cook, P.G., Walker, G.R. and Jolly, I.D. (1989) Spatial variability of groundwater recharge in a semi-arid region. *J. Hydrol.*, 111: 195-212.

Cortecci, G., and Longinelli, A. (1970) Isotopic composition of sulphate in rain water, Pisa, Italy. *Earth Planet. Sci. Lett.*, 8: 36-40.

Craig, H. (1954) Carbon 13 in plants and the relationship between carbon 13 and carbon 14 variations in nature. *J. Geol.*, 62: 115-141.

Craig, H. (1961) Isotopic variations in meteoric waters. *Science*, 133: 1702-1703.

Craig, H., Gordon, L. I. and Horibe, Y. (1963) Isotopic exchange effects in the evaporation of water. 1. Low-Temperature Experimental Results. *J. Geophy. Res.*, 68: 17, 5079-5087.

Dansgaard, W.F., (1964) Stable isotopes in precipitation. *Tellus*, 16: 436-439.

Darling, W G. and Bath, A.H. (1988) A stable isotope study of recharge processes in the English Chalk. *J. Hydrol.*, 101: 31-46.

Davie, R.F., Kellett, J.R., Fifield, L.K., Evans, W.R., Calf, G.E., Bird, J.R., Topham, S., and Ophel, T.R. (1989) Chlorine-36 measurements in the Murray Basin: preliminary results from the Victorian and South Australian Mallee region. *BMR J. Aust. Geol. Geophys.*, 11: 261-272.

Davies, G.R., and Krouse., H.R. (1975). Sulphur isotope distribution in Paleozoic evaporates, *Canadian Arctic Archipelago. Geo. Surv. Pap.*, 75-1 (B), pp. 221-225.

Davis, D.D., and Klauberg, G. (1975) Atmospheric gas phase oxidation mechanisms for the molecule SO_2. *Int. J. Chem. Kinet.*, 7: 543-556.

Deines, P. (1980) The isotopic composition of reduced organic carbon. In: P. Fritz and J.Ch. Fontes (Editors) Handbook of Environmental Isotope Geochemistry. The Terrestrial Environment, Vol. 1, pp. 330-406.

Deines, P., Langmuir, D., and Harmon, R. S. (1974) Stable carbon isotope ratios and the existence of a gas phase in the evolution of carbonate ground waters. *Geochim. Cosmochim. Acta*, 38: 1147-1164.

Dighton, J.C., Leaney, F.W. J., Herczeg, A.L., Allison, G.B., and Hughes, M.W. (1997) A rapid and robust method for the preparation of isotopically unaltered

hydrogen gas from water for stable isotope mass spectrometry. Sixth Australian-New Zealand Environmental isotope conference, Lower Hutt, New Zealand.

Dighton, J.C. and Allison G.B. (1985) Carbon dioxide profiles of nine sites in the Murray Basin. CSIRO, Division of Soils, Australia, Technical Memorandum No. 34.

Dincer, T., Al-Mugrin, A., and Zimmerman, U. (1974) Study of the infiltration and recharge through the sand dunes in arid zones with special reference to the stable isotopes and thermonuclear tritium. *J. Hydrol.*, 23: 79-109.

Domenico, P.A. (1972) *Concepts and Models in Groundwater Hydrology*. McGraw-Hill, New York, 406 pp.

Downing, R.A., Smith, D.B., Pearson, F.J., Monkhouse, R.A., and Otlet, R.L. (1977) The age of groundwater in the Lincolnshire Limestone, England and its relevance to the flow mechanism. *J. Hydrol.*, 33: 201-216.

Dowuona, G.N., Mermut, A.R., and Krouse, H.R. (1993) Stable isotope geochemistry of sulphate in relation to hydrogeology in southern Saskatchewan, Canada. *Appl. Geochem.*, 8: 255-263.

Drimmie, R.J., Aravena, R, Wassenaar, L.I., Fritz, P. Hendry, M.J., and Hut, G. (1991) Radiocarbon and stable isotopes in water and dissolved constituents, Milk River aquifer, Alberta, Canada. *Appl. Geochem.*, 6: 381-392.

Duce, R.A. (1981) Biogeochemical cycles and the air/sea exchange of aerosols. Working paper of SCOPE workshop on some perspectives of the major biogeochenical cycles, Orsundsbro, Sweden.

Edmunds, W.M., and Wright, E.P. (1979) Groundwater recharge and palaeoclimate in

the Sirte and Kufra Basins, Libya. *J. Hydrol.*, 40: 215-241.

Edmunds, W.M., Walton, N.R.G. (1980) A geochemical and isotopic approach to recharge evaluation in semi-arid zones: Past and Present. In Arid-Zone Hydrology Investigations with Isotope Techniques. IAEA, Vienna, Austria, pp. 47-67.

Edmunds, W.M., Smedley, P.L. and Spiro, B. (1995) Controls in the geochemistry of sulphur in the east midlands Triassic Aquifer, UK. In: International Symposium on Isotopes in Water Resources Management, IAEA, Vienna, Austria, Vol. 2, pp. 107-122.

Elliot, T. (1990) Geochemical indicators of groundwater ageing. Ph.D. Thesis, University of Bath, England.

Epstein, S., and Mayeda, T.K. (1953) Variations of ^{18}O content of waters from natural sources. *Geochim. Cosmochim. Acta*, 4: 213-224.

Eugster, H.P., and Jones, B.F. (1979) Behavior of major solutes during closed-basin brine evolution. *Am. Jour. Sci.*, 279: 609-631.

Evans, C.V., Otlet, R.L., Downing, R.A., Monkhouse, R.A., and Rae, G. (1978) Some problems in the interpretation of isotope measurements in United Kingdom Aquifers. In: Isotope Hydrology. IAEA, Vienna, Austria, pp. 679-708.

Evans, R.W. (1982) Factors affecting water quality in a regional fractured rock aquifer. Aust. Water Resources Council Conference on Groundwater in Fractured Rocks, Series 5, pp. 57-69.

Evans, R.W. and Kellett, R.J. (1989) The hydrology of the Murray Basin, southeastern Australia. *BMR, J. Aust. Geol. Geophys.*, 11: 147-166.

Faure, G. (1986) *Principles of Isotope Geology*. John Wiley & Sons, Inc. 589 pp.

Faure, G. (1992) *Principles and Applications of Inorganic Geochemistry*. Macmillan Inc. 626 pp.

Feth, J.H. (1981) Chloride in natural continental water-A review. *U.S. Geol. Sur. Water Supply Paper* 2176, 30 pp.

Firman, J.B. (1973) Regional stratigraphy of surficial deposits in the Murray Basin and Gambier Embayment. Geological Survey of South Australia, Report of Investigation, No. 39.

Fontes, J.Ch., and Garnier, J. (1979) Determination of the initial ^{14}C activity of the total dissolved carbon: A review of the existing models and a new approach. *Water Resour. Res.*, 15: 399-413.

Fontes. J.Ch. (1983) Dating of groundwater. In: Guidebook on Nuclear Techniques in Hydrology, IAEA. Vienna, Austria, pp. 285-317.

Frape, S.K. Fritz, P. and McNutt, R.H. (1984 a) The role of water-rock interaction in the chemical evolution of groundwaters from the Canadian shield. *Geochim. Cosmochim. Acta*, 48: 10-38.

Frape, S.K., and Fritz, P. (1982) The chemistry and isotopic composition of saline groundwaters from the Sudbury Basin, Ontario. Canadian. *J. Earth Sci.*, 19: 645-661.

Frape, S.K., Fritz, P. and McNutt, R.H. (1984 b) Water-rock interaction and chemistry of groundwaters from the Canadian shield. *Geochim. Cosmochim. Acta*, 48: 1617-1627.

Freeze, R.A. and Cherry, J.A. (1979) *Groundwater*. Prentice-Hall, New Jersey, 604 pp.

Fritz, P. and Frape, S.K. (1982) Saline groundwaters in the Canadian Shield-A first overview. *Chem. Geol.* 36: 179-190.

Fritz, P. and Frape, S.K. (1987) Saline waters and gases in crystalline rocks. *Geol. Assoc. Canada Spec. paper,* 33.

Fritz, P. Fontes, J.Ch., Frape, S.K., Louvat, D., Michelot, J.L., and Balderer, W. (1989) The isotope geochemistry of carbon in groundwater at Stripa. *Geochim. Cosmochim. Acta,* 48: 1765-1775.

Fritz, P., Basharmal, G.M., Drimmie, R.J., Ibsen, J., and Qureshi, R.M. (1989) Oxygen isotope exchange between sulphate and water during bacterial reduction of sulphate. *Chem. Geol.*, 79: 99-105.

Frohlich, K., Ivanovich, M., Hendry, M.J., Andrews, J.N., Davis, S.N., Drimmie, R.J., Fabryka-Martin, J. Florkowski, T., Fritz, P., Lehmann, B., Loosli, H.H., and Nolte, E. (1991) Application of isotopic methods to dating of very old groundwaters: Milk River aquifer, Alberta, Canada. *Appl. Geochem.*, 6: 465-472.

Fry B., Scalan, R.S., Winters, J.K., and Parker, P.L. (1992) Sulphur uptake by salt, grass, mangroves, and seagrass in anaerobic sediments. *Geochim. Cosmochim. Acta*, 46: 1121-1124.

Garland, J. (1978). Dry and wet removal of sulphur from the atmosphere. *Atmos. Environ.*, 12: 349-362.

Garrels, R.M. and Christ, C.L. (1965) *Solutions, Minerals, and Equilibria.* Harper and Row, New York, 449 pp.

Garrels, R.M., and Mackenzie, F.T. (1967) Origin of the chemical compositions of some springs and lakes. In R.F. Could (Editor) Equilibrium Concepts in Natural Water Systems. *Amer. Chem. Soc., Ser.* 67, pp. 222-242.

Gat, J.R. (1971) Comments on stable isotope methods in regional groundwater

investigations. *Water Resour. Res.*, 17: 980-993.

Georgii, H.W. (1978) Large-scale spatial and temporal distribution of sulphur compounds. *Atmos. Environ.*, 12: 681-690.

Goldich, S.S., and Gast, P.W. (1966) Effects of weathering on the Rb-Sr and K-Ar ages of biotite from the Morton Gneiss, Minnesota. *Earth Planet. Sci. Lett.*, 1: 372-375.

Gonfiantini, R. (1986) Environmental isotopes in lake studies. In P. Fritz and J.Ch. Fontes (Editors) Handbook of Environmental Isotope Geochemistry, Vol. 2. Elsevier, Amsterdam, pp. 113-168.

Gould, W.D., Krouse, H.R., McCready, R.G.L., and Rajan, S. (1989) Stable isotope composition of sulphate produced during bacterial oxidation of various metal sulphides. Proceedings of Biohydrometallugy International Symposium, Jackson Hole, Wyoming, pp. 81-93.

Graustein, W.C. (1987) $^{87}Sr/^{86}Sr$ ratios measure the sources and flow of strontium in terrestrial ecosystems: In P.W. Rundel, J.R. Ehleringer and K.A. Nagy (Editors) Stable Isotopes in Ecological Research, Springer-Verlag, New York, pp. 491-512.

Graustein, W.C., and Armstrong R.L. (1983) The use of strontium-87/strontium-86 ratios to measure atmospheric transport into forested watershed. *Science*, 219: 289-292.

Grinenko, V.A. and Thode, H.G. (1970) Sulphur isotope effects in volcanic gas mixtures. *Can. J. Earth Sci.*, 7: 1402-1409

Grinenko, V.A., and Grinenko, L.N. (1974) *Geochemistry of Sulphur Isotopes*. Nauka, Moscow, 272 pp.

Hanshaw, B.B., and Back, W. (1979) Major geochemical processes in the evolution of carbonate-aquifer systems. *J. Hydrol.*, 43: 287-312.

Harris, W.K. (1966) New and redefined names in South Australian Lower Tertiary stratigraphy, Geological Survey of South Australia, Quarterly Geological Notes, 20, pp. 1-3.

Harrison, A.G., and Thode, H.G. (1958) Mechanism of the bacterial reduction of sulphate from isotope fractionation studies. *Trans. Faraday Soc.,* 54: 84-92.

Heicklen, L. (1976) *Atmospheric Chemistry*. Academic press, New York, XIV, 406 pp.

Helgeson, H.C. (1968) Evaluation of irreversible reactions in geochemical processes involving minerals and aqueous solutions - I. Thermodynamic relations. *Geochim. Cosmochim. Acta*, 32: 853-877.

Helgeson, H.C., Garrels, R.M., and Mackenzie, F.T. (1969) Evaluation of irreversible reactions in geochemical processes involving minerals and aqueous solutions - II. Applications. *Geochim Cosmochim. Acta*, 34: 569-592.

Henderson, T. (1984) Geochemistry of ground-water in two sandstone aquifer systems in the Northern Great Plain in parts of Montana, Wyoming, North Dakota, and South Dakota. *U.S. Geol. Surv. Prof. Paper*, 1402-C.

Hendry, M.J., Krouse, H.R., and Shakur, M.A. (1989) Interpretation of oxygen and sulfur isotopes from dissolved sulfates in tills of Southern Alberta, Canada. *Water Resour. Res.*, 25: 3, 567-572.

Hendry, M.J. and Schwartz, F.W. (1988) An alternative view on the origin of chemical and isotopic patterns in groundwater from the Milk River Aquifer, Canada. *Water Resour. Res.*, 24: 10, 1747-1763.

Hendry, M.J. And Schwartz, F.W. and Robertson, C. (1991) Hydrogeology and

hydrochemistry of the Milk River aquifer system, Alberta, Canada: a review. *Appl. Geochem.*, 6: 369-380.

Herczeg, A.L. and Lyons, W.B. (1991) A chemical model for the evolution of Australian sodium chloride lake brines. *Palaeogeogr., Palaeoclimatol., Palaeoecol.,* 84: 43-53.

Herczeg, A.L., Barnes, C. J., Macumber, P.G., and Olley, J.M. (1992) A stable isotope investigation of groundwater-surface water interaction at Lake Tyrrell, Victoria, Australia. *Chem. Geol.*, 96: 19-32.

Herczeg, A.L., Leaney, F.W., Ghomari, R., Davie, R. and Fifield, L.K. (1989) Hydrochemistry of groundwaters in the south-western Murray Basin with special reference to the Woolpunda groundwater mound. Centre for groundwater studies, report No.13.

Herczeg, A.L., Simpson, H.J., and Mazor, E. (1993) Transport of soluble salts in a large semi-arid basin: River Murray, Australia. *J. Hydrol.*, 144: 59-84.

Herczeg, A.L., Torgerson, T., Chivas, A.R. and Habermehl, M.A. (1991) Geochemistry of ground waters from the Great Artesian Basin, Australia. *J. Hydrol.*, 126: 225-245.

Herut, B., Starinsky, A., and Katz, A. (1993) Strontium in rainwater from Israel: Sources, isotopes and chemistry. *Earth Planet. Sci. Lett.*, 120: 77-84.

Hess, J. Bender, M.J., and Schilling J-G. (1986) Evolution of the ratio of strontium-87 to strontium-86 in seawater from Cretaceous to present. *Science,* 231: 979-984.

Hines, M.E., Lyons, W.B., Lent, R.M., and Long, D.T. (1992) Sedimentary biogeochemistry of an acidic, saline groundwater discharge zone in Lake Tyrrell, Victoria, Australia. Chem. Geol., 96: 53-67.

Hodell, A.D., Mead, A.G., and Mueller, A.P. (1990) Variation in strontium isotopic composition of seawater (8 Ma to present): Implications for chemical weathering rates and dissolved fluxes to the oceans. *Chem. Geol.*, 80: 291-307.

Hodell, A.D., Mueller, A.P., and Garrido, R.J. (1991) Variations in strontium isotopic composition of seawater during the Neogene. *Geology*, 19: 24-27.

Holser, W.T., and Kaplan, I.R. (1966) Isotope geochemistry of sedimentary sulfates. *Chem. Geol.*, 1: 93-135.

Holt, B.D., and Kumar, R. (1984) Oxygen-18 study of high-temperature air oxidation of SO_2. *Atmos. Environ.*, 18: 2089-2094.

Holt, B.D., and Kumar, R. (1986) Oxygen-18 study of the atmospheric-aquatic linkage in Adirobdack Watersheds. *Water, Air, and Soil Pollution*, 31: 175-186.

Holt, B.D., Kumar R., and Cunningham, P.T. (1982) Primary sulfates in atmospheric sulfates: Estimation by Oxygen Isotope Ratio Measurements. *Science*, 217: 51-52.

Holt, B.D., Kumar, R., and Cunningham, P.T. (1981) Oxygen-18 study of the aqueous-phase oxidation of sulphur dioxide. *Atmos. Environ.*, 15: 557-566.

Holt, B.D., Cunningham, P. T., Engelkemeir, A. G., Graczyk, D. G., and Kumar, R. (1983) Oxygen-18 study of non aqueous-phase oxidation of sulfur dioxide. *Atmos. Environ.*, 17: 625-632.

Horita, J. and Gat, J. (188) Procedure for hydrogen isotope analysis of water from concentrated brines. *Chem. Geol.*, (Isotope Geoscience Section). 72: 85-88.

Hotzel, H., Job, C., Moser, H., Rauert, W., Stichler, W., and Zotl, J.G. (1980) Isotope methods as a tool for Quaternary studies in Saudi Arabia. In Arid-Zone Hydrology Investigations with Isotope Techniques. IAEA, Vienna, Austria, pp.

215-235.

Hufen, T.H., Lau, L.S., and Buddemeier, R. W. (1974) Radiocarbon, ^{13}C and tritium in water samples from Basaltic Aquifers and Carbonate Aquifers on the island of Oahu, Hawaii. In: Isotope Hydrology. IAEA, Vienna, Austria, pp. 111-127.

Hughes, M.W., Cook, P.G., Jolly, I.D., Beech, T.A., and Fiebiger, C.T. (1988 a) Recharge studies in the western Murray Basin. 1. Results of a drilling program at Borrika. CSIRO, Technical Memorandum 88/10.

Hughes, M.W., Jolly, I.D., Cook, P.G., Dighton, J.C., Beech, T.A., and Fiebiger, C.T. (1988 b) Recharge studies in the western Murray Basin. 2. Results of a drilling program at Wanbi. CSIRO, Technical Memorandum 88/11.

Hull, L. (1984) Geochemistry of ground water in the Sacramento Valley, California. *U.S. Geol. Surv. Prof. Paper,* 1401-D.

Husar, R.B., Lodge, J.P., and Moore, D.J. (1978) Sulphur in the Atmosphere. Proceedings of International Symposium, , *Atmos. Environ.*, 12: 25-796.

IAEA (1975) Sampling of water for carbon-14 analysis. Isotope Hydrology Laboratory, IAEA, Vienna, Austria.

Ingerson, E., and Pearson, F.J. (1964) Estimation of age and rate of motion of groundwater by the ^{14}C method. In Recent Researches in the Fields of Hydrosphere, Atmosphere and Nuclear Geochemistry, Maruzen, Tokyo, pp. 263-283.

Jack, R.L. (1921) The salt and gypsum resources of South Australia. *Geol. Surv. S. Aust., Bull.*, No. 8, pp.118.

Jacobson, G. (1988) Hydrology of Lake Amadeus, a groundwater-discharge playa in central Australia. BMR. *J. Aust. Geol. Geophys.*, 10: 301-308.

Jacobson, R.L., and Langmuir, D. (1970) The chemical history of some spring waters in carbonate rocks. *Ground Water*, 8: 5-9.

James, P.N., Bone, Y., and Kyser, K.T. (1993) Shallow burial dolomatization and dedolomatization of Mid-Cenozoic, cool-water, calcite, deep-shelf limestones, Southern Australia. *J. Sedim. petrol.*, 63: 3, 528-538.

Johnson, M. (1979) The origin of Australia's salt lakes. N.S.W. Geological. Survey. 19: 2, 221-266.

Jolly, I.D., Trenordan, M., Holub, A.N., Cook, P.G., and Dighton, J.C. (1990) Recharge studies in the western Murray Basin. 4. Results of a drilling program at Kulkami. CSIRO, Technical Memorandum 90/3.

Jones, B.F., Hanor, J.S. and Evans, R.W (1994) Sources of dissolved salts in the central Murray Basin, Australia. *Chem. Geol.*, 111: 135-154.

Jones, L.M., and Faure, G. (1978) A study of the strontium isotopes in lakes and surficial deposits of the ice-free valleys, Southern Victoria Land, Antarctica. *Chem. Geol.*, 22: 107-120.

Jorgensen, O.N., and Holm, M.P. (1995) Strontium-isotope studies of chloride-contaminated groundwater, Denmark. *Hyrogeol. J.*, 3: 2, 52-57.

Kaplan, I.R., and Rittenberg, S.C., (1964) Microbiological fractionation of sulphur isotopes. *J. Gen. Microbiol.*, 34: 195-212.

Kaplan, I.R., Emery, K.O., and Rittenberg, S.C. (1963) The distribution and isotopic abundance of sulphur in recent marine sediments of Southern California. *Geochim. Cosmochim. Acta*, 27: 297-331.

Katz, A., Sass, E., and Starinsky, A. (1972) Strontium behavior in the aragonite-calcite transformation: an experimental study at 40-98 °C. *Geochim Cosmochim Acta*,

36: 481-496.

Keay, J., Menage, P.M.A., and Dean, G.A., (1972) Automated method for the microdetermination of sulphur. *Analyst*., 97: 897-902.

Kellett, R.J., Evans, R.W., Allan, L.G., Davie, F.R., and Fifield, K.L. (1990) A study of stable chloride and chloride-36 in the Murray Group Limestone, Western Murray Basin. International Conference on Groundwater in Large Sedimentary Basins, Australian Water Council Conference, Series. 20, pp. 403-419.

Kemp, A.L., and Thode, H.G. (1968) The mechanisms of the bacterial reduction of sulphate and of sulphite from isotope fractionation studies. *Geochim. Cosmochim. Acta*, 32: 71-91.

Kennett-Smith, A., Cook, P.G., and Walker, G.R. (1994) Factors affecting groundwater recharge following clearing in the south western Murray Basin. *J. Hydrol.*, 154: 85-105.

King, D. (1951) Craigie plain gypsum deposit. Mining Review, Adelaide, 93, pp. 113-116.

Kinsman, J.J.D. (1969) Interpretation of Sr concentrations in carbonate minerals and rocks. *J. Sedim. petrol.*, 39: 486-508.

Krishnaswami, S., Trivedi, J.R, Sarin, M.M., Ramesh, R., and Sharma, K.K. (1992) Strontium isotope and rubidium in the Ganga-Brahmaputra river system: Weathering in the Himalaya, fluxes to the Bay of Bengal and contributions to the evolution of oceanic $^{87}Sr/^{86}Sr$. *Earth Planet. Sci. Lett.*, 109: 343-253.

Kroopnick, P., and Craig, H. (1972) Atmospheric oxygen: Isotope composition and solubility fractionation. *Science*, 175: 54-55.

Krouse, H.R., and McCready, R.G.L. (1979) Reductive processes. In: P.A. Trudinger

and D. Swaine (Editors) Biological Factors in Mineral Cycling. Elsevier, Amstrdam, pp. 315-368.

Langmuir, D. (1971) The geochemistry of some carbonate groundwaters in central Pennsylvania. *Geochim. Cosmochim. Acta*, 35: 1023-1045.

Lawrence, C.R. (1975) Geology, hydrodynamics and hydrochemistry of the southern Murray Basin. Geological Survey of Victoria. Memorandum No. 30.

Le Gal La Salle, C. (1992) Circulation des eaux souterraines dans l' aquifere captif du continental terminal: Bassin des iullemeden, Niger. Methodologie et application: Isotopes stables de la molecule d' eau, carbone-14, chlore-36, uranium et gaz nobles. Ph.D. Thesis, University of Paris, Paris, France.

Leaney, F.W. and Allison, G.B. (1986) Carbon-14 and stable isotope data for an area in the Murray Basin: its use in estimating recharge. *J. Hydrol.*, 88: 129-145.

Leaney, F.W., Herczeg, A.L., and Love, A.J. (1995) Fresh Groundwater in the S-W Murray Basin resulting from recharge during wet climatic periods. Murray Darling Workshop, Wagga Wagga, Australia, Record No. 1995/61, pp. 165-169.

Leaney, F.W., Herczeg, A.L., Love, A.J., and Robinson, M. (1994) The origin of fresh groundwater in the Southwest Murray Basin. Water Down Under, 2, Part 2, pp. 189-194.

Leaney, F.W., Herczeg, A.L. and Dighton, J.C. (1994) New developments for the direct CO_2 absorption method for radiocarbon analysis. *Quater. Geochron.*, 13: 171-178.

Lein, A.Yu. (1983) The sulphur cycle in the lithosphere. Part II, cycling. In: M.V. Ivanov, and J.R. Freney, (Editors) The Global Biogeochemical Sulphur Cycle.

SCOPE 19, pp. 95-129.

Libby, W.F. (1965) *Radiocarbon Dating*. University of Chicago Press, Chicago, III, 175 pp.

Lindsay, J.M. and Barnett, S.R. (1989) Aspects of stratigraphy and structure in relation to the Woolpunda Groundwater Interception Scheme, Murray Basin, South Australia. *BMR J. Aust. Geol. Geophys.*, 11, pp. 219-225.

LIoyd, J.W. (1980) An examination of recharge mound decay and fossil gradients in arid regional sedimentary basins. In Arid-Zone Hydrology Investigations with Isotope Techniques. IAEA, Vienna, Austria, pp. 69-75.

Lloyd, R.M., (1967) Oxygen-18 composition of oceanic sulfate. *Science*, 156:1228-1229.

Lloyd, R.M., (1968) Oxygen isotope behavior in the sulfate-water system. *J. Geophys. Res.*, 73: 6099-6110.

Long, D.T., Fegan, N.E., Lyons, W.B., Hines, M.E., Macumber, P.G. and Giblin, A.M. (1992) Geochemistry of acid brines: Lake Tyrrell, Victoria, Australia. *Chem. Geol.*, 96: 33-52.

Love, A.J., Herczeg, A.L., Leaney, F.W. Stadter, F., Dighton, J.C., and Armstrong, D. (1994) Groundwater residence time and palaeohydrology in the Otway Basin, South Australia: ^{2}H, ^{18}O and ^{14}C data. *J. Hydrol.*, 153: 157-187.

Love, A.J., Herczeg, A.L., Armstrong, D., Stadter, F., and Mazor, E. (1993) Groundwater flow regime within the Gambier Embayment of the Otway Basin, Australia: evidence from hydraulics and hydrochemistry. *J. Hydrol.*, 143: 297-338.

Lowrence, C.R., (1975) Geology, hydrodynamics and hydrochemistry of the southern

Murray Basin. Geological Survey of Victoria, Memorandum No. 30.

Ludbrook, N.H. (1961) Stratigraphy of the Murray Basin in South Australia. Geological Survey of South Australia. Bulletin 36.

Luly, J.G., Bowler, J.M., and Head, M.J. (1986) A radiocarbon chronology from the Playa Lake Tyrrell, northwestern Victoria, Australia. *Palaeogeogr., Palaeoclimatol., Palaeoecol.,* 54: 171-180.

Lyons, W.B., Tyler, S.W., Gaudette, H.E., and Long, D.T. (1995) The use of strontium isotopes in determining groundwater mixing and brine fingering in a playa spring zone, Lake Tyrrell, Australia. *J. Hydrol.*, 167: 225-239.

Macnamara, J., and Thode, H.G. (1950) Comparison of the isotopic constitution of terrestrial and meteoritic sulphur. *Phys. Rev.* 78, 307.

Macumber, P.G. (1990) Non- steady state hydrologyical equilibrium in the Murray Basin. In: International Conference on Groundwater in Large Sedimentary Basins, Australian Water Council Conference, Series. No.20, pp. 19- 27.

Macumber, P.G. (1991) Interaction between ground water and surface systems in northern Victoria. Department of Conservation & Environment, Victoria. 345 pp.

Magaritz, M., Nadler, A., Kafri, U. and Arad, A. (1984) Hydrogeochemistry of continental brackish waters in the southern Coastal Plain, Israel. *Chem. Geol.*, 42: 159-176.

Martin, R.E. and Harris, P.G. (1982) Hydrogeochemical study of groundwater from an unconfined aquifer in the vicinity of Perth, Western Australia, Australian Water Resources Council, Department of National Development and Energy, Technical paper, No. 67.

Mayer, B., Fritz, P., Knief, G. Li., Fischer, M., Rehfuess, K. E., and Krouse, H. R. (1991) Evaluating pathways of sulphate between the atmosphere and hydrosphere using stable sulphur and and oxygen isotope data. In Isotope Techniques in Water Resources Development. IAEA, Vienna, Austria. pp. 3-17.

Mayer, B., Fritz, P., Prietzel, J. and Krouse, H.R. (1995) The use of stable sulfur and oxygen isotope ratios for interpreting the mobility of sulphate in aerobic forest soils. *Appl. Geochem.*, 10: 161-173.

Mazor, E. (1976 b) Multitracing and multisampling in hydrologyical studies. In: Interpretation of Environmental Isotope and Hydrochemical data in Groundwater Hydrology. Proceedings of an Advisory Group Meeting, IAEA, Vienna, Austria, pp. 7-37.

Mazor, E. (1976 a) The Ram Crater Lake- A note on the revival of a 2000-year-old groundwater. In: Interpretation of Environmental Isotope and Hydrochemical Data in Groundwater Hydrology. Proceedings of an Advisory Group Meeting, IAEA, Vienna, Austria, pp. 179-183.

Mazor, E. (1992) Reinterpretation of ^{36}Cl data: physical processes, hydraulic interconnections and age estimates in groundwater systems. *Appl. Geochem.*, 7: 351-360.

Mazor, E., and George, R. (1992) Marine airborne salts applied to trace evapotranspiration, local recharge and lateral groundwater flow in Western Australia. *J. Hydrol.*, 139: 63-77.

Mazor, E., Vuataz, F.D., and Jaffe, F.C. (1985) Tracing groundwater components by chemical, isotopic and physical parameters-example: Schinznach, Switzerland.

J. Hydrol., 76: 233-246.

McCord, A.K. (1997) A description of land in the southern Mallee of South Australia. Primary Industries, South Australia, 223 pp.

Mckinney, C.R., McCrea, J.M., Epstein, S. Allen, H.A., and Urey, H.C. (1950) Improvements in mass spectrometers for the measurement of small differences in isotope abundance ratios. *Rev. Sci. Instrum.*, 21: 724-725.

McNutt, R.H. (1987) $^{87}Sr/^{86}Sr$ ratios as indicators of water/rock interaction: Application to brines found in Precambrian age rocks from Canada: In P. Fritz, and S.K. Frape (Editors) Saline water and gases in crystalline rocks. Geological. Association of Canada, Special Paper, 33. pp. 81-88.

McNutt, R.H., Frape, S.K., and Doller, P. (1987) A strontium, oxygen and hydrogen isotopic composition of brines, Michigan and Appalachian basins, Ontario and Michigan. *Appl. Geochem.*, 2: 495-505.

McNutt, R.H., Frape, S. K., and Fritz, P., (1984) Strontium isotopic composition of some brines from the Precambrian Shield of Canada. *Chem. Geol.*, (Isotope Geoscience Section), 2: 205-215.

McNutt, R.H., Frape, S.K., Fritz, P., Jones, M.G., and Macdonald, I.M. (1990) The $^{87}Sr/^{86}Sr$ values of Canadian Shield brines and fracture minerals with applications to groundwater mixing, fracture history, and geochronology. *Geochim Cosmochim Acta*, 54: 205- 215.

Meinzer, O.E. (1934) The history and development of ground-water hydrology. *J. Wash. Acad. Sci.*, 24: 1, 6-7.

Mekhtiyeva, V.L. Pankina, R.S., and Gavrilov, Ye.Ya. (1976). Distributions and isotopic compositions of forms of sulphur in water animals and plants.

Geochem. Int., 82-87.

Millipore Corporation (1989) Waters Ion Chomatography Cookbook, USA.

Mitchell, R.H., and Krouse, H.R. (1975) Sulphur isotope geochemistry of carbonates. *Geochim. Cosmochim. Acta,* 39: 1505-1513.

Mizutani, Y. and Rafter, T.A. (1973) Isotopic behavior of sulphate oxygen in the bacterial reduction of sulphate. *Geochem. J.*, 6: 183-191.

Mizutani, Y., and Rafter, T.A. (1969 a) Oxygen isotopic composition of sulphates-Part 4. Bacterial Fractionation of Oxygen Isotopes in the Reduction of Sulphate and in the Oxidation of Sulphur. *N.Z. J. Sci.*, 12: 60-68

Mizutani, Y., and Rafter, T.A. (1969 b) Oxygen isotopic composition of sulphates-Part 5. Isotopic Composition of Sulphate in Rain Water, Gracefield, New Zealand. *N.Z. J. Sci.*, 12: 69-80.

Mook, W.G. (1980) Carbon-14 in hydrogeological studies. In P. Fritz and J.Ch. Fontes (Editors) Handbook of Environmental Isotope Geochemistry. The Terrestrial Environment, Vol. 1, pp. 50-73.

Morse, J.W., and Mackenzie, F. T. (1990) *Geochemistry of Sedimentary Carbonates*: Developments in Sedimentology. Elsevier, Amsterdam, 702 pp.

Moser, H., Wolf, M., Fritz, P. Fontes, J.Ch., Florkowski, T., and Payne, B.R. (1989) Deuterium, oxygen-18, and tritium in Stripa groundwater. *Geochim. Cosmochim. Acta*, 48: 1757-1763.

Nakai, N., and Jensen, M.L. (1964) The kinetic isotope effect in the bacterial reduction and oxidation of sulphur. *Geochim. Cosmochim. Acta*, 28: 1893-1912.

Negrel, P., Fouillac, C., and Brach, M. (1997) A strontium isotope study of mineral and surface waters from the Cezallier (Massif Central, France): Implication for

mixing processes in areas of disseminated emergence of mineral waters. *Chem. Geol.*, 135: 89-101.

Neir, A.O., Ney, E.P. , and Inghram, M.G. (1947) A null method for the comparison of two ion currents in a mass spectrometer. *Rev. Sci. Instrum.*, 18: 294.

Newman, L., Krouse, H.R., and Grinenko V.A. (1991) Sulphur isotope variation in the atmosphere. In: H.R. Krouse, and V.A. Grinenko (Editors) Stable Isotopes, Natural and Anthropogenic Sulphur in the Environment. SCOPE 43, pp. 133-177.

Nielsen, H., Pilot, J., Grinenko, L.N., Grinenko, V.A., Lein, A.Yu., Smith, J.W., and Pankina, R.G. (1991). In: H.R. Krouse and V.A. Grinenko (Editors) Stable Isotopes, Natural and Anthropogenic Sulphur in the Environment. SCOPE 43, pp. 65-132.

Nienhuis, P.R., Appelo, C.A.J. and Willemsen, A. (1993) PHREEQM in a *M* ing-Cell flowtube, Free University- Amsterdam, Netherlands. Based on PHREEQE, Parkhurst D.L., Thorstenson, and D. C. Plummer L.N., (1980). Version July 24, 1987.

Nordstrom, D.K., Ball, J.W., Donahoe, R.J., and Whittemore, D. (1989) Groundwater chemistry and water-rock interactions at Stripa. *Geochim. Cosmochim. Acta*, 53: 1727-1740.

Norman, A.L. (1991) Stable isotope studies of atmospheric sulphur: Comparison of Alberta, Canada and Bermuda. Msc. Thesis. The University of Calgary, Alberta.

Norman, A.L. (1994) Isotope analysis of microgram quantities of sulfur: Applications to Soil Sulfur Mineralization Studies. Ph.D. Thesis. The University of Calgary,

Calgary, Alberta.

Norrish., K. and Chappell, B.W., (1977) X-ray fluorescence spectrometry. In: J. Zussman (Editor) Physical Methods in Determinative Mineralogy. Academic press, London, pp. 201-272.

Nriagu, J.O., Rees, C.E., Mekhtiyeva, V.L., Lein, A.Yu., Fritz, P., Drimmie, R.G., Pankina, R.G., Robinson, R.W., and Krouse, H.R. (1991) Hydrosphere. In: H. R. Krouse, and V.A. Grinenko (Editors) Stable Isotopes, Natural and Anthropogenic Sulphur in the Environment. SCOPE 43, pp. 175-265.

O'Brien, J.E. (1962) Automated analysis of Chlorides in sewage. Wastes Eng. 33, 670 pp.

Parkhurst, D.L., Thorstenson, and D.C. Plummer, L.N., (1980) PHREEQE, A computer program for geochemical calculations. *U.S. Geol. Sur. Water Resour. Inves.*, 80-96.

Pearson Jr.,F.J. and Swarzenki, W.V. (1974) ^{14}C evidence for the origin of arid region groundwater, Northern Province, Kenya. In Isotope Techniques in Groundwater Hydrology, IAEA, Vienna, Austria, pp. 95-109.

Phillips, F.M. (1993) Comments on "Reinterpretation of ^{36}Cl data: physical processes, hydraulic interconnections and age estimates in groundwater systems" by E. Mazor. *Appl. Geochem.*, 8: 643-647.

Pingitore, E.N.Jr., and Eastman, P.M. (1986) The coprecipitation of Sr^{2+} with calcite at 25 °C and 1 atm. *Geochim Cosmochim Acta*, 50: 2195-2203.

Plummer, L.N., and Back, W. (1980) The mass balance approach: Application to interpreting the chemical evolution of hydrologyic systems. *Amer. Jour. Sci.*, 280: 130-142.

Plummer, L.N., and Mackenzie, F.T. (1974) Predicting mineral solubility from rate data: application to the dissolution of magnesian calcite. *Am. J. Sci.,* 274: 61-83.

Plummer, L.N., Vacher, H.L., Mackenzie, F.T., Bricker, O.P., and Land, L.S. (1976) Hydrogeochemistry of Bermuda: A case history of groundwater-water diagenesis of biocalcarnites. *Geol. Soc. Amer. Bull.*, 87: 1301-1316.

Plummer, L.N., Parkhurst, D.L., and Thorstenson, D.C. (1983) Development of reaction models for ground -water systems. *Geochim. Cosmochim. Acta*, 47: 665-686.

Plummer, L.N., Prestemon, E.C. and Parkhurst, D.L. (1991) NETPATH- An interactive code (NETPATH) for modeling net geochemical reactions along a flow path. *U.S. Geol. Sur. Water Resour. Inves. Report,* 91- 4078.

Qureshi, R.M., Aravena, R., Fritz, P., and Drimmie, R. (1989) The CO_2 absorption method as an alternative to benzene synthesis method for ^{14}C dating. *Appl. Geochem.*, 4: 625-633.

Raven, M.D., (1992) XPLOT: Version 3-User manual. CSIRO, Division of Soils, Technical Memorandum, 24: 1990.

Reardon, E.J. and Fritz, P. (1979) Computer modeling of groundwater ^{13}C and ^{14}C isotope compositions. *J. Hydrol.*, 36: 201-224.

Reardon, E.J., Mozeto, A.A., and Fritz, P. (1980) Recharge in northern clime calcareous sandy soils: soil water chemical and carbon-14 evolution. *Geochim. Cosmochim. Acta*, 44: 1723-1735.

Rees, C.E., Jenkins, W.J., and Monster, J. (1978) The sulphur isotopic composition of ocean water sulphate. *Geochim. Cosmochim. Acta*, 42: 377-381.

Rees, C.E. (1973) A steady-state model for sulphur isotope fractionation in bacterial reduction processes. *Geochim. Cosmochim. Acta* 37: 1141-1162.

Rees, C.E. (1978) Sulphur isotope measurements using SO_2 and SF_6. *Geochim. Cosmochim. Acta*, 42: 383-389.

Revesz, K. and Woods, P.H. (1990) A method of extract soil water for isotope analysis. *J. Hydrol.*, 115: 397-406.

Rightmire, C.T., Pearson, .F.J., Back, W., Rye, R.O., and Hanshaw, B.B. (1974) Distribution of sulphate isotopes of sulphates in groundwaters from the principal artesian aquifer of Florida and the Edwards aquifer of Texas, United States of America. In: Isotope Techniques in Groundwater Hydrology. IAEA Vienna Austria, Vol. 2, pp. 191-206.

Robertson, F. (1987) Geochemistry of ground water in alluvial basins of Arizona and adjacent parts of Nevada, New Mexico, and California. *U.S. Geol. Surv.Prof. Paper* 1406-D.

Robertson, W.D. and Schiff, S.L. (1994) Fractination of sulphur isotopes during biogenic sulphate reduction below a sandy forested area in south-central Canada. *J. Hydrol.*, 158: 123-134.

Rozanski, K., Araguas.L., Gonfiantini, R. (1993) Isotopic patterns in modern global precipitation. In P.K. Swart, K.C. Lohmann, J. McKenzie, and S. Savin, (Editors) Climatic Change in Continental Isotopic Records. AGU Geophysical Monograph. *Amer. Geophy. Union*, Washington, D.C. 78, pp. 1-36.

Rye, R.O., Back, W., Hanshaw, B.B., Rightmire, C.T., and Pearson, Jr.F.J. (1980) The origin and isotopic composition of dissolved sulfide in groundwater from carbonate aquifers in Florida and Texas. *Geochim. Cosmochim. Acta*, 45: 1941-

1950.

Salati, E, Menezes, L.J., and Mendes, C.M. (1974) Environmental isotope used in a Hydrogeological study of Northeastern Brazil. In: Isotope Techniques in Groundwater Hydrology, IAEA, Vienna, Austria, pp. 259-283.

Sass, E., and Starinsky, A. (1979) Behavior of strontium in subsurface calcium chloride brines: southern Israel and Dead Sea Rift Valley. *Geochim Cosmochim Acta*, 43: 885- 895.

Schmid, R.M. (1985) Lake Torrens, South Australia: Sedimentation and Hydrology. Ph.D. Thesis, Flinders University of South Australia, Adelaide.

Schoen, R., and Rye, R.O. (1970) Sulfur isotope distribution in Solfatara, Yellowstone National Park. *Science*, 170: 1082-1084.

Schwartz, F.W., Muehlenbachs, K. and Chorley, D.W. (1981) Flow-system controls of the chemical evolution of groundwater. *J. Hydrol.,* 54: 225-243.

Seimbille, F.G., Manhes, G., and Allegre, C.J. (1988) Isotopic composition and content of strontium in rainwater. *Chem. Geol.*, 70: 16.

Shakur, M.A. (1982) $\delta^{34}S$ and $\delta\ ^{18}O$ variations in terrestrial sulphates. Ph.D. Thesis. University of Calgary, Calgary, Alberta, Canada.

Sheppard, S.F.M., Nielsen, R.L., and Tylor, H.P. (1969) Oxygen and hydrogen isotope ratios of clay minerals from porphyry deposits. Economic. *Geology*, 64: 755-777.

Siegel, D.I. (1989) Geochemistry of the Cambrian-Ordovician aquifer system in the Northern Midwest, United States. *U.S. Geol. Surv.Prof. Paper* 1405-D.

Simpson, H.J., and Herczeg, A.L. (1994) Delivery of marine chloride in precipitation and removal by rivers in the Murray-Darling Basin, Australia. *J. Hydrol.,* 154:

323-350.

Simpson, H.J., and Herczeg, A.L. (1991 a) Stable isotope as an indicator of evaporation in the River Murray, Australia. *Water Resour. Res.*, 27: 1925-1935.

Simpson, H.J., and Herczeg, A.L. (1991 b) Salinity and evaporation in the River Murray Basin, Australia. *J. Hydrol.*, 124: 1-27.

Smith, D.B., Downing, R.A., Monkhouse, R.A., Otlet, R.L. and Pearson, F.J. (1976) The age of groundwater in the Chalk of the London Basin. *Water Resour. Res.*, 12: 392-404.

Smith, D.B., Otlet, R.L., Downing, R.A., Monkhouse, R.A., and Pearson, F.J. (1975) Stable carbon and oxygen isotope ratios of groundwater from the Chalk and Lincolnshire Limestone. *Nature*, 257: 783-784.

Sonntag, C., Thoma, G., Munnich, K.O., Dincer, T., and Klitzsch, E. (1980). Environmental isotopes in North African groundwaters; and the Dahna sand-dune study, Saudi Arabia. In: Arid-Zone Hydrology Investigations with Isotope Techniques. IAEA, Vienna, Austria, pp. 77-83.

Sonntag, G., Klitzsch, E., Lohnert, E.P., El-Shazly, E.M., Munnich, K.O., Junghans, Ch.,Thorweihe, U., Weistroffer, K., and Swailem, F. M. (1978) Palaeoclimatic information from deuterium and oxygen-18 and carbon-14 dated North Saharian groundwaters. In: Isotope Hydrology, Vienna, Austria, Vol. 2, pp. 569-581.

Sprinkle, C.L. (1989) Geochemistry of the Floridian aquifer system in Florida and parts of Georgia, South Carolina, and Alabama. *U.S. Geol. Surv.Prof. Paper* 1403-I.

Starinsky, A., Bielski, M., Lazar, B., Steinitz, G., and Raab, M. (1983) Strontium isotope evidence on the history of oilfield brines, Mediterranean Coastal Plain, Israel. *Geochim Cosmochim Acta*, 47: 687- 695.

Strebel, O., Bottcher, J., and Fritz, P. (1991) Use of isotope fractionation of sulphate-sulfur and sulphate-oxygen to asses bacterial desulfurication in a sandy aquifer. *J. Hydrol.,* 121: 155-172.

Streich, V. (1893). Geology. *R. Soc. S. Aust., Trans.* 16, pp. 74-110.

Striegl, R.G., and Armstrong, D.E. (1990) Carbon dioxide retention and carbon exchange on unsaturated Quaternary sediments. *Geochim. Cosmochim. Acta*, 54: 2277-2283.

Stueber, M.A., Pushker, P., and Hetherington, A.E. (1984) A Strontium isotopic study of Smackover brines and associated solids, southern Arkansas. *Geochim Cosmochim Acta*, 48: 1637-1649.

Stueber, M.A., Walter, M.Lynn., Huston, J.T., and Pushkar, P. (1993) Formation waters from Mississippian-Pennsylvanian reservoirs, Illinois Basin, USA: Chemical and isotopic constraints on evolution and migration. *Geochim Cosmochim Acta*, 57: 763- 784.

Stumm, W., and Morgan, J.J. (1981) *Aquatic Chemistry*. John Wiley & Sons, Inc, 780 pp.

Stute, M., Clark, J.F., Schlosser, P., and Broecker, W.S. (1995) A 30,000 yr continental palaeotemparature record derived from noble gases dissolved in groundwater from the San Juan Basin, New Maxico. *Quater Res.* 43: 209-220.

Taylor, B.E., Wheeler, M.C., and Nordstrom, D.K. (1984 a) Isotope composition of sulphate in acid mine drainage as measure of bacterial oxidation. *Nature*, 308:

538-541.

Taylor, B.E., Wheeler, M. C., Nordstrom, D. K. (1984 b) Stable isotope geochemistry of acid mine drainage: Experimental oxidation of pyrite. *Geochim. Cosmochim. Acta*, 48: 2669-2678.

Telfer , A. (1990) Groundwater discharge from a confined aquifer through a zone of high upward leakage. International Conference on Groundwater in Large Sedimentary Basins, Australian Water Council Conference, Series. No.20, pp. 185-193.

Telfer, A. (1989) Groundwater-river water density contrast: its effect on the pattern of groundwater discharge to the River Murray. *J. Aust. Geol. Geophys.*, 11: 227-232.

Thode, H.G. (1991) Sulphur isotopes in nature and the environment: An overview. In: H.R. Krouse and V.A. Grinenko (Editors) Stable Isotopes, Natural and Anthropogenic Sulphur in the Environment. SCOPE 43, pp. 1-26.

Thode, H.G. and Monster, J. (1965). Sulfur-isotope geochemistry of petroleum, evaporates, and ancient seas. In: A. Young and J. E. Galley (Editors) Fluids in Subsurface Environments. *Mem. Am. Assoc. Petr. Geol.,* 4. pp. 367-377.

Thorstenson, D.C., Weeks, E.P., Haas, H. and Fisher, D.W. (1983) Distribution of gaseous $^{12}CO_2$, $^{13}CO_2$ and $^{14}CO_2$ in the sub-soil unsaturated zone of the Western US Great Plains. *Radiocarbon*, 25: 2, 315-346.

Thrailkill, J. (1968) Chemical and hydrologyic factors in excavation of limestone caves. *Bull. Geol. Soc. Amer.,* 79: 19-46.

Tickell, S.J. and Humphreys, W.G. (1987) Groundwater resources and associated salinity problems of the Victorian part of the Riverine Plain. Department of

Industry, Technology and Resources, Victoria, Geological Survey Report No. 84.

Todd, D.K. (1959) *Ground Water Hydrology*. Wiley & Sons, Inc., New York, 336 pp.

Todd, D.K. (1970) *The Water Encyclopedia*. Water Information Centre, Port Washington, New York.

Tolman, C.F. (1937) *Groundwater*, McGraw Hill, New York, 593 pp.

Tucker, M.E., and Wright, V.P. (1990) *Carbonate Sedimentology*. Blackwell Scientific publications, 482 pp.

Tudge, A.P., and Thode H.G. (1950) Thermodynamic properties of isotopic compounds of sulphur. *Can. J. Res*. 28: 567-578.

Turekian, K.K., and Kulp, L. J. (1956) The geochemistry of strontium. *Geochim. Cosmochim. Acta*, 10: 245-296.

Turner, S.M., Malin, G., and Liss, P.S. (1989) Dimethylsulfide and (dimethylsulfonio) propionate in European coastal and shelf waters. In E.S. Saltzman, and W.J. Cooper (Editors) Biogenic Sulphate in the Environment. Symposium, American Chemical Society, Washington D.C., Series No. 393.

Turner, S.M., Malin, G., Liss, P.S., Harbour, D.S., and Holligan, P.M. (1988) The seasonal variation of dimethylsulphide and dimethylsulfoniopropionate concentration in near shore waters. *Limnol Oceanogr.*, 33: 364-375.

Tyler, S.W., Chapman, S.H., Conrad, S H., Hammermeister, D.P., Blout, D.O., Miller, J.J., Sully, M.J., and Ginanni, J.M. (1996) Soil-water flux in the southern Great Basin, United States: Temporal and spatial variations over the last 120,000 years. *Water Resour. Res*., 32, pp. 1481-1499.

Urey, H.C. (1947) The thermodynamic properties of isotopic substances. *J. Chem.*

Soc., pp. 562-581.

Van Everdingen, R.O., and Krouse, H.R. (1985). Isotope composition of sulphates generated be bacterial and biological oxidation. *Nature,* 315: 395-396.

Van Everdingen, R.O., and Krouse, H.R. (1992) Control of $\delta^{18}O$ in Sulfate: Review of Experimental Data and Application to Specific Environment. In C.N. Alpers, and D.W. Blowes (Editors) Environmental Geochemistry of Sulfide Oxidation. *Amer. Chem. Soc*, pp. 447-479.

Van Everdingen, R.O., Shakur, M.A., and Krouse, H.R. (1982) Isotope geochemistry of dissolved, precipitated, airborne, and fallout sulfur species associated with springs near Paige Mountain, Norman Range, N. W. T. *Can. J. Earth. Sci.*, 19: 1395-1407.

Van Stempvoort, D.R. Reardon, E. J. and Fritz, P. (1990) Fractionation of sulfur and oxygen isotopes in sulfate by soil sorption. *Geochim. Cosmochim. Acta*, 54: 2817-2826.

Verhagen, B.Th., Mazor, E., and Sellschop, J.P.F. (1974) Radiocarbon and tritium evidence for direct recharge to groundwaters in the Northern Kalahari. *Nature,* 249: 643-644.

Vinogradov, A.P., Grinenko, V.A., and Ustinov, V.I. (1962) Isotopic composition of sulphur compounds in the Black Sea. *Geokhimiya*, 10: 973-997.

Vogel, J.C. (1966) Inversigations of groundwater flow with radiocarbon. In: Isotope Hydrology, IAEA, Vienna, Austria, pp. 355-367.

Volkov, I,I., and Rozanov, A.G., (1983) The sulphur cycle in oceans. In M.V. Ivanov, and J.R. Freney (Editors) The Global Biogeochemical Sulphur Cycle SCOPE 19, pp. 357-448.

Wakshal, E., and Nielsen H. (1982) Variations of $\delta^{34}S(SO_4)$, $\delta^{18}O(H_2O)$ and Cl/SO_4 ratio in rainwater over northern Israel, from the Mediterranean coast to Jordan Rift Valley and Golan Heights. *Earth Planet. Sci. Lett.*, 61: 272-282.

Walker, C.D., Brunel, J.P. Dunin, F.X., Edwards, W.R.N., Hacker, J.M., Hartmann, J., Jupp, D.L., Reyenga, W., Schwerdtfeger, P., Shao, Y. and Williams, A.E. (1990) A joint project on the water use of a Mallee community in late summer. In: J.C. Noble, P.J. Ross, and G.K. Jones (Editors) The Mallee lands: A Conservation Perspective. CSIRO, Melbourne, Victoria, pp. 114-119.

Walker, G.R., and Cook, P.G. (1991) The importance of considering diffusion when using carbon-14 to estimate groundwater recharge to an unconfined aquifer. *J. Hydrol.*, 128: 41-48.

Walker, G.R., Woods, P.H., and Allison, G.B. (1994) Inter-laboratory comparison of methods to determine the stable isotope composition of soil water. *Chem. Geol.*, (isotope Geoscience Section), 111: 297-306.

Wallick, E.I., and Toth, J. (1976) Methods of regional groundwater flow analysis with suggestions for the use of environmental isotopes. In: Interpretation of Environmental Isotope and Hydrochemical Data in Groundwater Hydrology. IAEA. Vienna, Austria, pp. 37-65.

Wasson, R.J., and Donnelly, T.H. (1991) Palaeooclimatic reconstruction for the last 30,000 years in Australia- a contribution to prediction of future climate. CSIRO, Division of Water Resources. Technical Memorandum 91/3.

Wickman, T., and Jacks, G. (1992) Strontium isotopes in weathering budgeting. In: Y.K. Kharaka, and A.S. Maest, (Editors) Water-Rock Interaction WRI-7, Proceedings of the 7th International Symposium. Park City, Utah, USA.

Balkema, Rotterdam, Vol. 1 pp. 611-614.

Wigley, T.M.L. (1973) Chemical evolution in the system calcite-gypsum-water. *Can. J. Earth Sci.*, 10: 306-315.

Wigley, T.M.L. (1975) Carbon 14 dating of groundwater from closed and open systems. *Water Resour. Res.*, 11: 324-328.

Wigley, T.M.L. (1976) Effect of mineral precipitation on isotopic composition and ^{14}C dating of groundwater. *Nature*, 263: 219-221.

Wigley, T.M.L., and Plummer L. N. (1976) Mixing of carbonate waters. *Geochim. Cosmochim. Acta*, 40: 989-995.

Wigley, T.M.L., Plummer L.N., and Pearson, Jr.F.J. (1978) Mass transfer and carbon isotope evolution in natural water systems. *Geochim. Cosmochim. Acta*, 42: 1117-1139.

Wigley, T.M.L., Plummer L.N., and Pearson, Jr.F.J. (1979) Errata: *Geochim. Cosmochim. Acta*, 43: 1393.

Wood, W.W., and Lmes, J.L. (1995) How wet is wet ? Precipitation constraints on late Quaternary climate in the Southern Arabian Peninsula. *J. Hydrol.*, 164: 263-268.

Wood, W.W., and Low, W.H. (1988) Solute geochemistry of the Snake River plain regional aquifer system, Idaho, and Eastern Oregon. *U.S. Geol. Surv.Prof. Paper* 1408-D.

Woolley, D.R., and Williams, R.M. (1978) Tertiary stratigraphy and hydrogeology of the eastern part of the Murray Basin, NSW. In: R.R. Storrier, and I.D. Kelly, (Editors) Proceedings of a symposium on the hydrogeology of the Riverine Plain of south-eastern Australia. Australian Society of Soil Science, Riverina

Branch, pp. 45-65.

Wopfner, H. and Twidale, C.R. (1967) Geomorphic history of the lake Eyre basin. In: J.N. Jennings and J.A. Mabbutt (Editors) Landform Studies from Australia and New Guinea. Australian National University Press, Canberra, A.C.T., pp. 118-143.

Zimmermann, U. Ehhalt, D. and Munnich, K.O. (1967) Soil-water movement and evapotranspiration: changes in the isotopic composition of the water. In: Isotope Hydrology. IAEA, Vienna, Austria, pp. 567-585.